UNIVERSITY OF URBINO CARLO BO

DEPARTMENT OF BIOMOLECULAR SCIENCES

PhD Course in Life Sciences, Health and Biotechnologies

Curriculum in Biochemical and Pharmacological Sciences and Biotechnologies

XXXIV Cycle

Advances in leishmaniasis: development of molecular diagnostic approaches and identification of new compounds against *Leishmania (Leishmania) infantum*

ACADEMIC DISCIPLINE: BIO-13

Coordinator:

Prof. Marco Bruno Luigi Rocchi

PhD Student:

Dr. Gloria Buffi

Supervisor:

Prof. Luca Galluzzi

Co-Supervisor:

Dr. Aurora Diotallevi

ACADEMIC YEAR 2020-2021

Summary

STRUCTURE OF THE THESIS

The thesis is composed of an introduction, 9 chapters and conclusions. Every chapter is introduced by a brief paragraph that explains the content. Chapters 1-4 and 6 report papers already published, chapter 7 is a work under review, while chapters 5, 8 and 9 contain unpublished data. During my Ph.D., I dealt with three *macro*-topics related to leishmaniasis: (i) the development and application of new molecular approaches for the parasite characterization at the species and strain level (chapters 1-5); (ii) the evaluation of current treatments, the problem of drug resistance and the screening and identification of new compounds active on *Trypanosomatidae* (chapters 6-8); (iii) host-pathogen interaction for the discovery of new infection markers (chapter 9). The references relating to each work are found at the end of each chapter.

INTRODUCTION

1.1 General Aspects

Leishmaniases are a group of anthropo-zoonic parasitic diseases caused by a *protozoan* belonging to *Leishmania* genus that affect millions of people worldwide, both in Old World (Europe, Asia, Africa) and New World (America) (Akhoundi et al., 2016; Alvar et al., 2012). According to the WHO, more than 1 billion people leave in endemic areas for leishmaniasis and are at risk of infection. Thirty thousand new cases of visceral leishmaniasis (VL) and more than 1 million new cases of cutaneous leishmaniasis (CL) have been estimated annually. In 2018, 92 and 83 countries and territories were considered endemic for leishmaniasis; most of them are developing countries (https://www.who.int/health-topics/leishmaniasis). Italy and the Mediterranean Basin are included in these areas where *L. infantum* species is the causative agent of human and canine leishmaniasis (CanL). The parasites are transmitted by the bite of female infected sandflies of the genus *Phlebotomus* or the genus *Lutzomyia*. The pathogens replicate in the vector middle intestine which injects the parasites into the vertebrate host during the blood meal. There are several vertebrate hosts for *Leishmania*, from canids to cats and wild rodents (Podinovskaia and Descoteaux, 2015) that have an important role as reservoirs of infection for humans.

In humans, there are three main forms of the disease: cutaneous (CL), mucocutaneous (MCL) and visceral leishmaniasis (VL). CL is characterized by papules and nodules that can evolve to skin ulcerative lesions nearby the phlebotomine bite site or regress spontaneously. The mucocutaneous leishmaniasis (MCL) shows destruction of the oro-nasopharyngeal tissue. VL is the most severe form of the disease and consists of a chronic infection of internal organs such as spleen, liver, and bone marrow; if left untreated is fatal (Podinovskaia and Descoteaux, 2015). The clinical manifestations depend on the species and the host's immune response to infection, and ranges from asymptomatic to fatal. VL is caused by *Leishmania donovani* complex that includes *L. donovani* and *L. infantum*; CL is related to Old World species like *L. major* and *L. tropica*, and New World species like *L. mexicana*. Although the form caused by species of the *Viannia* subgenus, including *L. braziliensis,* are generally responsible for the CL, the

parasite can also migrate to the oro-nasopharyngeal tissues and evolve in the MCL (Rogers *et al.*, 2011).

Even though the VL cases are decreasing due to surveillance projects introduced by the WHO, the disease still causes relevant problems in poor countries. On the other hand, the CL cases increase every year, probably because of globalization and climate change. Moreover, the prevention and the control of leishmaniasis are complex and require a combination of intervention strategies that involve humans, animal reservoir hosts, parasites, and vectors (WHO).

The treatments available are few and have severe limitations like toxicity, difficulty in administration, decrease efficacy, high production cost, and the most important, the presence of resistant strains (Sasidharan and Saudagar, 2021). Briefly, the current drugs are pentavalent antimonials, amphotericin B, pentamidine, miltefosine and paromomycin. The mechanism of action, when known, the characteristics and the limitations of these treatments will be described below.

For all these reasons, a rapid, cheap, and early diagnosis associated with effective therapy is pivotal to reduce the prevalence of the disease and to prevent disabilities and death. These two aspects will be discussed in the thesis and new data will be presented.

1.2 Classification

Leishmania genus belongs to *Protozoa* kingdom. The classification of this kingdom is quite complex and has undergone many changes over the year. More than 50,000 species have been identified, most of which are free-living organisms, but several are parasitic to humans. Some species are considered commensals and generally not harmful, whereas some others are pathogenic and can cause disease (Yaeger, 1996). The genus *Leishmania* belongs to the class of *Kinetoplastea* and the order of *Trypanosomatida*. All the kinetoplastids are characterized by the kinetoplast, a DNA-containing structure placed inside the single mitochondrion (Klatt et al., 2019). Until today, more than 50 species of *Leishmania* have been identified and classified in two *clade: Euleishmania* and *Paraleishmania* (Cupolillo et al., 2000). *Euleishmania* encompasses four subgenera (Figure 1): *Leishmania (Leishmania), Leishmania (Viannia), Leishmania (Sauroleishmania), Leishmania (mundinia)* also called *L. enriettii complex*.

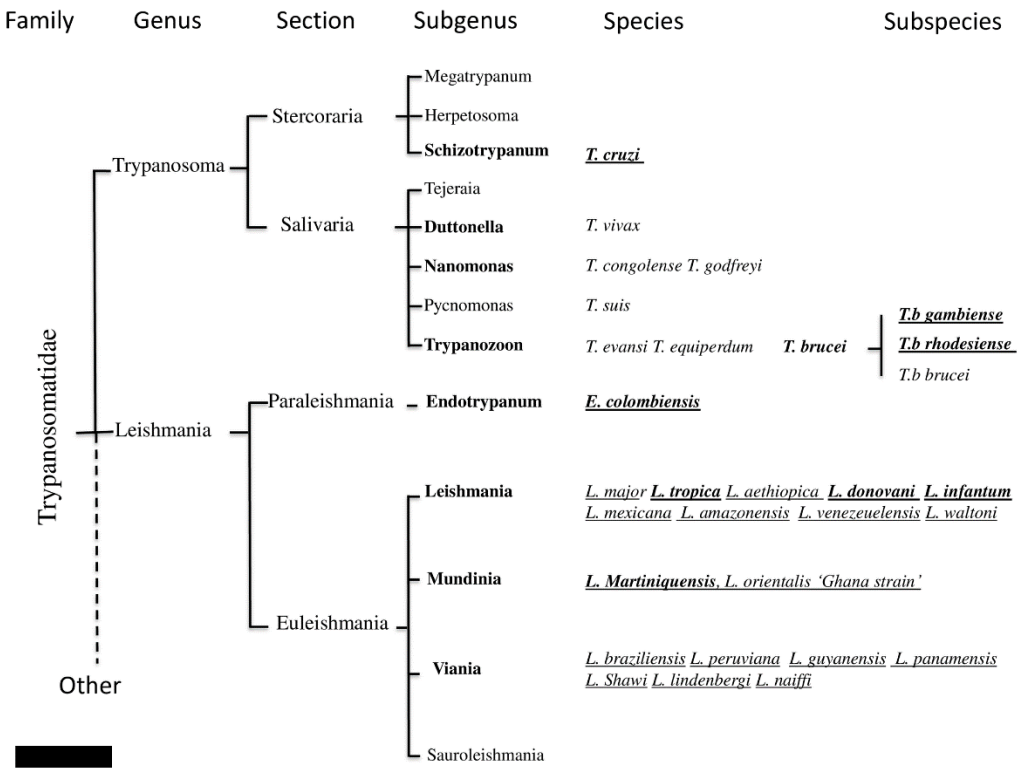

[Figure 1] Classification of human and animal pathogenic trypanosomatids. Human pathogenic species are underlined. In bold, pathogens causing systemic infection. (Sereno et al., 2020)

Among all the species, 20 are pathogenic to humans and cause leishmaniasis and belong to *Leishmania* subgenus (presents in both Old and New World) and *Viannia* subgenus (limited to Tropical America) (Akhoundi *et al.*, 2016). *Leishmania* subgenus includes *L. donovani* complex (*L. donovani, L. infantum,* also called *L. chagasi* in South America), the *L. mexicana* complex (L. *mexicana, L*. *amazonensis*), *L. tropica*, *L. major*, *L. aethiopica*, whereas *L. braziliensis, L. guyanensis, L. panamensis* and *L. peruviana* belong to subgenus *Viannia* (Figure 1).

In general, most of the species have been considered zoonotic agents because humans represent the secondary host except for *L. donovani*, the causative agent of anthroponotic visceral leishmaniasis (spread in India, Bangladesh, Sudan, Ethiopia, Kenya), and *L. tropica* that causes anthroponotic cutaneous leishmaniasis (spread in Middle East, Kenya, and North Africa).

1.3 Geographical Distribution

According to the WHO Expert Committee, countries are classifying as: (i) “endemic” if at least 1 autochthonous case has been reported and the entire cycle of transmission is demonstrated; (ii) “previously reported cases” if at least 1 autochthonous case have been reported but the cycle of transmission is not demonstrated; “not autochthonous cases reported” if no cases have been reported. As already cited, leishmaniasis has a worldwide distribution but continues to represent a health problem in four eco-epidemiological regions: the Americas, East Africa, North Africa and West and South East Africa (Ruiz-Postigo et al, 2021). Recently, it was published a report by the World Health Organization titled “Global leishmaniasis surveillance: 2019-2020, a baseline for the 2030 roadmap” (Ruiz-Postigo et al, 2021). According to this document, in 2020, among the 200 countries that reported to WHO, 98 (49%) were endemic for leishmaniasis; of those, 89 were endemic for CL, 79 were endemic for VL, and 71 were endemic for both. Of the endemic countries, 25 have been considered to have “high burden of leishmaniasis” (>100 VL cases or >2500 CL cases) since 2014: 13 countries for VL, 12 countries for CL, 1 country for both. In 2019-2020, 2 more countries have been added (Eritrea and Yemen). All the other endemic countries are considered as “having a low burden”. CL and VL are endemic in Africa, Americas, Eastern Mediterranean Region, Europe, South-East Asia, but most of the cases are referred in Eastern Mediterranean and Africa for CL and VL, respectively. Only one country, China, is endemic for both CL and VL in Western Pacific Region (Ruiz-Postigo et al, 2021).

In 2020, a total of 208,357 new CL cases and 12,838 new VL cases were reported to WHO. More than 90% of CL cases were in Eastern Mediterranean Region and South America with most of the cases in seven countries: Brazil, Colombia, Pakistan, Iraq, Algeria, Afghanistan, and the Syrian Arab Republic (Figure 2).

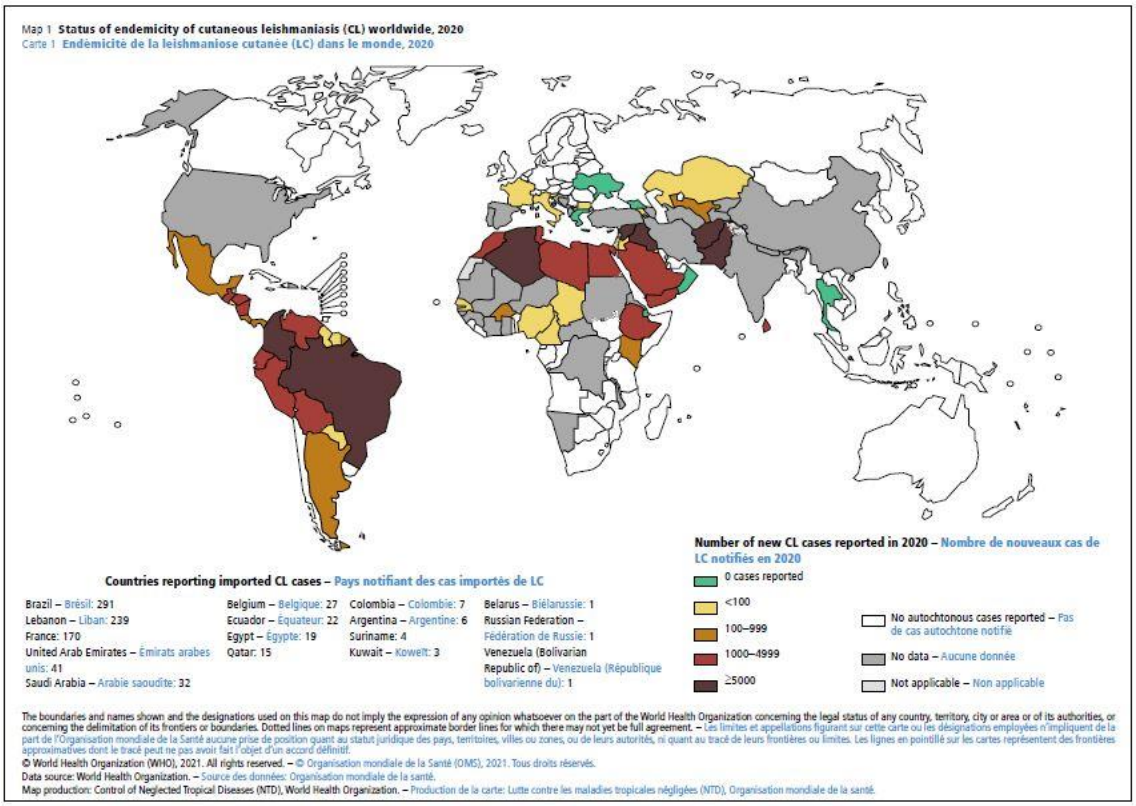

[Figure 2] Status of endemicity of CL worldwide, 2020
(Global leishmaniasis surveillance: 2019-2020, a baseline for the 2030 roadmap, WHO)

Regarding the VL cases, the hot spots are East Africa (Ethiopia, Eritrea, Kenya, Somalia, Sudan and Uganda), the Indian subcontinent (India, Nepal, Bangladesh) and Brazil (Figure 3).

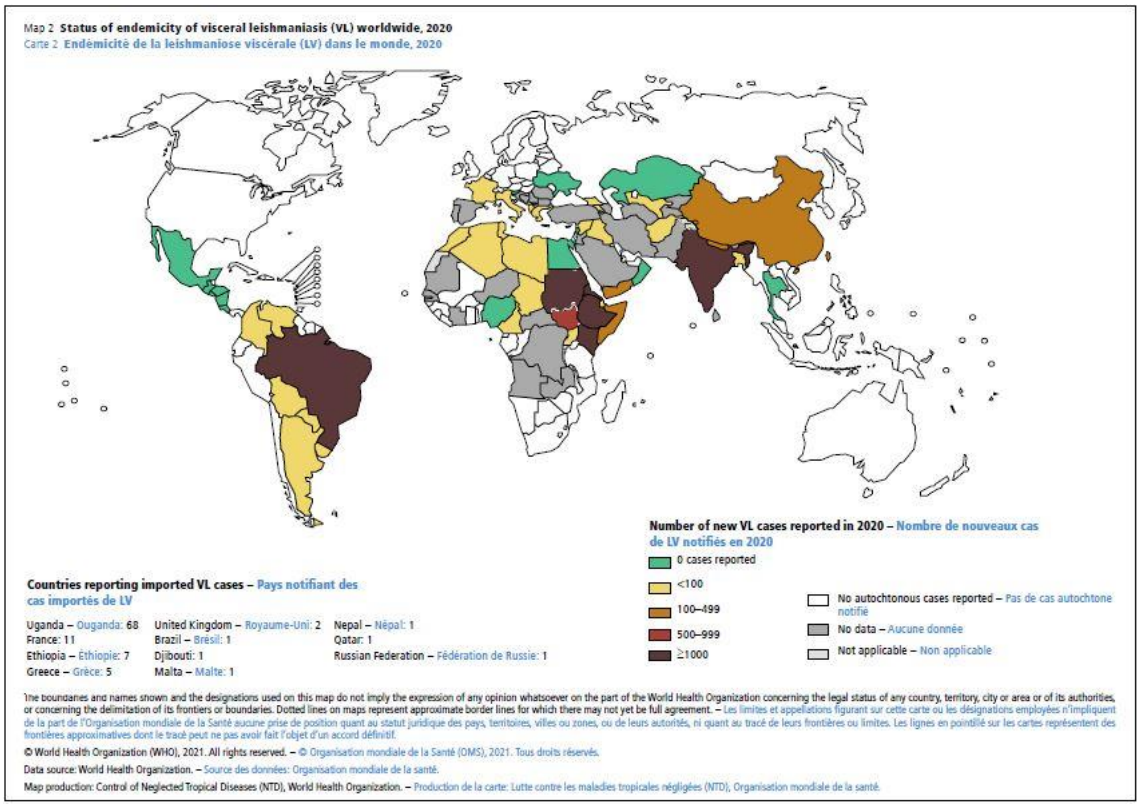

[Figure 3] Status of endemicity of VL worldwide, 2020
(Global leishmaniasis surveillance: 2019-2020, a baseline for the 2030 roadmap, WHO)

At a global level, there was a general increasing trend in the number of CL cases between 1998 and 2019 and an important decrease between 2019 and 2020, mainly due to the Europe trend. In the same way, also the number of VL has decreased consistently. A total of 3,813 VL deaths were reported in 2014-2020 with a case fatality rate of 3.3% in 2017, with a decrease to 2.7% in 2020. The report underlines the improvements made in leishmaniasis surveillance since 2014; nevertheless, the parasites continue to extend to new areas in endemic countries and to new countries (Ruiz-Postigo et al, 2021). The different *Leishmania* species with their respective reservoirs hosts and the geographical distribution are summarized in Table 1

Leishmania sp.	Reservoir hosts	Geographical distribution
L. donovani	Rodents and canines	India, China, Bangladesh, Sudan, Ethiopia, Burma, Kenya
L. chagasi	Opossums	South America
L. infantum	Dogs and rodents	East and Central Asia, Mediterranean countries, Pakistan, China, Central and South America, Europe, Africa, and French Guiana
L. amazonensis	Rodents and opposums	South America and Northern regions of Amazon
L. braziliensis	Rodents and dogs*	Central America and Mexico
L. major	Rodents	Africa, Middle East and Central Asia, North India, and Pakistan
L. aethiopica	Rock hyraxes	Ethiopia and Kenya
L. peruviana	Opposums and dogs*	Peru and Argentine highlands
L. panamensis	Sloths, procyonids, and dogs*	Brazil, Colombia, Costa Rica, and Panama
L. guyanensis	Opposums, sloths, and anteaters	Brazil and French Guiana

[Table 1] *Leishmania* spp. with their *reservoir* hosts and geographical distribution (Sasidharan and Saudagar, 2021)

1.3.1 Leishmaniasis in Italy

Italy and the South of Europe are endemic areas for VL and CL caused by *L. infantum* species, which is also responsible for the CanL. The first documented epidemic outbreak in Italy was observed between 1971 and 1972 near Bologna, with 60 new cases and 13 deaths. Subsequently, between 1989 and 2009, Italy recorded an increase in human VL, with 10-30 cases reported annually since 1950. The epidemic peak was reached between 2000 and 2004 with more than 200 cases/year (Gramiccia et al., 2013). Unfortunately, these data are rather old, and many regions suffer from under-notification while active surveillance programs have been set up in the Campania, Sicily, and Liguria regions. In 2020, Ortalli et al. found 12.5% prevalence of *Leishmania* infection in the blood donor in Bologna province (endemic area in northeastern Italy) indicating an elevated exposure and suggesting the importance of a surveillance system for monitoring *Leishmania* infection (Ortalli et al., 2020).

Although the number of human leishmaniasis cases in Italy are limited, the CanL distribution is more problematic. Since dogs represent one of the most important *reservoirs* of infection for humans, the control of infected dogs is important for public health and the development of prevention plans. Nevertheless, in some geographical areas, the direct association between the prevalence of CanL and the human VL is not clear. According to the latest data published on the website www.salute.gov.it from the "Ministero della Salute" in collaboration with "Centro di Referenza Nazionale per le Leishmaniosi" (C.Re.Na.L.), in Italy, the average percentage of dogs' serum prevalence in

2017 was 18.65% with a total number of 55,774 tests, of which 10,402 were positive (tests performed by IFAT) (Figure 4). In particular, Piemonte, Tuscany, Veneto and Sardinia regions showed a consistent circulation of the *Leishmania* parasite, higher compared to the past, a symptom not only of a greater spread of the parasite but also of poor surveillance of the pathology.

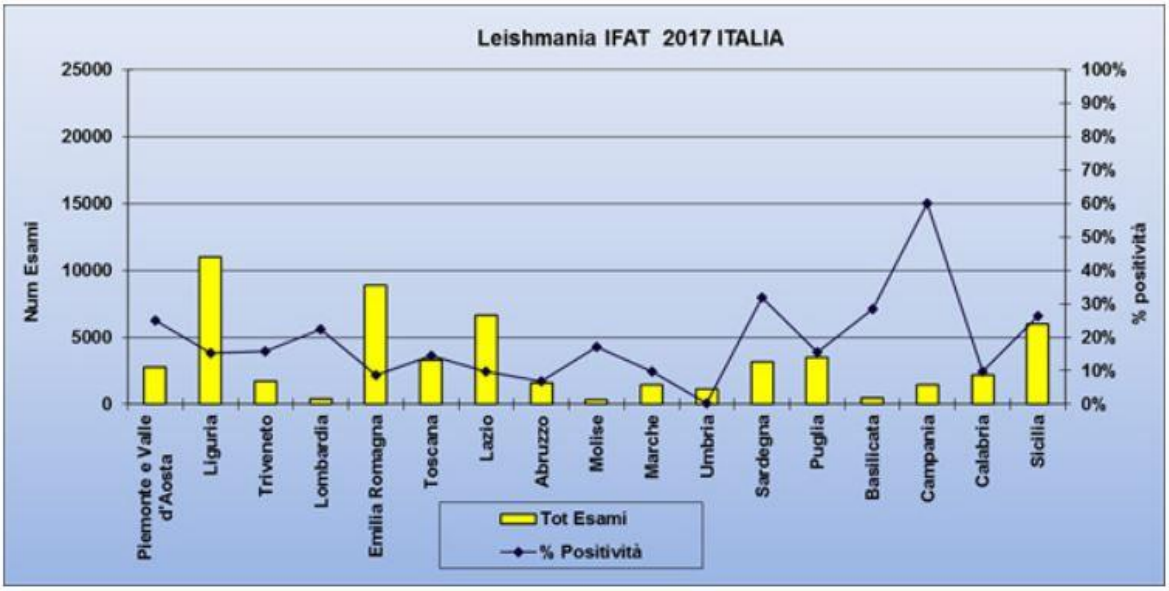

[Figure 4] Number of cases of CanL in different Italian regions in 2017. The X-axis shows the italian regions. The yellow bars indicate the total number of tests performed by IFAT, while the blue lines the percentage of positivity.
(https://www.salute.gov.it/portale/sanitaAnimale/dettaglioContenutiSanitaAnimale)

The average percentage of serum prevalence in 2017 was 14.21%, 7.42%, and 32.76%, in the North, center and South of Italy, respectively. The most affected regions were Piemonte/Valle d'Aosta and Lombardia in the North, Molise in the center and Sicily, Campania, and Sardinia in the South. Notably, territories that were considered CanL-free until some years ago, showed an increase of autochthonous infection, especially in the North. Surveillance plans are carried out in several regions and are focused to control the canine *reservoir* increasing in non-endemic areas and the rapid vector sand flies spread. The goal is to limit cases of infection by monitoring the vector and infected dogs and implementing proper disclosure among dog owners. Despite dogs historically represent the most important reservoir of infection, an increasing number of studies suggests that leishmaniasis also affect many other mammalian and avian species.

Domestic animals, in particular cats, pose a concern because of close contact with humans (Cardoso et al., 2021).

1.4 *Leishmania* Morphology and Life Cycle

The life cycle of *Leishmania* is digenetic and it involves two different hosts: mammalian and insect (Figure 5). The insect vector is the sandfly belonging to the *Phlebotomus* genus in the Old World and *Lutzomyia* genus in the New World (Sasidharan and Saudagar, 2021). During its life cycle, *Leishmania* undergoes important morphological changes depending on the environmental conditions present in the two hosts (Figure 6). In the vector stage, *Leishmania* is in the promastigote form. Promastigotes are flagelled and motile. The body measures 15-20 µm in length and 1.5-3.5 µm in width. The flagellar length is around 15-28 µm and helps the parasite attach to the gut of the sandfly (Sasidharan and Saudagar, 2021).

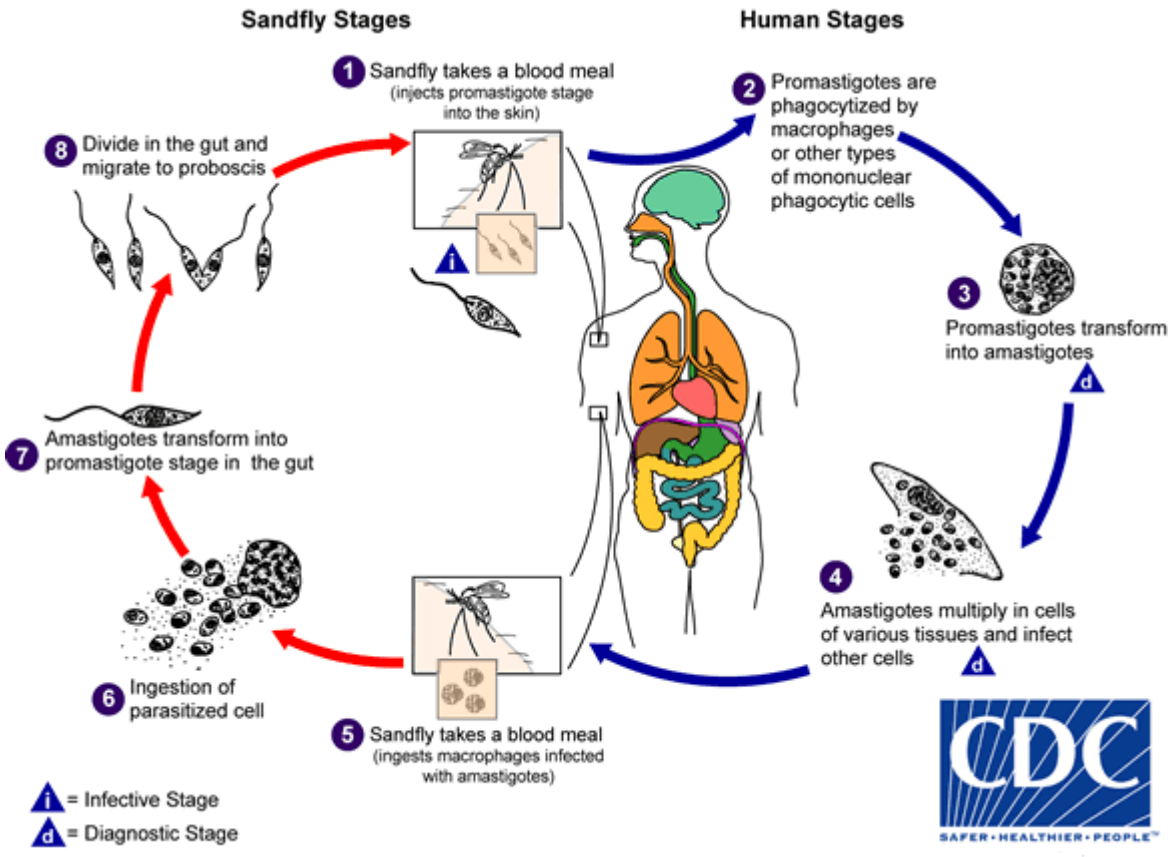

[Figure 5] Life cycle of *Leishmania* parasites (https://www.cdc.gov/dpdx/leishmaniasis/index.html)

The *Phlebotomus* gets infected after a blood meal from an infected host. Once in the insect, the parasites transform into the procyclic promastigotes, the replicative, but not infective for mammals' stage. This form divides in the sandfly's gut (in the hindgut for

parasites of the *Viannia* subgenus; in the midgut for the *Leishmania* subgenus). Subsequently, the procyclic promastigotes differentiate into the metacyclic promastigotes (the non-dividing form, infective for mammals) which migrate to the insect's proboscis.

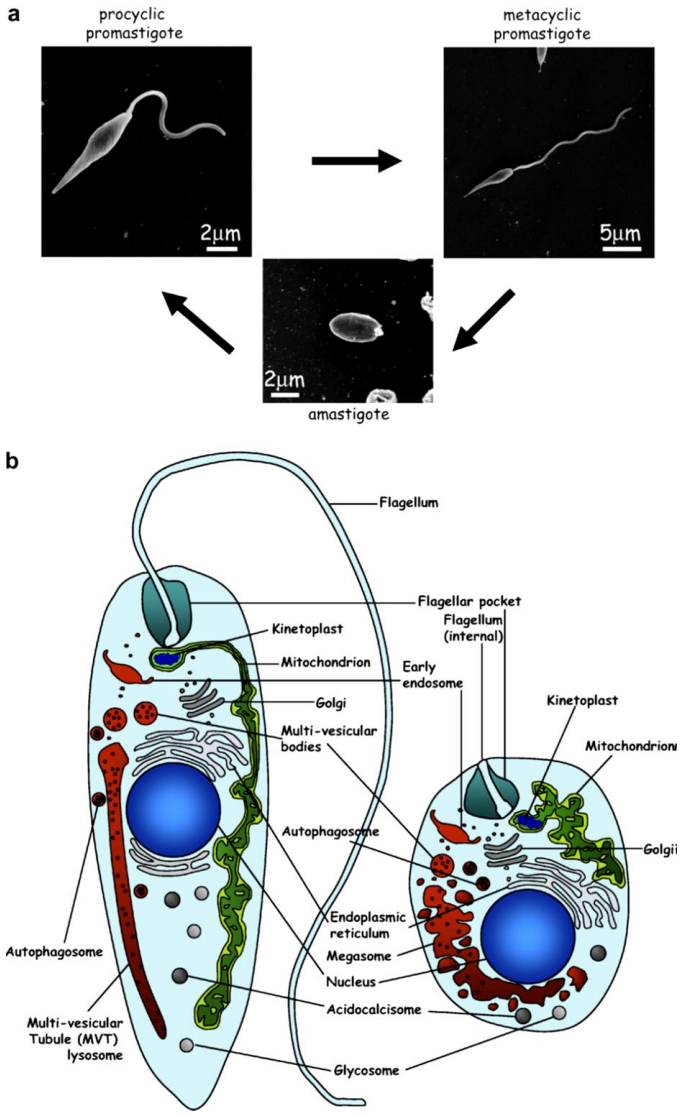

[Figure 6] Morphological *Leishmania* changes during its life cycle. (a) Scanning electron microscope images of the main *Leishmania* life cycle stages (b) Schematic representation of the main intracellular organelles of the *Leishmania* forms: promastigote (left) or amastigote (right).
(Besteiro et al., 2007)

This part of the life cycle is called metacyclogenesis and occurs in 7-10 days from the byte of the sandfly and the transmission to the mammalian host (Gossage et al., 2003). Following sandfly bite, the metacyclic promastigotes are phagocyted mainly by the

host's macrophages and infect the parasitophorous vacuole. Here the promastigotes change in the amastigote form. The amastigotes are unmotile, ovoid and it measures 2-4 µm in diameter. It's interesting to observe how the parasites can survive passing through different environments and conditions (changes in the availability and type of nutrients, temperature, oxygen, pH). *Leishmania* developed highly specialized and adapted forms, characterized by different nutritional needs, growth rate, expression of surface molecules and morphology. The amastigotes proliferate inside the parasitophorous vacuole until the macrophage ruptures and the release of all mature amastigotes in the surrounding tissues leading to a progressive infection. This situation can evolve to one of the clinical manifestations: the parasites infect cells nearby the inoculation site (CL), they spread to the mucous membranes (MCL), or they reach organs particularly rich in macrophages and histiocytes, such as liver, spleen, and bone marrow (VL).

1.5 *Leishmania* Genome

1.5.1 Genome Organisation

The trypanosomatids had separated very early from the rest of eukaryotes, which resulted in the development of cellular and molecular mechanisms and gene organization and expression unique to this group (Cavalier-Smith et al., 2014). In the past years, these differences have been investigated to better understand the pathogenesis and find potential targets for disease treatment (Maslov et al., 2018). First, it is not easy to define the ploidy of *Leishmania* parasites. This is due to the different evidence that shows that the parasite is subject to a natural aneuploidy (Mannaert et al., 2012). For example, according to some studies, *L. (V.) braziliensis* is predominantly triploid with some tetrasomy, as well as having a pentasomic chromosome (Chr. 31); in other strains, on the other hand, a more variable degree of ploidy is observed. This characteristic could represent an advantage in terms of adaptability to environment changes (different hosts, drugs selectivity pressure).

In general, Old and New World *Leishmania* species differ in the number of chromosomes: the Old World *Leishmania* karyotype is composed of 36 chromosomes, while the New World species, *L. (V.) braziliensis*, and *L. (L.) mexicana*, consist of 35 and 34 chromosomes, respectively, because of the fusion of some chromosomes (Real et al., 2013). Specific studies on the *L. (L.) major* genome defined in 32.8 megabases (MB) the dimensions of the nuclear genome organized in the 36 small chromosomes which, in turn, have an extension between 0.28 and 2.8 MB (Ivens et al., 2005), with over 8,200 coding genes and 97 pseudo-genes (Peacock et al., 2007). The genome is completely lacking introns and the genes are arranged as same-strand tandem arrays that may include up to hundreds of genes. These structures are like bacterial operons, but unlike them, trypanosomatid genes within the same cluster are not functionally related but seem to be arrayed randomly.

In addition, *Leishmania* (and the *Trypanosomatidae*) has attracted molecular biologists for the particular mechanisms of gene expression, such as polycistronic transcription, trans-splicing and RNA editing.

1.5.2 Gene Trascription

Most organisms control the gene expression at the early transcription level although regulation of gene expression can also be achieved during the elongation phases of the primary transcript, through the stability or transport of the RNA or in the translation phase. Although *Leishmania* is a eukaryotic organism, its mRNAs have a polycistronic origin, and the expression of genes is mainly regulated at the post-transcriptional level. The polycistronic transcriptional units are co-transcribed by polymerase II. The mature mRNA derives from a primary transcript that has undergone a particular splicing process, called trans-splicing, which is followed by polyadenylation (Clayton, 2002). The trans-splicing process was discovered in *Trypanosoma brucei* (Boothroyd and Cross, 1982), where a sequence of 39 nucleotides, defined spliced-leader sequence (SL) was discovered. This small sequence origins from a small RNA, defined SL RNA and transcribed by RNA polymerase II. The trans-splicing mechanism (Figure 7), presents in all *Trypanosmatidae*, is achieved through two successive transesterification reactions and the formation of a Y-shaped structure, unlike the ring structure found in other splicing processes. Although trans-splicing was first described in *Trypanosomes*, it has subsequently also been found in nematodes, flukes, euglenoids, and in chordates (Liang et al., 2003).

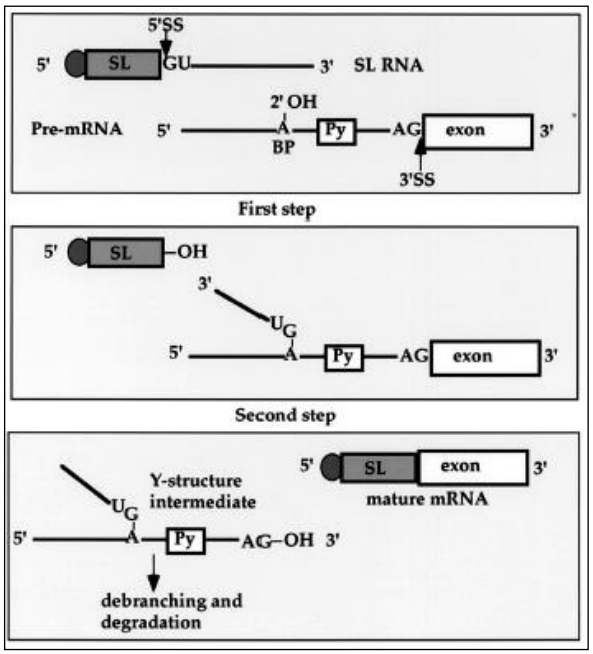

[Figure 7] Schematic representation of the SL RNA trans-splicing mechanism (Liang et al., 2003)

1.5.3 Kinetoplast DNA Organization

As already mentioned, *Leishmania* belongs to the order *Kinetoplastida*. The name derives from the presence of the kinetoplast at the flagellum base. The kinetoplast represents the unique and complex mitochondrion. This mitochondrion contains an abundant compact mass of mitochondrial DNA called kinetoplast DNA (kDNA). It was discovered in *L. tarantolae* (a species not pathogenic to humans) in the 1970s. Kinetoplast DNA is made of thousands of small circular DNA molecules, called **minicircles**, all linked together to form a network of DNA. Associated with this network, a small number (20-50) of larger circular molecules, defined as **maxicircles**, was also identified (figure 8) (Simpson and da Silva, 1971). The size of minicircles is specie-specific and varies from 460 to 2500 base pairs (bp) but contain different sequences even within the same network. Minicircles do not encode information for protein synthesis but replicate very actively. In contrast, the maxicircles, whose sizes vary from 23,000 to 30,000 bp in different species, carry information for mitochondrial proteins and mitochondrial rRNAs.

Although the minicircles of most species are heterogeneous in sequence, a common feature of their organization is the presence of at least one constant region of about 100-200 bp and a larger variable region (Jasmer and Stuart, 1986). In the *Leishmania* genus there is only a constant region of about 200 bp with a variable region of about 700 bp (Ponzi et al. 1984; Sugisaki et al., 1987). The function of these conserved regions is linked to the replication mechanism of the minicircles themselves (Simpson, 1997).

In the maxicircles there are genes coding for two rRNAs, some structural genes as well as some cryptic genes (Simpson, 1997). This term indicates the presence of a gene that could not be encoded unless a post-transcriptional modification, defined as RNA editing (Benne et al., 1986). Consequently, the mRNA regions, which need to be edited, are defined as pre-edited regions. The editing process consists in adding or subtracting some residues of uridine (U) to the mRNA transcript to obtain the mature form (Aphasizhev and Aphasizheva, 2011). In fact, without adding these residues, the correct mRNA translation is not possible. The editing process is mediated by small RNA molecules called guide RNA (gRNA) which are characterized by a tail of 13 residues of U at the 3' end (Simpson, 1997). Although the information for the gRNA synthesis can also be contained in the maxicircles, the greatest number of them is transcribed from the variable regions of the minicircles.

The minicircles network is an attractive diagnosis and genotyping target. As already know, it presents a variable region that could be exploited to design assays to species differentiation, not only in terms of sequence but also following the difference minicircle class abundance. This aspect is better explained below in some work published by our group (Ceccarelli et al., 2014; Ceccarelli et al., 2017; Ceccarelli et al., 2020; Diotallevi et al., 2020).

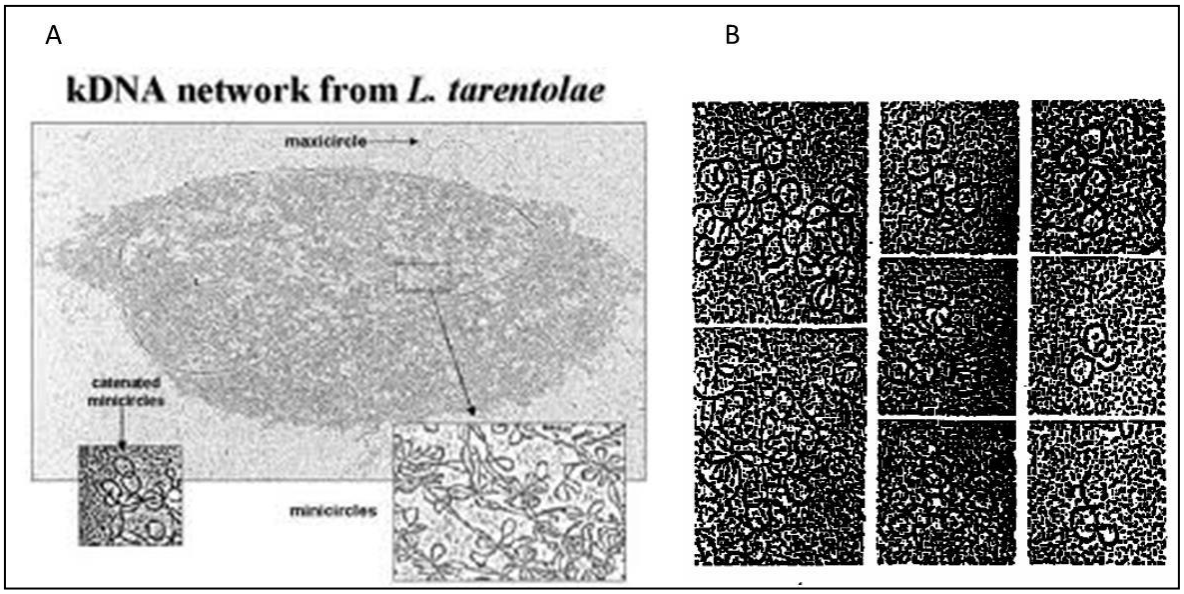

[Figure 8] Minicircles network A: minicircles and maxicircles network
B: Minicircles concatenation detail (adapted by Simpson and da Silva, 1971).

1.6 Pathogenesis

As already mentioned, macrophages are the host's cells mainly affected by the parasites. Differently from other parasites, *Leishmania* developed various strategies to infect cells and to survive and replicate in the macrophage's hostile environment. Understanding these mechanisms and the host immune response following infection is important to determine the clinical outcome and to identify novel drugs targets.

1.6.1 Early Infection Stages

Immediately after the vector bite and the promastigotes inoculation, macrophages, and neutrophils are rapidly recruited to the site of the bite (Peters et al., 2009). This is due to the proteophosphoglycans secreted by the parasites in the sand fly's midgut and inoculated into the host during the blood meal (Rogers et al., 2009; Rogers et al., 2010). Initial interaction between the promastigotes and the macrophages occurs through the parasite flagellum, leading to the release of intracellular survival factors by the parasite and subsequent modulation of macrophage phagocytic activity (Rotureau et al., 2009). *Leishmania* parasites interact with different macrophage receptors, including complement receptors (CRs), mannose receptors, fibronectin receptors and Fcγ receptors (FcγRs) (Ueno and Wilson, 2012). This choice depends on the *Leishmania* species and can influence the infection development. CR-mediated uptake may create favorable conditions for the parasite inhibiting inflammation, superoxide burst, and accumulation of the lysosomal markers LAMP1 and Cathepsin D; mannose receptor signaling may trigger inflammatory pathways and more efficient delivery of hydrolytic enzymes into the phagolysosome. FcγR-mediated phagocytosis leads to enhanced activation of NADPH oxidase on the newly formed phagosome (Ueno and Wilson, 2012). Following recognition at host cell surface, promastigotes can be internalized via caveolae that are composed of cholesterol-rich membrane lipid microdomains (Rodriguez et al., 2011). Moreover, the parasite internalization depends on actin-mediated uptake, and the integrity of the actin cytoskeleton of the host macrophage has been shown to be essential for *L. donovani* infectivity (Roy et al., 2014).

1.6.2 From Promastigotes to Amastigotes

Inside the host's macrophages, the promastigotes are internalized into the parasitophorous vacuole (PV) and transformed to amastigotes. Some authors proposed that, at this stage, some lysosomes may fuse with the PV and promote promastigote-to-amastigote differentiation (Forestier et al., 2011). The differentiation depends on the temperature increase and pH decrease. It was shown that the iron uptake and subsequent generation of hydrogen peroxide by *L. amazonensis* has an impact on parasite differentiation (Mittra and Andrews, 2013; Mittra et al., 2013). Iron mediates generation of reactive oxygen species (ROS), which are normally deleterious for pathogens, in this case, it was proposed to act as a signaling molecule regulating parasite differentiation. In fact, the *Leishmania* iron transporter LIT1 mediates iron acquisition by the parasite, which leads to parasite growth arrest and differentiation. Moreover, the differentiation is associated with a reduction in growth rate and the induction of a distinct metabolic state characterized by a decrease in uptake and utilization of glucose and amino acids, reduced organic acid secretion and increased fatty acid beta-oxidation. Catabolism of hexose and fatty acids provides substrates for glutamate synthesis, which is essential for amastigote growth and survival. These changes allow amastigote survival in the nutrient-poor intracellular environment (Podinovskaia and Descoteaux, 2015). Both promastigotes and amastigotes are able to divert the classical phagosome maturation pathway, which occurs via a set of highly regulated fusion and fission events with vesicles including endosomes and lysosomes and form PVs of very specific phenotypes.

1.6.3 Intracellular Parasite Growth

Once the infection within the macrophages has been established, *Leishmania* needs nutrients and additional membrane for phagosome expansion. For this reason, the PVs are highly dynamic organelle and interacts with the secretory pathway, which contains endoplasmic reticulum (ER) proteins destined for other organelles (Canton and Kima, 2012). Furthermore, intracellular parasites have complex nutritional needs that could limit the parasite's long-term survival within macrophages. The parasite can achieve some of its nutritional needs through the fusion of PV with ER-derived endosomes and

vacuoles (Ndjamen et al., 2010). Metabolites important to the parasite include hexoses, amino acids, polyamines, purines, vitamins, sphingolipids, heme and cations (i.e. Fe^{2+}, Mg^{2+}). Additionally, lipid bodies (LBs) in the macrophage can meet some of its nutritional requirements. LBs are organelles with a neutral lipid core mainly triacylglycerol and sterol esters, which can serve as nutrient sources for parasites. Therefore, the interaction between LB and PV can play a role in the maturation of phagosomes (Melo and Dvorak, 2012). Among all, iron represents an essential element for the growth and survival of *Leishmania*, the acquisition of which is favored by the ferric reductase LFR1, the ferrous iron transporter LIT1 and the heme transporter LHR1. In conclusion, *Leishmania* interacts with different intracellular components of the macrophage in order to guarantee all the elements needed for its growth and survival.

1.6.4 Macrophages Defenses

The macrophage is an extremely plastic cell, which encapsulates and digests dead cells and cell debris, foreign bodies, cancer cells and, most importantly, plays a central role in regulation of inflammation. There are several mechanisms through which the macrophage can respond to the presence of the parasite: to activate the classical cell-mediated response (Th1) through the synthesis of IFN-γ that leads to inflammatory state and inhibits *Leishmania* growth or, alternatively, the immune-mediated activation (Th2) that decreases inflammation through IL-10 production and stimulates the growth of *Leishmania* (Figure 9) (Liu and Uzonna, 2012).

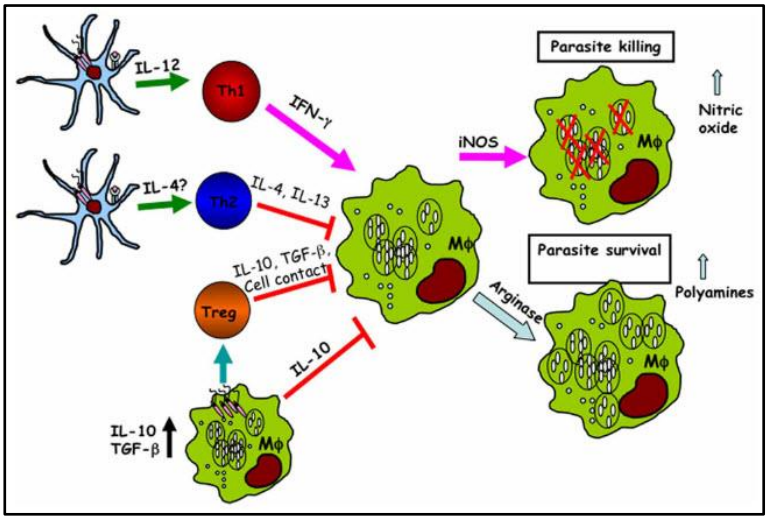

[Figure 9] Macrophages response following *Leishmania* infection (Liu and Uzonna, 2012).

Additionally, one of the main mechanisms used by macrophages to neutralize pathogens is the generation of oxygen free radicals (ROS) and reactive nitrogen intermediates (RNI). The assembly of NADPH oxidase in the *Leishmania*-containing phagosome stimulates ROS and superoxide production in the phagosomal lumen indicating an effort by macrophage defense mechanisms to induce oxidative damage to the parasite and compromise its survival capacity (Podinovskaia and Descoteaux, 2015).

1.6.5 Leishmania Evasion of *Host Defenses*

Once the infection is established, the parasite can modulate the host's response by altering the normal macrophages activation. Some of these mechanisms are summarized in Table 2 taken from the review of Podinovskaia and Descoteaux published in 2015 (Podinovskaia and Descoteaux, 2015). These modulation pathways will be briefly discussed below.

Macrophage defense	Molecular mediators targeted for evasion	Mechanism(s)	*Leishmania* factor(s)
Inflammation	IL-12	Activation of PTPs (PTP1B, TC-PTP, PTP-PEST, SHP-1)	GP63, CPB, LPG
	TNF		
	Phagolysosomal maturation		
	MHC II presentation		
	TLR4 signaling	↓ TRAF3 ↓ neutrophil elastase	ISP
	IL-17	Unknown	Unknown
	IL-6	↓ Protein Kinase R	ISP
Classical activation	iNOS	↑ PPAR-γ	Unknown
Oxidative damage	ROS	↓ mitochondrial UCP-2	Unknown
	ROS	↓ NADPH oxidase assembly	LPG, GP63
	NO	↑ autophagy, ↑ PPAR-γ	Unknown
Immune recognition	MHC II presentation	lipid microdomain disruption	GP63, LPG
	MHC I presentation	↓ VAMP8 ↓ NADPH oxidase	GP63

[Table 2] *Leishmania* evasion mechanisms and intracellular survival factors (Podinovskaia & Descoteaux, 2015).

1.6.5.1 Limitation Of The Inflammatory Process

During the parasite's inoculation by the vector, the secretory gel produced by the parasite, rich in proteophosphoglycans, intensifies the alternative activation by IL-4, which inhibits inflammation through the production of IL-10 and arginase upregulation, which favors the biosynthesis of polyamines, essential for cell proliferation and differentiation; therefore, it promotes the parasite survival in host macrophages (Rogers et al., 2009). The production of lipophosphoglycans (LPS) after murine peritoneal macrophages infection with *L. amazonensis*, leads to IL-12, IL-17 and IL-6 synthesis suppression. Some studies show that parasites induce host PPARγ expression, known as a repressor of inflammation, to protect host from excessive damage. *Leishmania* also induces protein tyrosine phosphatase (PTP) that leads to the reduction of inflammatory processes, the reduction of IL-12, NO, TNF, the phagolysosomal maturation and MHC class II antigen presentation (Liu and Uzonna, 2012; Gomez and Olivier, 2010). TRAF3 is another identified target of *L. donovani* promastigotes. Moreover, infected

macrophages are defective in the expression of activation-associated functions and are not responsive to IFN-γ (Shio et al., 2012).

1.6.5.2 Avoiding Oxidative Damage

ROS production could be critical to the host cells and, indirectly, to the parasite. *Leishmania* responses to oxidative stress depend on the species and host cell type (Olivier et al., 2012). A mechanism used by *L. donovani* amastigotes to impair cellular and mitochondrial ROS production is the induction of mitochondrial uncoupling protein 2 (UCP2) (Ball et al., 2014). *Leishmania* is also able to avoid oxidative damage by preventing NADPH oxidase assembly at the phagosomal membrane and the generation of ROS within the PV. Oxidative damage by ROS induces macrophages apoptosis, destroying the parasite's replicative niche. As such, apoptosis was found to be suppressed by *L. donovani* promastigotes in RAW 264.7 macrophages through the induction of the cytokine signaling suppressors, SOCS1 and SOCS3 (Srivastav et al., 2014).

1.6.5.3 Antigen Presentation

Antigen presentation is a critical phase of the immune response to pathogens. It involves the presentation of foreign proteins derived from the phagocytic process, cargo on MHC class I for subsequent detection by cytotoxic $CD8^+$ T cells and orchestration of a systemic immune response. As an antigen-presenting cell (APC), the macrophage participates in this process. Leishmania evades host immunity by inhibiting antigen presentation by cleavage of the SNARE VAMP8. Disruption of VAMP8 prevents NADPH oxidase assembly leading to more efficient phagosomes acidification and proteolysis, thereby inhibiting antigen presentation and T cell activation (Matheoud et al., 2013; Rybicka et al., 2012; Savina et al., 2006). Inhibition of antigen presentation was also achieved through the disruption of membrane lipid microdomains by the parasite (Chakraborty et al., 2005).

1.6.5.4 Intracellular Survival Factors

It has been shown that *Leishmania* has many surface molecules involved in the parasite protection from oxidative damage and phagolysosome proteolytic activity. Other survival factors are secreted and interact directly with the macrophage proteins, modulating the biogenesis of the phagosome, the host's defense mechanisms and the inflammatory process. Among these molecules, the most studied are lipophosphoglycans (LPG), zinc-dependent metalloprotease GP63 and glycosylinositol phospholipids (GIPLs), which are membrane-associated; while cysteine proteases (CPs) and secreted acid phosphatases (SAPs) are released through the flagellar pocket as virulence co-factors. Promastigotes can release exosomes into the extracellular environment to modulate macrophage activity. The exosome content is affected by external conditions, such as temperature and pH. The release of the exosome is up-regulated at 37°C and at low pH, the conditions that parasite encounters, following inoculation by the phlebotomine, in the mammalian host (Silverman et al., 2010).

1.6.5.5 Unfolded Protein Response

The endoplasmic reticulum (ER) is an organelle involved in several intracellular functions: synthesis, modification, folding and proteins transport, lipids and sterols synthesis, calcium storage and carbohydrates metabolism (Galluzzi et al., 2017). The ER physiological state can be altered in many conditions (i.e., imbalance in folding capacity, nutrient depletion, oxidative stress, hypoxia, calcium ion imbalance). To restore ER homeostasis and ensure cell survival, a process called the endoplasmic reticulum stress response or unfolded protein response (UPR) is activated. The initial aim is to compensate the damage by transcribing genes able to remove unfolded proteins. Despite this, when the ER stress is excessive and prolonged, apoptosis is induced.

In mammals, three ER transmembrane proteins are responsible for this process, which activate three signaling pathways that work in parallel: PERK (PKR-like endoplasmic reticulum kinase), IRE1 (inositol-requiring enzyme 1) and ATF6 (activating transcription factor 6). The activation of PERK and IRE1 occurs by dimerization and autophosphorylation, while ATF6 translocates into the Golgi apparatus where is activated through proteolytic cleavage.

Once activated, IRE1 causes a spincing reaction leading to the removal of 26 nucleotides from the XBP1 mRNA, generating the XBP1 spliced form (XBP1s), a transcription factor. XBP1s induces the expression of chaperones and proinflammatory cytokines (Martinon et al., 2010), proteins involved in the ERAD system (ER-associated degradation), in lipid synthesis and autophagy (Margariti et al., 2013). Under persistent stress conditions, IRE1 can also contribute to the degradation of mRNAs located in the ER membrane through a process known as IRE1-dependent decay (RIDD) (Kimmig et al., 2012). RIDD helps maintain ER homeostasis but, following prolonged stress, induces apoptosis (Maruel et al., 2014). Furthermore, IRE1 recruits TRAF2, which phosphorylates IκB by activating NF-κB, involved in the inflammatory response (Hu et al., 2006).

PERK phosphorylates the α-subunit of eIF2α, inducing a general translation and protein load reduction in the ER. Nevertheless, the transcription factor ATF4 evades translation inhibition through an alternative translation initiation site and induces the expression of the transcription factor DDIT3/CHOP and GADD34, a phosphatase that regulates the phosphorylation of eIF2α (Novoa et al., 2003). Furthermore, PERK induces the expression of genes related to the antioxidant response by the phosphorylation of the transcription factor NFE2L2 / NRF2 (Cullinan and Diehl, 2004).

ATF6 is a transmembrane protein containing a bZIP domain at the N-terminal. Under ER stress conditions, ATF6 is translocated into the Golgi apparatus, and it undergoes proteolytic cleavage, releasing the transcriptionally active N-terminal portion. The latter induces the transcription of XBP1 and contributes to the UPR.

Some studies revealed a correlation between *Leishmania* infection and UPR. It has been shown that infection of RAW 264.7 macrophages by *L. amazonensis* activates the IRE1-XBP1 branch in a TLR2-dependent manner leading to the expression of INF-β, involved in the pathogenesis (Vivarini et al., 2011). Furthermore, XBP1s is required for the HO-1 gene expression, an antioxidant that inhibits ROS production. These results suggest that activation of the IRE1-XBP1 branch plays a role during the infection by increasing IFN-β expression and protecting parasites from oxidative stress, thus promoting their survival and proliferation (Dias-Teixeira et al., 2016). Galluzzi et al. demonstrated that *L. infantum* infection is associated with a mild UPR response in both human and mouse macrophages. This response involved the up-regulation of various target genes related

to the ER stress process (CHOP, HSPA5, ATF3, ATF4, CEBPB, MAP1LC3B) (Galluzzi et al., 2016). The PERK/eIF2α/ATF4 pathway is known to play a key role in the regulation of autophagy. Indeed, MAP1LC3B, a gene essential for the autophagic process, can be induced by ER stress through ATF4 (B'chir et al., 2013). Although severe or prolonged ER stress is known to induce cell death, a slight level of stress can be beneficial to cells as it causes mild (adaptive) UPR and increases resistance to the next episode of stress. This process, called hormesis (Mollereau et al., 2014) is linked to the PERK-ATF4 and IRE1-XBP1 branches. Activating this process, *Leishmania* parasites could be able to survive and adapt within host macrophages.

1.6.5.6 Micro-RNA and *Leishmania* Infection

Micro-RNAs (miRNAs) are short single-strand non-coding RNAs (22-23 nucleotides) that regulate mRNA at the post-transcriptional level. They are synthesized inside the nucleus as primary transcripts, defined pri-miRNAs, which are folded in a hairpin structure composed of 70 nucleotides. They are coupled with Drosha RNase and DGCR8 leading to the formation of a second precursor, called pre-miRNA. The pre-miRNA is transferred into the cytoplasm through the Exportin 5 and processed by the Dicer which converts them into the mature form. The mature miRNA is loaded into the RNA-induced silencing complex (RISC) comprising the Argonaute (AGO) and TRBP proteins (Kim et al., 2009). At this point, the miRNA is able to recognize the target mRNA exploiting a small sequence located in position 2-7 at the 5' end of the miRNA, called "seed sequence", complementary with the mRNA (Lewis et al., 2005). MiRNAs are mostly considered negative post-transcriptional regulators (Fabian et al., 2010). A single miRNA could identify numerous target mRNAs and, at the same time, a single mRNA could be recognized by several miRNAs (Peter, 2010).

In the last years, several studies demonstrated how *Leishmania* infection induces alterations in human, murine, dog macrophages and dendritic cells miRNA profile, modifying the immune response against parasites (Acuña et al., 2020). Some miRNAs modulated during infection are implicated to macrophages polarization: miR-146 and miR-210 are related to M1 macrophages phenotype (Th1, pro-inflammatory response); miRNA-130a, miRNA-130b, miRNA-155, miRNA-21, miRNA-19a, miRNA-23a, miRNA-

125a, miRNA-125b, miRNA-26a, miRNA-26b, and miRNA-720 are related to M2 phenotype (Th2, anti-inflammatory response) (Li et al., 2018). *L. donovani* infection, downregulates miR-122 resulting in L-arginine depletion and parasites burden in mouse liver (Gosh et al., 2013). Furthermore, it has been shown that the induction of miR-30a-3p expression during *L. donovani* infection induces a decrease in the infectivity of the parasite by inhibiting autophagy through the negative regulation of Beclin 1 (BECN1) in THP-1 cells and primary human macrophages (Singh et al., 2016). Several groups identified miRNAs dysregulation connected with NO production: miR-294-3p and miR-721 were upregulated following *L. amazonensis* in BALB/c-BMDM (Muxel et al., 2017); miR-30e and miR-302d interfered with Nos2 mRNA expression, while miR-294 and miR-302d regulated Tnf mRNA levels and miR-294 altered Ccl2/Mcp-1 mRNA (Fernandez et al., 2019). In our previous work, we showed that *L. infantum* infection in human U937 and THP-1-derived macrophages upregulates miR-346 leading to the mRNA level decreasing of MHC class I and II genes, TAP1, RFX1 and BCAP31 (Diotallevi et al., 2018). Regarding *L. major*, it was observed the upregulation of various microRNAs, including miR-9, miR-132, miR-155, miR187 and miR-146a related to the control of TLR-receptor signaling, suggesting that these microRNAs are negative regulators of inflammatory response. Similarly, the induction of let-7a, miR-25, miR-26a, miR132 and miR-140 in human macrophages infected with *L. major* showed downregulation in the chemokine targets expression, including CCL2, CCL5, CXCL10, CXCL11 and CXCL12, inhibiting macrophages stimulation (Guerfali et al., 2008; Bazzoni et al., 2009; Lemaire et al., 2013). On the other hand, Geraci and colleagues reported let-7a, let-7b, and miR-103 upregulation in DCs and macrophages infected with *L. donovani*, but downregulated in *L. major* infections (Geraci et al., 2015). It has also been shown that the expression of miR-361-3p and miR-140-3p resulted significantly induced in skin lesions generated following *L. braziliensis* (Lago et al., 2018). *Leishmania* infection can also modify antigen presentation by deregulating the host's autophagy systems. The miRNAs miR-101c, miR-129-5p, miR-155, and miR-210-5p were related to the activation of the autophagic machinery and interfere with parasite clearance (Frank et al., 2015). Tiwari and colleagues identified 85 miRNAs whose expression was altered in macrophages infected with *L. donovani*. The in-silico analysis revealed the importance of 10 of these miRNAs

implicated in the survival of the parasite through the dysregulation of genes essential for the macrophage response to infection. MiR-6540, related to macrophage-parasite recognition, and miR-328, which regulates phagocytosis and phagocytic vacuole formation, were down-regulated. MiR-3473f, miR-763 and miR-8113 have been seen to be associated with the negative regulation of the apoptotic process, hampering normal macrophage activation functions. MiR-6996, involved in the immune response was up-regulated. MiR-3473f and miR-8113 appeared to be involved in switching from Th1 to Th2 response; furthermore, the first is linked to the inhibition of autophagy. MiR-6973a is associated with the biosynthesis of IL-12, a key molecule in the regulation of the immune system and essential for the activation of the Th1 response. MiR-3620 collaborates with the parasite in iron intake, and, together with miR-6385, regulates hypoxia. Finally, miR-763, miR-1264, and miR-3473f are implicated in the drug response mechanism. These results underline the importance of miRNAs in regulating the macrophage response during infection. Furthermore, they could be used as biomarkers to distinguish the various disease stages (infections in remission, symptomatic and asymptomatic) and be targets of new pharmacological strategies (Tiwari et al., 2017). In summary, these data appear to be quite heterogeneous and dependent on the cellular model, the *Leishmania* species, or the conditions of infection. Some of these results are summarized in Table 3 extracted from the review of Paul et al. (2020).

Leishmaniasis	*L. major*	miR-9 ↑	NFKB1	Control TLR-receptor signaling	Macrophages
		miR-132 ↑			
		miR-155 ↑	Myd88 and TRIF		
		miR-187 ↑	Unknown		
		miR-146a ↑	TRAF6, IRAK1		
		let-7a ↑	CCL2, CCL5, CXCL10, CXCL11, and CXCL12	Inhibits macrophages stimulation	
		miR-25 ↑			
		miR-26a ↑			
		miR-132 ↑			
		miR-140 ↑			
	L. braziliens	miR-361-3p ↑	TNF, GZMB, and FLG2	Worsening of tissue damage	Skin biopsies sample
		miR-140-3p ↑	NKG7		
		miR-193b ↓	CD40	Regulation of inflammatory response	
		miR-671 ↑	TNFR		
	L. infantum	miR-210 ↓	Procaspase-3	Inhibition of cell apoptosis	Macrophages
		miR-346 ↑	TAP1, RFX1, and BCAP31	Modulation of an immune response	
	L.donovani	miR-21 ↓	SMAD7	Regulation of TGF-β signaling	Monocytes
		miR-146b-5p ↑	TRAF6		
		miR-30a-3p ↑	BECN1	Inhibition of autophagic mechanism	Monocytes and macrophages
		miR-122 ↓	DICER1	Alteration of lipid metabolism	Huh7 cells

[Table 3] Relevant miRNAs involved in *Leishmania* infection (Paul et al., 2020)

1.7 Clinical Manifestations

As already described, there are three main forms of the leishmaniasis disease: CL, VL and MCL. The clinical manifestations are, generally, related to *Leishmania* species. There are two other rare types of the disease called diffuse cutaneous leishmaniasis (DCL) and post kala-azar dermal leishmaniasis (PKDL) (Sasidharan and Saudagar, 2021). The species responsible for the different symptoms, are summarized in Table 4. Among the three main forms, VL is the most severe and lethal type.

Causative species	Disease form	Geographical distribution
L. donovani	VL, PKDL	India, Nepal, Bangladesh, Sri Lanka, East Africa.
L. infantum	VL, PKDL	Mediterranean Basin, central and west Asia, Venezuela.
L. chagasi[*]	VL	Argentina, Bolivia, Brazil, Colombia, El Salvador, Guadeloupe, Guatemala, Honduras, Mexico, Nicaragua, Paraguay, Venezuela.
L. archibaldi[**]	VL	Sudan, East Africa
L. major	CL	North Africa, central and west Asia.
L. tropica	CL	Central and west Asia, western India.
L. aethiopica	CL, DCL	Ethiopia and Kenya.
L. braziliensis	CL, MCL	Argentina, Belize, Bolivia, Brazil, Colombia, Costa Rica, Ecuador, French Guyana, Guatemala, Honduras, Nicaragua, Panama, Peru, Venezuela.
L. amazonensis	CL, MCL, DCL	Bolivia, Brazil, Colombia, French Guyana, Paraguay.
L. mexicana	CL, DCL	Belize, Colombia, Costa Rica, Dominican, Ecuador, El Salvador, Guatemala, Honduras, Mexico, USA.
L. yucumensis	CL	Bolivia.
L. llanosmartini	CL, MCL	Bolivia.
L. guyanensis	CL, MCL	Brazil, French Guyana, Guyana, Venezuela.
L. lainsoni	CL	Brazil.
L. naiffi	CL	Brazil, French Guyana.
L. shawi	CL	Brazil.
L. colombiensis	CL	Colombia, Venezuela.
L. panamensis	CL, MCL	Colombia, Costa Rica, Honduras, Nicaragua, Panama.
L. aristedesi	CL	Panama.
L. peruviana	CL	Peru.
L. garnhami	CL	Venezuela.
L. pifanoi	CL	Venezuela.
L. venezuelensis	CL	Venezuela.

[Table 4] *Leishmania* species related with clinical manifestations and geographical distribution (Sasidharan and Saudagar, 2021).

1.7.1 Cutaneous Leishmaniasis

CL is the most common form of the disease. Although there are cases of diffuse cutaneous leishmaniasis and disseminated cutaneous leishmaniasis, usually CL refers to localized cutaneous leishmaniasis. Different *Leishmania* species cause CL in the Old and New world. *L. tropica, L. major*, and *L. aethiopica*, as well as *L. infantum* and *L. donovani* are the etiological agent of Old World CL; *L. mexicana* species complex (*L. mexicana, L.*

amazonensis, and L. venezuelensis) or the subgenus *Viannia [L. (V.) braziliensis, L. (V.) guyanensis, L. (V.) panamensis, and L. (V.) peruviana*], *L. infantum/L. chagasi* are responsible for New World CL. Cutaneous leishmaniasis is characterized by papules followed by nodules that can evolve to skin lesions with a raised border and central depression, which can be covered by scab or crust and lead to atrophic scars. This condition can persist for months, sometimes years and carries the disfiguration and stigmatization that remains even after the treatment. The evolution of the disease starts from the vector insect bite which, usually, is not perceived. The incubation period is generally 2-4 months but can range from a minimum of 10 days to 2 years. It's quite common for patients with localized cutaneous leishmaniasis to develop more than one primary lesion, on the same or different parts of the body. The progression of the disease evolves in five phases (Abdoli et al., 2017):

(i) Acute phase or initial inflammation: no epidermis changes
(ii) Silent phase: atrophic epidermis changes
(iii) Active phase: acute inflammatory response with nodular lesion
(iv) Ulcerative phase: inflammatory response with ulcerative lesion
(v) Healing phase: symptoms decreasing with epidermis remodeling

DCL is another form of CL with disfigurement resembling lepromatous leprosy (Sasidharan and Saudagar, 2021).

1.7.2 Mucocutaneous Leishmaniasis

An inadequate treatment of CL can evolve to MCL resulting in the parasites dissemination from the skin to the naso-oropharyngeal mucosa. The *Leishmania* species related to this form are belonging to the *Viannia* subgenus [especially *L. (V.) braziliensis* but also *L. (V.) panamensis* and sometimes *L. (V.) guyanensis*] but it also can be caused by *L. (Leishmania) amazonensis*. The lesions affect the oral-nasal as well as the pharyngeal cavity and cause extensive damage. If untreated, the disease can progress to ulcerative destruction of the naso-oropharyngeal mucosa and requires painful surgeries resulting in the disfigurement of the face.

1.7.3 Visceral Leishmaniasis

VL is usually caused by the species *L. donovani* and *L. infantum* and is characterized by the parasite's affection of the internal organs (particularly, spleen, liver, and bone marrow). VL is also called kala-azar, black fever in Hindi language, because of the black lesions observed in the body. The common VL symptoms are:

- Fever
- Cachexia: weight loss and muscle wasting
- Hepatosplenomegaly: enlargement of liver and spleen
- Pancytopenia: anemia, leukopenia, thrombocytopenia
- A high total protein level and a low albumin level, with hypergammaglobulinemia
- Lymphadenopathy

Additional symptoms are bleeding, headache, fatigue, myalgia, night sweating.

PKDL is a rare VL reoccurrence, even after 20 years after the first infection. This syndrome is characterized by skin lesions (such as macules, papules, nodules, and patches), typically first noticed on the face. According to Pandey et al., 50% of VL cases in Sudan and 5%-10% of VL cases in India tend to evolve to PKDL from 6 months to 2 years and sometimes even 10 years later VL treatment (Pandey et al., 2012).

Another emerging issue to prevent the disease is the HIV-VL co-infection due to the immune-compromised state of the patients. In the period 2014-2020, 3070 cases of VL-HIV co-infection have been reported from 42 countries (data from WHO).

1.7.4 Canine Leishmaniasis (CanL)

As already cited, dogs represent the main *reservoir* of infection for humans. CanL is mainly caused by *L. (L.) infantum* species and presents a complex range of clinical manifestations that occur simultaneously as visceral and cutaneous forms. The number of infected animals in Europe has been estimated at least 2.5/3 million cases with a seroprevalence in Italy in 2017 of 18.65%, but probably the cases are largely underestimated (www.salute.gov.it). The clinical manifestations are widely variable (Table 5), ranging from asymptomatic to polysymptomatic dogs and, in this case, it is

interesting to note that there is no clear correspondence between parasitic load and clinical symptoms (Geisweid et al., 2013).

Clinical manifestations
General
○ Generalized lymphadenomegaly
○ Loss of body weight
○ Decreased or increased appetite
○ Lethargy
○ Mucous membranes pallor
○ Splenomegaly
○ Polyuria and polydypsia
○ Fever
○ Vomiting
○ Diarrhea (including chronic colitis)
Cutaneous
○ Non-pruritic exfoliative dermatitis with or without alopecia
○ Erosive-ulcerative dermatitis
○ Nodular dermatitis
○ Papular dermatitis
○ Pustular dermatitis
○ Onychogryphosis
Ocular
○ Blepharitis (exfoliative, ulcerative, or nodular) and conjunctivitis (nodular)
○ Keratoconjunctivitis, either common or sicca
○ Anterior uveitis/Endophtalmitis
Other
○ Mucocutaneous and mucosal ulcerative or nodular lesions (oral, genital and nasal)
○ Epistaxis
○ Lameness (erosive or non-erosive polyarthritis, osteomyelitis, polymyositis)
○ Atrophic masticatory myositis
○ Vascular disorders (systemic vasculitis, arterial thromboembolism)
○ Neurological disorders

[Table 5] Main clinical symptoms related to CanL (Solano-Gallego et al., 2011).

Generally, the most frequent clinical symptoms are weight loss, alopecia, lymphadenomegaly (relates to the periscapular, popliteal and submandibular lymph nodes), lethargy, mucous membranes pallor, kidney disease (the principal cause of death), anemia, platelet disorders and a broad spectrum of skin lesions (exfoliative dermatitis, skin ulcers, fingertip lesions, skin depigmentations, periocular exfoliative alopecia) (Bourdeau et al., 2014). Moreover, an important clinical manifestation is given by a broad spectrum of ocular lesions (blepharitis and keratoconjunctivitis followed by chorioretinitis, uveitis, retinal detachment, cataract, glaucoma) which occur in 25% of cases (Peña et al., 2008). Regarding the pharmacological treatment, the pentavalent

antimonial drugs (organic salts of pentavalent antimony, meglumine antimoniate), allopurinol and miltefosine are the most commonly used.

1.8 Diagnosis

An accurate and reliable diagnostic method is pivotal for treatment choice and epidemiological studies. Leishmaniasis diagnosis is based on different methodologies including parasitological, immunological, and molecular assays. All of them have advantages and issues related to sensitivity, specificity, speed, accuracy, accessibility, ease to use, applicability, cost. For the assays, the ability to detect, quantify and discriminate *Leishmania* spp. in different clinical samples must be evaluated. The current methods need laboratories with specific equipment and qualified personnel (Akhoundi et al., 2017). Moreover, the most widely used tests are not able to discriminate all the species and are not suitable for areas endemic for several species. Cross-reactivity issues have been also reported. Because of the broad spectrum of clinical features and varieties of species involved in the disease development, a "gold standard" for *Leishmania* diagnosis is not available. The most common assays are described below.

1.8.1 Parasitological Methods

1.8.1.1 Microscopic Examination

Lesion biopsy smears for CL and aspirates of the spleen, bone marrow and lymph nodes for VL are examined under the microscope following Giemsa-staining (Akhoundi et al., 2013). This is a rapid and cheap but invasive approach because all tests need biopsy samples. Moreover, it does not allow species discrimination and the sensitivity is dependent on the parasite load as well as sample process and personnel technical skills. Nevertheless, it is a useful diagnostic approach for primary healthcare because of its cost-effectiveness and simplicity (Akhoundi et al., 2017).

1.8.1.2 Parasites Isolation

From the same samples used for cyto-histological investigations, it is possible to isolate *Leishmania* promastigotes for *in vitro* culture. Unfortunately, the parasites isolation is not easy to perform, it is time-consuming (at least one week) and relatively expensive since it requires specific media (such as Evans modified Tobie's, Schneider media)

(Berman, 1997). On the other hand, parasite isolation can be useful for DNA-based approach to discriminate *Leishmania* species.

1.8.2 Immunological Methods

Immunological methods are rapid, non-invasive and detect *Leishmania* antigens or antibodies in patients' samples (Kumari et al., 2021). However, these assays are not species-specific and are not indicated to evaluate follow-up, because the antibody titers tend to decrease too slowly even in the presence of clinical response to the treatment (Torres et al., 2010). Moreover, in some geographical areas cross-reactions with other protozoan are possible.

1.8.2.1 Indirect Fluorescent Antibody TEST (IFAT)

The test uses slides with fixed *Leishmania* cells (antigen) that will be put in contact with the serum (or plasma) samples. It is used in veterinary medicine for CanL diagnosis and in the clinic. Briefly, the antigen is incubated with serum scalar dilutions. After washes a secondary antibody conjugated with fluorescein isothiocyanate (FITC) is added. After further washing, the preparation is observed under a fluorescence microscope. In case of positivity, the promastigotes appear with a brilliant green fluorescence. This test has high sensitivity and specificity although cross-reactions with *Trypanosome* parasites have been reported (Coura-Vital et al., 2014). The need for proper laboratories and fluorescence microscopes remains a limitation.

1.8.2.2 Enzyme-linked Immunosorbent Assay (ELISA)

ELISA uses plates with antigens adhered in the wells. According to their nature, the antigens used can be classified into several groups: soluble extracts of promastigotes, soluble extracts of amastigotes, recombinant proteins, and purified proteins. If serum contains anti-*Leishmania* antibodies, they bind antigens. The antigen-antibody complexes' presence is highlighted by adding a secondary antibody conjugated with a specific enzyme, able to produce a colorimetric reaction that is read on the spectrophotometer. The sensitivity and specificity are generally high, but it depends on the antigen used which represents one of the main critical aspects. Moreover, is not

possible to distinguish between actual infection and recovery. In addition, the need for proper equipment and personnel represents a limitation to this technique.

1.8.2.3 Immunochromatographic Test (ICT)

ICT is a non-invasive and rapid screening test for VL using recombinant Kinesin-39 antigen (rK39) immobilized on nitro-cellulose paper. Briefly, serum, plasma or whole blood are mixed with a buffer containing conjugated antibodies. The mixture is loaded on the sample pad and flows through the membrane. If the antibodies are present in the patient sample, a colored line appears on the test line. It is useful for field purposes in endemic and non-endemic regions due to its low cost and minimum analysis time (10-15 minutes) (Karimi Kakh et al., 2020). Although the sensitivity and specificity are generally good, there are differences among varying populations: 90% and 100% in Brazil (Carvalho et al. 2003) and 100% and 93–98% in India, respectively (Sundar et al. 2002a, b). A study conducted in the Mediterranean showed the sensitivity of 78% in all VL patients (Bangert et al., 2018).

1.8.3 Molecular Methods

As already mentioned, the immunological and parasitological methods have some limitations regarding sensitivity, treatment relapse detection, cross-response, low antibody titers. In this view, the molecular methods sensibly improved the leishmaniasis diagnosis. They are characterized by high sensitivity and specificity, high-trhoughput, possibility of quantification, species discrimination. Different types of clinical samples can be analyzed: whole blood, plasma, serum, biopsy, cutaneous scrab, conjunctival swab. Although several molecular methods have been developed, PCR-based assays represent the gold standard of molecular diagnosis (Akhoundi et al., 2017).

1.8.3.1 Conventional PCR (cPCR)

Many *Leishmania* genomes have been entirely sequenced and are available in public databases (e.g. TRITRYPDB https://tritrypdb.org/tritrypdb/app/), allowing designing many assays for leishmaniasis diagnosis. Several targets can be exploited in this technique, i.e., ribosomal RNA (rRNA), internal transcribe spacer (ITS1), heat-shock proteins (hsp70), kDNA minicircles. A variant of this approach is **PCR-RFLP** (Restriction

Fragment Length Polymorphism), a method that detects variation in the pattern of DNA fragments produced by restriction enzyme digestion visualized by electrophoretic gel. Length and numbers of fragments can be used for *Leishmania* species discrimination, particularly when applied to ITS1 (Schönian et al., 2003). ITS1 region ranges from 50 to 350 bp and is located between the 18S rRNA and 5.8S rRNA genes. The ITS region between the two primers presents polymorphism that allows species typing.

Another application is **Nested-PCR** that uses two primer sets in two consecutive PCR. The second primer set is designed to recognize a sequence internal to the product obtained in the first amplification. The advantage is to reduce non-specific binding and obtain a product with little contamination from primer dimers (Akhavan et., 2010). However, due to the need to open the PCR tubes between the two PCR, the risk of contamination remains a downside of this method.

1.8.3.2 Real-time PCR or quantitative PCR(qPCR)

The qPCR can amplify and simultaneously quantify the target DNA molecule. It is a rapid quantification method with high sensitivity and reduced contamination risk because there is no requirement to open the reaction tubes. The amplified product can be visualized employing different chemistries, e.g. intercalant DNA dyes (SYBR Green I) or fluorescent probes (TaqMan). In previous works, we exploited **kDNA** minicircles to discriminate *Leishmania* subgenus from clinical samples using qPCR followed by high resolution melting (HRM) analysis. Since kDNA minicircles are present in thousands of copies per cell, they are an ideal target for highly sensitive *Leishmania* detection from biological samples with low parasite numbers (Ceccarelli et al., 2014). Several different subclasses of minicircles are present and their relative amount can vary among *Leishmania* species. This variability can be exploited to discriminate among species. Moreover, species discrimination could be achieved by HRM analysis that allow discrimination of amplicons differing in a single base. HRM measures changes in the fluorescence intensity of a DNA-intercalating dye during dissociation of double-stranded DNA to single-stranded DNA by a rising temperature of 0.1 °C each 2 sec. In this way, it is possible to distinguish species and/or population exploiting single nucleotide polymorphism (**SNP**). For example, Ceccarelli et al., (2018) developed a high-resolution

melt (HRM)-based assay exploiting the polymorphism 390T>G in the malic enzyme gene to rapidly differentiate the genotype 390T in *L. infantum* clinical isolates and clinical samples.

1.8.3.3 Multilocus Sequence Typing (MLST)

MLST is a method where multiple housekeeping genes are simultaneously amplified using PCR and subsequently sequenced. It is a great molecular typing method for phylogenetic research, epidemiological surveillance, and microbial population genetic structure analysis (El Kacem et al., 2021). This technique is used to evaluate genetic variability in *Leishmania* strains isolated in specific geographical endemic areas to perform epidemiological studies. MLST has allowed efficient discrimination between *L. braziliensis, L. guyanensis, L. naiffi* and *L. lainsoni* using four housekeeping genes (Boité et al., 2012). More recently was used to evaluate the genetic diversity of *L. tropica* in Morocco (El Kacem et al., 2021), of *Leishmania* strains isolated from atypical and typical CL patients from Iran (Hosseini et al., 2020) and among *L. donovani* isolates from a genetically homogeneous population in the Indian subcontinent (Banu et al., 2019).

1.9 Antileishmanial Treatment

The treatment available for leishmaniasis is based on few drugs. Historically, antimonials have been widely used in the treatment of this parasitosis, but now there are less toxic approaches, easier to administer or more effective even if more expensive. This is the case of liposomal formulation of amphotericin B, mostly used in human leishmaniasis. More recently, miltefosine, previously developed as an antineoplastic drug, resulted efficient as anti-*Leishmania* compound. Nevertheless, there are important limitations such as toxicities issues, administrations difficulties, high costs, efficacy decreasing, and the emergence of resistance strains. Because of all these reasons, the development of new therapies and the discovering of new targets is still a global challenge. In the following paragraphs, a brief description of the most frequently applied drugs and therapeutic protocols will be provided (Table 6)

Parameters	Chemical class	Mechanism of action	Mode of administration	Dosage regimen	Clinical application	Advantages	Disadvantages
Sodium Stibogluconate	Pentavalent antimonials	Inhibition of glycolysis, fatty acid oxidation, ATP and GTP synthesis	Intramuscular or intravenous or intralymphatic or intralesional	20 mg/kg daily for 20–30 days	Used as first-line anti-leishmanial therapy in South America, East Africa, and the Middle East with a cure rate of 35–95%. However, developed resistance in India	Budget-friendly, easily available, and intralesional route for CL showed reduced after-effects	Long treatment course, pain at the site of injection, cardiotoxicity, hepatotoxicity, and nephrotoxicity
Liposomal Amphotericin B	Polyene antibiotic	Pore formation in membrane or bind to ergosterol of cell membrane halting its synthesis	Intravenous	10–30 mg/kg total dose (single dose 3–5 mg/kg/ dose)	Indicated after treatment failure to antimonials. Valuable therapeutics against VL in India with an effective rate of cure >90%	Highly effective with decreased toxicity and a short course of treatment	Rigors and chills during slow infusion along with anaphylaxis, nephrotoxicity, hypokalemia
Miltefosine	Alkyl phospholipid	Modulate the cell surface receptors and alters sterol and phospholipid composition	Oral	1.5–2.5 mg/kg daily for 28 days	Recovery rate >90% in India and 60–90% in Africa but not effective as a single dose	Only oral drug available and effective in antimonials resistant cases	Long half-life, teratogenic, gastrointestinal disorders, nephrotoxicity and hepatotoxicity
Paromomycin	Amino-glycoside	Obstruct the machinery of protein synthesis as it binds to 30S smaller subunit of the ribosomal complex	Topical (CL) or intramuscular (VL)	20 mg/kg (17 days) or 15 mg/ kg (21 days)	Used for both CL and VL treatment. Cure rate >90% in India and 45–85% in Africa	Cost-effective and used in combination therapy	Pain at the site of injection, hepatotoxicity, nephrotoxicity, and ototoxicity

[Table 6] Overview of the drugs currently used to treat leishmaniasis (Kumari et al., 2021).

1.9.1 Pentavalent Antimonials

Antimonial compounds, applied in human and veterinary therapy, consist of organic salts of pentavalent antimony and have been the first-line drugs in the treatment of leishmaniasis for over 60 years (Ashutosh et al., 2007). These compounds are commercially available as sodium stibogluconate (Pentostam®) (figure 10a) and meglumine antimoniate, composed of pentavalent antimony and N-methyl-D-glucamine and available in Italy as an antimoniate of N-methylglucamine (Glucantime®). Although antimonials have been in use for a long time, their mechanism of action towards *Leishmania* is still not completely clear. The active form that produces antileishmanial effect is trivalent antimonial (Sb III) reduced from the prodrug pentavalent antimonial (Sb V). Some works reported trypanothione reductase and zinc finger proteins as potential targets of Sb III (Aruleba et al., 2020). The drug can be administered intramuscularly or intravenously. In human medicine, the recommended dose is 20 mg/kg per day for 21-28 days (Gradoni, 2001), while in veterinary medicine it is generally 100 mg/kg under the skin once a day for 4 weeks (GSLC, 2011). This treatment causes different side effects such as pancreatitis, pancytopenia, stiff joints, gastrointestinal problems, nephrotoxicity and, in rare cases, also cardiotoxicity (Brummitt and Porter, 1996; Gasser Jr et al., 1994; Zaghloul, 2004). Moreover, cases of resistance have been notified, especially in the geographical areas where the disease is more present (Ashutosh et al., 2007; Vanaerschot et al., 2011). In the veterinary field, antimonials are often associated with allopurinol therapy. This molecule has been used in human medicine for the treatment of gout due to its inhibitory effect on xanthine oxidase. The pharmacological effect in leishmaniasis is due to the fact that the molecule represents an analogous of purines, molecules that *Leishmania* cannot synthesize. The parasite, which normally uses the host's purines, also metabolizes allopurinol, transforming it into 4-aminopyrazole pyrimidine ribonucleotide triphosphate. This molecule, in turn, is incorporated into the parasite's RNA chains and this results in the alteration and blocking of its protein synthesis (Mirò et al., 2009).

1.9.2 Amphotericin B

Amphotericin B (figure 10b) is an antifungal isolated from an actinomycetes fungi: *Streptomyces nodosus.* The molecule interacts with 24-substituted sterol: ergosterol, the main component of the *Leishmania* cell membrane. This leads to the formation of pores in the membrane causing cell death. Unfortunately, the molecule is also active on cholesterol, widely spread on mammalian cell membranes, and this causes toxic effects, especially on the excretory system (Kamiński, 2014), like nausea, vomiting, diarrhea, stomach pain, weight loss, anorexia. To limit the toxicity of the drug, it is now administered in a liposomal solution (AmBisome®). This drug must be administered intravenously and leads to a high response against VL, although the costs of the treatment program are particularly high.

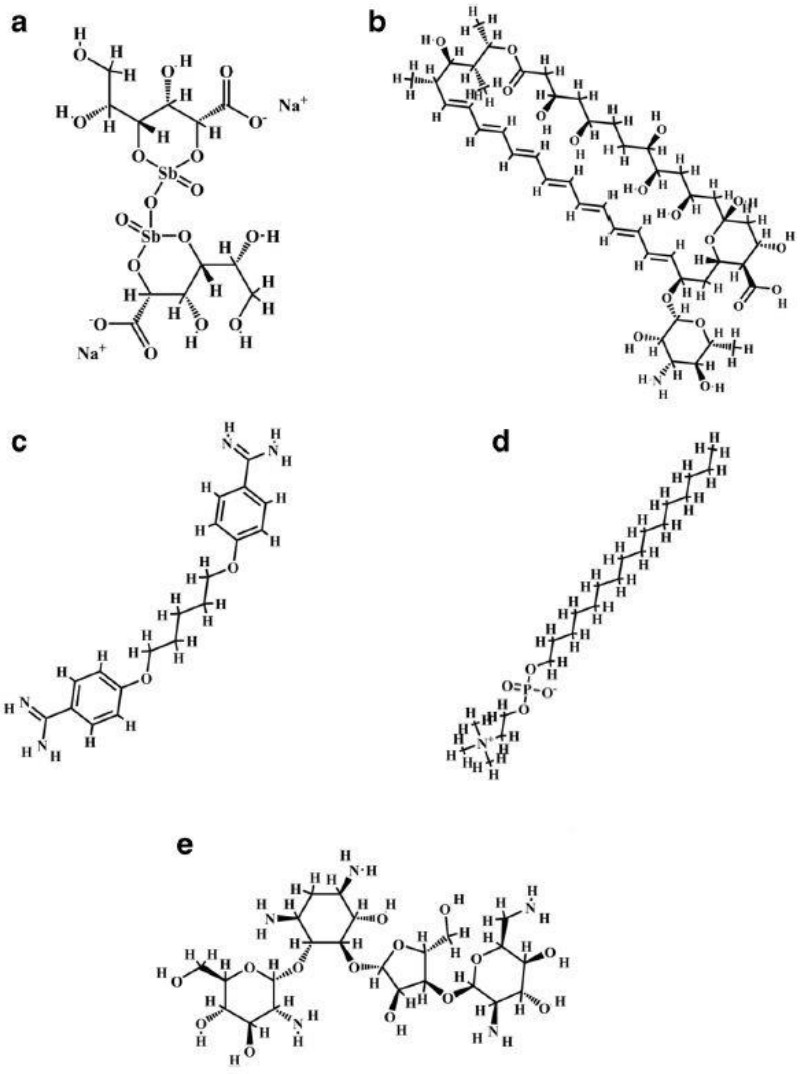

[Figure 10] Structure of antileishmanial drugs: (a) sodium stibogluconate, (b) amphotericin B, (c) pentamidine isethionate, (d) miltefosine, (e) paromomycin (Sasidharan and Saudaggar, 2021)

1.9.3 Miltefosine

Miltefosine (figure 10d) is a hexadecylphosphocholine, an analogous of phosphocholine, and it was originally developed as an antineoplastic agent against metastatic breast cancer. Since the late '90s (Sundar et al., 1998), the drug has been used with good results in VL treatment and is the only oral formulation available. The mechanisms involve the alteration of sterol and phospholipids composition, lipid metabolism, signal transduction and the production of nitric oxide (NO) inside the macrophages throw nitric oxide synthetase 2 (iNOS2) induction. This molecule is considered a first-line drug in the Indian subcontinent but, in this geographical area, drug resistance and therapeutic failures have been observed, as well as disease relapse (Rijal et al., 2013; Dorlo et al., 2014). Despite the high efficacy, side effects like gastrointestinal disturbances, renal and hepatotoxicity have been reported.

1.9.4 Pentamidine Isethionate

This drug is an aromatic diamine (figure 10c) and is administered intramuscular and intralesional for VL and CL treatment, respectively. The mechanism of action is not so clear: the efficacy seems to be due to the drug accumulation in the parasite mitochondrion. This causes the kDNA binding and the mitochondrial topoisomerase II inhibition (Mishra et al., 2007).

1.9.5 Paromomycin

Paromomycin (figure 10e) is an aminoglycoside antibiotic relatively new for the treatment of leishmaniasis, it has been approved for the VL treatment only in 2006 by the Indian government (Sasidharan and Saudaggar, 2021). The administration is topical to CL and intramuscular to VL. The mechanism remains elusive, but the inhibition of leishmanial protein synthesis has been confirmed (Maarouf et al. 1995). Among the side effects, there are elevated hepatic transaminases, hepatotoxicity, nausea, diarrhea (Khan and Kumar, 2011)

1.9.6 Vaccines Against Leishmaniasis

In the years, many efforts have been done to develop a vaccine against *Leishmania*. At present, there is no vaccine to immunize humans, but several possibilities are evaluated in clinical trials (Table 7). These vaccines include live attenuated cells, killed cells, DNA vaccine (Gamboa-Leòn et al., 2006), vector derived vaccines and peptides vaccines (Petitdidier et al., 2019).

Vaccine name	Mechanism	Classification	Clinical trial phase	Expected outcome
Leishvaccine	CD4+, CD8+, and B cell activation	First generation	III	Safe but no immune response
L. mexicana + BCG	T cell activation	First generation	–	Decrease in parasite incidence
ALM + BCG	T cell activation	First generation	II	Treatment of CL
L. mexicana + *L. amazonensis* + BCG	T cell activation	First generation	–	Higher cure rate in CL infection
Leishmune	T cell activation	First generation	III	Protection against VL in dogs
CaniLeish	Th1 induction	First generation	III	Approved in France against canine leishmaniasis
Gentamycin attenuated *L. infantum*	T and B cell activation	First generation	–	Protection against VL in dogs
Gentamycin attenuated *L. major*	Th1 induction	First generation	II	Treatment of CL
LEISH-F1	T cell activation	Second generation	I	Protection against VL in humans
LEISH-F2	T cell activation	Second generation	II	Protection against CL in humans
LEISH-F3	T cell activation	Second generation	I	Protection against VL in humans
Leish-Tec	T cell activation	Second generation	III	Protection against canine leishmaniasis
SMT and NH associated with GLA-SE	T cell activation	Second generation	I	Protection against VL in humans
Chad63-KH	Cd8+ T cell activation	Third generation	II	Protection against VL and PKDL in humans

[Table 7] Commercial and clinical trial *Leishmania* vaccine along with the mechanism, classification, and expected outcomes (Sasidharan and Saudaggar, 2021)

Currently, there are four vaccines approved for canine leishmaniasis: Leish-Tec® and Leishmune® in Brazil, CaniLeish® and LetiFend® in Europe. However, the clinical efficacy and the protection are still debated (Velez and Gállego, 2020).

1.10 References

Abdoli A, Maspi N, Ghaffarifar F (2017) Wound healing in cutaneous leishmaniasis: a double edged sword of IL-10 and TGF-β. Comp Immunol Microbiol Infect Dis 51:15–26

Acuña, S.M.; Floeter-Winter, L.M.; Muxel, S.M. MicroRNAs: Biological Regulators in Pathogen–Host Interactions. *Cells* **2020**, *9*, 113. https://doi.org/10.3390/cells9010113

Akhavan, A.A., Mirhendi, H., Khamesipour, A., Alimohammadian, M.H., Rassi, Y.,Bates, P., Kamhawi, S., Valenzuela, J.G., Arandian, M.H., Abdoli, H., Jalali-zand, N.,Jafari, R., Shareghi, N., Ghanei, M., Yaghoobi-Ershadi, M.R., 2010.Leishmaniaspecies: detection and identification by nested PCR assay from skin samples ofrodent reservoirs. Exp. Parasitol. 126, 552e556.

Akhoundi M, Downing T, Votýpka J, Kuhls K, Lukeš J, Cannet A, Ravel C, Marty P, Delaunay P, Kasbari M, Granouillac B, Gradoni L, Sereno D. Leishmania infections: Molecular targets and diagnosis. Mol Aspects Med. 2017 Oct;57:1-29. doi: 10.1016/j.mam.2016.11.012. Epub 2017 Jan 31. PMID: 28159546.

Akhoundi M, Kuhls K, Cannet A, Votýpka J, Marty P, Delaunay P, Sereno D, 2016. A Historical Overview of the Classification, Evolution, and Dispersion of *Leishmania* Parasites and Sandflies. PLoS Negl Trop Dis.; 3;10(3):e0004349. doi: 10.1371/journal.pntd.0004349.

Akhoundi, M., Hajjaran, H., Baghaei, A., Mohebali, M., 2013. Geographical distribu-tion ofleishmaniaspecies of human cutaneous leishmaniasis in Fars province, southern Iran. Iran. J. Parasitol. 8, 85e91

Alvar J, Velez ID, Bern C, Herrero M, Desjeux P, Cano J, Jannin J, den Boer M, 2012. Leishmaniasis worldwide and global estimates of its incidence. PLoS One 7:e35671. doi:10.1371/journal.pone.0035671.

Aphasizhev R. and Aphasizheva I. 2011. Uridine insertion/deletion editing in trypanosomes: a playground for rna-guided information transfer. Wiley Interdiscip Rev RNA. Sep-Oct; 2(5): 669-85

Aruleba RT, Carter KC, Brombacher F, Hurdayal R (2020) Can we harness immune responses to improve drug treatment in leishmaniasis? Microorganisms 8:1069

Ashutosh Sundar S. and Goyal N. 2007. Molecular mechanisms of antimony resistance in *Leishmania*. J Med Microbiol. Feb; 56(Pt 2): 143-53.

Ball WB, Mukherjee M, Srivastav S, Das PK, 2014. *Leishmania donovani* activates uncoupling protein 2 transcription to suppress mitochondrial oxidative burst through differential modulation of SREBP2, Sp1 and USF1 transcription factors. Int J Biochem Cell Biol.; 48:66-76. doi: 10.1016/j.biocel.2014.01.004.

Bangert M, Flores-Cha´vez MD, Llanes-Acevedo IP, Arcones C, Chicharro C, Garcı´a E, Ortega S, Nieto J, Cruz I (2018) Validation of rK39 immunochromatographic test and direct agglutination test for the diagnosis of Mediterranean visceral leishmaniasis in Spain. PLoS Negl Trop Dis 12(3):e0006277. https://doi.org/10.1371/journal.pntd.0006277

Banu SS, Meyer W, Ferreira-Paim K, Wang Q, Kuhls K, Cupolillo E, Schönian G, Lee R. A novel multilocus sequence typing scheme identifying genetic diversity amongst Leishmania donovani isolates from a genetically homogeneous population in the Indian subcontinent. Int J Parasitol. 2019 Jun;49(7):555-567. doi: 10.1016/j.ijpara.2019.02.010. Epub 2019 May 18. PMID: 31108098.

Bazzoni F, Rossato M, Fabbri M et al (2009) Induction and regulatory function of miR-9 in human monocytes and neutrophils exposed 3 Biotech (2020) 10:510 1 3 510 Page 14 of 16 to proinfammatory signals. Proc Natl Acad Sci USA 106:5282– 5287. https://doi.org/10.1073/pnas.0810909106

B'chir W, Maurin AC, Carraro V, Averous J, Jousse C, Muranishi Y, Parry L, Stepien G, Fafournoux P, Bruhat A, 2013. The eIF2alpha/ATF4 pathway is essential for stress-induced autophagy gene expression. Nucleic Acids Res.; 41(16):7683-99. doi: 10.1093/nar/gkt563.

Benne R, Van den Burg J, Brakenhoff JP, Sloof P, Van Boom JH, Tromp MC. Major transcript of the frameshifted coxII gene from trypanosome mitochondria contains four nucleotides that are not encoded in the DNA. Cell. 1986 Sep 12;46(6):819-26. doi: 10.1016/0092-8674(86)90063-2. PMID: 3019552.

Berman J. D., Human Leishmaniasis: Clinical, Diagnostic, and Chemotherapeutic Developments in the Last 10 Years, *Clinical Infectious Diseases*, Volume 24, Issue 4, April 1997, Pages 684–703, https://doi.org/10.1093/clind/24.4.684

Besteiro S, Williams RAM, Coombs GH, Mottram JC, 2007. Protein turnover and differentiation in Leishmania. Int J Parasitol.; 37(10): 1063–1075. doi: 10.1016/j.ijpara.2007.03.008.

Boité MC, Mauricio IL, Miles MA, Cupolillo E. New insights on taxonomy, phylogeny and population genetics of Leishmania (Viannia) parasites based on multilocus sequence analysis. PLoS Negl Trop Dis. 2012;6(11):e1888. doi: 10.1371/journal.pntd.0001888. Epub 2012 Nov 1. PMID: 23133690; PMCID: PMC3486886.

Boothroyd, J. C. and G. A. Cross. 1982. Transcripts coding for variant surface glycoproteins of *Trypanosoma brucei* have a short, identical exon attheir 5' end. Gene. Dec; 20(2): 281-9.

Bourdeau P., Saridomichelakis M. N., Oliveira A., Oliva G., Kotnik T., Gálvez R., Foglia Manzillo V., Koutinas A. F., Pereira da Fonseca I., Miró G. 2014. Management of canine leishmaniosis in endemic SW European regions: a questionnaire-based multinational survey. Parasit Vectors. Mar 24; 7:110.

Brummitt CF, Porter JA, Herwaldt BL (1996) Reversible peripheral neuropathy associated with sodium stibogluconate therapy for American cutaneous leishmaniasis. Clin Infect Dis 22:878–879

Canton J, Kima PE, 2012. Interactions of pathogen-containing compartments with the secretory pathway. Cell Microbiol.; 14(11):1676-86. doi: 10.1111/cmi.12000.

Cardoso L, Schallig H, Persichetti MF, Pennisi MG. New Epidemiological Aspects of Animal Leishmaniosis in Europe: The Role of Vertebrate Hosts Other Than Dogs. Pathogens. 2021 Mar 6;10(3):307. doi: 10.3390/pathogens10030307. PMID: 33800782; PMCID: PMC8000700.

Carvalho SF, Lemos EM, Corey R, Dietze R (2003) Performance of recombinant K39 antigen in the diagnosis of Brazilian visceral leishmaniasis. Am J Trop Med Hyg 68(3):321–324. https://doi.org/10.4269/ajtmh.2003.68.321

Cavalier-Smith T, Chao EE, Snell EA, Berney C, Fiore-Donno AM, Lewis R. Multigene eukaryote phylogeny reveals the likely protozoan ancestors of opisthokonts (animals, fungi, choanozoans) and Amoebozoa. Mol Phylogenet Evol. 2014 Dec;81:71-85. doi: 10.1016/j.ympev.2014.08.012. Epub 2014 Aug 23. PMID: 25152275.

Ceccarelli M, Diotallevi A, Andreoni F, Vitale F, Galluzzi L, Magnani M. Exploiting genetic polymorphisms in metabolic enzymes for rapid screening of Leishmania infantum genotypes. Parasit Vectors. 2018 Nov 1;11(1):572. doi: 10.1186/s13071-018-3143-7. PMID: 30382928; PMCID: PMC6211443.

Ceccarelli M, Galluzzi L, Migliazzo A, Magnani M. Detection and characterization of Leishmania (Leishmania) and Leishmania (Viannia) by SYBR green-based real-time PCR and high resolution melt analysis targeting kinetoplast minicircle DNA. PLoS One. 2014 Feb 13;9(2):e88845. doi: 10.1371/journal.pone.0088845. PMID: 24551178; PMCID: PMC3923818.

Ceccarelli, M., Galluzzi, L., Diotallevi, A. *et al.* The use of kDNA minicircle subclass relative abundance to differentiate between *Leishmania* (*L.*) *infantum* and *Leishmania* (*L.*) *amazonensis* . *Parasites Vectors* **10,** 239 (2017). https://doi.org/10.1186/s13071-017-2181-x

Ceccarelli, M.; Buffi, G.; Diotallevi, A.; Andreoni, F.; Bencardino, D.; Vitale, F.; Castelli, G.; Bruno, F.; Magnani, M.; Galluzzi, L. Evaluation of a kDNA-Based qPCR Assay for the Detection and Quantification of Old World *Leishmania* Species. *Microorganisms* **2020**, *8*, 2006. https://doi.org/10.3390/microorganisms8122006

Chakraborty D, Banerjee S, Sen A, Banerjee KK, Das P, Roy S. Leishmania donovani affects antigen presentation of macrophage by disrupting lipid rafts. J Immunol. 2005 Sep 1;175(5):3214-24. doi: 10.4049/jimmunol.175.5.3214. PMID: 16116212.

Clayton C. E. 2002. Life without transcriptional control? From fly to man and back again. EMBO J. Apr 15; 21(8):1881-8.

Coura-Vital W., Ker H. G., Roatt B. M., Guiar-Soares R. D., Leal G. G., Moreira N., Oliveira L. A., de Menezes Machado E. M., Morais M. H., Correa-Oliveira R., Carneiro M., Reis A. B. 2014. Evaluation of change in canine diagnosis protocol adopted by the visceral leishmaniasis control program in Brazil and a new proposal for diagnosis. PLoS One. Mar 7; 9(3): e91009.

Cullinan SB, Diehl JA, 2004. PERK-dependent activation of Nrf2 contributes to redox homeostasis and cell survival following endoplasmic reticulum stress. J Biol Chem.; 279(19):20108-17.

Cupolillo E, Medina-Acosta E, Noyes H, Momen H, Grimaldi G Jr, 2000. A revised classification for *Leishmania* and Endotrypanum. Parasitol Today.; 16: 142–144.

Dias-Teixeira KL, Calegari-Silva TC, dos Santos GR, Vitorino Dos Santos J, Lima C, Medina JM, Aktas BH, Lopes UG, 2016. The integrated endoplasmic reticulum stress response in *Leishmania amazonensis* macrophage infection: the role of X-box binding protein 1 transcription factor. FASEB J.; 30(4):1557-65. doi: 10.1096/fj.15-281550

Diotallevi A, Buffi G, Ceccarelli M, Neitzke-Abreu HC, Gnutzmann LV, da Costa Lima MS Jr, Di Domenico A, De Santi M, Magnani M, Galluzzi L. Real-time PCR to differentiate among Leishmania (Viannia) subgenus, Leishmania (Leishmania) infantum and Leishmania (Leishmania) amazonensis: Application on Brazilian clinical samples. Acta Trop. 2020 Jan;201:105178. doi: 10.1016/j.actatropica.2019.105178. Epub 2019 Oct 10. PMID: 31606374.

Diotavelli A, De Santi M, Buf G, Ceccarelli M, Vitale F, Galluzzi L, Magnani M (2018) Leishmania infection induces microRNA hsamiR-346 in human cell line-derived macrophages. Front Microbiol 9:1019

Dorlo T. P., Rijal S., Ostyn B., de Vries P. J., Singh R., Bhattarai N., Uranw S., Dujardin J. C., Boelaert M., Beijnen J. H., Huitema A. D. 2014. Failure of miltefosine in visceral leishmaniasis is associated with low drug exposure. J Infect Dis. Jul; 1, 210(1): 146-53.

El Kacem S, Kbaich MA, Daoui O, Charoute H, Mhaidi I, Ejghal R, Barhoumi M, Guizani I, Bennani H, Lemrani M. Multilocus sequence analysis provides new insight into population structure and genetic diversity of Leishmania tropica in Morocco. Infect Genet Evol. 2021 Sep;93:104932. doi: 10.1016/j.meegid.2021.104932. Epub 2021 May 21. PMID: 34023510.

Fabian MR, Sundermeier TR, Sonenberg N, 2010. Understanding how miRNAs post-transcriptionally regulate gene expression. Prog Mol Subcell Biol.; 50:1-20. doi: 10.1007/978-3-642-03103-8_1.

Fernandes, J.C.R.; Acuna, S.M.; Aoki, J.I.; Floeter-Winter, L.M.; Muxel, S.M. Long non-coding RNAs in the regulation of gene expression: Physiology and disease. Non-Coding RNA 2019, 5, 17

Forestier CL, Machu C, Loussert C, Pescher P, Spath GF, 2011. Imaging host cell- *Leishmania* interaction dynamics implicates parasite motility, lysosome recruitment, and host cell wounding in the infection process. Cell Host Microbe. 2011 Apr 21; 9(4):319-30. doi:10.1016/j.chom.2011.03.011.

Frank, B.; Marcu, A.; de Oliveira Almeida Petersen, A.L.; Weber, H.; Stigloher, C.; Mottram, J.C.; Scholz, C.J.; Schurigt, U. Autophagic digestion of leishmania major by host macrophages is associated with differential expression of bnip3, ctse, and the miRNAs mir-101c, mir-129, and mir-210. Parasites Vectors 2015, 8, 404

G.S.L.C. (Gruppo di Studio sulla Leishmaniosi Canina). 2011. Leishmaniosi Canina aggiornamenti su diagnosi e terapia. Parte II: terapia. Veterinaria. Ap; Anno 25, n. 2,.

Galluzzi L, Diotallevi A, De Santi M, Ceccarelli M, Vitale F, Brandi G, Magnani M, 2016. *Leishmania infantum* Induces Mild Unfolded Protein Response in Infected Macrophages. PLoS One.; 11(12): e0168339.

Galluzzi L, Diotallevi A, Magnani M, 2017. Endoplasmic reticulum stress and unfolded protein response in infection by intracellular parasites. Future Sci OA.; 3(3):FSO198. doi: 10.4155/fsoa-2017-0020.

Gamboa-León R et al (2006) Immunotherapy against visceral leishmaniasis with the nucleoside hydrolase-DNA vaccine of Leishmania donovani. Vaccine 24:4863–4873

Gasser RA Jr, Magill AJ, Oster CN, Franke ED, Grögl M, Berman JD (1994) Pancreatitis induced by pentavalent antimonial agents during treatment of leishmaniasis. Clin Infect Dis 18:83–90

Geisweid K., Weber K., Sauter-Louis C., Hartmann K. 2013. Evaluation of a conjunctival swab polymerase chain reaction for the detection of *Leishmania infantum* in dogs in a non-endemic area. Vet J. Oct; 198(1): 187-92.

Geraci NS, Tan JC, McDowell MA, 2015. Characterization of microRNA Expression Profiles in *Leishmania* Infected Human Phagocytes. Parasite Immunol.; 37(1):43-51. doi: 10.1111/pim.12156.

Ghosh J, Guha R, Das S, Roy S, 2013a. Liposomal cholesterol delivery activates the macrophage innate immune arm to facilitate intracellular *Leishmania donovani* killing. Infect Immun.; 82(2):607-17. doi: 10.1128/IAI.00583-13.

Global Health Observatory. Leishmaniasis. Geneva: World Health Organization; 2021 (https://www.who.int/data/gho/data/themes/topics/topic-details/GHO/leishmaniasis, accessed July 2021)

Gomez MA, Olivier M, 2010. Proteases and phosphatases during *Leishmania*-macrophage interaction: paving the road for pathogenesis. Virulence.;1(4):314-8. doi: 10.4161/viru.1.4.12194.

Gossage SM, Rogers ME, Bates PA. Two separate growth phases during the development of Leishmania in sand flies: implications for understanding the life cycle. Int J Parasitol. 2003 Sep 15;33(10):1027-34. doi: 10.1016/s0020-7519(03)00142-5. PMID: 13129524; PMCID: PMC2839921.

Gradoni L. 2001. Recenti sviluppi nella terapia delle leishmaniosi. Ann Ist Super Sanità. Vol. 37, n. 2, 255-263.

Gramiccia M, Scalone A, Di Muccio T, Orsini S, Fiorentino E, Gradoni L, 2013. The burden of visceral leishmaniasis in Italy from 1982 to 2012: a retrospective analysis of the multi-annual epidemic that occurred from 1989 to 2009. Euro Surveill.; 18(29): 20535

Guerfali, F.Z.; Laouini, D.; Guizani-Tabbane, L.; Ottones, F.; Ben-Aissa, K.; Benkahla, A.; Manchon, L.; Piquemal, D.; Smandi, S.; Mghirbi, O.; et al. Simultaneous gene expression profiling in human macrophages infected with leishmania major parasites using sage. BMC Genom. 2008, 9, 238.

Hosseini M, Nateghi Rostami M, Hosseini Doust R, Khamesipour A. Multilocus sequence typing analysis of Leishmania clinical isolates from cutaneous leishmaniasis patients of Iran. Infect Genet Evol. 2020 Nov;85:104533. doi: 10.1016/j.meegid.2020.104533. Epub 2020 Sep 10. PMID: 32919066.

Hu P, Han Z, Couvillon AD, Kaufman RJ, Exton JH, 2006. Autocrine tumor necrosis factor alpha links endoplasmic reticulum stress to the membrane death receptor pathway through IRE1-mediated NF-kB activation and downregulation of TRAF2 expression. Mol Cell Biol.; 26(8):3071-84.

Ivens A. C., Peacock C. S., Worthey E. A., Murphy L., Aggarwal G., Berriman M., Sisk E., Rajandream M. A., Adlem E., Aert R., Anupama A., Apostolou Z., Attipoe P., Bason N., Bauser C., Beck A., Beverley S. M., Bianchettin G., Borzym K., Bothe G., Bruschi C. V., Collins M., Cadag E., Ciarloni L., Clayton C., Coulson R. M., Cronin A., Cruz A. K., Davies R. M., De Gaudenzi J., *et al*. 2005. The genome of the kinetoplastid parasite, *Leishmania major*. Science. Jul 15; 309(5733): 436-42.

Jasmer D. P. and K. Stuart. 1986. Conservation of kinetoplastid minicircle characteristics without nucleotide sequence conservation. Mol Biochem Parasitol. Mar; 18(3): 257-69.

Kamiński D. M. 2014. Recent progress in the study of the interactions of amphotericin B with cholesterol and ergosterol in lipid environments. Eur Biophys J. Nov; 43(10-11): 453-67.

Karimi Kakh, M., Golchin, M., Kazemi Arababadi, M., Daneshvar, 2020. Application of the Leishmania infantum 21-kDa recombinant protein for the development of an immunochromatographic test. Parasite Immunol. 42, e12770.

Khan W, Kumar N (2011) Drug targeting to macrophages using paromomycin-loaded albumin microspheres for treatment of visceral leishmaniasis: an in vitro evaluation. J Drug Target 19:239–250

Kim VN, Han J, Siomi MC, 2009. Biogenesis of small RNAs in animals. Nat Rev Mol Cell Biol.; 10(2):126-39. doi: 10.1038/nrm2632

Kimmig P, Diaz M, Zheng J, Williams CC, Lang A, Aragón T, Li H, Walter P, 2012. The unfolded protein response in fission yeast modulates stability of select mRNAs to maintain protein homeostasis. Elife.; 1:e00048. doi: 10.7554/eLife.00048

Klatt S, Simpson L, Maslov DA, Konthur Z (2019) *Leishmania tarentolae*: Taxonomic classification and its application as a promising biotechnological expression host. PLOS Neglected Tropical Diseases 13(7): e0007424. https://doi.org/10.1371/journal.pntd.0007424

Kumari D, Perveen S, Sharma R, Singh K. Advancement in leishmaniasis diagnosis and therapeutics: An update. Eur J Pharmacol. 2021 Nov 5;910:174436. doi: 10.1016/j.ejphar.2021.174436. Epub 2021 Aug 21. PMID: 34428435.

Lago TS, Silva JA, Lago EL et al (2018) The miRNA 361-3p, a Regulator of GZMB and TNF is associated with therapeutic failure and longer time healing of cutaneous Leishmaniasis caused by L. (viannia) braziliensis. Front Immunol 9:2621. https://doi. org/10.3389/fmmu.2018.02621

Lemaire J, Mkannez G, Guerfali FZ, Gustin C, Attia H, Sghaier RM, Sysco-Consortium, Dellagi K, Laouini D, Renard P, 2013. MicroRNA expression profile in human macrophages in response to *Leishmania major* infection. PLoS Negl Trop Dis.; 7(10):e2478. doi: 10.1371/journal.pntd.0002478.

Lewis BP, Burge CB, Bartel DP, 2005. Conserved seed pairing, often flanked by adenosines, indicates that thousands of human genes are microRNA targets. Cell.; 120(1):15-20.

Li, H.; Jiang, T.; Li, M.Q.; Zheng, X.L.; Zhao, G.J. Transcriptional regulation of macrophages polarization by microRNAs. Front. Immunol. 2018, 9, 1175.

Liang X.-H., Haritan A., Uliel S. and Michaeli S. 2003. Mechanism, Factors, and Regulation Splicing in Trypanosomatids: cis and trans. Eukaryotic Cell. Oct; 2(5): 830-40.

Liu D, Uzonna JE, 2012. The early interaction of *Leishmania* with macrophages and dendritic cells and its influence on the host immune response. Front Cell Infect Microbiol.; 2:83. doi: 10.3389/fcimb.2012.00083.

Maarouf M, Lawrence F, Croft SL, Robert-Gero M (1995) Ribosomes ofLeishmania are a target for the aminoglycosides. Parasitol Res 81: 421–425

Mannaert A., Downing T., Imamura H. and Dujardin J.-C. 2012. Adaptive mechanisms in pathogens: universal aneuploidy in *Leishmania*. Trends in Parasitology. Sep; 28 (9): 370-6.

Margariti A, Li H, Chen T, Martin D, Vizcay-Barrena G, Alam S, Karamariti E, Xiao Q, Zampetaki A, Zhang Z, Wang W, Jiang Z, Gao C, Ma B, Chen YG, Cockerill G, Hu Y, Xu Q, Zeng L, 2013. XBP1 mRNA splicing triggers an autophagic response in endothelial cells through BECLIN-1 transcriptional activation. J Biol Chem.; 288(2):859-72. doi: 10.1074/jbc.M112.412783

Martinon F, Chen X, Lee A-H, Glimcher LH, 2010. Toll-like receptor activation of XBP1 regulates innate immune responses in macrophages. Nat Immunol.; 11(5):411-8. doi: 10.1038/ni.1857.

Maslov DA, Opperdoes FR, Kostygov AY, Hashimi H, Lukeš J, Yurchenko V. Recent advances in trypanosomatid research: genome organization, expression, metabolism, taxonomy and evolution. Parasitology. 2019 Jan;146(1):1-27. doi: 10.1017/S0031182018000951. Epub 2018 Jun 14. PMID: 29898792.

Matheoud D, Moradin N, Bellemare-Pelletier A, Shio MT, Hong WJ, Olivier M, Gagnon E, Desjardins M, Descoteaux A. Leishmania evades host immunity by inhibiting antigen cross-presentation through direct cleavage of the SNARE VAMP8. Cell Host Microbe. 2013 Jul 17;14(1):15-25. doi: 10.1016/j.chom.2013.06.003. PMID: 23870310.

Maurel M, Chevet E, Tavernier J, Gerlo S, 2014. Getting RIDD of RNA: IRE1 in cell fate regulation. Trends Biochem Sci.; 39(5):245-54. doi: 10.1016/j.tibs.2014.02.008.

Melo RC, Dvorak AM, 2012. Lipid body-phagosome interaction in macrophages during infectious diseases: host defense or pathogen survival strategy? PLoS Pathog 8(7): e1002729. doi.org/10.1371/journal.ppat.1002729

Mirò G., Oliva G., Cruz I., C. Cañavate, Mortarino M., Vischer C. e Bianciardi P. 2009. Multicentric, controlled clinical study to evaluate effectiveness and safety of miltefosine and allopurinol for canine leishmaniosis. Vet Dermatol. Oct; 20(5-6): 397-404.

Mishra J, Saxena A, Singh S (2007) Chemotherapy of leishmaniasis: past, present and future. Curr Med Chem 14:1153–1169

Mittra B, Andrews NW, 2013. IRONy OF FATE: role of iron-mediated ROS in *Leishmania* differentiation. Trends Parasitol.; 29(10):489-96. doi: 10.1016/j.pt.2013.07.007.

Mittra B, Cortez M, Haydock A, Ramasamy G, Myler PJ, Andrews NW, 2013. Iron uptake controls the generation of *Leishmania* infective forms through regulation of ROS levels. J Exp Med.; 210(2):401-16. doi: 10.1084/jem.20121368.

Mollereau B, Manie S, Napoletano F, 2014. Getting the better of ER stress. J Cell Commun Signal.; 8(4):311-21. doi: 10.1007/s12079-014-0251-9.

Muxel, S.M.; Laranjeira-Silva,M.F.; Zampieri, R.A.; Floeter-Winter, L.M. Leishmania (leishmania) amazonensis induces macrophage mir-294 and mir-721 expression and modulates infection by targeting nos2 and l-arginine metabolism. Sci. Rep. 2017, 7, 44141

Ndjamen B, Kang BH, Hatsuzawa K, Kima PE, 2010. *Leishmania* parasitophorous vacuoles interact continuously with the host cell's endoplasmic reticulum; parasitophorous vacuoles are hybrid compartments. Cell Microbiol.; 12(10):1480-94. doi: 10.1111/j.1462-5822.2010.01483.x.

Novoa I, Zhang Y, Zeng H, Jungreis R, Harding HP, Ron D, 2003. Stress-induced gene expression requires programmed recovery from translational repression. EMBO J.; 22(5):1180-7.

Olivier M, Atayde VD, Isnard A, Hassani K, Shio MT, 2012. *Leishmania* virulence factors: focus on the metalloprotease GP63. Microbes Infect.; 14(15):1377-89. doi: 10.1016/j.micinf.2012.05.014

Ortalli M, De Pascali AM, Longo S, Pascarelli N, Porcellini A, Ruggeri D, Randi V, Procopio A, Re MC, Varani S. Asymptomatic Leishmania infantum infection in blood donors living in an endemic area, northeastern Italy. J Infect. 2020 Jan;80(1):116-120. doi: 10.1016/j.jinf.2019.09.019. Epub 2019 Oct 1. PMID: 31585188.

Pandey K, Das VN, Singh D, Das S, Lal CS, Verma N, Bimal S, Topno RK, Siddiqui NA, Verma RB, Sinha PK, Das P. Post-kala-azar dermal leishmaniasis in a patient treated with injectable paromomycin for visceral leishmaniasis in India. J Clin Microbiol. 2012 Apr;50(4):1478-9. doi: 10.1128/JCM.05966-11. Epub 2012 Jan 25. PMID: 22278840; PMCID: PMC3318524.

Paul S, Ruiz-Manriquez LM, Serrano-Cano FI, Estrada-Meza C, Solorio-Diaz KA, Srivastava A. Human microRNAs in host-parasite interaction: a review. 3 Biotech. 2020 Dec;10(12):510. doi: 10.1007/s13205-020-02498-6. Epub 2020 Nov 5. PMID: 33178551; PMCID: PMC7644590.

Peacock CS, Seeger K, Harris D, Murphy L, Ruiz JC, Quail MA, Peters N, Adlem E, Tivey A, Aslett M, Kerhornou A, Ivens A, Fraser A, Rajandream MA, Carver T, Norbertczak H, Chillingworth T, Hance Z, Jagels K, Moule S, Ormond D, Rutter S, Squares R, Whitehead S, Rabbinowitsch E, Arrowsmith C, White B, Thurston S, Bringaud F, Baldauf SL, Faulconbridge A, Jeffares D, Depledge DP, Oyola SO, Hilley JD, Brito LO, Tosi LR, Barrell B, Cruz AK, Mottram JC, Smith DF, Berriman M. Comparative genomic analysis of three Leishmania species that cause diverse human disease. Nat Genet. 2007 Jul;39(7):839-47. doi: 10.1038/ng2053. Epub 2007 Jun 17. PMID: 17572675; PMCID: PMC2592530.

Peña M. T., Naranjo C., Klauss G., Fondevila D., Leiva M., Roura X., Davidson M. G., Dubielzig R. R. 2008. Histopathological features of ocular leishmaniosis in the dog. J Comp Pathol. Jan; 138(1): 32-9.

Peter ME, 2010. Targeting of mRNAs by multiple miRNAs: the next step. Oncogene.; 29(15):2161-4. doi: 10.1038/onc.2010.59.

Peters N. C. and Sacks D. L. 2009. The impact of vector-mediated neutrophil recruitment on cutaneous leishmaniasis. Cell. Microbiol. Sep; 11(9): 1290-6.

Petitdidier E et al (2019) Peptide-based vaccine successfully induces protective immunity against canine visceral leishmaniasis npj. Vaccines 4:1–9

Podinovskaia M, Descoteaux A, 2015. *Leishmania* and the macrophage: a multifaceted interaction. Future Microbiol.; 10(1):111-29. doi: 10.2217/fmb.14.103.

Ponzi M., C. Birago and P. A. Battaglia. 1984. Two identical symmetrical regions in the minicircle structure of *Tripanosoma lewisi* kinetoplast DNA. Mol. Biochem. Parasitol. Sep; 13(1): 111-9.

Real F., Oliveira Vidal R., Falsarella Carazzolle M., Costa Mondego J. M., Lacerda Costa G. G., Hirochi Herai R., Würtele M., de Carvalho L. M., Carmona e Ferreira R., Arruda Mortara R., Barbiéri C. L., Mieczkowski P., da Silveira J. F., Ribeiro da Silva Briones M., Guimarães Pereira G A. e Bahia D. 2013. The Genome Sequence of *Leishmania* (*Leishmania*) *amazonensis*: Functional Annotation and Extended Analysis of GeneModels. DNA Res. Dec; 20(6): 567-81.

Rijal S., Ostyn B., Uranw S., Rai K., Bhattarai N. R., Dorlo T. P., Beijnen J. H., Vanaerschot M., Decuypere S., Dhakal S. S., Das M. L., Karki P., Singh R., Boelaert M., Dujardin J. C. 2013. increasing failure of miltefosine in the treatment of Kala-azar in Nepal and the potential role of parasite drug resistance, reinfection, or noncompliance. Clin Infect Dis. Jun; 56(11): 1530-8.

Rodriguez NE, Gaur Dixit U, Allen LA, Wilson ME, 2011. Stage-specific pathways of *Leishmania infantum chagasi* entry and phagosome maturation in macrophages. PLoS One.; 6(4):e19000. doi: 10.1371/journal.pone.0019000.

Rogers M, Kropf P, Choi BS, Dillon R, Podinovskaia M, Bates P, Müller I, 2009. Proteophosophoglycans regurgitated by Leishmania-infected sand flies target the L-arginine metabolism of host macrophages to promote parasite survival. PLoS Pathog.; 5(8):e1000555. doi: 10.1371/journal.ppat.1000555.

Rogers ME, Corware K, Muller I, Bates PA, 2010. *Leishmania infantum* proteophosphoglycans regurgitated by the bite of its natural sand fly vector, Lutzomyia longipalpis, promote parasite establishment in mouse skin and skin-distant tissues. Microbes Infect.; 12(11):875-9. doi: 10.1016/j.micinf.2010.05.014.

Rogers, MB, Rogers MB, Hilley JD, Dickens NJ, Wilkes J, Bates PA, Depledge DP, Harris D, Her Y, Herzyk P, Imamura H, Otto TD, Sanders M, Seeger K, Dujardin JC, Berriman M, Smith DF, Hertz-Fowler C, Mottram JC. , 2011. Chromosome and gene copy number variation allow major structural change between species and strains of *Leishmania*. Genome Res.; 21(12):2129-42. doi: 10.1101/gr.122945.111.

Rotureau B, Morales MA, Bastin P, Spath GF, 2009. The flagellum-mitogen-activated protein kinase connection in trypanosomatids: a key sensory role in parasite signalling and development? Cell Microbiol.; 11(5):710-8. doi: 10.1111/j.1462-5822.2009.01295.x.

Roy S, Kumar GA, Jafurulla M, Mandal C, Chattopadhyay A, 2014. Integrity of the Actin Cytoskeleton of Host Macrophages is Essential for *Leishmania donovani* Infection. Biochim Biophys Acta.; 1838(8):2011-8. doi: 10.1016/j.bbamem.2014.04.017

Ruiz-Postigo JA, Jain S, Mikhailov A, Maia-Elkhoury AN, Valadas S, Warusavithana S, Osman M, Lin Z, Beshah A, Yajima A, Gasimovg E, 2021. Global leishmaniasis surveillance: 2019–2020, a baseline for the 2030 roadmap. https://www.who.int/publications/i/item/who-wer9635-401-419

Rybicka JM, Balce DR, Chaudhuri S, Allan ER, Yates RM. Phagosomal proteolysis in dendritic cells is modulated by NADPH oxidase in a pH-independent manner. EMBO J. 2012 Feb 15;31(4):932-44. doi: 10.1038/emboj.2011.440. Epub 2011 Dec 13. PMID: 22157818; PMCID: PMC3280544.

Sasidharan S, Saudagar P. Leishmaniasis: where are we and where are we heading? Parasitol Res. 2021 May;120(5):1541-1554. doi: 10.1007/s00436-021-07139-2. Epub 2021 Apr 7. PMID: 33825036.

Savina A, Jancic C, Hugues S, Guermonprez P, Vargas P, Moura IC, Lennon-Duménil AM, Seabra MC, Raposo G, Amigorena S. NOX2 controls phagosomal pH to regulate antigen processing during crosspresentation by dendritic cells. Cell. 2006 Jul 14;126(1):205-18. doi: 10.1016/j.cell.2006.05.035. PMID: 16839887.

Schönian G, Nasereddin A, Dinse N, Schweynoch C, Schallig HD, Presber W, Jaffe CL. PCR diagnosis and characterization of Leishmania in local and imported clinical samples. Diagn Microbiol Infect Dis. 2003 Sep;47(1):349-58. doi: 10.1016/s0732-8893(03)00093-2. PMID: 12967749.

Sereno D, Akhoundi M, Sayehmri K, Mirzaei A, Holzmuller P, Lejon V, Waleckx E. Noninvasive Biological Samples to Detect and Diagnose Infections due to Trypanosomatidae Parasites: A Systematic Review and Meta-Analysis. Int J Mol Sci. 2020 Feb 29;21(5):1684. doi: 10.3390/ijms21051684. PMID: 32121441; PMCID: PMC7084391.

Shio MT, Hassani K, Isnard A, Ralph B, Contreras I, Gomez MA, Abu-Dayyeh I, Olivier M, 2012. Host cell signalling and *Leishmania* mechanisms of evasion. J Trop Med.; 2012:819512. doi: 10.1155/2012/819512.

Silverman JM, Clos J, de'Oliveira CC, Shirvani O, Fang Y, Wang C, Foster LJ, Reiner NE. An exosome-based secretion pathway is responsible for protein export from Leishmania and communication with macrophages. J Cell Sci. 2010 Mar 15;123(Pt 6):842-52. doi: 10.1242/jcs.056465. Epub 2010 Feb 16. PMID: 20159964.

Simpson L. 1997. The genomic organization of guide RNA genes in kinetoplastid protozoa: several conundrums and their solutions. Mol Biochem Parasitol. Jun; 86(2): 133-41.

Simpson L., da Silva A. M. 1971 Isolation and characterization of kinetoplast DNA from *Leishmania tarentolae*. J. Mol. Biol. Mar 28; 56(3): 443-73.

Singh, A.K.; Pandey, R.K.; Shaha, C.; Madhubala, R. MicroRNA expression profiling of leishmania donovani-infected host cells uncovers the regulatory role of mir30a-3p in host autophagy. Autophagy 2016, 12, 1817–1831.

Solano-Gallego L., Miró G., Koutinas A., Cardoso L., Pennisi M. G., Ferrer L., Bourdeau P., Oliva G. e Baneth G. 2011 LeishVet guidelines for the practical management of canine leishmaniosis. Parasit Vectors. May 20; 4:86.

Srivastav, S. et al., 2014. Leishmania donovani prevents oxidative burst-mediated apoptosis of host macrophages through selective induction of suppressors of cytokine signaling (SOCS) proteins. J. Biol. Chem., 289(2), pp. 1092-1105.

Sugisaki H., and D. S. Ray. 1987. DNA sequence of *Crithidia fasciculata* kinetoplast minicircles. Mol. Biochem. Parasitol. Apr; 23(3): 253-63.

Sundar S, Jha TK, Thakur CP, Engel J, Sindermann H, Fischer C et al (2002a) Oral miltefosine for Indian visceral leishmaniasis. N Engl J Med 347:1739–1746. https://doi.org/10.1056/NEJMoa021556

Sundar S, Pai K, Sahu M, Kumar V, Murray HW (2002b) Immunochromatographic strip-test detection of anti-K39 antibody in Indian visceral leishmaniasis. Ann Trop Med Parasitol 96(1):19–23. https://doi.org/10.1179/000349802125000466

Sundar S., Rosenkaimer F., Makharia M. K., Goyal A. K., Mandal A. K., Voss A., Hilgard P., Murray H. W. 1998. Trial of oral miltefosine for visceral leishmaniasis. Lancet. Dec 5; 352(9143): 1821-3.

Tiwari, N.; Kumar, V.; Gedda, M.R.; Singh, A.K.; Singh, V.K.; Gannavaram, S.; Singh, S.P.; Singh, R.K. Identification and characterization of miRNAs in response to leishmania donovani infection: Delineation of their roles in macrophage dysfunction. Front. Microbiol. 2017, 8, 314

Torres M., Bardagí M., Roura X., Zanna G., Ravera I., Ferrer L. 2010. Long term follow-up of dogs diagnosed with leishmaniosis (clinical stage II) and treated with meglumine antimoniate and allopurinol. Vet J. Jun; 188(3): 346-51.

Ueno N, Wilson ME, 2012. Receptor-mediated phagocytosis of Leishmania: implications for intracellular survival. Trends Parasitol.; 28(8):335-44. doi: 10.1016/j.pt.2012.05.002..

Vanaerschot M., De Doncker S., Rijal S., Maes L., Dujardin J. C., Decuypereet S. 2011. Antimonial Resistance in *Leishmania donovani* is associated with increased in vivo parasite burden. PLoS One. 6(8): e23120.

Velez R, Gállego M. Commercially approved vaccines for canine leishmaniosis: a review of available data on their safety and efficacy. Trop Med Int Health. 2020 May;25(5):540-557. doi: 10.1111/tmi.13382. Epub 2020 Mar 2. PMID: 32034985.

Vivarini Ade C, Pereira Rde M, Teixeira KL, Calegari-Silva TC, Bellio M, Laurenti MD, Corbett CE, Gomes CM, Soares RP, Silva AM, Silveira FT, Lopes UG, 2011. Human cutaneous leishmaniasis: interferon-dependent expression of double-stranded RNA-dependent protein kinase (PKR) via TLR2. FASEB J.; 25(12):4162-73. doi: 10.1096/fj.11-185165

Yaeger, RG, 1996. Protozoa: Structure, Classification, Growth, and Development. Medical Microbiology. 4th edition.

Zaghloul I, Al-Jasser M (2004) Effect of renal impairment on the pharmacokinetics of antimony in hamsters. Ann Trop Med Parasitol 98: 793–800

AIMS

Leishmaniases are a group of anthropo-zoonic parasitic diseases caused by a *protozoan* belonging to *Leishmania* genus with a worldwide distribution that affects mainly the developing countries. The parasite has different hosts such as humans, dogs, and wild animals. Dogs, in particular, represent one of the most important reservoirs of infection for humans. Despite the surveillance programs introduced by the WHO, the disease still causes relevant problems in poor countries. Moreover, the treatments available are few and present several limitations such as toxicity, difficulty in administration, relapse, high production cost, and the appearance of resistant strains. In this view, an early diagnosis associated with effective therapy is pivotal to contain infection spread and prevent disabilities and death. Once entered in the host macrophages, *Leishmania* promastigotes are able to subvert the innate immune response and metabolic pathways of the host. The characterization of the molecular mechanisms underlying *Leishmania* infection and the pathogen survival in host cells can contribute to identifying new targets for therapeutic approaches. The aims of this thesis were:

(i) the development of molecular assays mainly based on qPCR and HRM analysis, and application to clinical samples and isolates from different geographic territories to differentiate the most common pathogenic species for humans, with particular attention on *L. infantum* species, endemic in the Mediterranean basin (chapters 1-5)

(ii) phenotypic screening of new classes of compounds to identify effective and safer drugs active on *L. infantum* (chapters 7-8)

(iii) the evaluation of the Unfolded Protein Response (UPR) and the expression of cfa-miR-346 in a canine macrophage-like cell line (DH82) infected with *Leishmania* spp. in an optic of “one-health” approach (chapter 9)

CHAPTER 1

In some geographical areas, like South America, several *Leishmania* species can coexist. In this contest, a rapid diagnostic approach is useful for epidemiological studies and treatments choice. This chapter consists of an original article about the application of a Real-time PCR assay on Brazilian clinical sample to differentiate *Leishmania* (*Viannia*) subgenus, *Leishmania* (*Leishmania*) *infantum* and *Leishmania* (*Leishmania*) *amazonensis.*

Original article (pre-print version) published in Acta Tropica
DOI: 10.1016/j.actatropica.2019.105178 Volume 201, January 2020, 105178

Real-time PCR to differentiate among *Leishmania* (*Viannia*) subgenus, *Leishmania* (*Leishmania*) *infantum* and *Leishmania* (*Leishmania*) *amazonensis*: application on Brazilian clinical samples

Aurora Diotallevi[a*], Gloria Buffi[a*], Marcello Ceccarelli[a], Herintha Coeto Neitzke-Abreu[b], Laisa Vieira Gnutzmann[b], Manoel Sebastião da Costa Lima Junior[c], Alice Di Domenico[a], Mauro De Santi[a], Mauro Magnani[a], Luca Galluzzi[a§]

[a]Department of Biomolecular Sciences, University of Urbino "Carlo Bo", Urbino (PU), Italy

[b]Programa de Pós-Graduação em Ciências da Saúde, Faculdade de Ciências da Saúde, Universidade Federal da Grande Dourados (UFGD), 79804-070, Dourados, MS, Brazil

[c]Fundação Oswaldo Cruz (FIOCRUZ), Instituto Aggeu Magalhães, 50740-465, Recife, PE, Brazil

*contributed equally

[§]corresponding author: luca.galluzzi@uniurb.it

Note: Supplementary data associated with this article

Abstract

Leishmaniasis is a complex disease caused by *Leishmania* species belonging to subgenera *Leishmania* and *Viannia*. In South America, *L*. (*L*.) *infantum* is considered the most important causative agent of visceral leishmaniasis, while *L*. (*L*.) *amazonensis* and *Viannia* subgenus species are responsible for the different cutaneous or mucocutaneous forms. In our previous work, we developed a diagnostic approach for *Leishmania* species discrimination based on two qPCRs (qPCR-ML and qPCR-ama) targeting the minicircle kDNA followed by melting analysis. This approach allowed to (i) differentiate the subgenera *Leishmania* and *Viannia*, and (ii) distinguish between *L*. (*L*.) *infantum* and *L*. (*L*.) *amazonensis*. The aim of this work was to demonstrate the applicability of the approach previously described, using human and canine clinical samples and strains from a Brazilian region, where *L.* (*L.*) *infantum, L.* (*L.*) *amazonensis* and *Viannia* subgenus species coexist. After validation on New World strains, the diagnostic approach was applied blindly to 36 canine clinical samples (peripheral blood and bone marrow) and 11 human clinical samples (peripheral blood and bone marrow). The sensitivity was 95.6% (95% confidence interval 77.3-100%) and 100% (95% confidence interval 76.9-100%) in the canine bone marrow samples and human (peripheral blood and bone marrow) samples, respectively, compared to conventional PCR assays. Concerning the *Leishmania* species identification, the conventional and qPCR-based methods showed kappa value of 0.876 (95% confidence interval 0.638-1.000), indicating good agreement. Therefore, this approach proved to be useful in both veterinary and human clinical context in regions co-endemic for *L.* (*L.*) *infantum*, *L.* (*L.*) *amazonensis,* and *Viannia* subgenus, helping to provide rapid diagnosis and to allow studies of species distribution.

Keywords: *Leishmania infantum*; *Leishmania amazonensis*; *Viannia*; qPCR; HRM; minicircle kDNA; diagnostics.

1. Introduction

Leishmaniasis is a neglected tropical disease caused by *Leishmania* species and transmitted by the bite of female phlebotomine sandflies. Leishmaniasis shows a worldwide distribution and affects about 12 million people. In fact, the parasite *Leishmania* is spread in Europe, Africa, Asia (Old World) as well as in the Americas (New World) with the highest number of cases in developing countries. A total of 0.7–1 million new cases of leishmaniasis and 20,000–30,000 deaths every year has been estimated (World Health Organization, 2018).

More than 20 *Leishmania* species, belonging to subgenera *Leishmania* and *Viannia*, cause infection in humans. The *Leishmania* (*Leishmania*) species are the etiological agents of visceral leishmaniasis (VL) and cutaneous leishmaniasis (CL). The *Leishmania* (*Viannia*) species, limited to tropical and subtropical America, are etiological agents of CL and mucocutaneous leishmaniasis (MCL) (Akhoundi et al., 2016). *Leishmania (L.) infantum* is the only *Leishmania* species reported in both the Old and New World. Recently, microsatellite analysis revealed that *L.* (*L.*) *infantum* in the New World (also known as *L. chagasi*) had been imported from southwest Europe (Kuhls et al., 2011).

In the New World, *Viannia* subgenus, *L.* (*L.*) *amazonensis* and occasionally *L.* (*L.*) *infantum* are responsible for the different cutaneous forms in humans (da Silva et al., 2010); importantly, *L*. (*L.*) *amazonensis* can also cause visceralization (de Souza et al., 2018). The cutaneous forms can be very heterogeneous (e.g., localized, diffuse, disseminated or mucosal forms) depending on the species of *Leishmania* and the immunological and nutritional status of the human host. Therefore, species identification could be one of the prognostic factors for the possible evolution of the disease (Anversa et al., 2018; Machado et al., 2019). Concerning canine leishmaniasis in South America, *L.* (*L.*) *infantum* and *L*. (*V*.) *braziliensis* are considered the most important causative agents (Dantas-Torres, 2009), although also *L*. (*L*.) *amazonensis* was isolated from dogs with visceral leishmaniasis in Brazil (Valdivia et al., 2017). These findings highlight the importance of using proper diagnostic assays to distinguish the *Leishmania* species involved in each case of leishmaniasis and coexisting in the same geographic area (Galluzzi et al., 2018). In this view, several PCR-based assays have been developed. In case of a generic PCR, the downstream analysis of PCR product is required to gain

information about parasite species. The most affordable technique is restriction fragment length polymorphism (RFLP) analysis, where electrophoretic analysis of the DNA fragments generated by a restriction enzyme may allow the species identification. Specifically, ITS1-PCR RFLP with the enzyme *Hae*III has been developed by Schonian et al. (Schönian et al., 2003) and further assessed by in silico RFLP analysis (Van der Auwera and Dujardin, 2015).

In previous work, we developed a new and affordable diagnostic approach for *Leishmania* species discrimination. This approach, based on two qPCRs (qPCR-ML and qPCR-ama) targeting the kDNA followed by High Resolution Melting (HRM) analysis, allowed to (i) differentiate the subgenera *Leishmania* and *Viannia*, and (ii) distinguish between *L*. (*L*.) *infantum* and *L*. (*L*.) *amazonensis*, exploiting the different abundance of minicircle subclasses (Ceccarelli et al., 2017) (Ceccarelli et al. Submitted manuscript). Briefly, the workflow of our method involves first a discrimination between subgenera *Viannia* and *Leishmania* based on HRM analysis of qPCR-ML amplicons. Then, to distinguish between *L.* (*L*.) *infantum* and *L*. (*L*.) *amazonensis*, the qPCR-ama is performed. The qPCR-ama assay is designed to amplify a minicircle subclass predominant in *L*. (*L*.) *amazonensis*, therefore discrimination between *L.* (*L*.) *infantum* and *L*. (*L*.) *amazonensis* is achieved through comparison of qPCR-ML and qPCR-ama Cq values.

This work aimed to validate the approach previously described, using human and canine clinical samples (peripheral blood and bone marrow) previously characterized and strains from a Brazilian region, where *L.* (*L*.) *infantum, L.* (*L*.) *amazonensis* and *Viannia* subgenus species can coexist.

2. Methods

2.1 Ethical statement

This research was approved by the Committee on Ethics in Animal (protocol number 27/2016) and by the Human Research Ethics Committee (protocol number 1.662.728/2016) of the Universidade Federal da Grande Dourados.

2.2 Experimental design

To test the field applicability of our previously developed qPCRs, which differentiate the subgenera *Leishmania* and *Viannia*, and distinguish between *L*. (*L*.) *infantum* and *L*. (*L*.) *amazonensis*, we used *Leishmania* strains and clinical samples from Mato Grosso do Sul (Brazil), where *L*. (*L*.) *infantum*, *L*. (*L*.) *amazonensis* and *Viannia* subgenus species can coexist. The experimental design is depicted in Fig. 1. Briefly, after serological test and/or optical microscopy examination, human and canine clinical samples were subjected to DNA extraction. The presence of *Leishmania* DNA, as well as *Leishmania* species characterization was first assessed using well consolidated molecular methods such as conventional PCR (genus and/or species specific). Then, clinical sample DNA, as well as lysates of certified *Leishmania* spp. Brazilian strains, were spotted on filter paper and sent to a different lab for ITS1-PCR RFLP, DNA sequencing and qPCR analysis. Finally, the results of qPCR assays and conventional methods (i.e. species-specific PCR, ITS1-PCR RFLP, DNA sequencing) were compared. All methods are explained in details below.

2.3 Canine and human samples

Thirty-six canine clinical samples and 11 human clinical samples were collected in Mato Grosso do Sul State, located in the Center-West Region of Brazil, an endemic area of leishmaniasis. The dog samples, i.e., 13 peripheral blood (A1-A9, B1-B4) and 23 bone marrow (B5-B9, C1-C9, D1-D9), were collected by the Control Center of Zoonoses (CCZ) of Campo Grande City. Peripheral blood was collected by jugular venipuncture, while the bone marrow was collected from the iliac crest or sternum bone, in EDTA tubes. Dogs were referred to CCZ for euthanasia because they were positive for visceral canine leishmaniasis (VCL) by the immunochromatographic Dual-Path Platform (DPP™, Bio-Manguinhos/Fiocruz, Rio de Janeiro, Brazil) and the ELISA test (EIE™; Bio-Manguinhos/Fiocruz, Rio de Janeiro, Brazil), serologic recommended tests by the Brazilian Ministry of Health, and direct identification of *Leishmania* amastigotes from Giemsa-stained smears analyzed by optical microscopy.

The human samples, 7 peripheral blood (E1, E5-E8, F2, F3) and 4 bone marrow (E2-E4, E9), were collected in Hospital Universitário of Dourados City from patients with a diagnosis of leishmaniasis. Peripheral blood was collected by venipuncture of the upper

limb, while the bone marrow was collected from sternum bone in EDTA tubes. Patients were diagnosed using serology rapid test (rK39) (Kalazar Detect™; InBios, Washington, US) and/or direct identification of *Leishmania* amastigotes from Giemsa-stained smears analyzed by optical microscopy, together with clinical evaluation. In details, patients E1 and F3 had anemia and splenomegaly, and they were diagnosed with visceral leishmaniasis. Samples E6 and E7 were from the same patient who had pancytopenia and hepatosplenomegaly. Sample E8 was from a 5 years old patient having hepatosplenomegaly, anemia, submandibular ganglia, fever, pancytopenia, abdominal distension. Sample E5 was from an AIDS patient with HIV dementia, fever, pancytopenia, hyporexia. Patient F2 had a nasal lesion with biopsy compatible with CL. Samples E2, E3, E4 were from the same patient who had a late diagnosis of VL and complications, which culminated in death. Diagnosis details are summarized in supplementary Table 1 (Data in Brief).

2.4 DNA extraction

DNA from canine and human clinical samples was obtained as described previously (Araújo et al., 2009), with some modifications. A 300 µl volume of blood was added to 500 µl of 20% SDS (Sodium Dodecyl Sulfate) (Sigma-Aldrich) and homogenized. Then, 400 µl of chloroform and 300 µl of protein precipitation solution (3M potassium acetate, 11% glacial acetic acid) were added. After centrifugation at 10,000 x g for 10 min, the supernatant was transferred to new tubes containing 1 ml of cold absolute ethanol, gently homogenized by inversion and centrifuged for 5 min at 10,000 x g. The pellets were washed twice with 1 ml of 70% cold ethanol each time and centrifuged for 2 min at 10,000 x g. The supernatant was discarded and the pellet was dried in a dry bath (AccuBlock) at 65°C for 5 min. The DNA pellet was resuspended in TE buffer (10 mM Tris, 1 mM EDTA, pH 8.0) to a final concentration of 200-500 ng/µl, stored at 4 °C for 24 h, and then frozen at -20 °C. For qPCR, DNA samples (8 µl) were spotted on filter paper (Macherey-Nagel MN 818), air-dried and stored at room temperature until analysis.

2.5 *Leishmania* spp. Brazilian strains

L. (*L.*) *infantum* MHOM/BR/2002/LPC-RPV, *L.* (*L.*) *amazonensis* WHOM/BR/75/JOSEFA and *L.* (*V.*) *braziliensis* MHOM/BR/1987/M11272 were cultivated in 199 Medium (Invitrogen) supplemented with 1% human urine, 10% fetal calf serum (Invitrogen) and 2 mM L-glutamine (Gibco-BR), at 25 °C in a B.O.D. incubator (Logen Scientific). The parasites were washed by centrifugation at 1,600 x g for 10 min with phosphate-buffered saline (PBS) pH 7.2. Parasites were counted in a Neubauer chamber, diluted with PBS at $1x10^4$ promastigotes/µl and stored at -20 °C until DNA extraction. The DNA was obtained by incubating 100 µl at 95 ºC for 30 min in a thermal cycler (Biorad, T100 Thermal Cycler); cell lysate was centrifuged at 13,000 x g for 1 min, the supernatant was transferred to a clean tube and used directly as amplification template (Marcussi et al., 2008). For qPCR, cell lysate containing DNA was spotted on filter paper (Macherey-Nagel MN 818) in duplicates, as described above.

2.6 Genus and species-specific PCR assays

Leishmania parasites were detected by PCR using genus-specific primers 13A and 13B targeting kDNA minicircle of both old world and new world species (Rodgers et al., 1990). The reaction (25 µl) contained 0.4 µM of each primer (Sigma), 1.5 mM $MgCl_2$, 0.2 mM dNTPs (Invitrogen), 1.5 U Taq DNA Polymerase (Phoneutria), 1X enzyme buffer and 2 µl extracted DNA (200-500 ng/µl). The amplification was performed in a thermal cycler (Biorad, T100 Thermal Cycler) at 95 °C for 5 min, followed by 35 cycles: 95 °C for 30 s, 61 °C for 30 s, 72 °C for 30 s.

L. (*L.*) *infantum* was detected by PCR using species-specific primers FLC2 and RLC2 targeting kDNA minicircle (Gualda et al., 2015). The reaction (25 µl) contained 0.2 µM of each primer (Sigma), 2 mM $MgCl_2$, 0.2 mM dNTPs (Invitrogen), 1.5 U Taq DNA Polymerase (Phoneutria), 1X enzyme buffer and 2 µl extracted DNA. The amplification was performed as described above, except for the annealing temperature (56 °C instead of 61 °C). DNAs from *L.* (*V.*) *braziliensis* MHOM/BR/1987/M11272, *L.* (*L.*) *amazonensis* WHOM/BR/75/JOSEFA and *L.* (*L.*) *infantum* MHOM/BR/2002/LPC-RPV were used as controls. Amplified fragments were visualized under UV light on 3% agarose gel stained with 0.1 µg/ml ethidium bromide.

2.7 ITS1-PCR RFLP

Leishmania species were identified in available human clinical samples by ITS1-PCR RFLP, as described by Schonian et al. (Schönian et al., 2003). Briefly, ITS1 PCR products were directly digested with 10 U *Hae*III (Thermo Fisher Scientifc) at 37 °C for 3 h. The restriction fragments were visualized on a 3.5% high-resolution MetaPhor (Cambrex) agarose gel stained with GelRed (Biotium, Hayward, CA). *L*. (*L*.) *amazonensis* WHOM/BR/75/JOSEFA, *L*. (*V*.) *braziliensis* MHOM/BR/1987/M11272, *L*. (*L*.) *infantum* MHOM/BR/2002/LPC-RPV and no template PCR reaction were used as controls. ITS1 PCR products were directly sequenced as previously described (Ceccarelli et al., 2018). Phylogenetic analysis was conducted using MEGA 6 software.

2.8 Quantitative PCR (qPCR) assays

The approach described in Ceccarelli et al. (Ceccarelli et al., 2017), consisting in running two qPCR reactions in parallel (qPCR-ML and qPCR-ama) to amplify different classes of minicircles, has been applied on sample DNA spotted on filter paper. Briefly, the workflow of our method involves first a discrimination between subgenera *Viannia* and *Leishmania* based on qPCR-ML HRM analysis, performed with primers MLF and MLR (Supplementary Table 2, Data in Brief); if this analysis indicates subgenus *Leishmania*, the discrimination between *L.* (*L.*) *infantum* and *L.* (*L.*) *amazonensis* is performed through comparison of qPCR-ML and qPCR-ama Cq values. The qPCR-ama was performed using the forward primer LMi-amaF and the reverse primer MLR (Supplementary Table 2, Data in Brief). All samples were tested blindly. To evaluate the DNA integrity and amplifiability in canine and human samples, canine beta-2-microglobulin (B2M) and human glyceraldehyde-3-phosphate dehydrogenase (GAPDH) were amplified. The primers were used as described previously (Ceccarelli et al., 2014b; Galluzzi et al., 2012) and should amplify 102 and 183 bp fragments, respectively. To ensure applicability with samples on filter paper, a pre-amplification step was introduced as follows. A punch of filter paper (2 mm in diameter) was placed in 40 µl reaction mixture containing 38 µl SYBR green PCR master mix (Diatheva srl, Fano, Italy) or RT2 SYBR Green ROX FAST Mastermix (Qiagen , Hilden, Germany) or TB Green premix ex TaqII Mastermix (Takara Bio Europe, France) and 200 nM of each primer

(Supplementary Table 2, Data in Brief). Tubes were placed in a thermal cycler (GeneAmp PCR System 2700), and pre-amplified under the following conditions: 94 °C for 5 min, 10 cycles at 94 °C for 30 s, 60 °C for 20 s and 72 °C for 20 s. At the end of this pre-amplification step, the tubes were centrifuged for few seconds and placed in ice; the filter paper was removed and the reaction was split into two PCR tubes (20 µl each tube). Then, the tubes were placed in the Rotor-Gene 6000 instrument and amplified as follows: 45 cycles at 94 °C for 30 s, 60 °C for 20 s and 72 °C for 20 s. As reference, PCR mixtures containing template DNA isolated from *L.* (*L.*) *infantum* MHOM/FR/78/LEM75, *L.* (*L.*) *amazonensis* MHOM/BR/00/LTB0016 and *L.* (*V.*) *braziliensis* MHOM/BR/75/M2904 were included in each run. *Trypanosoma cruzi* and human DNA were amplified using the conditions described above to confirm qPCRs specificity. The DNA concentration of reference strains was adjusted to have qPCR-ML Cq values comparable to Cq of tested samples. Moreover, a negative control (no template control) was included for each primer pair reaction. To confirm the absence of non-specific products or primer dimers, a melting analysis was performed from 79 to 95 °C at the end of each run, with a slope of 1 °C/s, and 5 s at each temperature. The Cq values were evaluated with quantification analysis of the RotorGene 6000 software.

2.9 High-resolution melt (HRM) analysis

The high-resolution melt (HRM) analysis was performed immediately after the amplification reactions in the Rotor-Gene 6000 instrument as previously described (Ceccarelli et al., 2014a). In brief, HRM analysis was conducted over the range from 79 °C to 90 °C, rising at 0.1 °C/s and waiting for 2 s at each temperature. Each sample was run in duplicate, and the gain was optimized before melting on all tubes. HRM curve analysis was performed with the derivative of the intensity of fluorescence at different temperatures (dF/dT), after smoothing, with the Rotor-Gene 6000 software. Only samples with Cq values < 30 were considered for analysis (Ceccarelli et al., 2014a; White and Potts, 2006). Template DNA isolated from *L.* (*L.*) *infantum* MHOM/FR/78/LEM75 and *L.* (*L.*) *amazonensis* MHOM/BR/00/LTB0016 were used as reference for *Leishmania* subgenus, while template DNA from *L.* (*V.*) *braziliensis* MHOM/BR/75/M2904 was used as reference for *Viannia* subgenus. Bins were set to define Tm of amplicons for each

species. Automated classification of genotypes (i.e. subgenus *Leishmania* or *Viannia*) of unknown samples was performed by the Rotor-Gene software according to the presence of a derivative peak located within a defined temperature bin.

2.10 Statistical analysis

The 95% confidence intervals for sensitivity in clinical samples were calculated using the modified Wald method (Agresti et al., 1998). The degree of agreement between conventional methods (i.e. *L*. *infantum* species-specific PCR and/or ITS1-PCR RFLP and/or DNA sequencing) and qPCR-based methods in all samples with information about *Leishmania* species was determined by calculating Kappa values with 95 % confidence intervals using GraphPad QuickCalcs (GraphPad Prism, 2018).

3. Results

3.1 Brazilian strains characterization

The approach based on two qPCRs to distinguish between *L*. (*L*.) *infantum* and *L*. (*L*.) *amazonensis* exploiting the different abundance of minicircle subclasses, previously developed with European *L*. (*L*.) *infantum* strains, was evaluated with additional New World strains. In particular, one New World *L.* (*L.*) *infantum* strain, one *L.* (*L.*) *amazonensis* strain and one *L.* (*V.*) *braziliensis* strain were tested blindly in duplicates. The contextual evaluation of qPCR-ML HRM peaks and qPCR-ML/qPCR-ama Cq values allowed to correctly identify the subgenus (*Leishmania* or *Viannia*) and the species (*infantum* or *amazonensis*) in each sample (Table 1). Samples F4 and F7 showed Cq (qPCR-ama) <Cq (qPCR-ML) and were classified as *L.* (*L.*) *amazonensis*. Samples F5, F6, F8, F9 showed Cq (qPCR-ML) <Cq (qPCR-ama) and were classified as *L.* (*L.*) *infantum* (F6, F9) and *Viannia* subgenus species (F5, F8), depending on the Tm of qPCR-ML amplicons determined by HRM analysis (Fig. 1).

3.2 Canine clinical samples characterization

Once confirmed the feasibility on New World strains, the approach described above was used to analyze 36 clinical sample DNAs, spotted on filter paper, from dogs with a diagnosis of leishmaniasis. Thirteen DNA samples (A1-A9, B1-B4) were from peripheral

blood and 23 from bone marrow (B5-B9, C1-C9, D1-D9). All peripheral blood samples were positive using conventional PCR with primers specific for genus *Leishmania*, and all bone marrow samples were positive using conventional PCR with primers specific for *L.* (*L.*) *infantum*.

Concerning the qPCR analysis, the amplifiability of DNA on filter paper was confirmed for all samples using canine B2M as a target. Regarding DNA samples isolated from peripheral blood, 8 out of 13 samples were not detectable with both qPCR-ML and qPCR-ama assays. The remaining 5 samples (A4, A5, A9, B3, B4) resulted positive with both qPCR-ML and qPCR-ama assays, with Cq (qPCR-ML) <Cq (qPCR-ama) (Supplementary Table 3, Data in Brief). Regarding DNA samples isolated from bone marrow, only one sample (D1) was not detectable with both qPCR-ML and qPCR-ama assays; 5 samples (C6, C8, C9, D2, D9) were positive with the qPCR-ML only; the remaining 17 samples were detected with both the assays, with Cq (qPCR-ML) <Cq (qPCR-ama) (Supplementary Table 3, Data in Brief).

After evaluation of HRM analysis, all samples were identified as *L.* (*L.*) *infantum* (Table 2). Compared to conventional PCR results in bone marrow samples, the sensitivity was 95.6% (95% confidence interval 77.3-100%). On the other hand, the sensitivity in peripheral blood samples was 38.5% (95% confidence interval 17.6-64.6%).

3.3 Human clinical samples characterization

In conventional PCR, 4 peripheral blood samples (E6-E8 and F3) and 3 bone marrow samples (E2-E4) were positive for the *Leishmania* genus. Samples E1, E9 and F2 were not detectable, while genus-specific PCR for sample E5 was not available. ITS1-PCR RFLP indicated the presence of *L*. (*L*.) *infantum* in samples E6, F2, F3, while sample E5 was characterized as *Viannia* subgenus species. The DNA sequence of F2 and F3 ITS1 amplicons confirmed the identification of those samples as *L.* (*L*.) *infantum* (Table 3) (Supplementary Fig. 1, Data in Brief).

Concerning the qPCR assays, the amplifiability of DNA on filter paper was confirmed for all samples using human GAPDH as a target. Regarding DNA samples isolated from peripheral blood, the samples E1, E6, E7 and E8 were positive with both qPCR-ML and qPCR-ama assays, with Cq (qPCR-ML) <Cq (qPCR-ama) (Supplementary Table 4, Data in

Brief). After HRM analysis, samples E1, E6 and E7 were identified as *L.* (*L.*) *infantum*, while in sample E8 both *L.* (*L.*) *infantum* and *Viannia* subgenus species were identified. The samples E5, F2 and F3 were positive with the qPCR-ML only. After HRM analysis, samples F2 and F3 were identified as *L.* (*L.*) *infantum*, while in sample E5 both *L.* (*L.*) *infantum* and *Viannia* subgenus species. were identified (Table 3). Regarding DNA samples isolated from bone marrow, the samples E2, E3 and E4 were identified as *L.* (*L.*) *infantum*, *L.* (*L.*) *amazonensis* and *L.* (*L.*) *infantum,* respectively (Table 3) (Supplementary Table 4, Data in Brief). The sample E9 was not detectable in conventional PCR but it was identified as *L.* (*L.*) *infantum* in qPCR. The sensitivity of the qPCR assays in both blood and bone marrow samples was 100% (95% confidence interval 76.9-100%).

The specificity of qPCR-ML and qPCR-ama with pre-amplification conditions from filter paper was confirmed using *Trypanosoma cruzi* and human DNA as template (Supplementary Fig. 2, Data in Brief).

3.4 Agreement between conventional and qPCR-based methods

The agreement between conventional and qPCR-based methods was evaluated among all samples having species information (including *Leishmania* strains) by calculating Kappa values. The samples were classified in 3 categories: *L.* (*L.*) *infantum*, *L.* (*L.*) *amazonensis* and *Viannia* subgenus. The strength of agreement was considered to be "very good" (Kappa=0.876; standard error=0.122; 95% confidence interval 0.638 - 1.000).

4. Discussion

In the New World, *L.* (*L.*) *infantum*, *L.* (*L.*) *amazonensis* and several *Viannia* subgenus species coexist in the same geographic area and can infect both humans and dogs (Tolezano et al., 2007). In particular, in Mato Grosso do Sul, *L.* (*L.*) *infantum*, *L.* (*L.*) *amazonensis* and *L.* (*V.*) *braziliensis* were identified as the etiologic agents of Leishmaniasis (Souza Castro et al., 2018).

In a previous investigation, a new diagnostic approach based on two qPCR assays (qPCR-ML and qPCR-ama) to differentiate the subgenera *Leishmania* and *Viannia* and to discriminate *L.* (*L.*) *infantum* from *L.* (*L.*) *amazonensis* exploiting differences in minicircle

subpopulations has been developed (Ceccarelli et al., 2017). This work represents a validation of the previously developed approach, using strains and clinical samples (canine and human) from Brazil, tested blindly.

The qPCR-ML and qPCR-ama results obtained with the Brazilian strains corroborated the results obtained previously. In particular, the *L.* (*L.*) *infantum* MHOM/BR/2002/LPC-RPV strain showed the same results obtained with European strains, i.e. Cq (qPCR-ML) <Cq (qPCR-ama), in agreement with previous studies showing identity between *L.* (*L.*) *infantum* from south Europe and *L.* (*L.*) *infantum* from New World (Kuhls et al., 2011). Importantly, these results suggest a homology between Old and New world strains also at the level of minicircle subclass composition.

Concerning canine samples, all samples with positive results were characterized as *L.* (*L.*) *infantum*, and the species identification was confirmed with the species-specific conventional PCR in all bone marrow samples. This was expected since all canine samples were from VCL cases. The qPCR sensitivity varied between peripheral blood (38.5%) and bone marrow (95.6%). The decreased sensitivity observed in blood samples could be due to the low parasite load in the peripheral blood compared to bone marrow or lymph node (Manna et al., 2008; Solano-Gallego et al., 2007) along with the low amount of template DNA, due to amplification of DNA from a punch of filter paper.

While dogs are mainly infected by *L.* (*L.*) *infantum*, and occasionally by *L.* (*V.*) *braziliensis* (Carvalho et al., 2015) or *L.* (*L.*) *amazonensis* (Sanches et al., 2016; Tolezano et al., 2007), humans can be infected by different *Leishmania* species giving heterogeneous clinical manifestations. The human samples E1, E2, E4, E6, E7, E9, F2 and F3 were characterized as *L.* (*L.*) *infantum*, E3 as *L.* (*L.*) *amazonensis*, E5 and E8 as co-infection *Viannia* subgenus species/*L.* (*L.*) *infantum*. The species characterization was in agreement with the clinical history of the patients. The fact that *L.* (*L.*) *infantum* was identified also in sample F2 (a CL patient) is not surprising since *L.* (*L.*) infantum has been identified also as a causative agent of cutaneous leishmaniasis in the state of Mato Grosso do Sul (Castro et al., 2016). Samples E2, E3, E4, which were from the same patient, were collected at different time points and were characterized as *L.* (*L.*) *infantum*, (E2 and E4) and as *L.* (*L.*) *amazonensis* (E3). The different species characterization could be due to the presence of a co-infection with two *Leishmania* species or to infection with *L.* (*L.*) *infantum* and *L.* (*L.*)

amazonensis occurring at different times in the same patient. This is plausible also because some *Lutzomyia* spp. are supposed to transmit more than one *Leishmania* spp. In particular, *Lu. longipalpis*, the main vector of *L.* (*L.*) *infantum* in Latin America, has also been found infected by *L.* (*V.*) *braziliensis* and *L.* (*L.*) *amazonensis* in Brazil (Guimarães-e-Silva et al., 2017).

On the whole, the agreement between conventional methods and qPCR-based methods for *Leishmania* species identification, determined by Kappa test, was "very good". The agreement was not perfect due to a possible co-infection [*L.* (*L.*) *infantum* and *Viannia* subgenus species] revealed by qPCR in human sample E5, but not detected with ITS1-PCR RFLP. Importantly, concerning the methodology, the species characterization in canine or human samples was reached regardless the qPCR master mix used (Diatheva, Qiagen or Takara) -provided that reference strains are included in each run as internal controls- demonstrating the robustness of this approach (Supplementary Table 3 and 4, Data in Brief). Since there is no PCR-based method considered as gold standard for species determination, DNA sequencing was performed on two representative samples (F2 and F3) to confirm the results obtained with qPCR-based assays. However, due to limited sample size, caution is still needed and the results should be considered as preliminary for the South American clinical context.

Nevertheless, the fact that the closed-tube format of the assays helps to minimize contamination and accelerate the workflow, could make this approach a potential alternative to conventional PCR and/or PCR-RFLP methods (Souza Castro et al., 2018). For example, this has been demonstrated in endemic areas of Iran, where qPCR assays have shown highest sensitivity, specificity, positive and negative predictive values both in canine and human samples (Mohammadiha et al., 2013b, 2013a). On the other hand, high costs of qPCR reagents and equipment could still impair the use of this approach in low-income settings.

In conclusion, the applicability of the method developed in (Ceccarelli et al., 2017) was demonstrated in clinical samples from a Brazilian endemic area. Our data indicate that this approach could be useful in a clinical context in regions co-endemic for *L.* (*L.*) *infantum*, *L.* (*L.*) *amazonensis,* and *Viannia* subgenus, helping to provide rapid diagnosis and to allow studies of species distribution.

Acknowledgments

We would like to thank Dr Margherita Carletti for assistance in statistical analysis; Dr Francesca Andreoni and Dr Daniela Bencardino for DNA sequencing. This work was partially supported by the Department of Biomolecular Sciences of University of Urbino. The funder had no role in study design, data collection and analysis, interpretation of the data.

References

Agresti, A., Coull, B.A., Statistician, T.A., May, N., 1998. Approximate Is Better than "Exact" for Interval Estimation of Binomial Proportions. Am Stat 52, 119–126.

Akhoundi, M., Kuhls, K., Cannet, A., Votýpka, J., Marty, P., Delaunay, P., Sereno, D., 2016. A Historical Overview of the Classification, Evolution, and Dispersion of Leishmania Parasites and Sandflies. PLoS Negl Trop Dis 10, e0004349. doi:10.1371/journal.pntd.0004349

Anversa, L., Tiburcio, M.G.S., Richini-Pereira, V.B., Ramirez, L.E., Anversa, L., Tiburcio, M.G.S., Richini-Pereira, V.B., Ramirez, L.E., 2018. Human leishmaniasis in Brazil: A general review. Rev Assoc Med Bras 64, 281–289. doi:10.1590/1806-9282.64.03.281

Araújo, F.R. de, do Nascimento Ramos, C.A., Luíz, H.L., Hany Fuzeta Schabib Péres, I.A., Marçal Oliveira, R.H., Fernando de Souza, I.I., dos Santos Russi, L., 2009. Avaliação de um Protocolo de Extração de DNA Genômico a Partir de Sangue Total. Embrapa Comun Técnico 120, 1–5.

Carvalho, F.S., Wenceslau, A.A., Albuquerque, G.R., Munhoz, A.D., Gross, E., Carneiro, P.L.S., Oliveira, H.C., Rocha, J.M., Santos, I.A., Rezende, R.P., 2015. Leishmania (Viannia) braziliensis in dogs in Brazil: epidemiology, co-infection, and clinical aspects. Genet Mol Res 14, 12062–12073. doi:10.4238/2015.October.5.19

Castro, L.S., França, A. de O., Ferreira, E. de C., Hans Filho, G., Higa Júnior, M.G., Gontijo, C.M.F., Pereira, A.A.S., Dorval, M.E.M.C., 2016. Leishmania infantum as a causative agent of cutaneous leishmaniasis in the state of Mato Grosso do Sul, Brazil. Rev Inst Med Trop Sao Paulo 58, 23. doi:10.1590/S1678-9946201658023

Ceccarelli, M., Diotallevi, A., Andreoni, F., Vitale, F., Galluzzi, L., Magnani, M., 2018. Exploiting genetic polymorphisms in metabolic enzymes for rapid screening of Leishmania infantum genotypes. Parasit Vectors 11, 572. doi:10.1186/s13071-018-3143-7

Ceccarelli, M., Galluzzi, L., Diotallevi, A., Andreoni, F., Fowler, H., Petersen, C., Vitale, F., Magnani, M., 2017. The use of kDNA minicircle subclass relative abundance to differentiate between Leishmania (L.) infantum and Leishmania (L.) amazonensis. Parasit Vectors 10, 239. doi:10.1186/s13071-017-2181-x

Ceccarelli, M., Galluzzi, L., Migliazzo, A., Magnani, M., 2014a. Detection and Characterization of Leishmania (Leishmania) and Leishmania (Viannia) by SYBR Green-Based Real-Time PCR and High Resolution Melt Analysis Targeting Kinetoplast Minicircle DNA. PLoS One 9, e88845. doi:10.1371/journal.pone.0088845

Ceccarelli, M., Galluzzi, L., Sisti, D., Bianchi, B., Magnani, M., 2014b. Application of qPCR in conjunctival swab samples for the evaluation of canine leishmaniasis in borderline cases or disease relapse and correlation with clinical parameters. Parasit Vectors 7, 460. doi:10.1186/s13071-014-0460-3

da Silva, L.A., de Sousa, C.S.C. dos S., da Graca, G.C., Porrozzi, R., Cupolillo, E., da Graça, G.C., Porrozzi, R., Cupolillo, E., 2010. Sequence analysis and PCR-RFLP profiling of the hsp70 gene as a valuable tool for identifying Leishmania species associated with human leishmaniasis in Brazil. Infect Genet Evol 10, 77–83. doi:10.1016/j.meegid.2009.11.001

Dantas-Torres, F., 2009. Canine leishmaniosis in South America. Parasit Vectors 2 Suppl 1, S1. doi:10.1186/1756-3305-2-S1-S1

de Souza, C.S.F., Calabrese, K.S., Abreu-Silva, A.L., Carvalho, L.O.P., Cardoso, F. de O., Dorval, M.E.M.C., Oshiro, E.T., Quaresma, P.F., Gontijo, C.M.F., Pacheco, R.S., Rossi, M.I.D., da Costa, S.C.G., Zaverucha do Valle, T., 2018. Leishmania amazonensis isolated from human visceral leishmaniasis: histopathological analysis and parasitological burden in different inbred mice. Histol Histopathol 33, 705–716. doi:10.14670/HH-11-965

Galluzzi, L., Ceccarelli, M., Diotallevi, A., Menotta, M., Magnani, M., 2018. Real-time PCR applications for diagnosis of leishmaniasis. Parasit Vectors 11, 273. doi:10.1186/s13071-018-2859-8

Galluzzi, L., De Santi, M., Crinelli, R., De Marco, C., Zaffaroni, N., Duranti, A., Brandi, G., Magnani, M., 2012. Induction of endoplasmic reticulum stress response by the indole-3-carbinol cyclic tetrameric derivative CTet in human breast cancer cell lines. PLoS One 7, e43249. doi:10.1371/journal.pone.0043249

GraphPad Prism, 2018. GraphPad Software, QuickCalcs [WWW Document]. URL http://www.graphpad.com/quickcalcs/ (accessed 6.18.19).

Gualda, K.P., Marcussi, L.M., Neitzke-Abreu, H.C., Aristides, S.M.A., Lonardoni, M.V.C., Cardoso, R.F., Silveira, T.G.V., 2015. New primers for detection of Leishmania infantum using polymerase chain reaction. Rev Inst Med Trop Sao Paulo 57, 377–383. doi:10.1590/S0036-46652015000500002

Guimarães-e-Silva, A.S., Silva, S. de O., Ribeiro da Silva, R.C., Pinheiro, V.C.S., Rebêlo, J.M.M., Melo, M.N., 2017. Leishmania infection and blood food sources of phlebotomines in an area of Brazil endemic for visceral and tegumentary leishmaniasis. PLoS One 12, e0179052. doi:10.1371/journal.pone.0179052

Kuhls, K., Alam, M.Z., Cupolillo, E., Ferreira, G.E.M., Mauricio, I.L., Oddone, R., Feliciangeli, M.D., Wirth, T., Miles, M.A., Schönian, G., 2011. Comparative Microsatellite Typing of New World Leishmania infantum Reveals Low Heterogeneity among Populations and Its Recent Old World Origin. PLoS Negl Trop Dis 5, e1155. doi:10.1371/journal.pntd.0001155

Machado, G.U., Prates, F.V., Machado, P.R.L., 2019. Disseminated leishmaniasis: clinical, pathogenic, and therapeutic aspects. An Bras Dermatol 94, 9–16. doi:10.1590/abd1806-4841.20198775

Manna, L., Reale, S., Vitale, F., Picillo, E., Pavone, L.M., Gravino, A.E., 2008. Real-time PCR assay in Leishmania-infected dogs treated with meglumine antimoniate and allopurinol. Vet J 177, 279–282. doi:10.1016/j.tvjl.2007.04.013

Marcussi, V.M., Marcussi, L.M., Barbosa-Tessmann, I.P., Lonardoni, M.V.C., Silveira, T.G.V., 2008. Leishmania (Viannia) braziliensis: New primers for identification using polymerase chain reaction. Exp Parasitol 120, 300–305. doi:10.1016/j.exppara.2008.08.005

Mohammadiha, A., Haghighi, A., Mohebali, M., Mahdian, R., Abadi, A.R.R., Zarei, Z., Yeganeh, F., Kazemi, B., Taghipour, N., Akhoundi, B., Barati, M., Mahmoudi, M.R.R., 2013a. Canine visceral leishmaniasis: A comparative study of real-time PCR, conventional PCR, and direct agglutination on sera for the detection of Leishmania infantum infection. Vet Parasitol 192, 83–90. doi:10.1016/j.vetpar.2012.10.013

Mohammadiha, A., Mohebali, M., Haghighi, A., Mahdian, R., Abadi, A.R., Zarei, Z., Yeganeh, F., Kazemi, B., Taghipour, N., Akhoundi, B., 2013b. Comparison of real-time PCR and conventional PCR with two DNA targets for detection of Leishmania (Leishmania) infantum infection in human and dog blood samples. Exp Parasitol 133, 89–94. doi:10.1016/j.exppara.2012.10.017

Rodgers, M.R., Popper, S.J., Wirth, D.F., 1990. Amplification of kinetoplast DNA as a tool in the detection and diagnosis of Leishmania. Exp Parasitol 71, 267–75.

Sanches, L. da C., Martini, C.C. de, Nakamura, A.A., Santiago, M.E.B., Dolabela de Lima, B., Lima, V.M.F. de, 2016. Natural canine infection by Leishmania infantum and Leishmania amazonensis and their implications for disease control. Rev Bras Parasitol Vet 25, 465–469. doi:10.1590/S1984-29612016071

Schönian, G., Nasereddin, A., Dinse, N., Schweynoch, C., Schallig, H.D.F.., Presber, W., Jaffe, C.L., 2003. PCR diagnosis and characterization of Leishmania in local and imported clinical samples. Diagn Microbiol Infect Dis 47, 349–358. doi:10.1016/S0732-8893(03)00093-2

Solano-Gallego, L., Rodriguez-Cortes, A., Trotta, M., Zampieron, C., Razia, L., Furlanello, T., Caldin, M., Roura, X., Alberola, J., 2007. Detection of Leishmania infantum DNA by fret-based real-time PCR in urine from dogs with natural clinical leishmaniosis. Vet Parasitol 147, 315–319. doi:10.1016/j.vetpar.2007.04.013

Souza Castro, L., de Oliveira França, A., de Castro Ferreira, E., da Costa Lima Júnior, M.S., Gontijo, C.M.F., Pereira, A.A.S.,

Dorval, M.E.C., 2018. Characterization of Leishmania species from Central-West Region of Brazil. Parasitol Res 117, 1839–1845. doi:10.1007/s00436-018-5871-1

Tolezano, J.E., Uliana, S.R.B., Taniguchi, H.H., Araújo, M.F.L., Barbosa, J.A., Barbosa, J.E., Floeter-Winter, L.M., Shaw, J.J., 2007. The first records of Leishmania (Leishmania) amazonensis in dogs (Canis familiaris) diagnosed clinically as having canine visceral leishmaniasis from Araçatuba County, São Paulo State, Brazil. Vet Parasitol 149, 280–284. doi:10.1016/j.vetpar.2007.07.008

Valdivia, H.O., Almeida, L. V, Roatt, B.M., Reis-Cunha, J.L., Pereira, A.A.S., Gontijo, C., Fujiwara, R.T., Reis, A.B., Sanders, M.J., Cotton, J.A., Bartholomeu, D.C., 2017. Comparative genomics of canine-isolated Leishmania (Leishmania) amazonensis from an endemic focus of visceral leishmaniasis in Governador Valadares, southeastern Brazil. Sci Rep 7, 40804. doi:10.1038/srep40804

Van der Auwera, G., Dujardin, J.-C., 2015. Species Typing in Dermal Leishmaniasis. Clin Microbiol Rev 28, 265–294. doi:10.1128/CMR.00104-14

White, H., Potts, G., 2006. Mutation scanning by high resolution melt analysis. Evaluation of RotorGene 6000 (Corbett Life Science), HR1 and 384 well LightScanner (Idaho Technology). National Genetics Reference Laboratory (Wessex).

World Health Organization, 2018. Leishmaniasis [WWW Document]. World Heal Org Fact Sheet. URL http://www.who.int/mediacentre/factsheets/fs375/en/ (accessed 3.16.18).

Figures and tables

Fig. 1. Flow diagram of experimental design. See text for details.

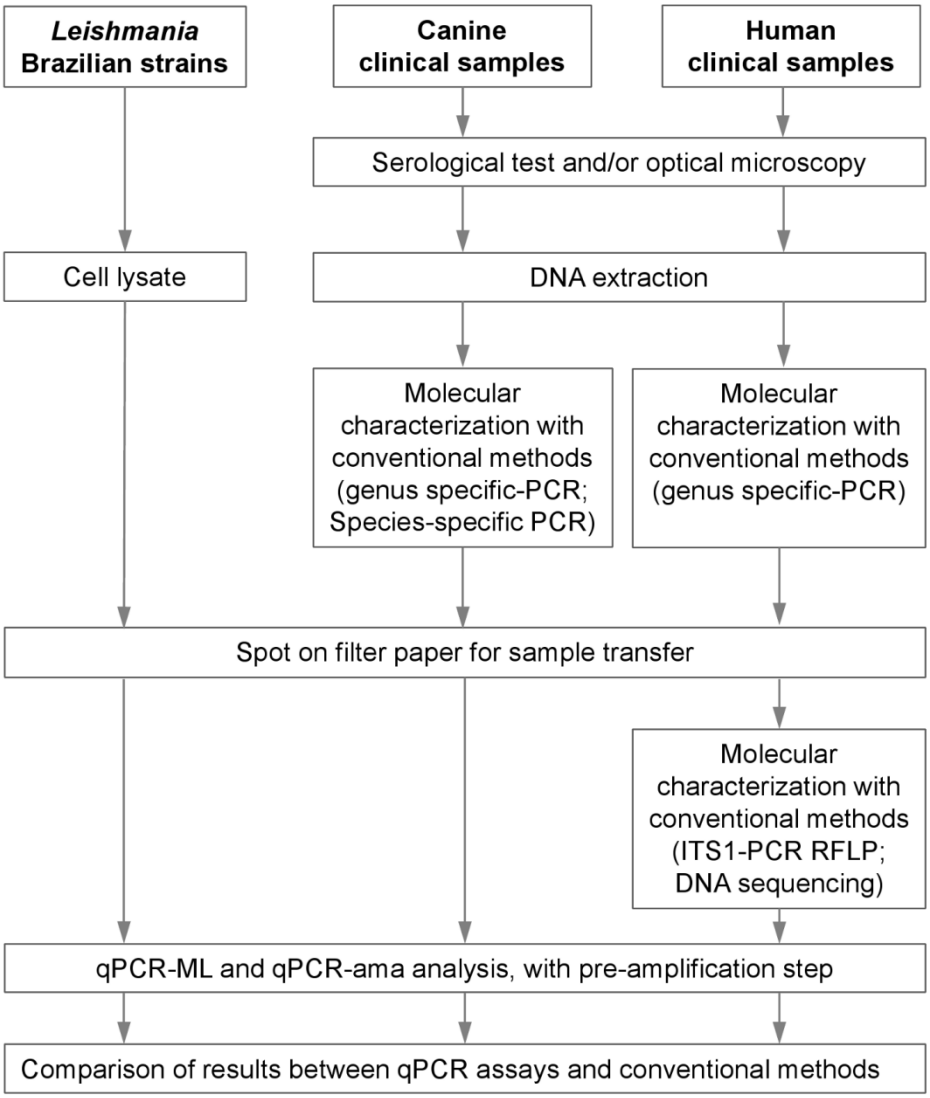

Fig. 2. Example of high resolution melting curve analysis for qPCR-ML amplicons. The plot of the negative derivative of fluorescence (dF/dT) vs temperature is presented, showing melting transitions as peaks. Replicates are grouped for clarity. **a)** Curves obtained from reference strains *L.* (*V.*) *braziliensis* MHOM/BR/75/M2904 (Bin A), *L.* (*L.*) *amazonensis* MHOM/BR/00/LTB0016 (Bin B) and *L.* (*L.*) *infantum* MHOM/FR/78/LEM75 (Bin C); **b)** same curves including sample F8, assigned to *Viannia* subgenus (blue arrow); **c)** same curves including sample F6, assigned to *Leishmania* subgenus.

a

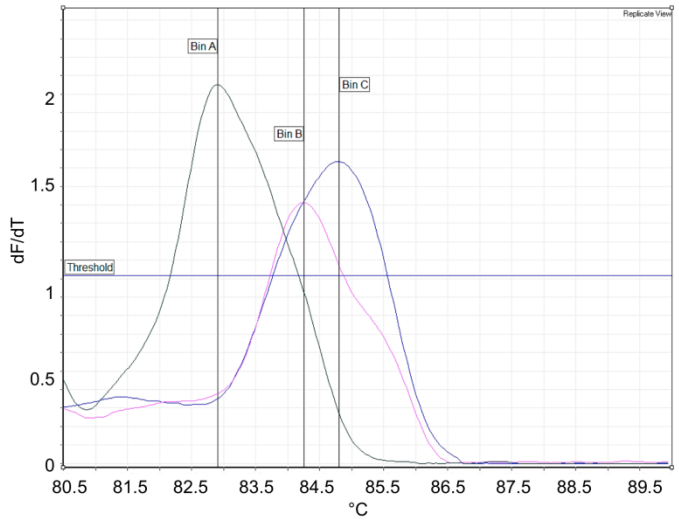

Name	Genotype	Peak 1
MHOM/FR/78/LEM75	Leishmania	84.83 (Bin C)
MHOM/FR/78/LEM75	Leishmania	84.73 (Bin C)
MHOM/BR/00/LTB0016	Leishmania	84.30 (Bin B)
MHOM/BR/00/LTB0016	Leishmania	84.20 (Bin B)
MHOM/BR/75/M2904	Viannia	82.93 (Bin A)
MHOM/BR/75/M2904	Viannia	82.88 (Bin A)

b

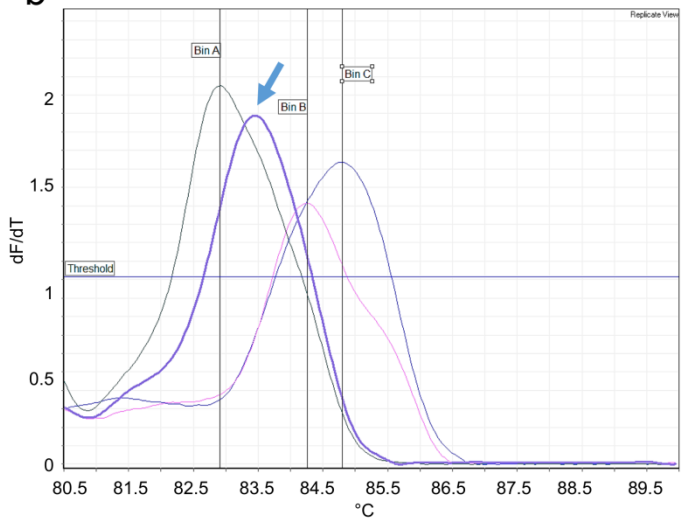

Name	Genotype	Peak 1
MHOM/FR/78/LEM75	Leishmania	84.83 (Bin C)
MHOM/FR/78/LEM75	Leishmania	84.73 (Bin C)
MHOM/BR/00/LTB0016	Leishmania	84.30 (Bin B)
MHOM/BR/00/LTB0016	Leishmania	84.20 (Bin B)
MHOM/BR/75/M2904	Viannia	82.93 (Bin A)
MHOM/BR/75/M2904	Viannia	82.88 (Bin A)
F8	Viannia	83.50 (Bin A)
F8	Viannia	83.42 (Bin A)

c

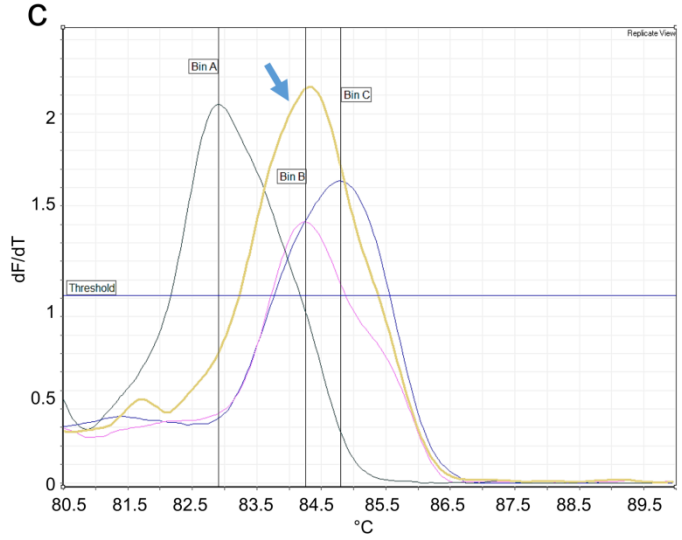

Name	Genotype	Peak 1
MHOM/FR/78/LEM75	Leishmania	84.83 (Bin C)
MHOM/FR/78/LEM75	Leishmania	84.73 (Bin C)
MHOM/BR/00/LTB0016	Leishmania	84.30 (Bin B)
MHOM/BR/00/LTB0016	Leishmania	84.20 (Bin B)
MHOM/BR/75/M2904	Viannia	82.93 (Bin A)
MHOM/BR/75/M2904	Viannia	82.88 (Bin A)
F6	Leishmania	84.30 (Bin B)
F6	Leishmania	84.33 (Bin B)

Table 1. qPCR-ML and qPCR-ama results in Brazilian strains

Species/strain	Sample ID	qPCR-ML (Cq ± SD)	qPCR-ama (Cq ± SD)	qPCR-ML (HRM T_m °C)	Species identification
L. (*L.*) *amazonensis* WHOM/BR/75/JOSEFA	F4	n.d.	18.38±0.17	n.d.	*L.*(*L.*) *amazonensis*
L. (*V.*) *braziliensis* MHOM/BR/1987/M11272	F5	29.67±0.15	35.54±0.02	83.56±0.01	*Viannia* subgenus
L. (*L.*) *infantum* MHOM/BR/2002/LPC-RPV	F6	20.37±0.06	31.39±0.31	84.30±0.04	*L.* (*L.*) *infantum*
L. (*L.*) *amazonensis* WHOM/BR/75/JOSEFA	F7	36.39±1.26	17.80±0.49	u.	*L.*(*L.*) *amazonensis*
L. (*V.*) *braziliensis* MHOM/BR/1987/M11272	F8	28.80±0.33	33.84±1.15	83.46±0.04	*Viannia* subgenus
L. (*L.*) *infantum* MHOM/BR/2002/LPC-RPV	F9	24.45±0.18	37.94±0.12	84.37±0.04	*L.* (*L.*) *infantum*

n.d. = not detectable

u. = unreliable since qPCR-ML Cq>>30

Table 2. Summary of results from canine samples

Source	sample ID	Serology[1]	Microscopy Identification[2]	Conventional PCR	Species identification (qPCR-ML and qPCR-ama)
Peripheral blood	A1	+	+	genus *Leishmania*[3]	-
	A2	+	+	genus *Leishmania*[3]	-
	A3	+	+	genus *Leishmania*[3]	-
	A4	+	+	genus *Leishmania*[3]	*L.* (*L.*) *infantum*
	A5	+	+	genus *Leishmania*[3]	*L.* (*L.*) *infantum*
	A6	+	+	genus *Leishmania*[3]	-
	A7	+	+	genus *Leishmania*[3]	-
	A8	+	+	genus *Leishmania*[3]	-
	A9	+	+	genus *Leishmania*[3]	*L.* (*L.*) *infantum*
	B1	+	+	genus *Leishmania*[3]	-
	B2	+	+	genus *Leishmania*[3]	-
	B3	+	+	genus *Leishmania*[3]	*L.* (*L.*) *infantum*
	B4	+	+	genus *Leishmania*[3]	*L.* (*L.*) *infantum*
Bone marrow	B5	+	+	*L.* (*L.*) *infantum*[4]	*L.* (*L.*) *infantum*
	B6	+	+	*L.* (*L.*) *infantum*[4]	*L.* (*L.*) *infantum*
	B7	+	+	*L.* (*L.*) *infantum*[4]	*L.* (*L.*) *infantum*

	B8	+	+	*L.* (*L.*) *infantum*[4]	*L.* (*L.*) *infantum*
	B9	+	+	*L.* (*L.*) *infantum*[4]	*L.* (*L.*) *infantum*
	C1	+	+	*L.* (*L.*) *infantum*[4]	*L.* (*L.*) *infantum*
	C2	+	+	*L.* (*L.*) *infantum*[4]	*L.* (*L.*) *infantum*
	C3	+	+	*L.* (*L.*) *infantum*[4]	*L.* (*L.*) *infantum*
	C4	+	+	*L.* (*L.*) *infantum*[4]	*L.* (*L.*) *infantum*
	C5	+	+	*L.* (*L.*) *infantum*[4]	*L.* (*L.*) *infantum*
	C6	+	+	*L.* (*L.*) *infantum*[4]	*L.* (*L.*) *infantum*
	C7	+	+	*L.* (*L.*) *infantum*[4]	*L.* (*L.*) *infantum*
	C8	+	+	*L.* (*L.*) *infantum*[4]	*L.* (*L.*) *infantum*
	C9	+	+	*L.* (*L.*) *infantum*[4]	*L.* (*L.*) *infantum*
	D1	+	+	*L.* (*L.*) *infantum*[4]	-
	D2	+	+	*L.* (*L.*) *infantum*[4]	*L.* (*L.*) *infantum*
	D3	+	+	*L.* (*L.*) *infantum*[4]	*L.* (*L.*) *infantum*
	D4	+	+	*L.* (*L.*) *infantum*[4]	*L.* (*L.*) *infantum*
	D5	+	+	*L.* (*L.*) *infantum*[4]	*L.* (*L.*) *infantum*
	D6	+	+	*L.* (*L.*) *infantum*[4]	*L.* (*L.*) *infantum*
	D7	+	+	*L.* (*L.*) *infantum*[4]	*L.* (*L.*) *infantum*
	D8	+	+	*L.* (*L.*) *infantum*[4]	*L.* (*L.*) *infantum*
	D9	+	+	*L.* (*L.*) *infantum*[4]	*L.* (*L.*) *infantum*

[1]immunochromatographic Dual-Path Platform and the ELISA test

[2]direct identification of suggestive forms of *Leishmania* amastigotes from Giemsa-stained smears analyzed by optical microscopy

[3]conventional PCR with primers specific for genus *Leishmania* (Rodgers et al., 1990)

[4]conventional PCR with primers specific for *L.* (*L.*) *infantum* (Gualda et al., 2015)

Source	sample ID	Serology[1]	Microscopy identification[2]	Conventional PCR[3]	ITS1-PCR RFLP[4]	ITS1 DNA sequencing	Species identification (qPCR-ML and qPCR-ama)
Peripheral blood	E1	+	n.a.	-	n.a.	n.a.	*L.* (*L.*) *infantum*
	E5	-	+	n.a.	*Viannia* subgenus	n.a.	*L.* (*L.*) *infantum* *Viannia* subgenus
	E6	+	n.a.	genus *Leishmania*	*L.* (*L.*) *infantum*	n.a.	*L.* (*L.*) *infantum*
	E7	+	n.a.	genus *Leishmania*	-	n.a.	*L.* (*L.*) *infantum*
	E8	+	n.a.	genus *Leishmania*	-	n.a.	*L.* (*L.*) *infantum* *Viannia* subgenus
	F2	n.a.	+*	-	*L.* (*L.*) *infantum*	*L.* (*L.*) *infantum*	*L.* (*L.*) *infantum*
	F3	n.a.	n.a.	genus *Leishmania*	*L.* (*L.*) *infantum*	*L.* (*L.*) *infantum*	*L.* (*L.*) *infantum*
Bone marrow	E2	-	+	genus *Leishmania*	n.a.	n.a.	*L.* (*L.*) *infantum*
	E3	-	+	genus *Leishmania*	-	n.a.	*L.* (*L.*) *amazonensis*

	E4	-	+	genus *Leishmania*	n.a.	n.a.	*L.* (*L.*) *infantum*
	E9	n.a.	n.a.	-	n.a.	n.a.	*L.* (*L.*) *infantum*

Table 3. Summary of results from human samples

[1]Rapid Test (rK39) for visceral leishmaniasis

[2]direct identification of suggestive forms of *Leishmania* amastigotes from Giemsa-stained smears analyzed by optical microscopy

[3]convencional PCR with primers specific for the genus *Leishmania* (Rodgers et al., 1990)

[4]ITS1-PCR RFLP according to Schonian et al (Schönian et al., 2003)

*from lesion of patient

n.a. not available

CHAPTER 2

This chapter contains the supplementary data, tables and images related to the article "Real-time PCR to differentiate among *Leishmania* (*Viannia*) subgenus, *Leishmania* (*Leishmania*) *infantum* and *Leishmania* (*Leishmania*) *amazonensis*: application on Brazilian clinical samples" of the previous chapter

Data article published in Data in Brief (pre-print version)

DOI: 10.1016/j.dib.2019.104914 Volume 28, February 2020, 104914

Data on the differentiation among *Leishmania* (*Viannia*) spp., *Leishmania* (*Leishmania*) *infantum* and *Leishmania* (*Leishmania*) *amazonensis* in Brazilian clinical samples using real-time PCR

Authors

Aurora Diotallevi[1], Gloria Buffi[1], Marcello Ceccarelli[1], Herintha Coeto Neitzke-Abreu[2], Laisa Vieira Gnutzmann[2], Manoel Sebastião da Costa Lima Junior[3], Alice Di Domenico[1], Mauro De Santi[1], Mauro Magnani[1], Luca Galluzzi[1]

Affiliations

1. Department of Biomolecular Sciences, University of Urbino "Carlo Bo", Urbino (PU), Italy
2. Programa de Pós-Graduação em Ciências da Saúde, Faculdade de Ciências da Saúde, Universidade Federal da Grande Dourados (UFGD), 79804-070, Dourados, MS, Brazil
3. Fundação Oswaldo Cruz (FIOCRUZ), Instituto Aggeu Magalhães, 50740-465, Recife, PE, Brazil

Corresponding author

Luca Galluzzi - luca.galluzzi@uniurb.it

1. Abstract

This article contains the data regarding *Leishmania* species identification in human and canine clinical samples from a Brazilian region endemic for *Leishmania* (*Viannia*) spp., *Leishmania* (*Leishmania*) *infantum* and *Leishmania* (*Leishmania*) *amazonensis*, using a previously developed approach involving two qPCR assays (qPCR-ML and qPCR-ama). The data are related to the article "Real-time PCR to differentiate among *Leishmania* (*Viannia*) subgenus, *Leishmania* (*Leishmania*) *infantum* and *Leishmania* (*Leishmania*) *amazonensis*: application on Brazilian clinical samples" [1] and include also details of

clinical evaluation/diagnosis of human patients and primers sequences used in the qPCR assays. The *Leishmania* species has been determined in 27 canine samples and 11 human samples, exploiting HRM analysis of qPCR-ML and Cq values of qPCR-ML and qPCR-ama, as reported previously [2]. The results were in agreement with the species characterization obtained with other methods such as conventional species-specific PCR, ITS1 PCR-RFLP or DNA sequencing. Despite the limited number of clinical samples, the results are encouraging for a potential application in regions where *L.* (*Viannia*) spp., *L*. (*L*.) *infantum* and *L*. (*L*.) *amazonensis* are co-endemic.

Keywords

Leishmania infantum; *Viannia*; *Leishmania amazonensis*; qPCR; real-time PCR; HRM

Specifications Table

Subject	Parasitology
Specific subject area	Molecular diagnostics
Type of data	Table Figure
How data were acquired	The qPCR assays were performed using Rotor-Gene 6000 instrument (Corbett life science). The qPCR runs were analyzed with Rotor-Gene software version 1.7 to obtain Cq values and High resolution melting temperatures.
Data format	Analyzed
Parameters for data collection	DNA extracted from clinical samples and strains was spotted on filter paper for storage and laboratory transfer. The qPCR assays (qPCR-ML and qPCR-ama), as well as ITS1 PCR, were performed directly from a punch of filter paper, with a pre-amplification step.

Description of data collection	HRM data obtained with qPCR-ML allowed to discriminate between subgenera *Viannia* and *Leishmania*. In case of subgenus *Leishmania*, the discrimination between *L. (L.) infantum* and *L. (L.) amazonensis* is performed through comparison of qPCR-ML and qPCR-ama Cq values. Both HRM and Cq data were collected by amplification of DNA extracted from clinical samples and spotted on filter paper.
Data source location	**Canine samples** Institution: Control Center of Zoonoses (CCZ) City/Town/Region: Campo Grande City/Mato Grosso do Sul Country: Brazil **Human samples** Institution: Hospital Universitário City/Town/Region: Dourados City/Mato Grosso do Sul Country: Brazil
Data accessibility	With the article
Related research article	Aurora Diotallevi, Gloria Buffi, Marcello Ceccarelli, Herintha Coeto Neitzke-Abreu, Laisa Vieira Gnutzmann, Manoel Sebastião da Costa Lima Junior, Alice Di Domenico, Mauro De Santi, Mauro Magnani, Luca Galluzzi. Real-time PCR to differentiate among *Leishmania* (*Viannia*) subgenus, *Leishmania* (*Leishmania*) *infantum* and *Leishmania* (*Leishmania*) *amazonensis*: application on Brazilian clinical samples. Acta Tropica, submitted paper

Value of the Data

- These data are useful to point out the potential field application of our SYBR Green-based qPCR assays to distinguish among *Leishmania* (*Viannia*) subgenus, *L*. (*L*.) *infantum* and *L*. (*L*.) *amazonensis*, exploiting HRM and Cq values.
- The rapid Leishmania species identification can be particularly useful for diagnosis in regions where *Leishmania* (*Viannia*) subgenus, *L*. (*L*.) *infantum* and *L*. (*L*.) *amazonensis* are co-endemic.

- These data can be considered to further develop qPCR-based assays for other species differentiation in the *Viannia* subgenus (e.g. *L*. (*V*.) *braziliensis* and *L*. (*V*.) *panamensis*) or in the *Leishmania* subgenus (e.g. *L*. (*L*.) *amazonensis* and *L*. (*L*.) *mexicana*).

Data

The presented data first describe the Clinical evaluation/diagnosis of human patients (Table 1) and the primers used in the qPCR assays targeting *Leishmania* minicircle kDNA (qPCR-ML and qPCR-ama) and host genes (Table 2). Then, the Cq and HRM values obtained from qPCR-ML and qPCR-ama used for *Leishmania* species identification in canine (n=36) and human (n=11) clinical samples spotted on filter paper are presented (Table 3 and Table 4, respectively). As a further confirmation of *Leishmania infantum* species identification, ITS1 amplicons from two human clinical samples were directly sequenced and a phylogenetic analysis was performed with ITS1 sequences from *L. (V.) braziliensis* (n=21) *L*. (*L*.) *infantum* (n=7) and *L*. (*L*.) *amazonensis* (n=4) available in genbank database (Fig. 1). Moreover, the data also show the specificity of qPCR-ML and qPCR-ama assays in the conditions used to amplify DNA samples from filter paper (Fig. 2).

2. Experimental Design, Materials, and Methods

2.1 Canine and human clinical samples

Thirty-six canine clinical samples and 11 human clinical samples were collected in Mato Grosso do Sul (Brazil), an endemic area of leishmaniasis. The canine samples consisted in 13 peripheral blood (A1-A9, B1-B4) and 23 bone marrow (B5-B9, C1-C9, D1-D9), collected by the Control Center of Zoonoses (CCZ) of Campo Grande City. Dogs were diagnosed positive for visceral canine leishmaniasis (VCL) by the immunochromatographic Dual-Path Platform (DPP™, Bio-Manguinhos/Fiocruz, Rio de Janeiro, Brazil) and the ELISA test (EIE™; Bio-Manguinhos/Fiocruz, Rio de Janeiro, Brazil), and direct identification of Leishmania amastigotes from Giemsa-stained smears analyzed by optical microscopy.

The human samples consisted in 7 peripheral blood (E1, E5-E8, F2, F3) and 4 bone marrow (E2-E4, E9), collected in Hospital Universitário of Dourados City from patients with a diagnosis of leishmaniasis. After evaluation of clinical signs (Table 1), patients were diagnosed using serology rapid test (rK39) (Kalazar Detect™; InBios, Washington, US) and/or direct identification of Leishmania amastigotes from Giemsa-stained smears analyzed by optical microscopy.

2.2 DNA extraction

DNA from canine and human clinical samples, positive for *Leishmania* infection, was obtained as follows. A 300 µl volume of sample was added to 500 µl of 20% Sodium Dodecyl Sulfate (Sigma-Aldrich) and homogenized. Then, 400 µl of chloroform and 300 µl of protein precipitation solution (3M potassium acetate, 11% glacial acetic acid) were added. After centrifugation at 10,000 x g for 10 min, the supernatant was transferred to new tubes containing 1 ml of cold absolute ethanol, gently homogenized by inversion and centrifuged for 5 min at 10,000 x g. The pellets were washed twice with 1 ml of 70% cold ethanol each time and centrifuged for 2 min at 10,000 x g. The supernatant was discarded and the pellet was dried in a dry bath (AccuBlock) at 65°C for 5 min. The DNA pellet was resuspended in TE buffer (10 mM Tris, 1 mM EDTA, pH 8.0) to a final concentration of 200-500 ng/µl, stored at 4 °C for 24 h, and then frozen at -20 °C. For sample transfer, DNA samples (8 µl) were spotted on filter paper (Macherey-Nagel MN 818), air-dried and stored at room temperature until analysis.

2.3 Quantitative PCR (qPCR) assays

The approach described in Ceccarelli et al. [2], consisting in running two qPCR reactions in parallel (qPCR-ML and qPCR-ama) to amplify different classes of minicircles, has been applied on sample DNA spotted on filter paper. The workflow of this approach involves first a discrimination between subgenera *Viannia* and *Leishmania* based on qPCR-ML HRM analysis, performed with primers MLF and MLR (Table 2); if this analysis indicates subgenus *Leishmania*, the discrimination between *L*. (*L*.) *infantum* and *L.* (*L*.) *amazonensis* is performed through comparison of qPCR-ML and qPCR-ama Cq values. The qPCR-ama was performed using the forward primer LMi-amaF and the reverse primer MLR (Table 2). All samples were tested blindly. To evaluate the DNA integrity and

amplifiability in canine and human samples, canine beta-2-microglobulin (B2M) and human glyceraldehyde-3-phosphate dehydrogenase (GAPDH) were amplified under the same conditions as the qPCR-ML and qPCR-ama (described below).

To ensure applicability with samples on filter paper, a pre-amplification step was introduced as follows. A punch of filter paper (2 mm in diameter) was placed in 40 µl SYBR green reaction mixture containing 200 nM of each primer. Three different PCR master mix were tested: SYBR green PCR master mix (Diatheva srl, Fano, Italy), RT2 SYBR Green ROX FAST Mastermix (Qiagen , Hilden, Germany), TB Green premix ex TaqII Mastermix (Takara Bio Europe, France). Tubes were placed in a thermal cycler (GeneAmp PCR System 2700), and pre-amplified under the following conditions: 94 °C for 5 min, 10 cycles at 94 °C for 30 s, 60 °C for 20 s and 72 °C for 20 s. At the end of this pre-amplification step, the tubes were centrifuged for few seconds and placed in ice; the filter paper was removed and the reaction was split into two PCR tubes (20 µl each tube). Then, the tubes were placed in the Rotor-Gene 6000 instrument and amplified as follows: 45 cycles at 94 °C for 30 s, 60 °C for 20 s and 72 °C for 20 s. As reference, PCR mixtures containing template DNA isolated from *L. (L.) infantum* MHOM/FR/78/LEM75, *L. (L.) amazonensis* MHOM/BR/00/LTB0016 and L*. (V.) braziliensis* MHOM/BR/75/M2904 were included in each run. A no template control (NTC) was included for each primer pair reaction. To monitor non-specific products or primer dimers, a melting analysis was performed from 79 to 95 °C at the end of each run, with a slope of 1 °C/s, and 5 s at each temperature. The Cq values were evaluated using the quantification analysis of the RotorGene 6000 software.

Trypanosoma cruzi and human DNA were amplified using the conditions described above to confirm qPCR_ML and qPCR-ama specificity with the three master mix used and including the pre-amplification step. The absence of specific amplicons was confirmed by visualization on 2% agarose gel electrophoresis.

2.4 High-resolution melt (HRM) analysis

The high-resolution melt (HRM) analysis was performed immediately after the amplification reactions in the Rotor-Gene 6000 instrument. HRM analysis was

conducted over the range from 79 °C to 90 °C, rising at 0.1 °C/s and waiting for 2 s at each temperature. Each sample was run in duplicate, and the gain was optimized before melting on all tubes. HRM curve analysis was performed with the derivative of the intensity of fluorescence at different temperatures (dF/dT), after smoothing, with the Rotor-Gene 6000 software. Only samples with Cq values < 30 were considered for analysis.Template DNA isolated from *L. (L.) infantum* MHOM/FR/78/LEM75 and L*. (L.) amazonensis* MHOM/BR/00/LTB0016 were used as reference for *Leishmania* subgenus, while template DNA from *L. (V.) braziliensis* MHOM/BR/75/M2904 was used as reference for *Viannia* subgenus. Bins were set to define Tm of amplicons for each species. Automated classification of genotypes (i.e. subgenus *Leishmania* or *Viannia*) of unknown samples was performed by the Rotor-Gene software according to the presence of a derivative peak located within a defined temperature bin.

2.5 ITS1 DNA sequencing and phylogenetic analysis

To confirm *Leishmania* species identification, ITS1 fragments, obtained by ITS1-PCR RFLP [3], were sequenced in two human samples (F2 and F3) as follows. The ITS1 amplicons were directly digested with 10 U HaeIII (Thermo Fisher Scientifc) at 37 °C for 3 h. The restriction fragments were visualized on a 3.5% high-resolution MetaPhor (Cambrex) agarose gel stained with GelRed (Biotium, Hayward, CA). The larger fragment was excised from gel, purified using MinElute Gel Extraction kit (Qiagen) and directly sequenced. DNA sequencing was performed using the BigDye Terminator v. 1.1 Cycle Sequencing Kit on an ABI PRISM 310 Genetic Analyzer (Applied Biosystems). The F2 and F3 sequences were aligned with ITS1 sequences from *L*. (*L*.) *infantum* (n=7), *L. (V.) braziliensis* (n=21) and *L*. (*L*.) *amazonensis* (n=4) available in GenBank database, using BioEdit Sequence Alignment Editor using default options. The phylogenetic analysis of aligned ITS1 fragments was conducted with MEGA 6 software. Phylogenetic relationships were inferred by using the maximum likelihood method and Tamura-Nei model. Bootstrap values were calculated from 100 replications.

Acknowledgments

We would like to thank Dr Francesca Andreoni and Dr Daniela Bencardino for DNA sequencing.

References

[1] A. Diotallevi, G. Buffi, M. Ceccarelli, H. Coeto Neitzke-Abreu, L. Vieira Gnutzmann, M. S. da Costa Lima Junior, A. Di Domenico, M. De Santi, M. Magnani, L. Galluzzi, Real-time PCR to differentiate among Leishmania (Viannia) subgenus, Leishmania (Leishmania) infantum and Leishmania (Leishmania) amazonensis: application on Brazilian clinical samples, Acta Tropica, submitted paper.

[2] Ceccarelli M., Galluzzi L., Diotallevi A., Andreoni F., Fowler H., Petersen C., Vitale F., Magnani M., 2017. The use of kDNA minicircle subclass relative abundance to differentiate between Leishmania (L.) infantum and Leishmania (L.) amazonensis. Parasit Vectors. 10, 239. https://doi.org/10.1186/s13071-017-2181-x.

[3] Schönian, G., Nasereddin, A., Dinse, N., Schweynoch, C., Schallig, H.D.F., Presber, W., Jaffe, C.L., 2003. PCR diagnosis and characterization of Leishmania in local and imported clinical samples. Diagn Microbiol Infect Dis 47, 349–358. https://doi:10.1016/S0732-8893(03)00093-2

Table 1. Diagnosis and clinical evaluation of human patients

sample ID	Diagnosis	Patient clinical evaluation
E1	VL	Anemia, splenomegaly
E2, E3, E4	VL	No clinical information
E5	VL	HIV patient, fever, pancytopenia, hyporexia
E6, E7	VL	Pancytopenia, hepatosplenomegaly
E8	VL	5 years old; hepatosplenomegaly, anemia, submandibular ganglia, fever, pancytopenia, abdominal distension
E9	n.a.	No clinical information
F2	CL	Nasal lesion
F3	VL	Anemia, splenomegaly

Table 2. Primer sequences for qPCR.

Target	Forward primer (5'-3')	Reverse primer (5'-3')
B2M canine	GTCCCACAGATCCCCCAAAG	CTGGTGGATGGAACCCTGAC
GAPDH human	CCATGTTCGTCATGGGTGTG	GGTGCTAAGCAGTTGGTGGTG
kDNA (qPCR-ML)	**MLF** - CGTTCTGCGAAAACCGAAA	**MLR** - CGGCCCTATTTTACACCAACC
kDNA (qPCR-ama)	**LMi-amaF** - AAAATGAGTGCAGAAACCC	**MLR** - CGGCCCTATTTTACACCAACC

B2M canine, *Canis familiaris* Beta-2-Microglobulin;

GAPDH human, *Homo sapiens* glyceraldehyde-3-phosphate dehydrogenase.

Table 3. qPCR-ML and qPCR-ama results in canine clinical samples.

Source	clinical sample (ID)	qPCR-ML (Cq ± SD)	qPCR-ama (Cq ± SD)	qPCR-ML (HRM T_m °C)	Results
Peripheral blood	A1 [1]	n.d.	n.d.	n.d.	-
	A2 [1]	n.d.	n.d.	n.d.	-
	A3 [1]	n.d.	n.d.	n.d.	-
	A4 [1]	20.58±0.62	31.83±0.89	84.08±0.11	*L.* (*L.*) *infantum*
	A5 [1]	26.51±0.40	n.d.	84.12±0.02	*L.* (*L.*) *infantum*
	A6 [1]	n.d.	n.d.	n.d.	-
	A7 [1]	n.d.	n.d.	n.d.	-
	A8 [1]	n.d.	n.d.	n.d.	-
	A9 [1]	27.60±1.39	39.23±0.81	84.03±0.04	*L.* (*L.*) *infantum*
	B1 [1]	n.d.	n.d.	n.d.	-
	B2 [1]	n.d.	n.d.	n.d.	-
	B3 [1]	23.69±0.14	32.28±0.66	83.64±0.01	*L.* (*L.*) *infantum*
	B4 [1]	18.16±0.35	24.77±0.16	83.95±0.32	*L.* (*L.*) *infantum*
Bone marrow	B5 [1]	17.96±0.17	26.09±0.09	83.94±0.08	*L.* (*L.*) *infantum*
	B6 [1]	22.90±0.30	30.34±0.08	84.08±0.11	*L.* (*L.*) *infantum*
	B7 [1]	17.39±4.53	25.93±3.47	83.79±0.02	*L.* (*L.*) *infantum*
	B8 [1]	18.18±3.62	25.12±2.64	84.05±0.14	*L.* (*L.*) *infantum*
	B9 [1]	25.58±1.20	33.57±0.86	84.90±0.04	*L.* (*L.*) *infantum*
	C1 [1]	17.41±3.39	26.27±2.25	83.85±0.02	*L.* (*L.*) *infantum*

	C2 [1]	14.80±0.23	22.62±0.01	83.96±0.08	*L.* (*L.*) *infantum*
	C3 [1]	16.02±0.13	23.73±0.07	84.12±0.02	*L.* (*L.*) *infantum*
	C4 [1]	17.53±0.06	25.20±0.06	83.97±0.07	*L.* (*L.*) *infantum*
	C5 [1]	14.57±0.22	22.43±0.13	83.90±0.07	*L.* (*L.*) *infantum*
	C6 [1]	25.95±10.55	n.d.	84.86±0.05	*L.* (*L.*) *infantum*
	C7 [1]	20.38±0.50	26.40±3.57	84.10±0.05	*L.* (*L.*) *infantum*
	C8 [1]	22.52±0.50	n.d.	84.05±0.05	*L.* (*L.*) *infantum*
	C9 [1]	30.81±0.35	n.d.	84.10±0.07	*L.* (*L.*) *infantum*
	D1 [1]	n.d.	n.d.	n.d.	-
	D2 [1]	28.51±3.35	n.d.	84.03±0.05	*L.* (*L.*) *infantum*
	D3 [2]	20.04±0.12	32.36±0.35	80.44±0.04	*L.* (*L.*) *infantum*
	D4 [2]	17.65±0.18	28.62±0.93	80.08±0.09	*L.* (*L.*) *infantum*
	D5 [2]	12.14±0.01	23.68±0.32	79.95±0.03	*L.* (*L.*) *infantum*
	D6 [2]	12.17±0.09	22.63±0.17	80.13±0.11	*L.* (*L.*) *infantum*
	D7 [2]	8.72±0.01	18.85±0.13	80.06±0.04	*L.* (*L.*) *infantum*
	D8 [2]	8.38±0.18	18.50±0.05	80.07±0.08	*L.* (*L.*) *infantum*
	D9 [1]	30.75±0.04	n.d.	84.10±0.08	*L.* (*L.*) *infantum*

n.d. = not detectable

[1]Samples tested with SYBR green PCR master mix (Diatheva srl)

[2]Samples tested with RT2 SYBR Green ROX FAST Mastermix (Qiagen)

Table 4. qPCR-ML and qPCR-ama results in human clinical samples.

Source	Human clinical sample (ID)	qPCR-ML (Cq ± SD)	qPCR-ama (Cq ± SD)	qPCR-ML (HRM T_m °C)	Results
Peripheral blood	E1 [1]	28.28±0.72	34.08±0.71	84.20±0.05	*L.* (*L.*) *infantum*
	E5 [2]	28.81±2.36	n.d.	83.27±0.05* 83.15±0.07	*L.* (*L.*) *infantum* *L.* (*V.*) *sp*
	E6 [1]	19.12±0.06	27.35±0.23	84.20±0.01	*L.* (*L.*) *infantum*
	E7 [1]	31.12±0.31	34.93±0.74	83.94±0.08	*L.* (*L.*) *infantum*
	E8 [2]	28.34±0.76	28.76±0.30	83.47±0.02* 82.75±0.28	*L.* (*L.*) *infantum* *L.* (*V.*) *sp*
	F2 [1]	33.85±3.11	n.d.	84.18±0.04	*L.* (*L.*) *infantum*
	F3 [1]	29.19±0.18	n.d.	84.14±0.06	*L.* (*L.*) *infantum*
Bone marrow	E2 [3]	27.80±0.84	n.d.	80.06±0.13	*L.* (*L.*) *infantum*
	E3 [3]	n.d.	30.35±1.55	n.d.	*L.* (*L.*) *amazonensis*
	E4 [3]	31.99±1.31	n.d.	80.65±0.05	*L.* (*L.*) *infantum*
	E9 [1]	27.78±1.34	n.d.	84.62±0.07	*L.* (*L.*) *infantum*

n.d. = not detectable

[1]Samples tested with SYBR green PCR master mix (Diatheva srl)

[2]Samples tested with SYBR green PCR master mix (Diatheva srl) and TB Green premix ex TaqII Mastermix (Takara)

[3]Samples tested with RT2 SYBR Green ROX FAST Mastermix (Qiagen)

* values obtained with TB Green premix ex TaqII Mastermix (Takara)

Fig. 1. Phylogenetic analysis of ITS1 fragments of F2 and F3 samples (red dotted line). The phylogenetic tree was constructed by using the maximum likelihood method and Tamura-Nei model. Numbers below branches represent bootstrap support.

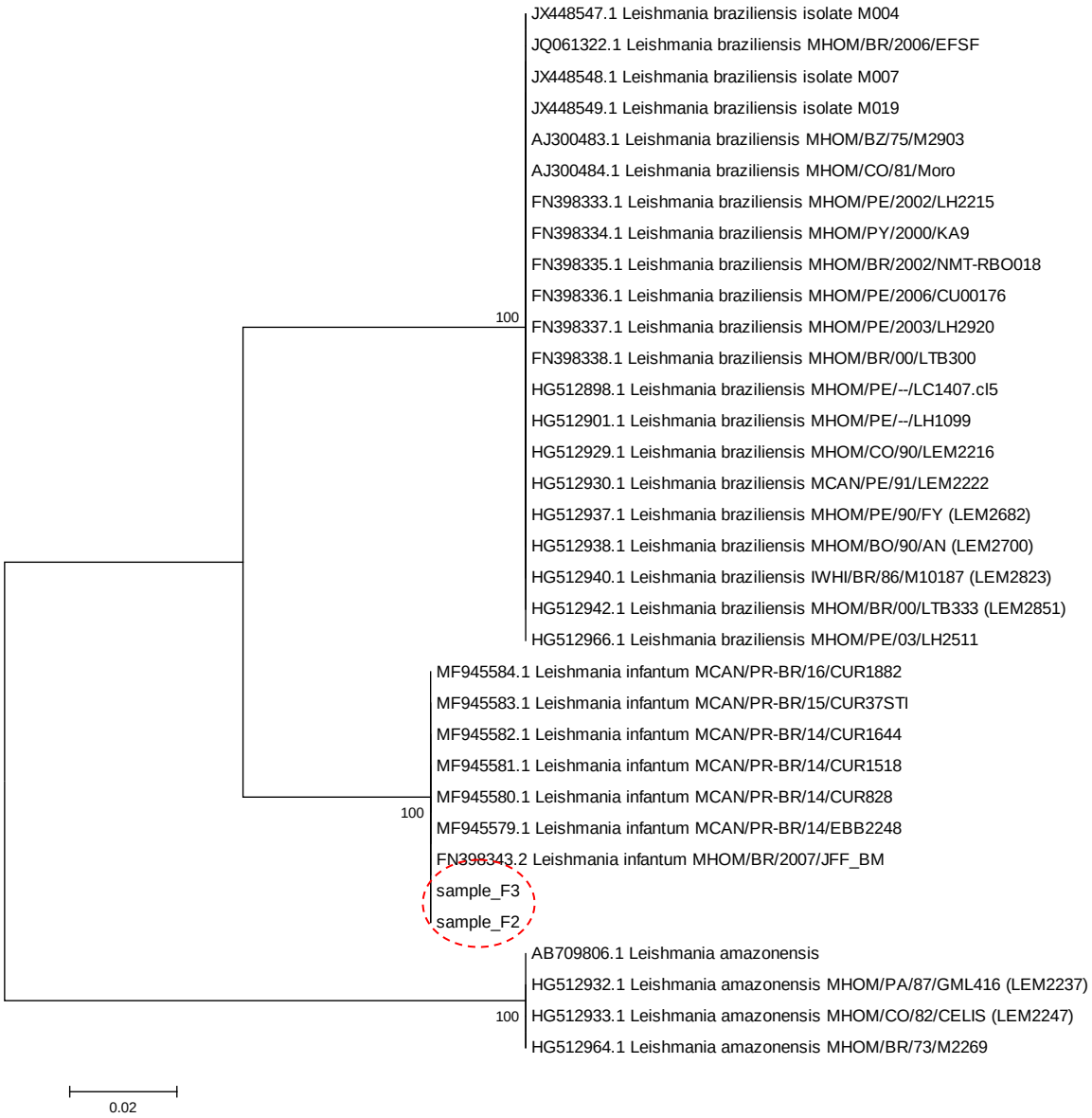

Fig. 2. Specificity of qPCR-ML (A) and qPCR-ama (B). qPCR amplicons were run on a 2 % agarose gel. Both qPCR assays were performed using three different PCR master mix: SYBR green PCR master mix, Diatheva (I); RT2 SYBR Green ROX FAST Mastermix, Qiagen (II); TB Green premix ex TaqII Mastermix, Takara Bio (III). For each master mix, DNA from *L.* (*L.*) *infantum* (0,006 ng/µl)*, L.* (*L.*) *amazonensis* (0,15 ng/µl)*, Trypanosoma cruzi* (0,1 ng/µl) and human DNA (30 ng/µl) were tested with the condition described in the manuscript. As negative control, a no template control was used for each qPCR run. M: ΦX174 DNA/BsuRI (HaeIII) Marker, 9 (ThermoFisher Scientific); NTC: no template control.

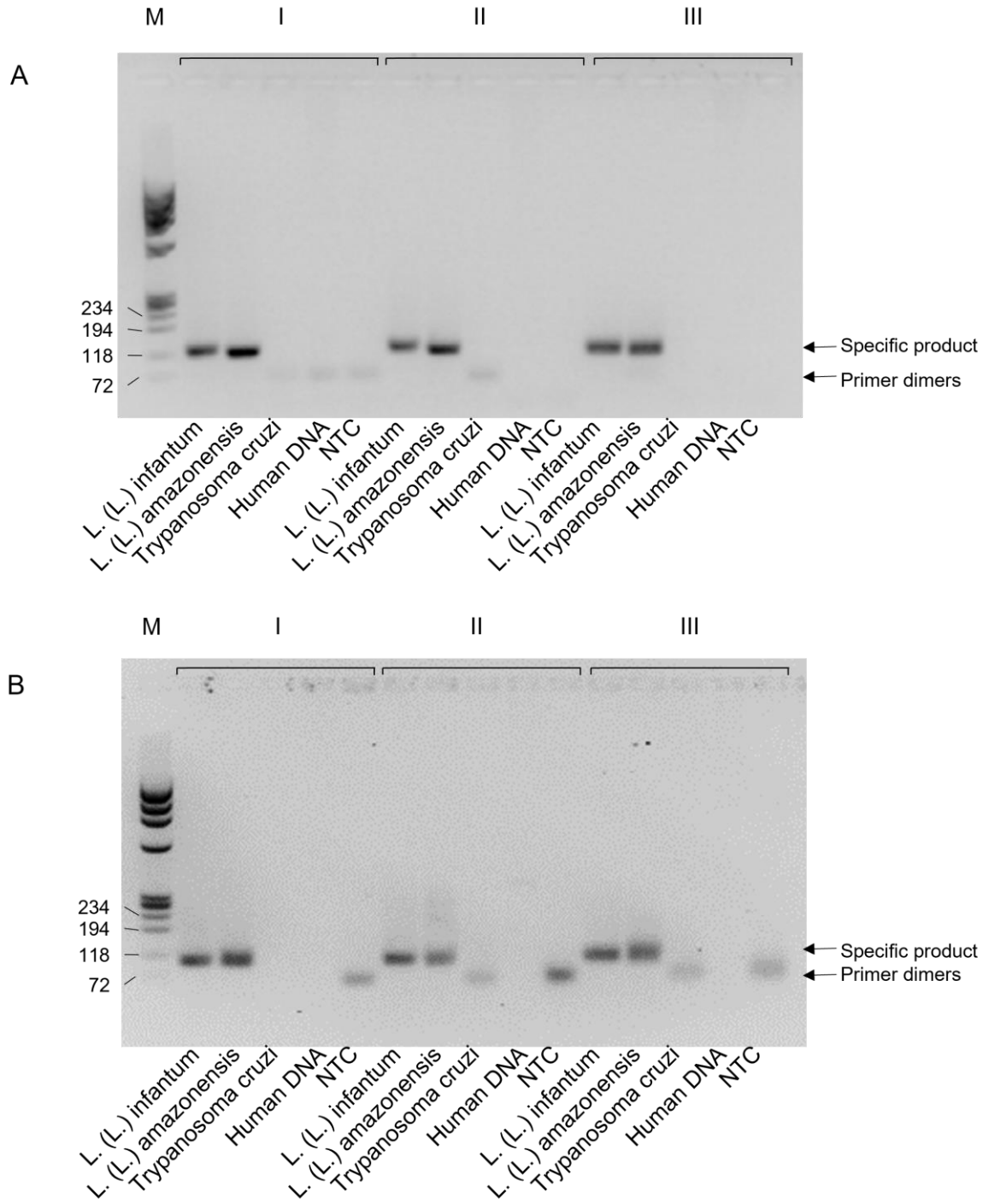

CHAPTER 3

This chapter consists of an original article about the application of sequential qPCR Assays and High-Resolution Melt Analysis to differentiate *Leishmania* (*L*.) *infantum*, *Leishmania* (*L*.) *amazonensis* and *Leishmania* (*L*.) *mexicana.*

Original article published in Microorganism

DOI: 10.3390/microorganisms8060818
Volume 8, Issue 6, 2020, 818

microorganisms

MDPI

Article

Differentiation of *Leishmania* (*L.*) *infantum*, *Leishmania* (*L.*) *amazonensis* and *Leishmania* (*L.*) *mexicana* Using Sequential qPCR Assays and High-Resolution Melt Analysis

Marcello Ceccarelli [1], Aurora Diotallevi [1], Gloria Buffi [1], Mauro De Santi [1], Edith A. Fernández-Figueroa [2,3], Claudia Rangel-Escareño [2,4], Said A. Muñoz-Montero [2], Ingeborg Becker [3], Mauro Magnani [1] and Luca Galluzzi [1,*]

[1] Department of Biomolecular Sciences, University of Urbino "Carlo Bo", 61029 Urbino (PU), Italy; m.ceccarelli3@campus.uniurb.it (M.C.); aurora.diotallevi@uniurb.it (A.D.); g.buffi@campus.uniurb.it (G.B.); mauro.desanti@uniurb.it (M.D.S.); mauro.magnani@uniurb.it (M.M.)

[2] Department of Population Genomics, Computational and Integrative Genomics, National Institute of Genomic Medicine, 14610 Mexico City, Mexico; efernandez@inmegen.gob.mx (E.A.F.-F.); crangel@inmegen.gob.mx (C.R.-E.); samunoz@inmegen.edu.mx (S.A.M.-M.)

[3] Centro de Medicina Tropical, Unidad de Investigación en Medicina Experimental, Facultad de Medicina, Universidad Nacional Autónoma de México, Hospital General de México, 04360 México City, México; becker@unam.mx

[4] School of Engineering and Sciences, Tecnologico de Monterrey, 76130 Queretaro, Mexico

***** Correspondence: luca.galluzzi@uniurb.it; Tel.: +39-0722-304976

Received: 8 April 2020; Accepted: 28 May 2020; Published: 29 May 2020

Abstract

Leishmania protozoa are the etiological agents of visceral, cutaneous and mucocutaneous leishmaniasis. In specific geographical regions, such as Latin America, several *Leishmania* species are endemic and simultaneously present; therefore, a diagnostic method for species discrimination is warranted. In this attempt, many qPCR-based assays have been developed. Recently, we have shown that *L. (L.) infantum* and *L. (L.) amazonensis* can be distinguished through the comparison of the Cq values from two qPCR assays (qPCR-ML and qPCR-ama), designed to amplify kDNA minicircle subclasses more represented in *L. (L.) infantum* and *L. (L.) amazonensis*, respectively. This paper describes the application of this approach to *L. (L.) mexicana* and introduces a new qPCR-ITS1 assay followed by high-resolution melt (HRM) analysis to differentiate this species from *L. (L.) amazonensis*. We show that *L. (L.) mexicana* can be distinguished from *L. (L.) infantum* using the same approach we had previously validated *for L. (L.)*

amazonensis. Moreover, it was also possible to reliably discriminate *L. (L.) mexicana* from *L. (L*.) *amazonensis* by using qPCR-ITS1 followed by an HRM analysis. Therefore, a diagnostic algorithm based on sequential qPCR assays coupled with HRM analysis was established to identify/differentiate *L. (L.) infantum*, *L. (L.) amazonensis*, *L. (L.) mexicana* and *Viannia* subgenus. These findings update and extend previous data published by our research group, providing an additional diagnostic tool in endemic areas with co-existing species.

Keywords: leishmania infantum; leishmania amazonensis; leishmania mexicana; qPCR; high resolution melting; kDNA; ITS1

---

1. Introduction

Leishmaniasis is caused by many *Leishmania* species belonging to subgenera *Leishmania* (*Leishmania*) and *Leishmania* (*Viannia*), creating a global public health problem with 0.2–0.4 million cases of visceral leishmaniasis (VL) and 0.7–1.2 million cases of cutaneous leishmaniasis (CL) per year [1]. In specific geographical regions, such as Central and South America, many *Leishmania* species are endemic and simultaneously present and, in some cases, can give rise to the same clinical form [2]. For instance, *L. (L.) amazonensis* and *L. (L.) mexicana* are responsible for the cutaneous manifestations and have a wide geographic distribution from Mexico to the north of Argentina. The epidemiological heterogeneity and difficulties in clinical approaches make species identification a critical step in clinical diagnosis and management, especially in case of co-infections. Therefore, an accurate diagnostic method allowing species identification is necessary [3]. Since the microscopic analysis does not provide information for species discrimination and the isoenzymatic characterization (i.e., multilocus enzyme electrophoresis) is a challenging and time-consuming technique, many biomolecular assays have been developed for *Leishmania* detection and species identification [4,5]. In particular, many qPCR assays have been designed to target the ribosomal DNA (rDNA) sequences and the kinetoplast DNA (kDNA) minicircle network that characterizes the *Leishmania* genus [6,7]. The rDNA sequence is repeated tens or

hundreds of times per cell, allowing acceptable sensitivity also with DNA from clinical samples. Moreover, the variability of the internal transcribed spacer (ITS) sequences can be exploited for typing at the species level [8]. The kDNA minicircles are about 800 bp long and are present in several thousands of copies per cell, which makes them ideal targets for highly sensitive PCR-based assays. Minicircles are characterized by conserved regions in their replication origin [9], which allows the design of PCR primers with broad taxonomic coverage. On the other hand, the minicircle network is composed of different subclasses presenting high sequence variability, with exception of the conserved regions [10]. The number and identity of minicircle subclasses vary greatly among *Leishmania* species [11–13]. These features make the design of qPCR assays for identification at the species level difficult to perform, even using probes or melting analysis [14–17]. To differentiate *L. (L.) infantum* from *L. (L.) amazonensis*, we recently proposed an approach based on the evaluation of relative abundance of minicircle subclasses by using two qPCR assays [18–20]. However, our previous works did not include *L. (L.) mexicana*, which is closely related to *L. (L.) amazonensis* [21].

In this paper, we also applied this diagnostic approach to *L. (L.) mexicana* species, with the aim to extend the validity of our previous work. Results showed that, as previously demonstrated for *L. (L.) amazonensis*, *L. (L.) mexicana* can also be distinguished from *L. (L.) infantum* by exploiting the two qPCR assays designed on minicircle kDNA. Moreover, it was also possible to reliably distinguish *L. (L.) mexicana* from *L. (L.) amazonensis* species using a new high-resolution melt (HRM) assay designed on the ITS1 region (qPCR-ITS1).

2. Materials and Methods

2.1. Leishmania Strains, Clinical Samples and DNA Extraction

The *Leishmania* strains and isolates used in this study are listed in Table 1. The *L*. (*L*.) *mexicana* clinical isolates 2, 3 and 5 were from diffuse cutaneous leishmaniasis lesions, whereas the clinical isolates 14, 17 and MHOM/MX/2011/Lacandona were from localized cutaneous leishmaniasis lesions. The clinical samples were taken from individuals from Quintana Roo, an endemic area of leishmaniasis in Mexico, as well as from patients treated at the Tropical Medicine Center, Medical Faculty, National

Autonomous University of Mexico (UNAM); all patients were clinically diagnosed as diffuse or localized cutaneous leishmaniasis by Giemsa-stained smears of the lesions and by ELISA test for *Leishmania* (Table 2).

The DNA was extracted from promastigote cultures and from clinical samples using phenol-chloroform standard procedures followed by ethanol precipitation and the High Pure PCR Template Preparation Kit (Roche, Mannheim, Germany). The DNA was quantified using a Qubit fluorometer (Life Technologies, Carlsbad, USA) and stored at −20 °C until being used.

Table 1. *Leishmania* spp reference strains/clinical isolates used in this study.

Species	Strain/Isolate
L. (L.) infantum	MHOM/TN/80/IPT1
L. (L.) infantum	MHOM/IT/86/ISS218
L. (L.) infantum	MHOM/FR/78/LEM75
L. (L.) amazonensis	MHOM/BR/00/LTB0016
L. (L.) amazonensis	IFLA/BR/67/PH8
L. (L.) amazonensis	Clinical isolate
L. (V.) braziliensis	MHOM/BR/75/M2904
L. (L.) mexicana	MHOM/MX/2011/Lacandona
L. (L.) mexicana	Clinical isolate 2
L. (L.) mexicana	Clinical isolate 3
L. (L.) mexicana	Clinical isolate 5
L. (L.) mexicana	Clinical isolate 14
L. (L.) mexicana	Clinical isolate 17

Table 2. Clinical samples used in this study.

Sample	Species Identification (ITS1-PCR RFLP)	Species Identification (*ALAT* sequencing)	CL Form
Px1	*L. (L.) mexicana*	n.a. [1]	LCL
Px2	*L. (L.) mexicana*	*L. (L.) mexicana*	LCL
Px3	*L. (L.) mexicana*	*L. (L.) mexicana*	LCL
Px4	*L. (L.) mexicana*	n.a. [1]	LCL
Px5	*L. (L.) mexicana*	n.a. [1]	DCL
Px7	*L. (L.) mexicana*	n.a. [1]	LCL
Px9	*L. (L.) mexicana*	*L. (L.) mexicana*	DCL
Px10	*L. (L.) mexicana*	*L. (L.) mexicana*	LCL
PxGSF	*L. (L.) mexicana*	n.a. [1]	LCL
PxCMU	n.a. [1]	n.a. [1]	n.a. [1]
PxJLC	*L. (L.) mexicana*	*L. (L.) mexicana*	LCL

[1] not available.

2.2. ITS1-PCR RFLP

The *L*. (*L*.) *mexicana* strains and clinical samples were typed using ITS1-PCR RFLP according to Monroy-Ostria et al. [22]. Briefly, the PCR was performed using primers LITSR and L5.8S, following the amplification protocol—94 °C for 4 min followed by 36 cycles of 94 °C for 40 s, 54 °C for 30 s and 72 °C for 1 min and a final extension at 72 °C for 6 min. PCR products were nested using the same PCR conditions for 18 cycles. PCR products were digested with *Hae*III for 3 h at 37 °C and for 20 min at 80 °C to inactivate the enzyme. The restriction fragments were subjected to electrophoresis on a 4% agarose gel.

2.3. DNA Sequencing and Phylogenetic Analysis

The alanine aminotransferase (*ALAT*) gene was amplified in clinical samples px2, px3, px9, px10, pxJLC and in *L.* (*L.*) *mexicana* MHOM/MX/2011/Lacandona according to Marco et al. [23] using primers ALAT.F and ALAT.R. The amplification conditions were—94 °C for 3 min followed by 40 cycles of 94 °C for 30 s, 55 °C for 30 s and 72 °C for 30 s. PCR products were purified using the Agencourt AMPure XP kit (Beckman Coulter, Brea, CA, USA) and sequenced using the BigDye Terminator v3.1 Cycle Sequencing Kit (Thermo Fisher Scientific, Waltham, MA, USA) on ABI 3730xL DNA Analyzer (Thermo Fisher Scientific, Waltham, MA, USA). Chromatograms were visualized with ApE software and consensus sequences were generated and compared between them and with other validated species of *L. (L.) mexicana* deposited in GenBank using the Blastn tool available in the same platform. A phylogenetic reconstruction based on the Maximum Likelihood (ML) method was generated and a phylogenetic tree was constructed with 10,000 bootstrap replications, using the close-neighbor interchange method in Mega 6.0.

2.4. qPCR Assays

The qPCR-ML (amplifying kDNA minicircle subclass more represented in *L.* (*L.*) *infantum*) and qPCR-ama (amplifying kDNA minicircle subclass more represented in *L*. (*L*.) *amazonensis*) were performed as previously described [18]. The new assay qPCR-ITS1 was performed using the new primers ITS1mexama_F (5'-GGATCATTTTCCGATGATTACACC-3') and ITS1mexama_R (5'-

CTGCAAATGTTGTTTTTGAGTACA-3'), flanking a portion of ITS1 sequence containing differences between *L*. (*L*.) *amazonensis* and *L.* (*L.*) *mexicana* (Figure 1). The primers were designed using Primer BLAST and were verified against the ITS1 sequences of *L*. (*L*.) *amazonensis* (*n* = 32) and *L.* (*L.*) *mexicana* (*n* = 30) encompassing forward and/or reverse primers, available in the Genbank database.

```
DQ182536.1   753  GTAGGTGAACCT---GCAGCTGGATCATTTTCCGATGATTACACCaaaaaaa-CATATAC  808
                  ||||||||||||   |||||||||||||||||||||||||||||||||| |||||||
AF466382.1   1    GTAGGTGAACCTGCAGCAGCTGGATCATTTTCCGATGATTACACCAAAAAAAACATATAC  60

DQ182536.1   809  --AAAACTCTCGGGGAGACCTATTCTTTCGATAGGCGCCTTTCCCACACAT--ACACAGC  864
                    ||||||||||||||| |||||||||||||||||||||||||||||||  |||||||
AF466382.1   61   AAAAAACTCTCGGGGAGGCCTATTCTTTCGATAGGCGCCTTTCCCACACATACACACAGC  120

DQ182536.1   865  AAAGTTTTTGTACTCAAAAACAACATTTGCAGTAAACAAAAAATGGCCGATCGACGTTAT  924
                  ||||||||||||||||||||||||||||||||||||||||||| ||||||||||||||||
AF466382.1   121  AAAGTTTTTGTACTCAAAAACAACATTTGCAGTAAACAAAAAAAGGCCGATCGACGTTAT  180
```

Figure 1. Alignment of ITS1 partial sequence of *L*. (*L*.) *amazonensis* MHOM/BR/73/M2269 (acc. n. DQ182536.1) and *L*. (*L*.) *mexicana* MHOM/MX/98/UNAM (acc. n. AF466382.1). Highlighted sequences represent primers ITS1mexama_F and ITS1mexama_R. Sequences are representative of *L*. (*L*.) *amazonensis* (*n* = 32) and *L*. (*L*.) *mexicana* (*n* = 30) ITS1 sequences available in the Genbank database.

For all assays, PCR reactions were carried out in a 25 µL volume with 1–3 µL of template DNA using SYBR green PCR master mix (Diatheva srl, Fano, Italy) or TB Green premix ex TaqII Mastermix (Takara Bio Europe, France) and 200 nM of each primer in a Rotor-Gene 6000 instrument (Corbett Life Science, Mortlake, Australia). The amplification conditions were—94 °C for 10 min, 40 cycles at 94 °C for 25 s, 60 °C for 20 s and 72 °C for 20 s. At the end of each run, a melting curve analysis was performed from 78 to 92 °C with a slope of 1 °C/s, and 5 s at each temperature. The reactions were performed in duplicate. Dilution curves (from 1.0 to 1 × 10^{-5} ng/reaction) were established using *L.* (*L.*) *mexicana* MHOM/MX/2011/Lacandona DNA for qPCR-ML, qPCR-ama and qPCR-ITS1. The threshold cycles (Cq) were determined using the quantitation analysis of the Rotor-Gene 6000 software, setting a threshold to 0.15. To evaluate the potential interference of host DNA as a background in the qPCR analysis, 30 ng of human DNA was spiked in the reaction tubes.

2.5. High-Resolution Melt (HRM) Analysis

The qPCR-ML, qPCR-ama and qPCR-ITS1 amplicons were analyzed by HRM protocol on a Rotor-Gene 6000 instrument as described previously [24] with few modifications.

Briefly, HRM was carried out over the range from 80 to 90 °C (qPCR-ML, qPCR-ama) or 75 to 85 °C (qPCR-ITS1), rising at 0.1 °C/s and waiting for 2 s at each temperature. Each sample was run in duplicate, and the gain was optimized before melting on all tubes.

2.6. Ethics Approval

This study was conducted according to the principles expressed in the Declaration of Helsinki. This research was approved by the Institutional Ethics Committee of the Medical Faculty of the National Autonomous University of Mexico (FM/DI/013/SR/2019). Guidelines established by the Mexican Health Authorities were strictly followed. All patients received treatment and clinical care by health authorities and signed a written informed consent for the collection of samples and subsequent analysis.

2.7. Statistical Analysis

Statistical analysis was performed with GraphPad Prism 5.0 (GraphPad Software, San Diego, CA, USA). Normal distribution of data was assessed by D'Agostino and Pearson omnibus normality test (alpha = 0.05). Difference between Tm mean values was evaluated using the nonparametric Mann–Whitney test.

3. Results

3.1. Both L. (L.) mexicana and L. (L.) amazonensis Can be Distinguished from L. (L.) infantum Exploiting A Differential qPCR Targeting Minicircle kDNA

Previously, we have shown that *L.* (*L.*) *infantum* and *L.* (*L.*) *amazonensis* can be distinguished by comparing the Cq values of two qPCR assays (qPCR-ML and qPCR ama). In this work, the qPCR-ML and qPCR-ama were sequentially performed using DNA from *L.* (*L.*) *mexicana* MHOM/MX/2011/Lacandona, isolate 2, isolate 3, isolate 5, isolate 14 and isolate 17 as templates. As already shown for *L.* (*L.*) *amazonensis* strains, Cq values obtained with qPCR-ama were much lower compared to those obtained with qPCR-ML (Table 3).

Table 3. qPCR-ML and qPCR-ama results in strains/clinical isolates.

Leishmania Species, Strain/Isolate	DNA Template (ng)	qPCR-ML (Cq ± SD)	qPCR-ama (Cq ± SD)
L. (*L.*) *mexicana* MHOM/MX/2011/Lacandona	1.0	31.61 ± 2.03	14.25 ± 0.69
L. (*L.*) *mexicana* MHOM/MX/2011/Lacandona	1.0×10^{-1}	33.43 ± 2.09	17.48 ± 1.13
L. (*L.*) *mexicana* MHOM/MX/2011/Lacandona	1.0×10^{-2}	37.53 ± 1.27	20.68 ± 1.46
L. (*L.*) *mexicana* MHOM/MX/2011/Lacandona	1.0×10^{-3}	n.d. [1]	24.07 ± 1.09
L. (*L.*) *mexicana* MHOM/MX/2011/Lacandona	1.0×10^{-4}	n.d. [1]	27.37 ± 1.05
L. (*L.*) *mexicana* MHOM/MX/2011/Lacandona	1.0×10^{-5}	n.d.[1]	31.36 ± 0.93
L. (*L.*) *mexicana* Isolate 2	1.0	33.19 ± 1.34	16.78 ± 0.06
L. (*L.*) *mexicana* Isolate 3	1.0	33.62 ± 2.14	18.62 ± 1.12
L. (*L.*) *mexicana* Isolate 5	1.0	38.19 ± 1.01	20.14 ± 0.43
L. (*L.*) *mexicana* Isolate 14	1.0	34.59 ± 0.51	16.54 ± 0.17
L. (*L.*) *mexicana* Isolate 17	1.0	35.94 ± 1.20	19.15 ± 1.00
L. (*L.*) *amazonensis* MHOM/BR/00/LTB0016	1.0×10^{-1}	33.95 ± 0.34	21.1 ±1.02
L. (*L.*) *infantum* MHOM/FR/78/LEM75	1.0	14.42 ± 0.75	28.02 ± 0.98

[1] not detectable.

The Cq difference between qPCR-ama and qPCR-ML allowed us to include *L.* (*L.*) *mexicana* among the *Leishmania* (*Leishmania*) species that can be distinguished from *L.* (*L.*) *infantum.* Results from *L.* (*L.*) *amazonensis* MHOM/BR/00/LTB0016 and *L.* (*L.*) *infantum* MHOM/FR/78/LEM75 were included as representative results obtained previously. As a consequence of different minicircle subclass amplified, the qPCR-ML and qPCR-ama showed a different limit of detection, allowing to amplify up to 1.0×10^{-2} and 1.0×10^{-5} ng of *L.* (*L.*) *mexicana* MHOM/MX/2011/Lacandona DNA, respectively (Table 3). In the qPCR-ML, the presence of 30 ng of purified human DNA delayed the limit of detection to 1.0×10^{-1} ng (Figure S1). With regard to qPCR-ama, the efficiency and detection limit were evaluated using 10-fold *L.* (*L.*) *mexicana* MHOM/MX/2011/Lacandona DNA serial dilutions (from 1.0 to 1×10^{-5} ng) in three independent experiments. There was a linear correlation between the log of DNA concentration and Cq value (slope = −3.3909, $R^2 = 0.9716$) with a reaction efficiency of 97%. In order to evaluate the interference of host DNA, the DNA dilutions were spiked with 30 ng of purified human DNA, showing a delay on the Cq values but with

comparable efficiency and limit of detection (Figure 2). The efficiency and detection limit obtained with *L.* (*L.*) *mexicana* DNA were in agreement with previous results obtained using DNA template from *L*. (*L*.) *amazonensis* [18].

The qPCR-ML/qPCR-ama approach was also applied to 11 clinical samples. These samples were characterized as *L.* (*L.*) *mexicana* by ITS1-PCR RFLP (Figure S2), with the exception of pxCMU, for which a digestion profile could not be obtained. Moreover, the genotype of five clinical samples (px2, px3, px9, px10, pxJLC) were further confirmed as *L.* (*L.*) *mexicana* by sequencing and phylogenetic analysis of the alanine aminotransferase (ALAT) gene (Figure S3). All samples showed Cq qPCR-ama <Cq qPCR-ML (Table 4), confirming the presence of *L.* (*L.*) *mexicana* parasites.

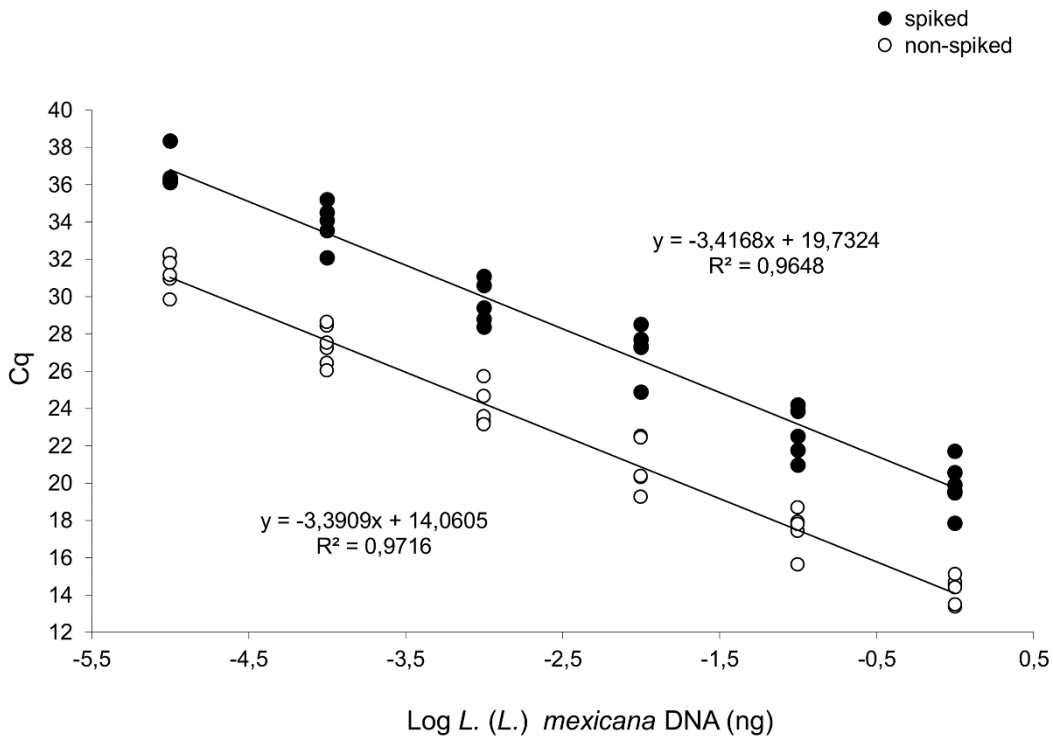

Figure 2. qPCR-ama curves constructed with serial dilutions of *L*. (*L*.) *mexicana* MHOM/MX/2011/Lacandona DNA. The curves were obtained with serial dilutions ranging from 1.0 to 1.0 × 10^{-5} ng/tube, spiked with 30 ng human DNA (upper curve, y = −3.4168x + 19.73; R^2 = 0.9648) or nonspiked (lower curve, y = −3.3909x + 14.0605; R^2 = 0.9716). Results were from three independent experiments in duplicate.

Table 4. qPCR-ML and qPCR-ama results in clinical samples.

Sample ID	qPCR-ML (Cq ± SD)	qPCR-ama (Cq ± SD)
Px1	n.d. [1]	27.71 ± 0.08
Px2	n.d. [1]	25.79 ± 0.55
Px3	n.d. [1]	24.57 ± 0.58
Px4	36.21 ± 1.99	29.59 ± 0.80
Px5	n.d. [1]	28.99 ± 1.57
Px7	35.31 ± 1.47	28.04 ± 0.25
Px9	n.d. [1]	28.35 ± 1.93
Px10	n.d. [1]	24.92 ± 0.87
PxGSF	36.38 ± 1.70	29.49 ± 0.53
PxCMU	36.53 ± 1.36	31.48 ± 0.36
PxJLC	n.d. [1]	34.87 ± 1.93

[1] not detectable.

3.2. L. (L.) amazonensis Can be Differentiated from L. (L.) mexicana by qPCR-ITS1 HRM Analysis

In the attempt to differentiate *L.* (*L.*) *mexicana* and *L.* (*L.*) *amazonensis*, HRM analyses were performed after qPCR-ML and qPCR-ama using the *L.* (*L.*) *mexicana* and *L.* (*L.*) *amazonensis* samples indicated in Tables 1 and 2. However, both assays did not allow us to distinguish the two species reliably. In particular, the qPCR-ML assay showed overly high Cq values (>30) in *L.* (*L.*) *mexicana* samples. Concerning the qPCR-ama assay, HRM analysis of all *L.* (*L.*) *mexicana* and *L.* (*L.*) *amazonensis* samples showed heterogeneous profiles (Figure S4). Moreover, despite that the mean Tm of PCR products from *L.* (*L.*) *mexicana* and *L.* (*L.*) *amazonensis* were significantly different (Mann–Whitney test, $p < 0.01$), the Tm value distributions partly overlapped, de facto making the distinction between the two species unreliable (Figure 3).

Therefore, a new qPCR assay and HRM analysis were designed on ITS1 sequences. The in silico analysis showed that PCR product lengths were 125–126 and 129–131 bp for *L.* (*L.*) *amazonensis* and *L.* (*L.*) *mexicana*, respectively. The qPCR-ITS1 efficiency and detection limit were evaluated using 10-fold *L.* (*L.*) *mexicana* MHOM/MX/2011/Lacandona DNA serial dilutions (from 1.0 to 1×10^{-4} ng). A linear correlation between the log of DNA concentration and Cq value was demonstrated (slope = −3.6227, $R^2 = 0.997$), with a reaction efficiency of 89%. As shown for the qPCR-ama, spiking with 30 ng of purified human DNA induced a delay on the Cq values, but

efficiency and limit of detection were not affected (Figure 4). The Tm analysis of qPCR-ITS1 amplicons obtained from all amplified *L.* (*L.*) *amazonensis* and *L.* (*L.*) *mexicana* samples allowed full discrimination between the two species (Mann–Whitney test, $p < 0.001$) (Figure 5) (Table S1). However, three clinical samples failed to amplify (Px7, PxGSF, PxCMU). Overall, the qPCR-ITS1 HRM assay for *amazonensis*/*mexicana* species discrimination showed 84.2% sensitivity and 100% specificity.

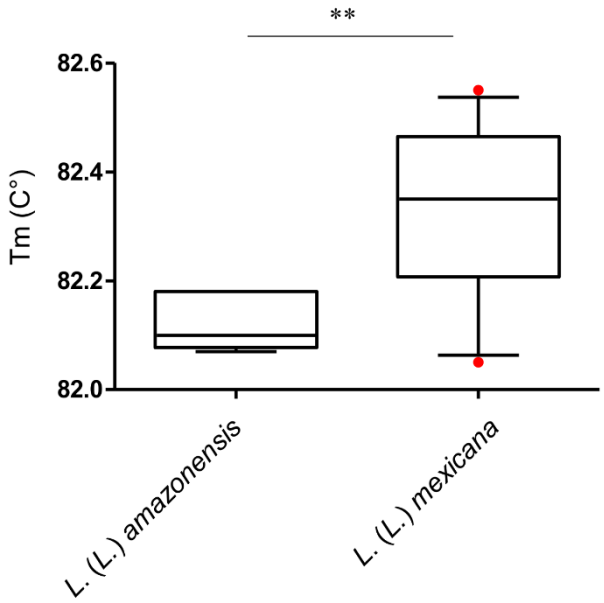

Figure 3. Box and whisker plot with 5–95% confidence interval showing Tm values distribution obtained with high-resolution melt (HRM) analysis of qPCR-ama amplicons of *L.* (*L.*) *mexicana* ($n = 32$) and *L.* (*L.*) *amazonensis* ($n = 6$). Line within the box represents the median and the red dots above and below the whiskers represent the outliers that are either greater than 95th or less than 5th percentile. ** $p < 0.01$.

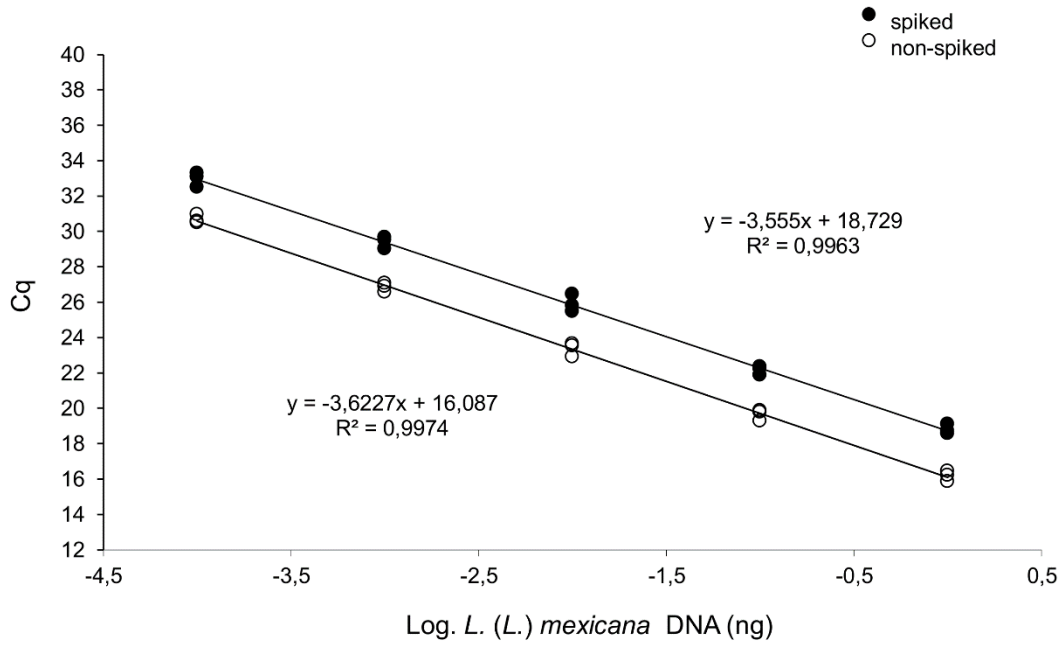

Figure 4. qPCR-ITS1 curves constructed with serial dilutions of *L*. (*L*.) *mexicana* MHOM/MX/2011/Lacandona DNA. The curves were obtained with serial dilutions ranging from 1.0 to 1.0 × 10^{-4} ng/tube, spiked with 30 ng human DNA (upper curve, y = −3.555x + 18.729; R^2 = 0.996) or nonspiked (lower curve, y = −3.623x + 16.087; R^2 = 0.997). Triplicates of the PCR amplification are represented.

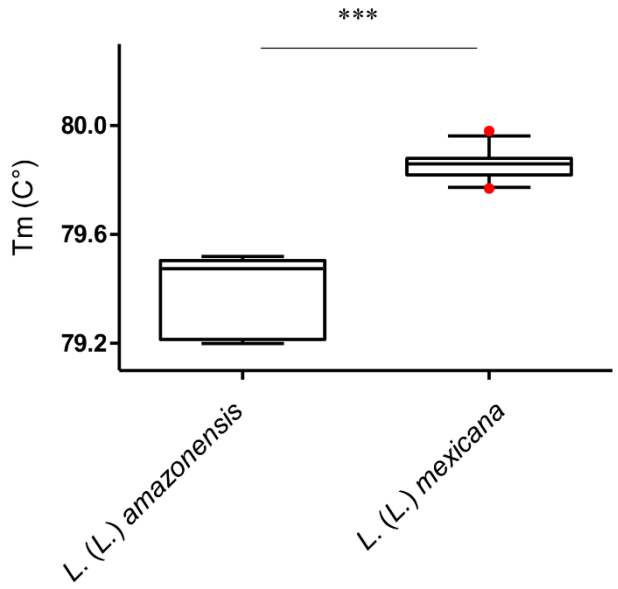

Figure 5. Box and whisker plot with 5–95% confidence interval showing Tm value distribution obtained with HRM analysis of qPCR-ITS1 amplicons of *L*. (*L*.) *mexicana* (*n* = 26) and *L*. (*L*.) *amazonensis* (*n* = 6). Line within the box represents the median and the red dots above and below the whiskers represent the outliers that are either greater than 95th or less than 5th percentile. *** $p < 0.001$.

4. Discussion

The identification of *Leishmania* species is an important diagnostic aspect, especially in Latin America, not only for epidemiological studies but also for the accurate monitoring of clinical disease evolution. In fact, the only species causing VL in this geographical region is *L*. (*L*.) *infantum* (syn. *chagasi*), while cutaneous or mucocutaneous (MCL) manifestations can also be generated by *Viannia* subgenus and *L.* (*L*.) *mexicana* complex. In this epidemiological and clinical context, the species discrimination appears pivotal, e.g., to monitor a cutaneous lesion that could evolve in VL, MCL or disseminated CL, depending on the species. In this view, molecular diagnostic tools allowing species discrimination can be helpful. The kDNA minicircles are ideal targets for highly sensitive molecular detection of *Leishmania* spp. since they are present in thousands of copies per cell [25]. Since the pioneering work of Nicolas et al. [26], many qPCR assays have been designed on conserved regions of minicircles to detect/quantify *Leishmania* parasites. Moreover, several authors investigated the possibility to exploit minicircle sequences to discriminate *Leishmania* parasites at the species level, reaching only partial results due to the variability of minicircle subclasses [15,16]. Previously, we proposed an SYBR Green qPCR-based approach to distinguish *L*. (*L*.) *infantum* from *L*. (*L*.) *amazonensis*, exploiting the different abundance of minicircle subclasses rather than targeting a species-specific sequence. Using this approach, which relies on two qPCR assays (qPCR-ML and qPCR-ama) and evaluation of Cq values, we were able to distinguish the two species adequately [18].

In this work, we tested this approach with *L.* (*L*.) *mexicana*, which is genetically close to *L.* (*L*.) *amazonensis*. The comparison of Cq values of qPCR-ML and qPCR-ama confirmed results previously obtained with *L*. (*L*.) *amazonensis,* allowing us to include *L.* (*L.*) *mexicana* among the *Leishmania* (*Leishmania*) species that can be differentiated from *L.* (*L*.) *infantum*, therefore extending the conclusion of our previous work. Importantly, this approach was successfully applied to cutaneous lesions of 11 patients diagnosed with diffuse or localized cutaneous leishmaniasis. Notably, the clinical sample pxCMU, which was negative in ITS1-PCR RFLP, was identified as *L*. (*L*.) *mexicana*/*amazonensis*, evidencing the highest sensitivity of our qPCR assays targeting minicircles. These results further support the possibility of exploiting the relative

abundance of minicircles for *Leishmania* species discrimination. Moreover, we confirmed the use of an adequate diagnostic approach based on consecutive qPCR assays to define species [18], as also proposed by other authors [27].

The distinction between *L.* (*L.*) *amazonensis* and *L. (L.) mexicana* is important for epidemiological studies and disease monitoring, but it can be challenging [28]. For instance, *hsp70* analysis by Fraga et al. [29] did not resolve between these species. On the other hand, other authors were able to separate these species based on multilocus sequence typing (MLST) [30] or sequential real-time PCR assays [27].

The qPCR coupled with HRM analysis is considered as a good option in molecular diagnostics since it avoids the use of modified oligonucleotides, it is accurate, allows high-throughput applications and is faster and cheaper than other types of analysis such as MLST, RFLP or single-gene DNA sequencing. Moreover, since the qPCR is a closed-tube system, the potential for carryover contamination will be reduced. In the attempt to discriminate between *L*. (*L.*) *amazonensis* and *L.* (*L.*) *mexicana*, HRM profiles of amplicons from qPCR-ama were investigated; however, their heterogeneity did not us allow to distinguish these two species reliably. Since Schönian et al. demonstrated the possibility to discriminate the two species using ITS1-PCR RFLP [31], we designed an HRM-based assay exploiting differences in *L*. (*L.*) *amazonensis* and *L.* (*L.*) *mexicana* ITS1 sequences, in order to avoid restriction digestion and electrophoretic analysis. This process allows saving a considerable amount of time to perform the analysis and avoids possible difficulties in restriction fragment identification. As expected from the in silico sequence analysis, the observed HRM Tm values of all *L.* (*L.*) *mexicana* samples were significantly higher as those of all *L*. (*L.*) *amazonensis* samples, allowing a robust distinction between these two species. The fact that three clinical samples did not amplify (Px7, PxGSF, PxCMU) was probably due to the lower sensitivity of qPCR-ITS1 as compared to the assay targeting kDNA minicircles.

5. Conclusions

In the attempt to use a qPCR-based approach to differentiate *Leishmania* species co-existing in the New World, sequential qPCR assays and HRM analysis have been implemented. The results showed that—(i) *L.* (*L.*) *infantum* can be distinguished from *L.*

(*L.*) *mexicana* comparing the Cq values of qPCR-ML and qPCR-ama, as previously shown for *L.* (*L.*) *amazonensis*; (ii) this distinction was possible not only using strains/isolates but also in clinical samples; (iii) the differentiation between *L.* (*L.*) *amazonensis* and *L.* (*L.*) *mexicana* was achieved by qPCR-ITS1 HRM analysis. Therefore, it was possible to design/update an algorithm that allows us to identify/differentiate *L*. (*L*.) *infantum*, *L*. (*L*.) *amazonensis*, *L.* (*L.*) *mexicana* and *Viannia* subgenus with sequential qPCR assays coupled with HRM analysis targeting minicircle kDNA and ITS1 sequence (Figure 6), which further extends our previous work.

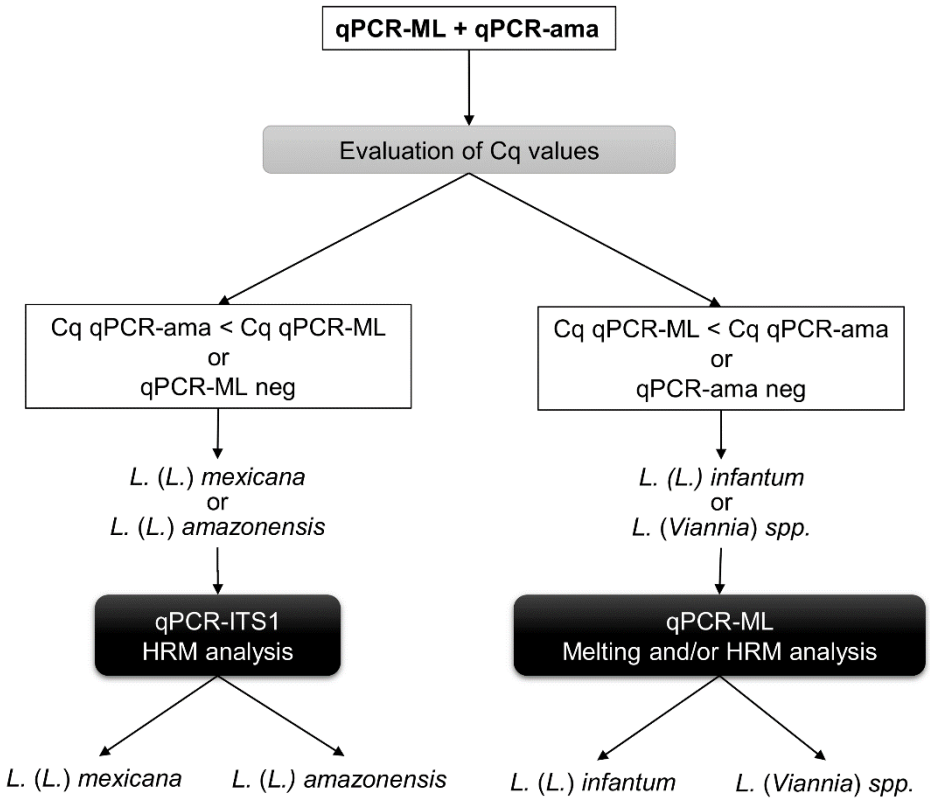

Figure 6. Updated sequential qPCR and HRM approach targeting minicircle kDNA and ITS1 sequence for the identification of *L*. (*L*.) *infantum*, *L*. (*L*.) *amazonensis*, *L.* (*L.*) *mexicana* and *Viannia* subgenus. First, the qPCR-ML and qPCR-ama followed by HRM analysis are performed. The evaluation of Cq values and HRM profiles for both assays will allow discriminating among *L*. (*Viannia*) spp, *L*. (*L*.) *infantum* and the two species *L.* (*L*.) *mexicana/amazonensis*. Then, qPCR-ITS1 HRM analysis is performed to discriminate between *L*. (*L*.) *amazonensis* and *L.* (*L*.) *mexicana.*

6. Supplementary matherials

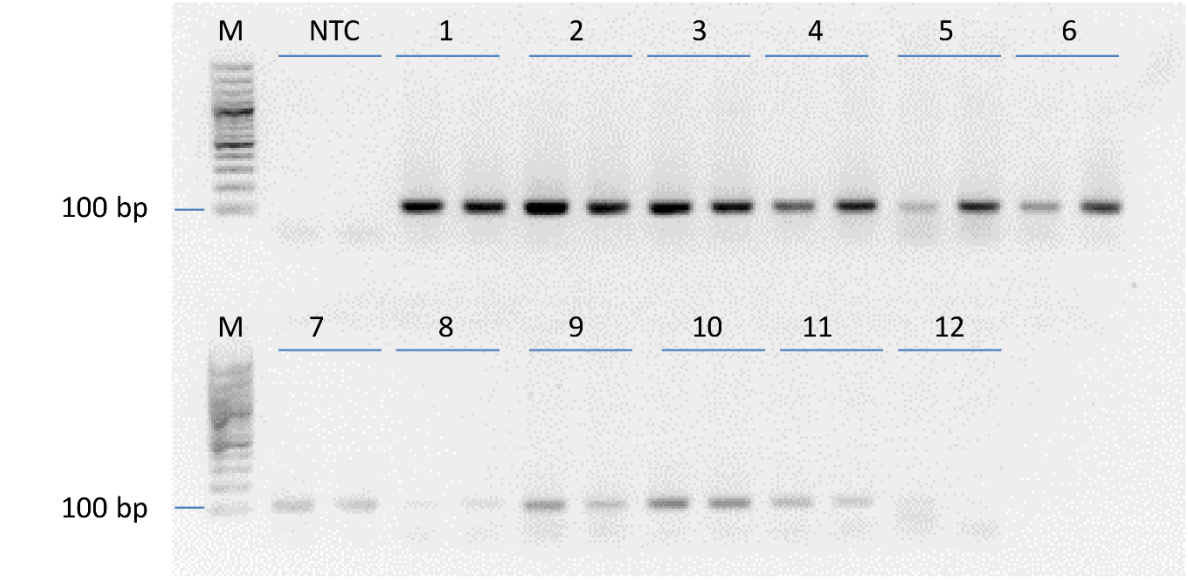

Figure S1. Electrophoretic analysis of qPCR-ML products. Lane 1: *L.* (*L.*) *infantum* MHOM/TN/80/IPT1; Lane 2: *L.* (*L.*) *infantum* MHOM/IT/86/ISS218; Lane 3: *L.* (*V.*) *braziliensis* MHOM/BR/75/M2904; Lane 4: *L.* (*L.*) *amazonensis* MHOM/BR/00/LTB0016; Lanes 5-8: *L.* (*L.*) *mexicana* MHOM/MX/2011/Lacandona serial dilution ranging from 10.0 to 0.01 ng DNA/reaction tube; Lanes 9-12: *L.* (*L.*) *mexicana* MHOM/MX/2011/Lacandona serial dilution ranging from 10.0 to 0.01 ng DNA/reaction tube spiked with 30 ng of human DNA. Abbreviations: M, 100 bp DNA ladder; NTC, no template control.

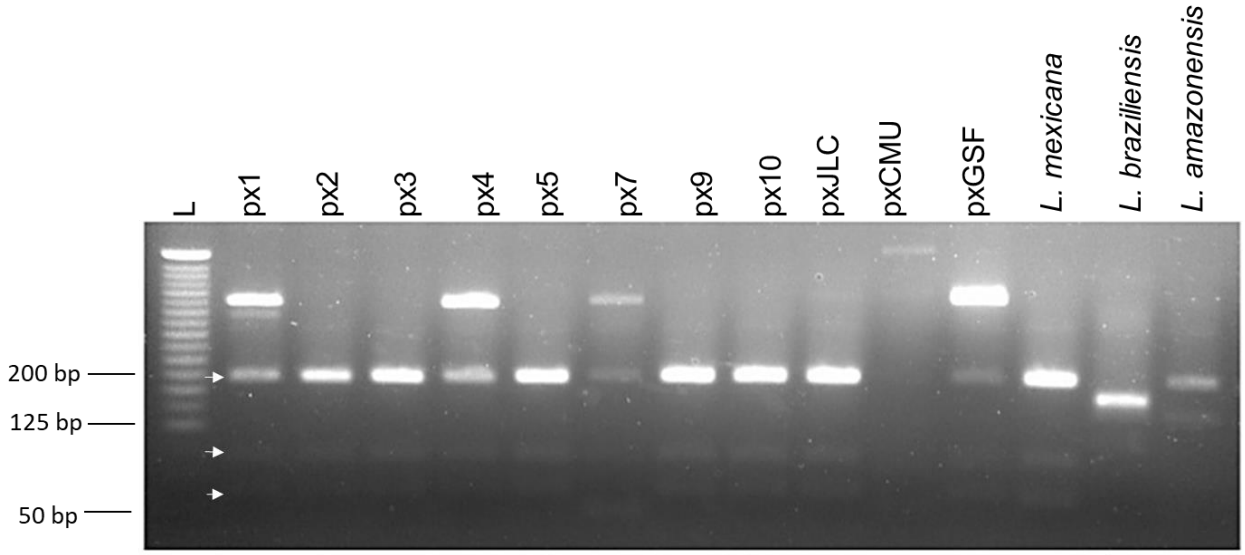

Figure S2. Digestion of ITS1 amplicons of clinical samples and reference *Leishmania* strains with the restriction endonuclease HaeIII. The following strains of *Leishmania* have been used as reference: *L. mexicana* MHOM/MX/2011/Lacandona, *L. braziliensis* MHOM/BR/75/M2904, *L. amazonensis* MHOM/BR/00/LTB0016. Fragments were separated on a 4% agarose gel. The fragments specific for *L. mexicana* are indicated by arrows. L: 25bp ladder.

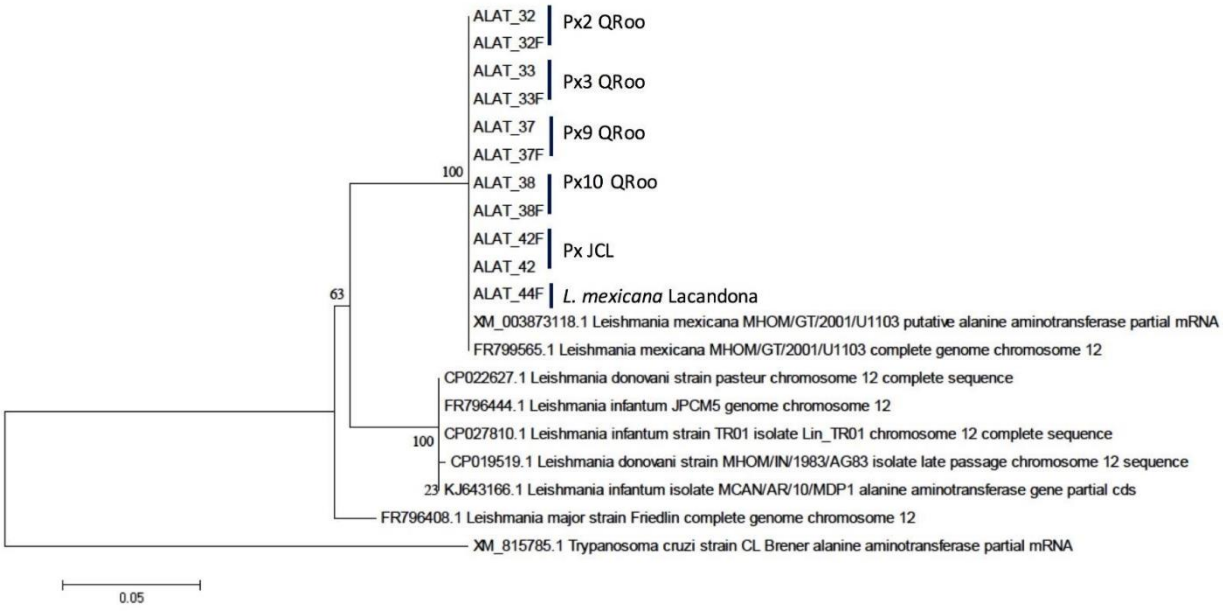

Figure S3. Maximum likelihood phylogenetic tree of ALAT amplicons. The tree was constructed with MEGA 6.0 software using the close neighbor interchange method.

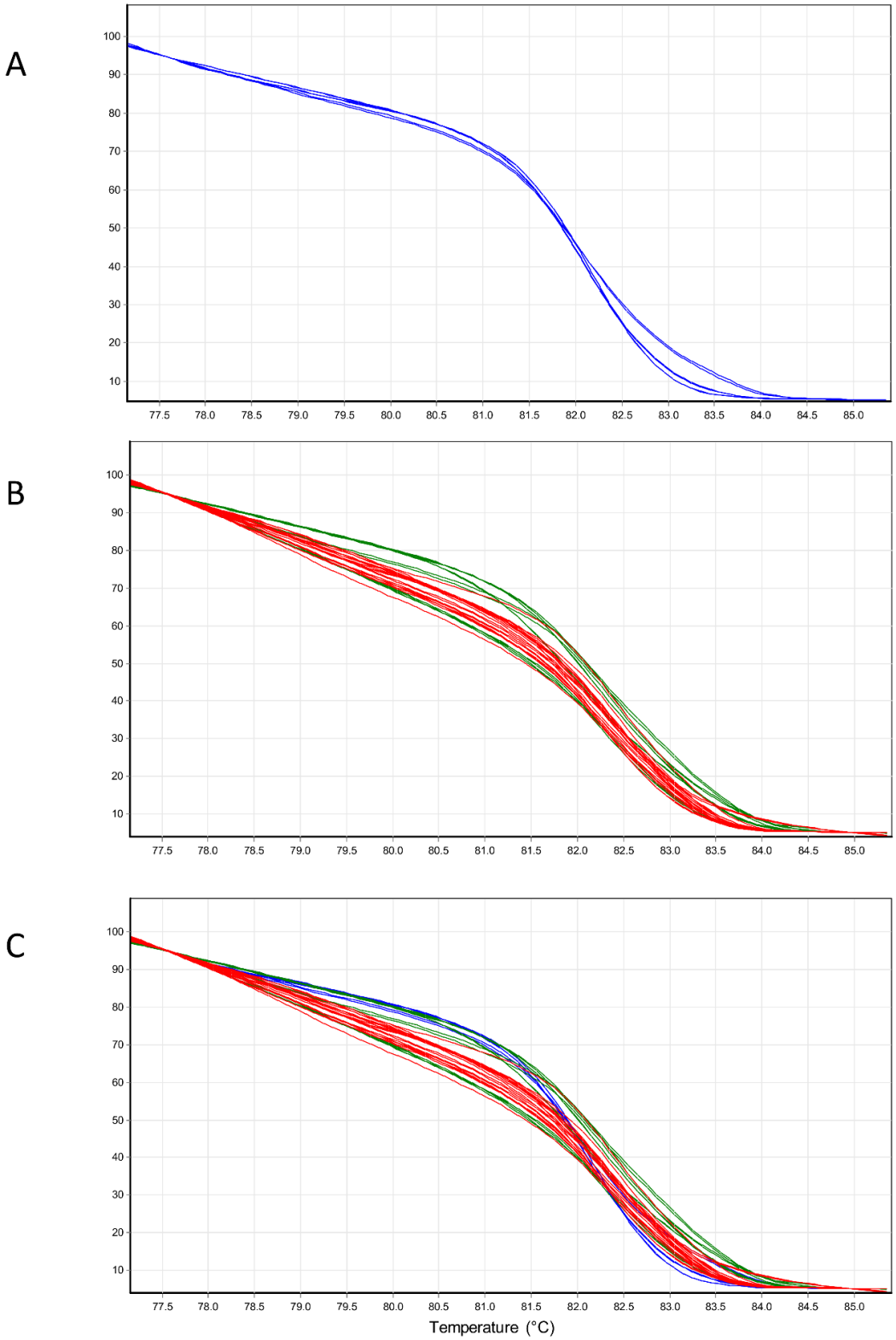

Figure S4. HRM analysis of qPCR-ama amplicons. A) Normalized HRM curves obtained from amplicons of *L*. (*L*.) *amazonensis* MHOM/BR/00/LTB0016, *L*. (*L*.) *amazonensis* clinical isolate and *L*. (*L*.) *amazonensis* IFLA/BR/67/PH8 (blue lines); B) Normalized HRM curves obtained from amplicons of *L*. (*L*.) *mexicana* isolates 2, 3, 5, 14, 17, MHOM/MX/2011/Lacandona (green lines) and *L*. (*L*.) *mexicana* clinical samples (n=11) (red lines); C) Merged curves from panels A and B. Each sample was tested in duplicate.

Table S1 Results of qPCR-ITS1 HRM analysis from *L*. (*L*.) *amazonensis* and *L*. (*L*.) *mexicana* samples.

Species	Strain/isolate/clinical sample	qPCR-ITS1 HRM (°C)±SD
L. (*L*.) *mexicana*	MHOM/MX/2011/Lacandona	79.90±0.028
L. (*L*.) *mexicana*	Isolate 2	79.82±0.005
L. (*L*.) *mexicana*	Isolate 3	79.82±0.006
L. (*L*.) *mexicana*	Isolate 5	79.91±0.035
L. (*L*.) *mexicana*	Isolate 14	79.89±0.014
L. (*L*.) *mexicana*	Isolate 17	79.88±0.005
L. (*L*.) *mexicana*	Px1	n.a.
L. (*L*.) *mexicana*	Px2	79.88±0.007
L. (*L*.) *mexicana*	Px3	79.85±0.005
L. (*L*.) *mexicana*	Px4	79.93±0.078
L. (*L*.) *mexicana*	Px5	79.85±0.005
L. (*L*.) *mexicana*	Px7	-
L. (*L*.) *mexicana*	Px9	79.78±0.007
L. (*L*.) *mexicana*	Px10	79.80±0.005
L. (*L*.) *mexicana*	PxGSF	-
L. (*L*.) *mexicana*	PxCMU	-
L. (*L*.) *mexicana*	PxJLC	79.88±0.035
L. (L.) amazonensis	MHOM/BR/00/LTB0016	79.48±0.035
L. (L.) amazonensis	IFLA/BR/67/PH8	79.21±0.014
L. (L.) amazonensis	Clinical isolate	79.51±0.014

n.a.: not available

-: negative result

Author Contributions: Conceptualization, M.C. and L.G.; methodology, M.C., A.D. and L.G.; validation, M.C., L.G., E.A.F.-F., C.R.-E., S.A.M.-M., I.B. and M.M.; formal analysis, L.G., A.D. and E.A.F.-F.; investigation, M.C., A.D., M.D.S., G.B. and E.A.F.-F.; resources, C.R.-E., I.B. and M.M.; writing—original draft preparation, M.C. and L.G.; writing—review and editing, A.D., G.B., E.A.F.-F., C.R.-E., S.A.M.-M., I.B., M.D.S. and M.M. All authors have read and agreed to the published version of the manuscript.

Funding: This research was partially funded by the Department of Biomolecular Sciences of University of Urbino and by INMEGEN-08/2013/I.

Acknowledgments: We thank Fabrizio Vitale and Christine Petersen for providing *Leishmania* spp DNA. We also thank Marco Quintanilla for providing the clinical samples of patients from Quintana Roo.

Conflicts of Interest: The authors declare no conflict of interest. The funders had no role in the design of the study; in the collection, analyses, or interpretation of data; in the writing of the manuscript, or in the decision to publish the results.

References

1. Alvar, J.; Vélez, I.D.; Bern, C.; Herrero, M.; Desjeux, P.; Cano, J.; Jannin, J.; den Boer, M. Leishmaniasis Worldwide and Global Estimates of Its Incidence. *PLoS ONE* **2012**, *7*, e35671.
2. Hashiguchi, Y.; Velez, L.N.; Villegas, N.V.; Mimori, T.; Gomez, E.A.L.; Kato, H. Leishmaniases in Ecuador: Comprehensive review and current status. *Acta Trop.* **2017**, *166*, 299–315.
3. Goto, H.; Lindoso, J.A. Current diagnosis and treatment of cutaneous and mucocutaneous leishmaniasis. *Expert Rev. Anti Infect. Ther.* **2010**, *8*, 419–433.
4. Akhoundi, M.; Downing, T.; Votýpka, J.; Kuhls, K.; Lukeš, J.; Cannet, A.; Ravel, C.; Marty, P.; Delaunay, P.; Kasbari, M.; et al. Leishmania infections: Molecular targets and diagnosis. *Mol. Asp. Med.* **2017**, *57*, 1–29.
5. Recalde, O.D.S.; Brunelli, J.P.; Rolon, M.S.; De Arias, A.R.; Aldama, O.; Gómez, C.V. First molecular report of Leishmania (Leishmania) amazonensis and Leishmania (Viannia) guyanensis in paraguayan inhabitants using high-resolution melt-PCR. *Am. J. Trop. Med. Hyg.* **2019**, *101*, 780–788.
6. Galluzzi, L.; Ceccarelli, M.; Diotallevi, A.; Menotta, M.; Magnani, M. Real-time PCR applications for diagnosis of leishmaniasis. *Parasites Vectors* **2018**, *11*, 273.
7. Medkour, H.; Varloud, M.; Davoust, B.; Mediannikov, O. New Molecular Approach for the Detection of Kinetoplastida Parasites of Medical and Veterinary Interest. *Microorganisms* **2020**, *8*, 356.
8. Schonian, G.; Kuhls, K.; Mauricio, I.L. Molecular approaches for a better understanding of the epidemiology and population genetics of Leishmania. *Parasitology* **2011**, *138*, 405–425.
9. Jensen, R.E.; Englund, P.T. Network News: The Replication of Kinetoplast DNA. *Annu. Rev. Microbiol.* **2012**, *66*, 473–491.
10. Brewster, S.; Barker, D. Analysis of minicircle classes in Leishmania (Viannia) species. *Trans. R. Soc. Trop. Med. Hyg.* **2002**, *96*, S55–S63.
11. Lee, S.-Y.; Lee, S.-T.; Chang, K.-P. Transkinetoplastidy-A Novel Phenomenon Involving Bulk Alterations of Mitochondrion-Kinetoplast DNA of a Trypanosomatid Protozoan 1, 2. *J. Protozool.* **1992**, *39*, 190–196.
12. Simpson, L. The genomic organization of guide RNA genes in kinetoplastid protozoa: Several conundrums and their solutions. *Mol. Biochem. Parasitol.* **1997**, *86*, 133–141.
13. Kocher, A.; Valière, S.; Bañuls, A.-L.; Murienne, J. High-throughput sequencing of kDNA amplicons for the analysis of Leishmania minicircles and identification of Neotropical species. *Parasitology* **2017**, *145*, 1–8.
14. Mary, C.; Faraut, F.; Lascombe, L.; Dumon, H. Quantification of Leishmania infantum DNA by a real-time PCR assay with high sensitivity. *J. Clin. Microbiol.* **2004**, *42*, 5249–5255.
15. Pita-Pereira, D.; Lins, R.; Oliveira, M.P.; Lima, R.B.; Pereira, B.A.S.; Moreira, O.C.; Brazil, R.P.; Britto, C. SYBR Green-based real-time PCR targeting kinetoplast DNA can be used to discriminate between the main etiologic agents of Brazilian cutaneous and visceral leishmaniases. *Parasites Vectors* **2012**, *5*, 15.
16. Ceccarelli, M.; Galluzzi, L.; Migliazzo, A.; Magnani, M. Detection and Characterization of Leishmania (Leishmania) and Leishmania (Viannia) by SYBR Green-Based Real-Time PCR and High Resolution Melt Analysis Targeting Kinetoplast Minicircle DNA. *PLoS ONE* **2014**, *9*, e88845.
17. Losada-Barragán, M.; Cavalcanti, A.; Umaña-Pérez, A.; Porrozzi, R.; Cuervo-Escobar, S.; Vallejo, A.F.; Sánchez-Gómez, M.; Cuervo, P. Detection and quantification of Leishmania infantum in naturally and experimentally infected animal samples. *Vet. Parasitol.* **2016**, *226*, 57–64.
18. Ceccarelli, M.; Galluzzi, L.; Diotallevi, A.; Andreoni, F.; Fowler, H.; Petersen, C.; Vitale, F.; Magnani, M. The use of kDNA minicircle subclass relative abundance to differentiate between *Leishmania* (L.) infantum and *Leishmania* (L.) amazonensis. *Parasites Vectors* **2017**, *10*, 239.
19. Diotallevi, A.; Buffi, G.; Ceccarelli, M.; Neitzke-Abreu, H.C.; Gnutzmann, L.V.; da Costa Lima, M.S.; Di Domenico, A.; De Santi, M.; Magnani, M.; Galluzzi, L. Real-time PCR to differentiate among Leishmania (Viannia) subgenus, Leishmania (Leishmania) infantum and Leishmania (Leishmania) amazonensis: Application on Brazilian clinical samples. *Acta Trop.* **2020**, *201*, 105178.
20. Diotallevi, A.; Buffi, G.; Ceccarelli, M.; Di Domenico, A.; De Santi, M.; Magnani, M.; Galluzzi, L.; Neitzke-Abreu, H.C.; Gnutzmann, L.V.; da Costa Lima Junior, M.S. Data on the differentiation among Leishmania (Viannia) spp., Leishmania

(Leishmania) infantum and Leishmania (Leishmania) amazonensis in Brazilian clinical samples using real-time PCR. *Data Brief* **2020**, *28*, 104914.

21. Tschoeke, D.A.; Nunes, G.L.; Jardim, R.; Lima, J.; Dumaresq, A.S.R.; Gomes, M.R.; De Mattos Pereira, L.; Loureiro, D.R.; Stoco, P.H.; De Matos Gliedes, H.L.; et al. The Comparative Genomics and Phylogenomics of Leishmania Amazonensis Parasite. *Evol. Bioinform.* **2014**, *10*, EBO.S13759.
22. Monroy-Ostria, A.; Nasereddin, A.; Monteon, V.M.; Guzmán-Bracho, C.; Jaffe, C.L. lTS1 PCR-RFLP Diagnosis and Characterization of Leishmania in Clinical Samples and Strains from Cases of Human Cutaneous Leishmaniasis in States of the Mexican Southeast. *Interdiscip. Perspect. Infect. Dis.* **2014**, *2014*, 1–6.
23. Marco, J.D.; Barroso, P.A.; Locatelli, F.M.; Cajal, S.P.; Hoyos, C.L.; Nevot, M.C.; Lauthier, J.J.; Tomasini, N.; Juarez, M.; Estévez, J.O.; et al. Multilocus sequence typing approach for a broader range of species of Leishmania genus: Describing parasite diversity in Argentina. *Infect. Genet. Evol.* **2015**, *30*, 308–317.
24. Ceccarelli, M.; Diotallevi, A.; Andreoni, F.; Vitale, F.; Galluzzi, L.; Magnani, M. Exploiting genetic polymorphisms in metabolic enzymes for rapid screening of Leishmania infantum genotypes. *Parasites Vectors* **2018**, *11*, 572.
25. Quaresma, P.F.; Murta, S.M.F.; Ferreira, E. de C.; da Rocha-Lima, A.C.V.M.; Xavier, A.A.P.; Gontijo, C.M.F. Molecular diagnosis of canine visceral leishmaniasis: Identification of Leishmania species by PCR-RFLP and quantification of parasite DNA by real-time PCR. *Acta Trop.* **2009**, *111*, 289–294.
26. Nicolas, L.; Prina, E.; Lang, T.; Milon, G. Real-Time PCR for Detection and Quantitation of Leishmania in Mouse Tissues. *J. Clin. Microbiol.* **2002**, *40*, 1666–1669.
27. Hernández, C.; Alvarez, C.; González, C.; Ayala, M.S.; León, C.M.; Ramírez, J.D. Identification of Six New World Leishmania species through the implementation of a High-Resolution Melting (HRM) genotyping assay. *Parasites Vectors* **2014**, *7*, 501.
28. Zampieri, R.A.; Laranjeira-Silva, M.F.; Muxel, S.M.; Stocco de Lima, A.C.; Shaw, J.J.; Floeter-Winter, L.M. High Resolution Melting Analysis Targeting hsp70 as a Fast and Efficient Method for the Discrimination of Leishmania Species. *PLoS Negl. Trop. Dis.* **2016**, *10*, e0004485.
29. Fraga, J.; Montalvo, A.M.; De Doncker, S.; Dujardin, J.-C.; Van der Auwera, G. Phylogeny of Leishmania species based on the heat-shock protein 70 gene. *Infect. Genet. Evol.* **2010**, *10*, 238–245.
30. Van der Auwera, G.; Ravel, C.; Verweij, J.J.; Bart, A.; Schonian, G.; Felger, I. Evaluation of Four Single-Locus Markers for Leishmania Species Discrimination by Sequencing. *J. Clin. Microbiol.* **2014**, *52*, 1098–1104.
31. Schönian, G.; Nasereddin, A.; Dinse, N.; Schweynoch, C.; Schallig, H.D.F..; Presber, W.; Jaffe, C.L. PCR diagnosis and characterization of Leishmania in local and imported clinical samples. *Diagn. Microbiol. Infect. Dis.* **2003**, *47*, 349–358.

CHAPTER 4

This chapter consists of a brief report regarding a kDNA-Based qPCR Assay, previously proposed to distinguish *L.* (*L.*) *infantum* and *L.* (*L.*) *amazonensis* from *L. Viannia* species, for the Detection and Quantification of Old World *Leishmania* species.

Brief report published in Microorganism

DOI: 10.3390/microorganisms8122006 Volume 8, Issue 12, 2020, 2006

microorganisms

MDPI

Brief Report

Evaluation of a kDNA-Based qPCR Assay for the Detection and Quantification of Old World *Leishmania* species

Marcello Ceccarelli [1], Gloria Buffi [1], Aurora Diotallevi [1], Francesca Andreoni [1], Daniela Bencardino [1], Fabrizio Vitale [2], Germano Castelli [2], Federica Bruno [2], Mauro Magnani [1] and Luca Galluzzi [1,*]

[1] Department of Biomolecular Sciences, University of Urbino "Carlo Bo", 61029 Urbino (PU), Italy; m.ceccarelli3@campus.uniurb.it (M.C.); g.buffi@campus.uniurb.it (G.B.); aurora.diotallevi@uniurb.it (A.D.); francesca.andreoni@uniurb.it (F.A.); daniela.bencardino@uniurb.it (D.B.); mauro.magnani@uniurb.it (M.M.)

[2] National Reference Center for Leishmaniasis (C.Re.Na.L.), Istituto Zooprofilattico Sperimentale della Sicilia, 90129 Palermo, Italy; fabrizio.vitale@izssicilia.it (F.V.); germanocastelli@gmail.com (G.C.); federica.bruno@izssicilia.it (F.B.)

* Correspondence: luca.galluzzi@uniurb.it; Tel.: +39-0722-304976

Received: 8 September 2020; Accepted: 14 December 2020; Published: 16 December 2020

Abstract

The parasite protozoan Leishmania, the causative agent of leishmaniasis, includes two subgenera of medical interest: Leishmania (Leishmania) and Leishmania (Viannia). Parasite species detection and characterization is crucial to choose treatment protocols and to monitor the disease evolution. Molecular approaches can speed up and simplify the diagnostic process. In particular, several molecular assays target the mitochondrial DNA minicircle network (kDNA) that characterizes the Leishmania genus. We previously proposed a qPCR assay targeting kDNA, followed by high resolution melt (HRM) analysis (qPCR-ML) to distinguish L. (L.) infantum and L. (L.) amazonensis from L. Viannia species. Successively, this assay has been integrated with other qPCR assays, to differentiate L. (L.) infantum, L. (L.) amazonensis and L. (L.) mexicana. In this work, we tested the applicability of our qPCR-ML assay on L. (L.) donovani, L. (L.) major, L. (L.) tropica and L. (L.) aethiopica, showing that the qPCR-ML assay can also amplify Old World species, different from L. (L.) infantum, with good quantification limits (1 × 10−4–1 × 10−6 ng/pcr tube). Moreover, we evaluated 11 L. (L.) infantum strains/isolates, evidencing the

variability of the kDNA minicircle target molecules among the strains/isolates of the same species, and pointing out the possibility of quantification using different strains as reference. Taken together, these data account for the consideration of qPCR-ML as a quantitative pan-Leishmania assay.

Keywords: *Leishmania*; *Viannia*; qPCR; Old World; high resolution melting; kDNA

---

1. Introduction

Leishmania spp. is a protozoan parasite widespread in Asia, Africa, Europe and America. The parasite is the etiological agent of leishmaniasis, one of the most important tropical diseases that encompasses a broad spectrum of clinical manifestations. The genus *Leishmania* ascribes two subgenera of medical interest: *Leishmania* (*Leishmania*) and *Leishmania* (*Viannia*) [1]. The subgenus *Leishmania* (*Leishmania*) includes species responsible for visceral leishmaniasis (VL) [*L.* (*L.*) *donovani*, *L.* (*L.*) *infantum*] and cutaneous leishmaniasis (CL) [*L.* (*L.*) *infantum*, *L.* (*L.*) *major*, *L.* (*L.*) *tropica*, *L.* (*L.*) *aethiopica*, *L.* (*L.*) *mexicana*, *L.* (*L.*) *amazonensis*], while the species belonging to the subgenus *Leishmania* (*Viannia*) are the etiological agents of CL and mucocutaneous leishmaniasis (MCL) [2]. However, a few *Leishmania* (*Leishmania*) species [i.e., *L.* (*L.*) *infantum*, *L.* (*L.*) *major* and *L.* (*L.*) *tropica*] have also been reported to be the etiological agent of MCL [3]. The diagnosis of leishmaniasis is based on a combination of clinical manifestations, epidemiological data and laboratory test (i.e., serological, parasitological or molecular methods). However, a real gold-standard method for human or veterinary leishmaniasis is still lacking [4]. Among the diagnostic methods, molecular assays allow to obtain fast results and high sensitivity. In particular, a number of PCR-based assays are targeting the mitochondrial DNA minicircle network (kDNA) that characterizes the *Leishmania* genus, ensuring very high sensitivity [5]. Previously, we proposed a qPCR assay targeting the conserved region of kDNA minicircles using primers MLF and MLR (qPCR-ML), followed by high resolution melt (HRM) analysis to detect and distinguish *L*. (*Leishmania*) from *L.* (*Viannia*) subgenus [6]. Successively, this assay has been integrated with other qPCR assays to differentiate *L.*

(*L*.) *infantum* from *L.* (*L*.) *amazonensis* [7] and from *L.* (*L*.) *mexicana* [8]. These approaches have also been applied to Brazilian clinical samples, allowing to distinguish different species causing infection in the New World [9]. However, considering the Old World *Leishmania* species, the qPCR-ML assay has been tested only on *L.* (*L*.) *infantum*. In this work, we tested the applicability of our qPCR-ML assay in Old World *Leishmania* species different from *L.* (*L*.) *infantum* [i.e., *L.* (*L*.) *donovani*, *L.* (*L*.) *major*, *L.* (*L*.) *tropica* and *L.* (*L*.) *aethiopica*], in an attempt to test the pan-*Leishmania* potential of our approach. Moreover, we quantitatively evaluated the target sequence of qPCR-ML in different *L.* (*L*.) *infantum* strains and isolates to investigate the possibility of quantification in clinical applications.

2. Materials and Methods

2.1. *Leishmania* Strains, Clinical Isolates and Clinical Samples

Leishmania strains or isolates used in this study are listed in Table 1. The DNA from all strains and isolates was Chelex-purified from cultured promastigotes and was provided by the Istituto Zooprofilattico Sperimentale della Sicilia, OIE Reference Laboratory, National Reference Center for Leishmaniasis (C.Re.Na.L.), (Palermo, Italy), with the following exceptions: *L.* (*L*.) *donovani* MHOM/IN/02/BPK282/0cl4, provided by the Istituto Zooprofilattico Sperimentale della Lombardia e dell'Emilia-Romagna (Modena, Italy); *L.* (*V*.) *braziliensis* MHOM/BR/1987/M11272, provided by Universidade Federal da Grande Dourados (Brazil); *L.* (*L*.) *amazonensis* MHOM/BR/1973/M2269, *L.* (*L*.) *donovani* MHOM/SD/62/1S, *L.* (*L*.) *major* SV39 and *L. (S.) tarentolae* Parrot Tar II, provided by Instituto de Investigação e Inovação em Saúde Universidade do Porto, Portugal. Moreover, the *L.* (*V*.) *braziliensis* clinical isolate AN1 was obtained from a pharyngo-laryngeal biopsy during routine diagnosis of a human patient with MCL. The human clinical samples Psalb and Daedio were obtained during routine diagnosis of two patients with VL (blood) [10] and CL (cutaneous biopsy), respectively. The DNA samples were quantified using a Qubit fluorometer 3 (Thermofisher, Carlsbad, CA, USA).

Table 1. *Leishmania* spp. reference strains, clinical isolates and clinical samples used in this study.

Subgenus	Species	Strain/Isolate
Leishmania	*L. infantum*	MHOM/TN/80/IPT1
Leishmania	*L. infantum*	MHOM/FR/78/LEM75
Leishmania	*L. infantum*	Clinical isolate V2921
Leishmania	*L. infantum*	MHOM/IT/08/31U
Leishmania	*L. infantum*	MHOM/IT/08/49U
Leishmania	*L. infantum*	Clinical isolate 10816
Leishmania	*L. infantum*	Clinical isolate 791
Leishmania	*L. infantum*	MHOM/DZ/82/LIPA59
Leishmania	*L. infantum*	MHOM/ES/81/BCN1
Leishmania	*L. infantum*	MHOM/IT/86/ISS218
Leishmania	*L. infantum*	MHOM/IT/93/ISS822
Leishmania	*L. donovani*	MHOM/IN/80/DD8
Leishmania	*L. donovani*	MHOM/NP/02/BPK282/0cl4
Leishmania	*L. donovani*	MHOM/SD/62/1S
Leishmania	*L. major*	MHOM/SU/73/5ASKH
Leishmania	*L. major*	MRHO/SU/59/P-strain *
Leishmania	*L. major*	SV39 *
Leishmania	*L. tropica*	MHOM/SU/74/K27
Leishmania	*L. aethiopica*	MHOM/ET/72/L100
Leishmania	*L. amazonensis*	MHOM/BR/00/LTB0016
Leishmania	*L. amazonensis*	MHOM/BR/1973/M2269
Leishmania	*L. mexicana*	MHOM/MX/2011/Lacandona
Leishmania	*L. infantum*	Clinical sample Psalb
Leishmania	*L. infantum*	Clinical sample Daedio
Viannia	*L. panamensis*	Clinical isolate
Viannia	*L. guyanensis*	Clinical isolate
Viannia	*L. braziliensis*	Clinical isolate AN1
Viannia	*L. braziliensis*	Clinical isolate IZS
Viannia	*L. braziliensis*	MHOM/BR/1987/M11272

Viannia	*L. braziliensis*	MHOM/BR/75/M2904
Sauroleishmania	*L. tarentolae*	Parrot Tar II

* synonym strains coming from two different laboratories.

2.2. qPCR Assay

The qPCR assays were performed using MLF-MLR primer pair (MLF: 5'-CGTTCTGCGAAAACCGAAA-3'; MLR: 5'-CGGCCCTATTTTACACCAACC-3') as previously reported [6]. Briefly, the reactions were carried out in 25 µL volume with 1 µL of template DNA and 24 µL TB Green Premix Ex TaqII Mastermix (Takara Bio Europe, France) containing 200 nM MLF and MLR primers. The reactions were performed in a Rotor-Gene 6000 instrument (Corbett Life Science, Mortlake, Australia). The cycle threshold (Cq) values were determined using the quantitation analysis of the Rotor-Gene 6000 software, setting a threshold to 0.15.

Standard curves were established using 1×10^{0} to 1×10^{-7} ng DNA of *L.* (*L.*) *major* MHOM/SU/73/5ASKH, *L.* (*L.*) *donovani* MHOM/IN/80/DD8, *L.* (*L.*) *aethiopica* MHOM/ET/72/L100, *L.* (*L.*) *tropica* MHOM/SU/74/K27, *L.* (*L.*) *infantum* MHOM/FR/78/LEM75 and *L. (S.) tarentolae* Parrot Tar II. To evaluate the potential interference of host DNA as background in the qPCR assay, 30 ng of human DNA purified from human cell line (CACO-2 or MCF7) was spiked in each qPCR reaction tube (with the exception of *L. (S.) tarentolae* Parrot Tar II because not pathogenic to humans). The standard curves were obtained from two independent experiments for each strain, processed in duplicate.

To determine the variability of kDNA minicircle target sequences in *L.* (*L.*) *infantum* species, 0.02 ng DNA extracted from 11 *L.* (*L.*) *infantum* strains/isolates were amplified in 6 independent experiments and Cq were compared by Kruskal–Wallis nonparametric test.

2.3. High-Resolution Melt (HRM) Analysis

The qPCR-ML amplicons, obtained by all stains/isolates listed in Table 1, were analyzed by HRM protocol on a Rotor-Gene 6000 instrument as described previously [6] with slight modifications. Briefly, HRM was carried out over the range from 77 °C to 89 °C, rising at 0.1 °C/s and waiting for 2 s at each temperature. Each sample was run in

duplicate and the gain was optimized before melting on all tubes. HRM curve analysis was performed with the derivative of the raw data, after smoothing, with the Rotor-Gene 6000 software. Only the samples with Cq values <30 were considered [11]. The HRM temperature average and the standard deviation derived from 3 independent experiments.

2.4. PCR Product Sequencing

The qPCR-ML products obtained from *L.* (*L*.) *major* MHOM/SU/73/5ASKH, *L.* (*L*.) *major* MRHO/SU/59/P-strain, *L.* (*L*.) *donovani* MHOM/IN/80/DD8, *L.* (*L*.) *aethiopica* MHOM/ET/72/L100, *L.* (*L*.) *tropica* MHOM/SU/74/K27, *L.* (*L*.) *infantum* MHOM/FR/78/LEM75, *L.* (*V*.) *braziliensis* MHOM/BR/75/M2904 were purified using the MinElute PCR purification kit (Qiagen) and directly sequenced, using both MLF and MLR primers, as previously described [6,7]. The DNA sequencing was performed using the BigDye Terminator v. 1.1 Cycle Sequencing Kit on ABI PRISM 310 Genetic Analyzer (Applied Biosystems, Foster City, CA, USA). Sequences were manually edited and nucleotide composition analyses were conducted using MEGA6 [12]. A phylogenetic tree based on the Maximum Likelihood method was constructed with 10,000 bootstrap replications, using the nearest neighbor interchange method in MEGA6 [12].

2.5. Statistical Analysis

To compare the variability on Cq values on *L.* (*L*.) *infantum* strains/isolates, a Kruskal–Wallis nonparametric test followed by Dunn's multiple-comparison post-test was performed. To evaluate the different HRM temperatures between the *Leishmania* and *Viannia* subgenera, a Mann–Whitney test was performed. All statistical tests were performed using GraphPad Prism version 5 (GraphPad Software, Inc., La Jolla, CA, USA). A p value ≤ 0.05 was considered statistically significant.

3. Results

3.1. The qPCR-ML Assay Can Amplify All Medically Relevant Old World *Leishmania* Species

The qPCR-ML was applied to the strains listed in Table 1 to verify the amplifiability of all *Leishmania* species with MLF-MLR primers. All Old World species [i.e., *L.* (*L.*) *infantum*, *L.* (*L.*) *donovani*, *L.* (*L.*) *major*, *L.* (*L.*) *tropica*, *L.* (*L.*) *aethiopica*, *L. (S.) tarentolae*] were successfully amplified. The calibration curves evidenced a limit of quantification of 1×10^{-4} ng/PCR tube for *L.* (*L.*) *tropica* and *L.* (*L.*) *aethiopica*, 1×10^{-5} ng/PCR tube for *L.* (*L.*) *major*, 1×10^{-6} ng/PCR tube for *L.* (*L.*) *donovani*, 1×10^{-7} ng/PCR tube for *L.* (*L.*) *infantum* and 1×10^{-6} ng/PCR tube for *L. (S.) tarentolae* Parrot Tar II, with PCR efficiencies ≥ 94.5% and $R^2 > 0.97$ (Figure 1)**. A**lthough out of linearity range, the limit of detection for *L.* (*L.*) *donovani* MHOM/IN/80/DD8 and *L.* (*L.*) *tropica* MHOM/SU/74/K27 were 1×10^{-7} (Cq 32.48 ± 0.46) and 1×10^{-5} (Cq 33.56 ± 1.14) ng/PCR tube, respectively. In the presence of human DNA as background, the Cq were slightly delayed, but the linearity and limit of quantification of the assay remained unchanged (Figure 1).

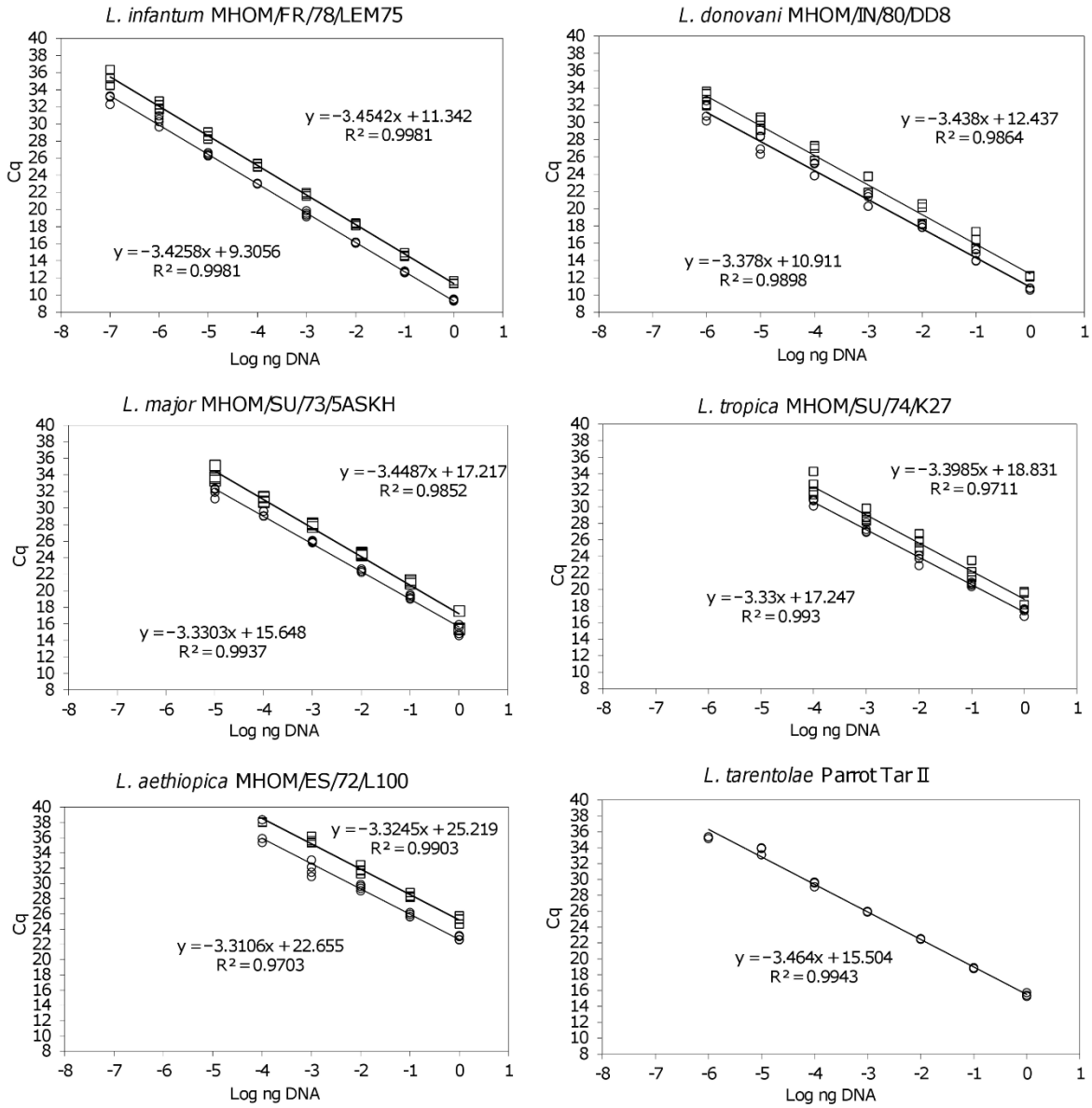

Figure 1. qPCR-ML standard curves obtained from DNA serial dilutions of *L.* (*L.*) *infantum* MHOM/FR/78/LEM75, *L.* (*L.*) *donovani* MHOM/IN/80/DD8, *L.* (*L.*) *major* MHOM/SU/73/5ASKH, *L.* (*L.*) *tropica* MHOM/SU/74/K27, *L.* (*L.*) *aethiopica* MHOM/ET/72/L100, *L. (S.) tarentolae* Parrot Tar II. The standard curves were spiked (upper curve, square points) or non-spiked (lower curve, circle points) with 30 ng human DNA. The standard curve of *L. (S.) tarentolae* Parrot Tar II, not pathogenic to humans, was not spiked. Each point derived from a duplicate of two independent experiments.

The variability of kDNA minicircle target sequence was investigated among 11 *L.* (*L.*) *infantum* strains by amplification of 0.02 ng promastigote DNA. Dunn's post-test analysis of Cq values revealed significant differences among V2921 clinical isolate, MHOM/IT/86/ISS218 strain and clinical isolate 10816 (Figure 2). The average Cq was 19.36 ± 1.14, very close to the value obtained for the strain MHOM/FR/78/LEM75 (19.44

± 0.56), suggesting that this strain could be used as reference to obtain approximate quantification values for illness caused by *L.* (*L*.) *infantum*.

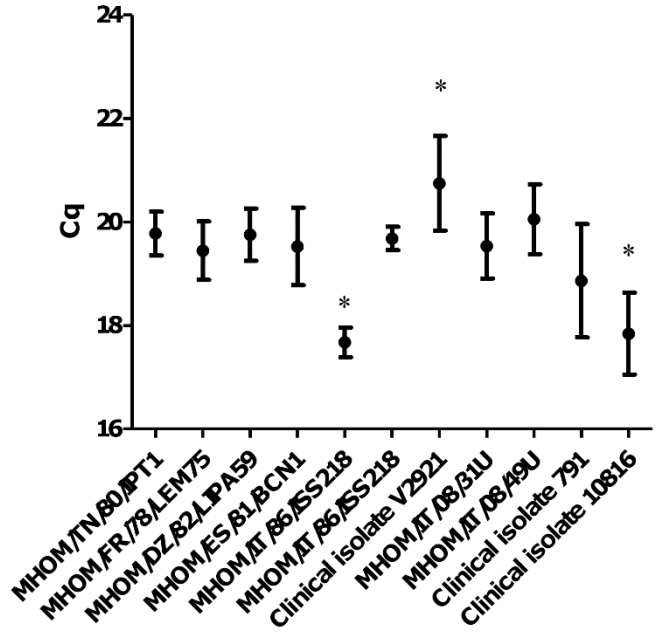

Figure 2. qPCR-ML Cq values obtained from 11 *L.* (*L*.) *infantum* strains/isolates. The results were obtained from six independent experiments. * $p < 0.01$ Dunn's Multiple Comparison Test.

3.2. The subgenera *Leishmania* and *Viannia* can be Differentiated by HRM Analysis

Species discrimination power of qPCR-ML assay was also evaluated by analysis of HRM profiles on all *Leishmania* species listed in Table 1. Despite the impossibility to reliably discriminate each species using HRM profiles, the assay evidenced the lower Tm of amplicons belonging to *Viannia* subgenus, confirming the possibility to discriminate between *Leishmania* and *Viannia* subgenus, as previously demonstrated with a limited number of species [6] (Figure 3A). However, the Tm of *L.* (*L*.) *tropica* MHOM/SU/74/K27 amplicon showed a partial overlapping with *L.* (*V*.) *panamensis*, hence the two species were not fully distinguishable (Figure 3B). Accordingly, the specificity of this assay can be considered 96.6%. Nevertheless, this drawback can be overcome by considering the geographical origin of the sample since *L.* (*L*.) *tropica* is an Old World species. It is also noteworthy that *L. (S.) tarentolae* Parrot Tar II HRM temperature was 80.92 ± 0.08, clearly distinguishable from *Viannia* and *Leishmania* subgenera.

The sequence analysis of qPCR-ML products evidenced that the GC content found in *L. Viannia* strains was lower than that found in *L. Leishmania* strains (<48.2% and

>48.6%, respectively), accounting for the lower Tm observed in the *Viannia* amplicons. In addition, a maximum likelihood phylogenetic tree of qPCR-ML amplicons was performed, confirming the clusterization in two groups of the amplicons obtained from the two subgenera, with the exception of *L.* (*L.*) *tropica*, which clusterizes independently (Figure S1).

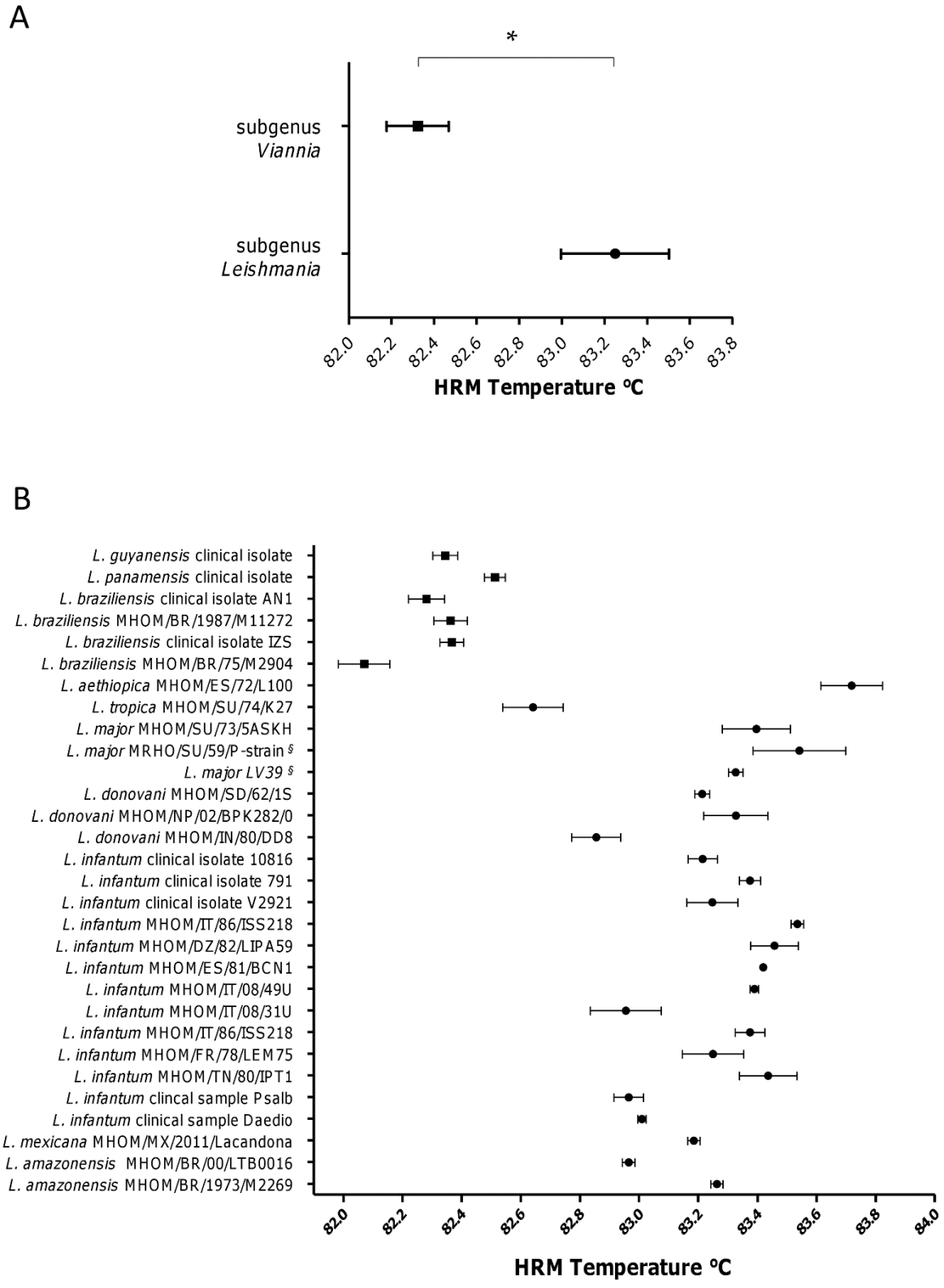

Figure 3. *Leishmania* spp. qPCR-ML HRM temperatures analysis. (**A**) Comparison between HRM temperatures (mean and standard deviation) of all tested samples belonging to subgenus *Leishmania* (n = 24) and *Viannia* (n = 6). * $p < 0.05$ Mann–Whitney test. (**B**) HRM temperature distribution of all samples tested. Squares and circles represent species belonging to subgenus *Viannia* and *Leishmania*, respectively. Mean values and standard deviations of at least three replicates are shown. § synonym strains coming from different laboratories.

4. Discussion

Although leishmaniasis is considered a neglected disease, it affects about 12 million people in Africa, Americas, Asia and Europe, with a heterogeneous clinical spectrum [13]. The diagnosis is complicated, as well as for the different species spread in the world. To improve the diagnostic process and classification, a number of molecular assays have been developed. In particular, qPCR techniques allow obtaining rapid parasitic load estimation and potential species discrimination through melting analysis. Due to their high copy number per cell, the kDNA minicircles are considered molecular targets that allow to design very sensitive assays [14]. However, due to the different composition of minicircle classes in the various species, an assay designed on a particular species can show lower sensitivity in another [7]. For this reason, many works describe minicircle-based qPCR assays targeting only few species or complex. For example, some authors developed qPCR assay for New World species [15,16], while some others tested their primers in Old World species [17,18]. Since different reports describe the infection in travelers [19,20] and in military personnel operating in country endemic for leishmaniasis [21–23], the availability of a rapid pan-*Leishmania* assay, highly sensitive and able to provide a quantification and a partial classification, can certainly be useful. Moreover, a pan-*Leishmania* assay can also be exploited in eco-epidemiological studies, including identification of vectors and reservoirs [24]. In recent years, only a few attempts to develop pan-*Leishmania* assays based on nucleic acids amplification (i.e., SL RNA, rDNA or kDNA minicircles) have been made [24–27]. We previously showed that qPCR-ML was able to detect Old World *L.* (*L.*) *infantum* and New world species [i.e., *L.* (*L.*) *chagasi/infantum*, *L.* (*L.*) *amazonensis*, *L.* (*L.*) *mexicana*, *L.* (*V.*) *guyanensis*, *L.* (*V.*) *panamensis*, *L.* (*V.*) *braziliensis*] and among these species, distinguishing between *Leishmania* and *Viannia* subgenera [6,8]. In this work, we show for the first time that the qPCR-ML assay can also amplify the Old World species different from *L.* (*L.*) *infantum* with good quantification limits (1×10^{-4}–1×10^{-6} ng/pcr tube), including *L. (S.) tarentolae*, not pathogenic to humans. The differences in the limit of quantification of the different species can be explained by different amount of minicircle class amplified by ML primers, as already shown for other species [7]. Importantly, we confirmed that species related to *Viannia* subgenus can be

distinguished from Old World species of *Leishmania* subgenus by HRM analysis, with the only exception of *L.* (*L*.) *tropica* that, however, is distinguishable from *Viannia* subgenus by phylogenetic analysis. Moreover, although caution should be taken due to the few strains tested, it is interesting to note that the related species *L.* (*L*.) *tropica* and *L.* (*L*.) *aethiopica* can be distinguished through HRM analysis (Figure 3). *L.* (*L*.) *aethiopica* is geographically restricted to Kenya and Ethiopia, while *L.* (*L*.) *tropica* is widely distributed from the Eastern Mediterranean to Eastern India and in Africa. These species were distinguished by microsatellite analysis [28] but, to our knowledge, this is the first evidence of their separation using an HRM-based approach. In fact, *L.* (*L*.) *aethiopica* is a species rarely tested using HRM analysis and, when done, it is without discrimination from other species [29]. On the whole, due to its good sensitivity especially in Old World species, the qPCR-ML assay appears to be applicable in human and veterinary medicine in Europe, Africa and Middle East. Similar approaches having ITS1 region as target have been previously published [30,31]. Although these ITS1-based assays have the great potential to discriminate among *Leishmania Leishmania* species through HRM analysis [30], their contextual application with the *Viannia* subgenus has not been reported. Moreover, the use of FRET probes for species discrimination [31] could increase the cost compared to approaches based on intercalating dyes. The lack of species specificity of the qPCR-ML assay can be overcome using sequential PCR assays, as already demonstrated [8] or, in part, with the contextualization between the clinical presentation and the geographical origin of the patient.

Finally, we quantitatively evaluated the minicircle subclass amplified by qPCR-ML in 11 different *L.* (*L*.) *infantum* strains/isolates, to verify the possible differences in terms of Cq values. We confirmed the presence of significant variability among some strains/isolates, as previously reported in literature [14,32]. This variation could have an impact on absolute quantification, but the use of a reference strain with average minicircle kDNA amplifiable sequences could minimize the variability of results. Moreover, it could have a negligible consequence on the biological and clinical interpretation of diagnostic results, as already pointed out by Mary et al. [14].

5. Conclusions

In conclusion, the present work represents an update of our assay mentioned above and it demonstrates the applicability of qPCR-ML to detect and to quantify a large spectrum of *Leishmania* species, including also the Old World species, with a good limit of quantification and detection. We believe that this assay could be now considered as a quantitative pan-*Leishmania* assay, because it has been tested in the most common *Leishmania* species of the New and Old World, including *L. (S.) tarentolae*.

Supplementary Materials: The following are available online at www.mdpi.com/xxx/s1, Figure S1: Maximum likelihood phylogenetic tree of qPCR-ML amplicons.

Author Contributions: Conceptualization, M.C. and L.G.; methodology, M.C., G.B., A.D., F.A. and D.B.; validation, M.C., L.G., F.V. and M.M.; formal analysis, L.G., A.D., F.A., D.B. and G.B.; investigation, M.C., A.D., G.B., G.C. and F.B.; resources, F.V. and M.M.; writing—original draft preparation, M.C. and L.G.; writing—review and editing, A.D., G.B., G.C., F.B. and M.M. All authors have read and agreed to the published version of the manuscript.

Funding: This research was partially funded by the Department of Biomolecular Sciences of University of Urbino and by FanoAteneo.

Acknowledgments: We would like to thank Gianluca Rugna and Elena Carra for providing *L. donovani* MHOM/IN/02/BPK282/0cl4 DNA, and Nuno Santarém and Anabela Cordeiro Da Silva for providing DNA from *L. amazonensis* MHOM/BR/1973/M2269, *L. donovani* MHOM/SD/62/1S, *L. major* SV39 and *L tarentolae* Parrot Tar II.

Conflicts of Interest: The authors declare no conflict of interest. The funders had no role in the design of the study; in the collection, analyses, or interpretation of data; in the writing of the manuscript, or in the decision to publish the results.

References

1. Sereno, D.; Akhoundi, M.; Sayehmri, K.; Mirzaei, A.; Holzmuller, P.; Lejon, V.; Waleckx, E. Noninvasive Biological Samples to Detect and Diagnose Infections due to Trypanosomatidae Parasites: A Systematic Review and Meta-Analysis. *Int. J. Mol. Sci.* **2020**, *21*, 1684.
2. World Health Organization Leishmaniasis. Available online: http://www.who.int/mediacentre/factsheets/fs375/en/ (accessed on 16 March 2018).
3. Shirian, S.; Oryan, A.; Hatam, G.R.; Daneshbod, Y. Three *Leishmania*/*L.* species—*L. infantum*, *L. major*, *L. tropica*—As causative agents of mucosal leishmaniasis in Iran. *Pathog. Glob. Health* **2013**, *107*, 267–272.
4. Rodriguez-Cortes, A.; Ojeda, A.; Francino, O.; Lopez-Fuertes, L.; Timon, M.; Alberola, J. Leishmania Infection: Laboratory Diagnosing in the Absence of a "Gold Standard." *Am. J. Trop. Med. Hyg.* **2010**, *82*, 251–256.
5. Galluzzi, L.; Ceccarelli, M.; Diotallevi, A.; Menotta, M.; Magnani, M. Real-time PCR applications for diagnosis of leishmaniasis. *Parasit. Vectors* **2018**, *11*, 273.
6. Ceccarelli, M.; Galluzzi, L.; Migliazzo, A.; Magnani, M. Detection and Characterization of *Leishmania* (Leishmania) and *Leishmania* (Viannia) by SYBR Green-Based Real-Time PCR and High Resolution Melt Analysis Targeting Kinetoplast Minicircle DNA. *PLoS ONE* **2014**, *9*, e88845.
7. Ceccarelli, M.; Galluzzi, L.; Diotallevi, A.; Andreoni, F.; Fowler, H.; Petersen, C.; Vitale, F.; Magnani, M. The use of kDNA minicircle subclass relative abundance to differentiate between *Leishmania* (L.) *infantum* and *Leishmania* (L.) *amazonensis*. *Parasit. Vectors* **2017**, *10*, 239.

8. Ceccarelli, M.; Diotallevi, A.; Buffi, G.; De Santi, M.; Fernández-Figueroa, E.A.; Rangel-Escareño, C.; Muñoz-Montero, S.A.; Becker, I.; Magnani, M.; Galluzzi, L. Differentiation of *Leishmania* (L.) *infantum*, *Leishmania* (L.) *amazonensis* and *Leishmania* (L.) *mexicana* Using Sequential qPCR Assays and High-Resolution Melt Analysis. *Microorganisms* **2020**, *8*, 818.
9. Diotallevi, A.; Buffi, G.; Ceccarelli, M.; Neitzke-Abreu, H.C.; Gnutzmann, L.V.; da Costa Lima, M.S.; Di Domenico, A.; De Santi, M.; Magnani, M.; Galluzzi, L. Real-time PCR to differentiate among *Leishmania* (Viannia) *subgenus*, *Leishmania* (Leishmania) *infantum* and *Leishmania* (Leishmania) *amazonensis*: Application on Brazilian clinical samples. *Acta Trop.* **2020**, *201*, 105178.
10. Ceccarelli, M.; Diotallevi, A.; Andreoni, F.; Vitale, F.; Galluzzi, L.; Magnani, M. Exploiting genetic polymorphisms in metabolic enzymes for rapid screening of *Leishmania infantum* genotypes. *Parasit. Vectors* **2018**, *11*, 572.
11. White, H.; Potts, G. *Mutation Scanning by High Resolution Melt Analysis. Evaluation of RotorGene 6000 (Corbett Life Science), HR1 and 384 Well LightScanner (Idaho Technology)*; National Genetics Reference Laboratory: Wessex, UK, 2006.
12. Tamura, K.; Stecher, G.; Peterson, D.; Filipski, A.; Kumar, S. MEGA6: Molecular Evolutionary Genetics Analysis version 6.0. *Mol. Biol. Evol.* **2013**, *30*, 2725–2729.
13. Alvar, J.; Vélez, I.D.; Bern, C.; Herrero, M.; Desjeux, P.; Cano, J.; Jannin, J.; Boer, M. den Leishmaniasis Worldwide and Global Estimates of Its Incidence. *PLoS ONE* **2012**, *7*, e35671.
14. Mary, C.; Faraut, F.; Lascombe, L.; Dumon, H. Quantification of Leishmania infantum DNA by a real-time PCR assay with high sensitivity. *J. Clin. Microbiol.* **2004**, *42*, 5249–5255.
15. de Paiva Cavalcanti, M.; Dantas-Torres, F.; da Cunha Gonçalves de Albuquerque, S.; Silva de Morais, R.C.; de Brito, M.E.F.; Otranto, D.; Brandão-Filho, S.P. Quantitative real time PCR assays for the detection of *Leishmania* (Viannia) *braziliensis* in animals and humans. *Mol. Cell. Probes* **2013**, *27*, 122–128.
16. Pita-Pereira, D.; Lins, R.; Oliveira, M.P.; Lima, R.B.; Pereira, B.A.S.; Moreira, O.C.; Brazil, R.P.; Britto, C. SYBR Green-based real-time PCR targeting kinetoplast DNA can be used to discriminate between the main etiologic agents of Brazilian cutaneous and visceral leishmaniases. *Parasit. Vectors* **2012**, *5*, 15.
17. Nicolas, L.; Prina, E.; Lang, T.; Milon, G. Real-Time PCR for Detection and Quantitation of Leishmania in Mouse Tissues. *J. Clin. Microbiol.* **2002**, *40*, 1666–1669.
18. De Monbrison, F.; Mihoubi, I.; Picot, S. Real-time PCR assay for the identification of cutaneous Leishmania parasite species in Constantine region of Algeria. *Acta Trop.* **2007**, *102*, 79–83.
19. Mansueto, P.; Seidita, A.; Vitale, G.; Cascio, A. Leishmaniasis in travelers: A literature review. *Travel Med. Infect. Dis.* **2014**, *12*, 563–581.
20. Pavli, A.; Maltezou, H.C. Leishmaniasis, an emerging infection in travelers. *Int. J. Infect. Dis.* **2010**, *14*, e1032–e1039.
21. Mody, R.M.; Lakhal-Naouar, I.; Sherwood, J.E.; Koles, N.L.; Shaw, D.; Bigley, D.P.; Co, E.M.A.; Copeland, N.K.; Jagodzinski, L.L.; Mukbel, R.M.; et al. Asymptomatic Visceral *Leishmania infantum* Infection in US Soldiers Deployed to Iraq. *Clin. Infect. Dis.* **2019**, *68*, 2036–2044.
22. Kniha, E.; Walochnik, J.; Poeppl, W.; Mooseder, G.; Obwaller, A.G. Leishmania spp. seropositivity in Austrian soldiers returning from the Kosovo. *Wien. Klin. Wochenschr.* **2020**, *132*, 47–49.
23. Bailey, M.S.; Langman, G. Misdiagnosis of cutaneous leishmaniasis and recurrence after surgical excision. *J. R. Army Med. Corps* **2013**, *160*, 314–316.
24. Pareyn, M.; Hendrickx, R.; Girma, N.; Hendrickx, S.; Bockstal, L.V.; Houtte, N.V.; Shibru, S.; Maes, L.; Leirs, H.; Caljon, G. Evaluation of a pan—Leishmania SL RNA qPCR assay for parasite detection in laboratory-reared and field-collected sand flies and reservoir hosts. *Parasit. Vectors* **2020**, *13*, 1–10.
25. Nateghi Rostami, M.; Darzi, F.; Farahmand, M.; Aghaei, M.; Parvizi, P. Performance of a universal PCR assay to identify different Leishmania species causative of Old World cutaneous leishmaniasis. *Parasit. Vectors* **2020**, *13*, 431.
26. Adams, E.R.; Schoone, G.; Versteeg, I.; Gomez, M.A.; Diro, E.; Mori, Y.; Perlee, D.; Downing, T.; Saravia, N.; Assaye, A.; et al. Development and Evaluation of a Novel Loop-Mediated Isothermal Amplification Assay for Diagnosis of Cutaneous and Visceral Leishmaniasis. *J. Clin. Microbiol.* **2018**, *56*, 56.
27. Gow, I.; Millar, D.; Ellis, J.; Melki, J.; Stark, D. Semi-Quantitative, Duplexed qPCR Assay for the Detection of Leishmania spp. Using Bisulphite Conversion Technology. *Trop. Med. Infect. Dis.* **2019**, *4*, 135.
28. Krayter, L.; Schnur, L.F.; Schönian, G. The Genetic Relationship between Leishmania aethiopica and Leishmania tropica Revealed by Comparing Microsatellite Profiles. *PLoS ONE* **2015**, *10*, e0131227.

29. Schulz, A.; Mellenthin, K.; Schonian, G.; Fleischer, B.; Drosten, C. Detection, Differentiation, and Quantitation of Pathogenic Leishmania Organisms by a Fluorescence Resonance Energy Transfer-Based Real-Time PCR Assay. *J. Clin. Microbiol.* **2003**, *41*, 1529–1535.
30. Talmi-Frank, D.; Nasereddin, A.; Schnur, L.F.; Schönian, G.; Töz, S.Ö.; Jaffe, C.L.; Baneth, G. Detection and Identification of Old World Leishmania by High Resolution Melt Analysis. *PLoS Negl. Trop. Dis.* **2010**, *4*, e581.
31. Toz, S.O.; Culha, G.; Zeyrek, F.Y.; Ertabaklar, H.; Alkan, M.Z.; Vardarlı, A.T.; Gunduz, C.; Ozbel, Y. A Real-Time ITS1-PCR Based Method in the Diagnosis and Species Identification of Leishmania Parasite from Human and Dog Clinical Samples in Turkey. *PLoS Negl. Trop. Dis.* **2013**, *7*, e2205.
32. Weirather, J.L.; Jeronimo, S.M.B.; Gautam, S.; Sundar, S.; Kang, M.; Kurtz, M.A.; Haque, R.; Schriefer, A.; Talhari, S.; Carvalho, E.M.; et al. Serial Quantitative PCR Assay for Detection, Species Discrimination, and Quantification of *Leishmania* spp. in Human Samples. *J. Clin. Microbiol.* **2011**, *49*, 3892–3904.

CHAPTER 5

The multilocus enzyme electrophoresis (MLEE) has been historically considerer by WHO the reference technique for *Leishmania* species characterization. Since this test is time-consuming and needs parasites isolation, the aim of this work was to develop an HRM-based assay for the rapid and cheap characterization of *L. Infantum* species. Moreover, these new assays were applied on *L. Infantum* clinical isolates/samples from the Mediterranean region, including the borderline territory of Pantelleria island, to explore the genetic variability that characterizes *L. (L.) infantum*. The study was made in collaboration with National Reference Center for Leishmaniasis (C.Re.Na.L.), Istituto Zooprofilattico Sperimentale della Sicilia (Palermo, Italy) and financed by the project “ricerca corrente IZS SI 01/17”

(Unpublished data)

Development and application of an MLST panel for the identification of informative polymorphisms in *Leishmania infantum* strains in the Mediterranean region

Abstract

Leishmaniasis is a zoonotic disease endemic in the Mediterranean region, where the causative agent of human and canine infection is *Leishmania infantum*. The spread of leishmaniasis is associated with population movements, ecology of phlebotomine vectors, and reservoir host. We used multilocus sequence typing (MLST) to explore the genetic variability of *L. infantum* strains in the Mediterranean region, including the borderline territory of Pantelleria island, and identify informative polymorphisms for rapid identification of genotypes through high-resolution melting (HRM)-based assays. A customized sequencing panel targeting 14 housekeeping genes was designed and MLST analysis was performed using the Ion Torrent S5 on 9 *L. infantum* strains/isolates: 5 canine isolates (3 from Pantelleria Island and 2 from central Italy), and 4 human isolates/strains from Tunisia, France, central and southern Italy. MLST results and in silico analysis of sequences available in Genbank allowed to select two informative polymorphisms on malic enzyme (ME) and 6-phosphogluconate dehydrogenase (GPI) genes (390T/G and 1834A/G, respectively) used to develop two HRM-based assays for fast screening of 39 clinical samples. The MLST analysis identified a single *L. infantum* clonal complex regardless of the geographic origin or host (human or canine), except for the human isolate from central Italy that showed polymorphisms in 11 out of 14 housekeeping genes, and clustered independently in molecular phylogenetic analysis. Successively, the screening through HRM-based assays of 39 clinical samples from central/south Italy and Pantelleria island allowed to identify 6 genotypes. Interestingly, the sequence type 390T/1834A was found only in Pantelleria island (prevalence 75%). This study represents a description of the genetic variability of *L. infantum* through a first approach based on MLST and then by HRM analysis on selected polymorphisms. The HRM assays could be used as fast and cheap tools for epidemiological surveillance of *L. infantum*.

1. Introduction

Leishmaniasis is a zoonotic disease endemic in the Mediterranean basin caused by *Leishmania infantum* species, the etiological agent of human cutaneous and visceral leishmaniasis (CL and VL) and canine leishmaniasis (CanL). The species characterization is performed by multilocus enzyme electrophoresis (MLEE) technique, considered the reference method for parasite typing by the World Health Organization (World Health Organization, 2010). This enzymatic technique, developed at the Centre for Leishmaniasis of Montpellier (France) (MON system), is based on the different electrophoretic mobility of 15 metabolic enzymes: malate dehydrogenase, malic enzyme, isocitrate dehydrogenase, 6-phosphogluconate dehydrogenase, glucose-6-phosphate dehydrogenase, glutamate dehydrogenase, NADH diaphorase, purine nucleoside phosphorylase 1, purine nucleoside phosphorylase 2, glutamate–oxaloacetate transaminases 1 and 2, phosphoglucomutase, fumarate hydratase, mannose-phosphate isomerase, glucose phosphate isomerase (Aït-Oudhia et al., 2011). The comparison of isoenzyme mobility with a reference strain identified over 300 zymodemes, also termed MON. Regarding *L. infantum*, 45 zymodemes have been identified. Zoonotic VL and CanL are mainly caused by MON-1, MON-24, MON-34, MON-72, MON-77, MON-80, MON-98, MON-105, MON-108, MON-199, MON-199 NP1130 variant and MON-281. In particular, MON-1 is the most frequent zymodeme in humans and dogs (Kuhls et al., 2011; Pratlong et al., 2013), while MON-72 is the second more diffuse in CanL, but has been identified also in patients (Aït-Oudhia et al., 2011). On the other hand, some zymodemes (i.e., MON-11, MON-27, MON-28, MON-29, MON-33, MON-189), were isolated only in humans (Millán et al., 2014). Moreover, several non-MON 1 parasites have been reported in HIV patients (Gramiccia, 2003). This evidence questions the role of dogs, historically considered the main reservoir of infection for humans. In fact, the zymodeme's homogeneity relieved in the canine population does not reflect the heterogeneity found in humans. Unfortunately, the *Leishmania* characterization based on MLEE presents some limitations: it is time-consuming and cumbersome, requires parasites isolation and cultivation and can be performed only in a few laboratories. To overcome these problems, some biomolecular approaches have been proposed such as multilocus sequence typing (MLST) (Mauricio et al., 2006) and multilocus microsatellite typing (MLMT) (Gouzelou et al., 2012). Nevertheless, also these techniques are time-consuming, expensive, and can require

parasite isolation; therefore, their applicability in epidemiological studies is poor. In this view, in a previous study, we developed an alternative technique, a high-resolution melting (HRM)-based assay able to differentiate the most common zymodemes (i.e., MON-1, MON-72, MON-201, except for MHOM/TN/80/IPT1, a MON-1 strain from Tunisia) exploiting the polymorphism 390T>G in the malic enzyme evidencing a partial agreement, although not univocal, between genotyping results and MLEE. This assay has been successfully applied for rapid characterization of *L. infantum* clinical isolates and clinical samples, without the need for parasite isolation (Ceccarelli et al., 2018). This work represents an update of the previous one. We designed an MLST panel with the aim of: (i) identifying polymorphisms useful for *L. infantum* typing in the Mediterranean region through an MLST-based approach; (ii) developing HRM-based test on the most informative polymorphisms for the rapid and cheap characterization of *L. infantum* strains; (iii) investigating genetic variability of *L. infantum* strains in border territory in the Mediterranean (Pantelleria island).

2. Material and methods

2.1 MLST panel design, library preparation and NGS sequencing

A customized sequencing panel was designed with Ion AmpliSeq™ designer v7.0.6 (Thermo-Fisher-Scientific), using the *L. infantum* JPCM5 genome as reference, to target the coding DNA sequences of the 14 genes listed in Table 1 (partially in common with MLEE enzymes). This panel consisted of two primer pools with 88 different amplicons. The *Leishmania* strains and isolated sequenced are summarized in Table 2. The DNA library preparation was performed by Ion AmpliSeq™ Library Kit Plus (Thermo-Fisher-Scientific) following the protocol instructions, starting from a total of 5 ng of DNA.

Name	Chromosome	Chr_Start	Chr_End	Num Amplicons	Total Bases	Covered Bases	Missed Bases	Overall Coverage
Elongation initiation factor 2alpha	LinJ03	386699	387940	7	1241	1241	0	1
Spermidine synthase1	LinJ04	235535	236437	6	902	902	0	1
Isocitrate dehydrogenase	LinJ10	130500	131500	7	1000	1000	0	1
glucose-6-phosphate isomerase	LinJ12	291650	292850	7	1200	1165	35	0.971
Nucleoside hydrolase-like protein (NH2)	LinJ14	31980	33040	6	1060	1060	0	1
Nucleoside hydrolase(iunh) (NH1)	LinJ18	686250	687250	6	1000	864	136	0.864
malic_enzyme	LinJ24	280800	282400	9	1600	1500	100	0.938
mannose_phosphate_isomerase	LinJ32	621550	622150	4	600	600	0	1
glucose-6-phosphate dehydrogenase	LinJ34	26850	28050	7	1200	1200	0	1
malate_dehydrogenase	LinJ34	47355	48308	6	953	930	23	0.976
arginase(ARG)	LinJ35	570876	571865	7	989	989	0	1
6-phosphogluconate dehydrogenase	LinJ35	1288100	1288800	4	700	513	187	0.733
phosphomannomutase(PMM)	LinJ36	782734	783477	4	743	743	0	1
N-acetylglucosamine-1-phosphate transferase(NAGT)	LinJ36	1632000	1633300	8	1300	1300	0	1

[Table 1] Genes and genomic coordinates of the MLST panel designed with Ion AmpliSeq™ designer (ID: IAD170409)

NGS was performed using the Ion Torrent S5 instrument. After sequencing, reads were mapped to *L. infantum* JPCM5 genome using Torrent Browser. Variants were called using LoFreq in Galaxy (Galaxy Version 2.1.5+galaxy0) (Wilm et al., 2012) using default settings. Integrative Genomics Viewer or Ugene were used for variant visualization. Subsequently, a

molecular phylogenetic analysis by Maximum Likelihood method based on the General Time Reversible model (Nei et al., 2000) has been performed using MEGA6 software.

Sample ID	Description	Host species	Disease	Geographical origin
1	*L. infantum* isolate 30	dog	CanL	Pantelleria island
2	*L. infantum* isolate 42	dog	CanL	Pantelleria island
3	*L. infantum* MHOM/TN/80/IPT1	human		Tunisia
4	*L. infantum* MHOM/FR/78/LEM75	human		France
5	*L. infantum* isolate 64	dog	CanL	Pantelleria island
6	*L. infantum* isolate Leo-Ani	human	CL	Marche (Central Italy)
7	*L. infantum* MHOM/IT/08/31U	dog	CanL	Sicily (South Italy)
8	*L. infantum* isolate Brina (Bra-Aii)	dog	CanL	Marche (Central Italy)
9	*L. infantum* isolate Scagnetti (Els-Sci)	dog	CanL	Marche (Central Italy)

[Table 2] Samples selected for MLST analysis

2.2 Collected samples and DNA extraction

L. infantum strains, clinical samples and isolates used in this study are listed in Table 3. The samples 1-14 and 29-55 were provided by the National Reference Center for Leishmaniasis (C.Re.Na.L.), Istituto Zooprofilattico Sperimentale della Sicilia (Palermo, Italy) (Castelli et al., 2020; Vitale et al., 2020). Human samples (15,18,19) were obtained from the Infectious Diseases Department of Muraglia Hospital (Ospedali Riuniti Marche Nord, Pesaro - Italy) for diagnostic purposes. The parasite isolation of sample 15 was performed as previously described (Diotallevi et al., 2021). The canine clinical samples (16,17,20-29) were provided from the veterinary clinic “Santa Teresa” in Fano (Italy). DNA from buffy-coat, biopsies, bone marrow and lymph node aspirates were extracted using the DNeasy Blood & Tissue kit (Qiagen, Valencia, USA) following the protocol indications and quantified using a Qubit fluorometer (Life Technologies, Carlsbad, USA). DNA from conjunctival swab was obtained from raw lysate by incubation for 2 h at 56°C in 200 µl lysis buffer (10 mM Tris–HCl pH 8.3,

50 mM KCl, 0.5% Nonidet P40, 0.5% Tween 20, 0.1 mg/ml proteinase K). After swab elimination, the samples were incubated for 10 min at 95°C and centrifuged at 10,000 × g for 10 min (Ceccarelli et al., 2014a). All human and veterinary samples were diagnosed positive for *Leishmania* spp. through objective evaluation, serological tests and/or cytohistological exams. Moreover, samples positivity has been evaluated with qPCR-ML analysis (Ceccarelli et al., 2014b). *L. infantum* species characterization was performed with ITS1-PCR RFLP according to Schönian et al. (Schönian et al., 2003). Briefly, the PCR products were digested with 10U HaeIII (Thermo Fisher Scientific) at 37 °C for 3h. The restriction fragments were visualized on 3.5% high-resolution MetaPhor (Cambrex) agarose gel.

Number	ID Sample	Type of sample	Host	Geographic origin
1	**MHOM/FR/78/LEM75**	Strain (MON-1)	human	France
2	**MHOM/TN/80/IPT1**	Strain (MON-1)	human	Tunisia
3	**MHOM/DZ/82/LIPA59**	Strain (MON-24)	human	Algeria
4	**MHOM/ES/81/BCN1**	Strain (MON-29)	human	Spain
5	**MHOM/IT/86/ISS218**	Strain (MON-72)	human	Italy
6	**MHOM/IT/93/ISS822**	Strain (MON-201)	human	Italy
7	**MHOM/IT/08/31U**	Strain (MON-1)	human	Italy
8	**MHOM/IT/08/49U**	Strain (MON-1)	human	Italy
9	**30**	Clinical isolate	dog	Pantelleria (Italy)
10	**42**	Clinical isolate	dog	Pantelleria (Italy)
11	**64**	Clinical isolate	dog	Pantelleria (Italy)
12	**10816**	Clinical isolate	cat	Italy
13	**V2921**	Clinical isolate	marten	Italy
14	**791**	Clinical isolate	cat	Italy
15	**Leo-Ani**	Clinical isolate	human	Italy
16	**Elr-Sci**	Clinical isolate	dog	Italy
17	**Bra-Aii**	Clinical isolate	dog	Italy
18	**PsAlb**	Clinical sample	human	Italy
19	**Dae-Dio**	Clinical sample	human	Italy
20	**Aro-Sai**	Clinical sample	dog	Italy
21	**Els-Mai**	Clinical sample	dog	Italy
22	**Toy-Gai**	Clinical sample	dog	Italy
23	**Koa-Cro**	Clinical sample	dog	Italy
24	**Zeo-sci**	Clinical sample	dog	Italy
25	**Gia-Spi**	Clinical sample	dog	Italy

26	**Grg-Rao**	Clinical sample	dog	Italy
27	**Vea-Fri**	Clinical sample	dog	Italy
28	**Jon-Doe**	Clinical sample	dog	Italy
29	**1038U**	Clinical sample	human	Italy
30	**1522U**	Clinical sample	human	Italy
31	**1536U**	Clinical sample	human	Italy
32	**1538U**	Clinical sample	human	Italy
33	**1578U**	Clinical sample	human	Italy
34	**1810U**	Clinical sample	human	Italy
35	**2618U**	Clinical sample	human	Italy
36	**2619U**	Clinical sample	human	Italy
37	**1**	Clinical sample	dog	Pantelleria (Italy)
38	**4**	Clinical sample	dog	Pantelleria (Italy)
39	**5**	Clinical sample	dog	Pantelleria (Italy)
40	**6**	Clinical sample	dog	Pantelleria (Italy)
41	**9**	Clinical sample	dog	Pantelleria (Italy)
42	**10**	Clinical sample	dog	Pantelleria (Italy)
43	**12**	Clinical sample	dog	Pantelleria (Italy)
44	**13**	Clinical sample	dog	Pantelleria (Italy)
45	**14**	Clinical sample	dog	Pantelleria (Italy)
46	**15**	Clinical sample	dog	Pantelleria (Italy)
47	**16**	Clinical sample	dog	Pantelleria (Italy)
48	**19**	Clinical sample	dog	Pantelleria (Italy)
49	**20**	Clinical sample	dog	Pantelleria (Italy)
50	**21**	Clinical sample	dog	Pantelleria (Italy)
51	**22**	Clinical sample	dog	Pantelleria (Italy)
52	**24**	Clinical sample	dog	Pantelleria (Italy)
53	**26**	Clinical sample	dog	Pantelleria (Italy)
54	**27**	Clinical sample	dog	Pantelleria (Italy)
55	**28**	Clinical sample	dog	Pantelleria (Italy)

[Table 3] *L. infantum* strains, clinical isolates and clinical samples processed in this study

2.3 Primers design

MLST results and in silico analysis of sequences available in Genbank allowed to select two informative polymorphisms on malic enzyme (ME) and 6-phosphogluconate dehydrogenase (GPI) genes (390T/G and 1834A/G, as in reference sequences DQ449701.1 and AJ620647.1

respectively) useful to develop two HRM-based assays for fast screening of clinical samples, updating the genotyping method previously described and applied by Ceccarelli et al. on ME gene (Ceccarelli et al., 2018). Primers for each assay have been designed: two external primers to perform the pre-amplification step with conventional PCR (cPCR) and an internal couple of primer for the second amplification with quantitative PCR (qPCR), followed by HRM-analysis. Primers were designed with PrimerBLAST (Ye et al., 2012) using *L. infantum* MHOM/FR/78/LEM75 and MHOM/TN/80/IPT1 sequences as reference. The primers are listed in Table 4 and their position on the target genes is shown in Figures 1 and 2.

Target Gene	Reference sequence	Primer	Sequence	qPCR assay
ME	DQ449701.1	MEint_F*	TCAGAACCTTCGCAAGACGA	PCR-MEint-ME65
		MEint_R*	CACTTGCCGATGCTGATGC	
		ME65_R	GGCCGAGAATGCGGGAG	
GPI	AJ620647.1	GPIext_F	CTCAAGTCCGGCAACATCGT	PCR-GPIext-GPI88
		GPIext_R	ACATGCACTTCGCAGCTCT	
		GPI88_F	ACGAACGGCCTGATCAACAT	
		GPI88_R	ACATGCACTTCGCAGCTCTA	

[Table 4] *Primers* used in this study. ME: malic_enzyme; GPI: 6-phosphogluconate dehydrogenase; F: forward; R: reverse. *(Ceccarelli et al., 2018).

[Figure 1] Sequence of *L. infantum* MHOM/FR/78/LEM75 (DQ449701.1) ME gene and primers used for PCR-MEint-ME65. The polymorphic position (390T/G) is in red. MEint_F is in common for both PCR assays.

[Figure 2] Sequence of *L. infantum* MHOM/TN/80/IPT1 (AJ620647.1) GPI gene and primers used for PCR-GPIext-GPI88. The polymorphic position (1834A/G) is in red.
GPI88_R differs from GPIext_R by an extra base at 3' (in bold).

2.4 Pre-amplification step by cPCR

To ensure the amplification of clinical samples with low parasite load, a pre-amplification step by conventional PCR (cPCR) was introduced. The cPCR was performed in total 50 µl with 4 µl of template, 200 µM dNTP, 2.5 mM MgCl2, 200 nM of each primer and 1 unit of Hot-Rescue DNA polymerase (Diatheva s.r.l., Fano, Italy). Amplification was carried out in a GeneAmp® PCR System 2700 thermocycler (Applied Biosystems, Foster City, USA). The thermal cycling profile was as follows: 94 °C for 7 min; followed by 15 cycles at 94 °C for 30 s, 60 °C for 20, 72 °C for 15 s. A no template tube was introduced as a negative control.

2.5 Quantitative PCR (qPCR) and high-resolution melting (HRM) analysis

The quantitative PCR-ME65 and PCR-GPI88 amplify products of 65 bp and 88 bp, respectively. The PCR products encompass the single nucleotide polymorphisms (SNPs) 390T/G (PCR-ME65) and 1834G/A (PCR-GPI88). All qPCRs were carried out in 25 µl of total volume containing 1 µl of template DNA (genomic for control samples and pre-amplified by cPCR for clinical samples) and 24 µl of TB Green PreMix ex Taq II Master Mix (Takara Bio Europe, France), with 200 nM of each primer. The qPCR reactions were performed in a Rotor-Gene 6000 instrument (Corbett Life Science, Mortlake, Australia). The thermal cycling profile was as follows: 94 °C for 10 min, followed by 45 cycles at 94 °C for 20 s, 60 °C for 20 s and 72 °C for 20 s. Each sample was run in duplicate, and a no template control was processed in each run. After amplification, HRM analysis was performed over the range 77-88 °C, rising by 0.1 °C/s and waiting for 2 s at each temperature. Raw HRM curves were normalized by the Rotorgene 6000 v.1.7 software. In PCR-ME65, MHOM/FR/78/LEM75 and MHOM/TN/80/IPT1 strains were used as reference for genotypes 390T and 390G, respectively. In PCR-GPI88, MHOM/FR/78/LEM75, MHOM/TN/80/IPT1 and MHOM/IT/93/ISS822 strains were used as standards for 1834G, 1834A and 1834R (heterozygote) genotypes. The assignment of the 390T/G and 1834G/A genotypes was performed by the instrument software with a confidence ≥ 85%.

To evaluate the specificity of the new primer pairs (Meint_F/ME65_R and GPI88_F/GPIext_R), a qPCR was performed as described previously using $1x10^{-2}$ ng of MHOM/FR/78/LEM75, MHOM/TN/80/IPT1 DNA, and 30 ng of human, canine, feline and *Tryanosoma cruzi* DNA as template. Amplified fragments were analyzed by 1.8% agarose gel electrophoresis with Midori Green Advance DNA stain (NIPPON Genetics EUROPE GmBh). The gels were visualized under UV light using a gel doc apparatus (Bio-Rad, Hercules, USA). GeneRuler 100 bp Plus DNA Ladder (Thermo Fisher Scientific) was included as size standard.

To estimate ME65 and GPI88 qPCRs sensitivity and applicability on clinical samples, standard curves were established using serial dilutions of MHOM/FR/78/LEM75 DNA, from $1×10^{0}$ to $1×10^{-5}$ ng. To evaluate the potential interference of host DNA as background in the qPCR assay, 30 ng of human and canine DNA purified from human and canine cell lines (MCF7 and DH82) were spiked in each qPCR reaction tube. The standard curves were obtained from two independent experiments and processed in duplicate.

2.6 Sequencing

To confirm the genotype assigned by the Rotorgene software, the amplification products of the reference strains and some clinical samples, were purified using the Minelute PCR purification kit (Qiagen, Hilden, Germany) and directly sequenced. DNA sequencing was performed using the BigDye Terminator v.11 Cycle Sequencing Kit on an ABI PRISM 310 Genetic Analyzer (Applied Biosystems). The electropherogram was analyzed and the sequences were aligned using the BioEdit Sequence Alignment Editor (Hall et al., 1999). The heterozygous genotype was attributed when two different overlapping peaks were observed in the same position.

3. Results

3.1 MLST on *L. infantum* strains and isolates

The MLST custom panel has been applied on 9 *L. infantum* samples: 5 canine isolates (3 from Pantelleria Island and 2 from central Italy), and 4 human isolates/strains from Tunisia, France, central and southern Italy. The results showed identical sequences (1-3 mismatches compared to reference genome JPCM5 out of 15545 bases, i.e., <0.0002%) in all the samples, regardless of geographic origin or host, except for the human isolate from central Italy Leo-Ani that showed 25 mismatches compared to reference genome JPCM5 (i.e., 0.0016%) (Table 5).

Chr		1 Isolate 30	2 Isolate 42	3 MHOM/TN/80/IPT1	4 MHOM/FR/78/LEM75	5 Isolate 64	6 Isolate Leo-Ani	7 MHOM/IT/08/31U	8 Isolate Brina	9 Isolate Scagnetti
LinJ03	elongation_initiation_factor_2alpha LINF_030014900									
LinJ04	spermidine_synthase1 LINF_040010800									
LinJ10	isocitrate_dehydrogenase LINF_100008300						130806 C 131265 Y 131511 T			
LinJ12	glucose-6-phosphate_isomerase LINF_120010600	292519 A 292809 A	292519 A	292519 A 292809 A	292519 A	292519 A 292809 A	292519 A 292809 A	292519 A	292519 A 292809 A	292519 A
LinJ14	nucleoside_hydrolase-like_protein(NH2) LINF_140006200						32800 T			
LinJ18	nucleoside_hydrolase(iunh)(NH1) LINF_180021400						686833 G			
LinJ24	malic_enzyme LINF_240012800			281164 G			280978 Y 281103 G 281164 G 281281 G 281617 Y 281693 R		281164 G	
LinJ32	mannose_phosphate_isomerase LINF_320021600						621512 K			
LinJ34	glucose-6-phosphate_dehydrogenase LINF_340005700						26839 S 26878 C 27181 C 27947 R			
LinJ34	malate_dehydrogenase LINF_340006400						47256 R 47877 C 48169 M 48225 G			
LinJ35	arginase(ARG) LINF_350019900						571026 M			
LinJ35	phosphogluconate_dehydrogenase LINF_350038800						1288246 C			
LinJ36	phosphomannomutase(PMM) LINF_360026300						783228 S			
LinJ36	N-acetylglucosamine-1-phosphate_transferase(NAGT) LINF_360051000									

[Table 5] Polymorphisms identified in samples sequenced by MLST, compared to the reference genome JPCM5. (In yellow, missense mutation; in green, silent mutation; in grey, non-coding)

In fact, phylogenetic analysis showed that Leo-Ani isolate clustered independently from the other *L. infantum* strains/isolates (Figure 3).

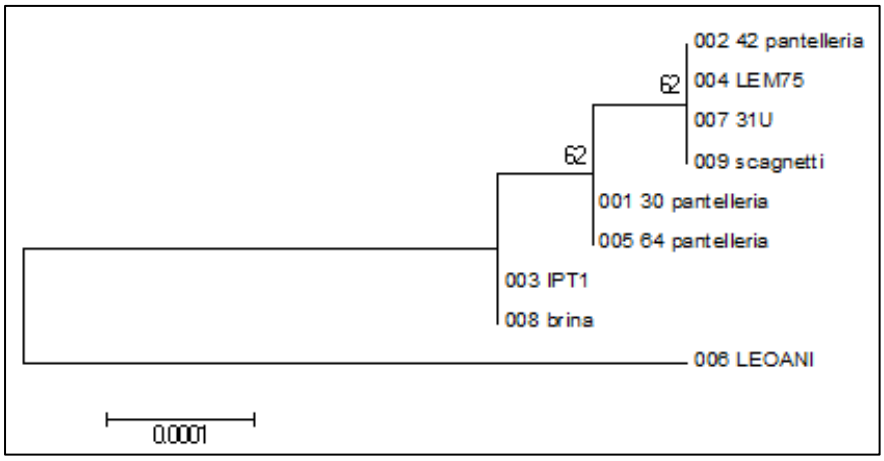

[Figure 3] Molecular Phylogenetic analysis by Maximum Likelihood method. The tree is drawn to scale, with branch lengths measured in the number of substitutions per site. Evolutionary analyses were conducted in MEGA6

Based on MLST panel results and in silico analysis of sequences available in Genbank, an informative polymorphism on GPI genes (1834A/G) has been identified and select to develop an HRM-based assay for screening of clinical samples, used in association with the genotyping method previously developed and applied by Ceccarelli et al. on ME gene (Ceccarelli et al., 2018).

3.2 Specificity and sensitivity evaluation

The new pairs of primers (Meint_F/ME65_R and GPI88_F/GPI88_R) were first tested by qPCR to evaluate specificity. As templates, 30 ng of human, canine, feline and *Trypanosoma cruzi* and $1x10^{-2}$ ng of MHOM/FR/78/LEM75, MHOM/TN/80/IPT1 were used. Amplified fragments were analyzed by agarose gel electrophoresis as described in methods. The products obtained were of the expected size and non-specific amplification was not detected (Figure 4)

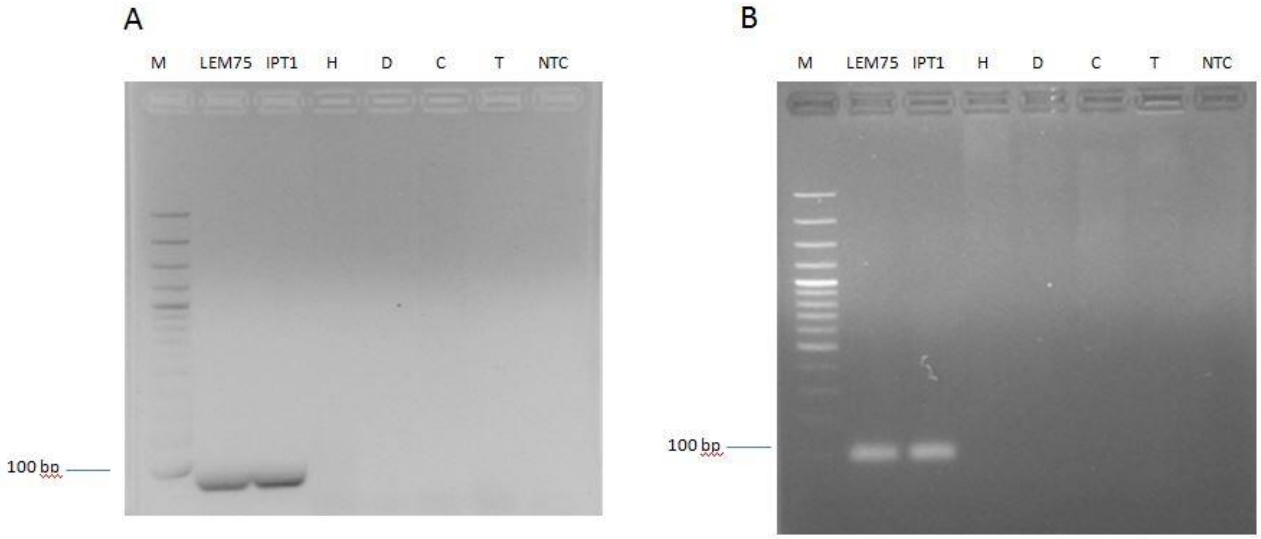

[Figure 4] Specificity evaluation of primers Meint_F/ME65_R (A) and GPI88_F/GPI88_R (B). M: marker 100 bp DNA ladder; Lem: MHOM/FR/78/LEM75; IPT1: MHOM/TN/80/IPT1; H: human DNA; D: dog DNA; C: cat DNA; T: *Trypanosoma cruzi* DNA; NTC: no template control.

The sensitivity curves for ME65 and GPI88 evidenced a limit of quantification of 1×10^{-4} ng/PCR tube with R^2>0.99 (Figure 5). In the presence of human and canine DNA as background, the Cq was slightly delayed, but the linearity and limit of quantification of the assay remained unchanged.

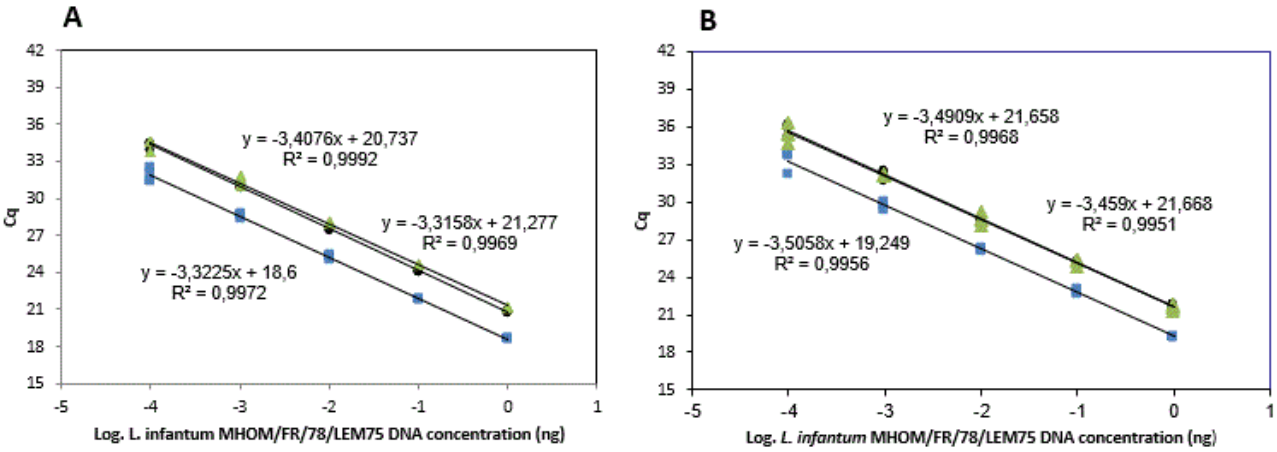

[Figure 5] Sensitivity curves of ME65 (A) and GPI88 (B). The standard curves were spiked with 30 ng of human or canine DNA (upper curves partially overlapping, circles and triangles points, respectively) or non-spiked (lower curve, square points). Each point is derived from a duplicate of two independent experiments.

3.3 HRM assays application on *L. infantum* strains

The two qPCR assays (qPCR-ME65 and qPCR-GPI88) were first tested on *L. infantum* strains MHOM/FR/78/LEM75 and MHOM/TN/80/IPT1, whose ME/GPI polymorphisms were 390T/1834G and 390G/1834A, respectively. The qPCR assays were performed as described in methods. At the end of the amplification, HRM analysis was performed. The evaluation of the dissociation curves generated by the Rotorgene software allowed to discriminate the two genotypes (Figure 6).

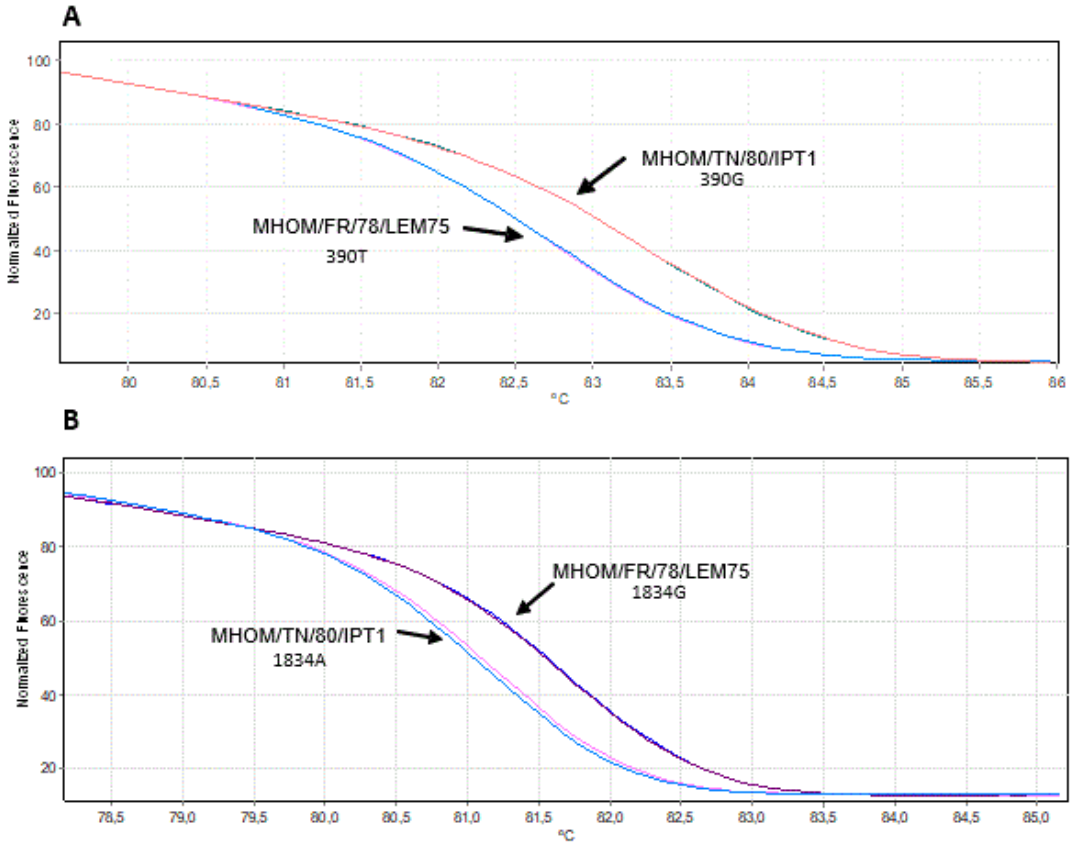

[Figure 6] HRM analysis of *L. infantum* strains. (A) HRM profiles obtained by qPCR-ME65 of MHOM/TN/80/IPT1 (genotype 390G) and MHOM/FR/78/LEM75 (genotype 390T). (B) HRM profiles were obtained by qPCR-GPI88 of MHOM/TN/80/IPT1 (genotype 1834A) and MHOM/FR/78/LEM75 (genotype 1834G).

3.4 HRM assays application on *L. infantum* clinical samples/isolates

Once demonstrated the possibility to discriminate 390T/390G and 1834G/1834A genotypes on reference strains, the two PCR assays have been tested on 9 clinical isolates and 38 human and canine clinical samples from central/south Italy and Pantelleria island (borderline territory of the Mediterranean), in order to evaluate the genetic variability of *L. Infantum* in

this area and obtain epidemiological information. First, the presence of *L. infantum* in clinical samples was confirmed by ITS1-PCR RFLP (Schönian et al., 2003) and/or by amplification of minicircles kDNA (qPCR-ML) (Ceccarelli et al., 2014b). To increase the sensitivity and robustness of the HRM analysis on clinical samples in which the parasite DNA was poorly represented, 15 cycles of pre-amplification step were introduced using the external primers pair. Subsequently, 2 µl of the reaction were used as template for qPCR. The qPCR-ME65 and qPCR-GPI88 assays allowed to discriminate the genotype of 37 and 30 out of 38 clinical samples available, showing a sensitivity of 97.4% and 78.9%, respectively, while on clinical isolates the sensitivity has reached 100% (9 out of 9 with both the assays) (Table 5). An example of dissociation curve and % of confidence obtained with clinical samples are shown in Figures 7 and 8. The sequences of selected samples confirmed data obtained with PCR.

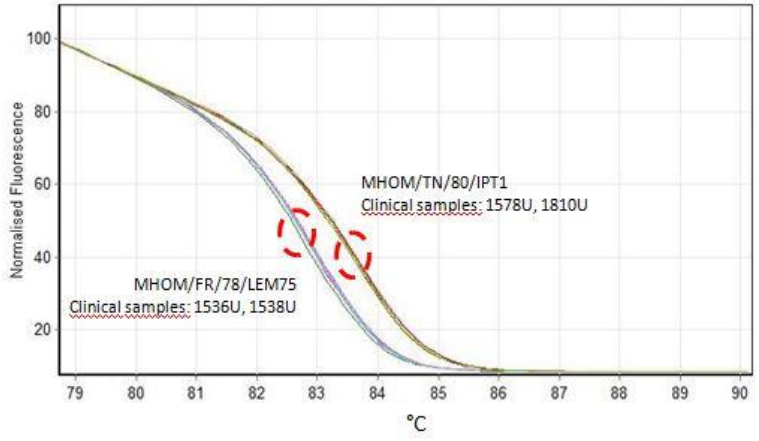

No.	Colour	Name	Genotype	Confidence %
7		ME65 IPT1	390G	99,92
8		ME65 IPT1	390G	99,92
9		ME65 LEM75	390T	98,48
10		ME65 LEM75	390T	98,48
15		ME65 1536U	390T	98,57
16		ME65 1536U	390T	97,14
17		ME65 1538U	390T	91,30
18		ME65 1538U	390T	95,38
19		ME65 1578U	390G	93,19
20		ME65 1578U	390G	96,81
21		ME65 1810U	390G	99,69
22		ME65 1810U	390G	99,16

[Figure 7] HRM dissociation curves analysis and % of confidence of reference strains and clinical isolates processed with qPCR-ME65

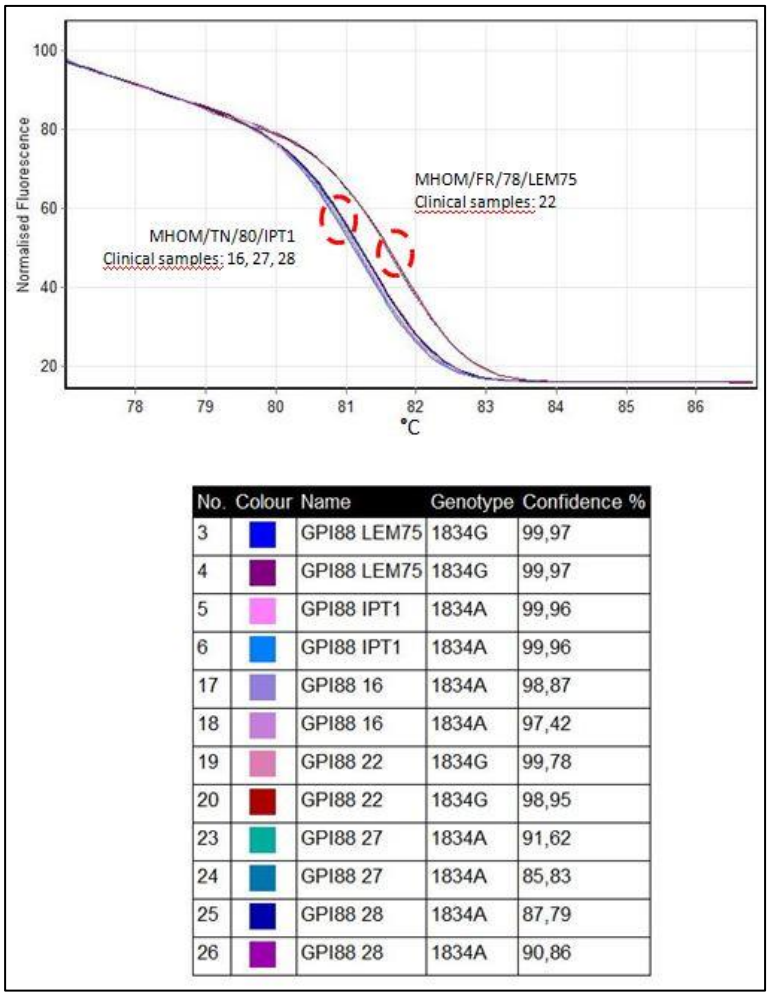

No.	Colour	Name	Genotype	Confidence %
3		GPI88 LEM75	1834G	99,97
4		GPI88 LEM75	1834G	99,97
5		GPI88 IPT1	1834A	99,96
6		GPI88 IPT1	1834A	99,96
17		GPI88 16	1834A	98,87
18		GPI88 16	1834A	97,42
19		GPI88 22	1834G	99,78
20		GPI88 22	1834G	98,95
23		GPI88 27	1834A	91,62
24		GPI88 27	1834A	85,83
25		GPI88 28	1834A	87,79
26		GPI88 28	1834A	90,86

[Figure 8] HRM dissociation curves analysis and % of confidence of reference strains and clinical isolates processed with qPCR-GPI88

3.5 Genotype identification

From the simultaneous analysis of the two polymorphisms, it was possible to identify 6 genotypes (Table 6)

Genotype	ME	GPI
G1	390T	1834G
G2	390G	1834G
G3	390G	1834A
G4	390T	1834R
G5	390G	1834R
G6	390T	1834A

[Table 6] Genotype identified in the study

The genotyping results obtained by the processing of all *L. infantum* strains, clinical samples and clinical isolates with qPCR-ME65 and qPCR-GPI88 are summarized in Table 7. The genotype distribution is depicted in Figure 9.

ID Sample	Type of sample	Host	Geographic origin	ME	GPI	Genotype
MHOM/FR/78/LEM75	Strain (MON-1)	human	France	390T	1834G	1
MHOM/TN/80/IPT1	Strain (MON-1)	human	Tunisia	390G	1834A	3
MHOM/DZ/82/LIPA59	Strain (MON-24)	human	Algeria	390G	1834A	3
MHOM/ES/81/BCN1	Strain (MON-29)	human	Spain	390G	1834G	2
MHOM/IT/86/ISS218	Strain (MON-72)	human	Italy	390T	1834G	1
MHOM/IT/93/ISS822	Strain (MON-201)	human	Italy	390T	1834R	4
MHOM/IT/08/31U	Strain (MON-1)	human	Italy	390T	1834G	1
MHOM/IT/08/49U	Strain (MON-1)	human	Italy	390T	1834G	1
30	Clinical isolate	dog	Pantelleria (Italy)	390T	1834A	6
42	Clinical isolate	dog	Pantelleria (Italy)	390T	1834G	1
64	Clinical isolate	dog	Pantelleria (Italy)	390T	1834A	6
10816	Clinical isolate	cat	Italy	390T	1834G	1
V2921	Clinical isolate	marten	Italy	390G	1834R	5
791	Clinical isolate	cat	Italy	390T	1834G	1
LEO ANI	Clinical isolate	human	Italy	390G	1834A	3
Elr-Sci	Clinical isolate	dog	Italy	390T	1834G	1
Bra-Aii	Clinical isolate	dog	Italy	390G	1834A	3
PsAlb	Clinical sample	human	Italy	390T	1834G	1
Dae-Dio	Clinical sample	human	Italy	390G	1834R	5
Aro-Sai	Clinical sample	dog	Italy	390T	1834G	1
Els-Mai	Clinical sample	dog	Italy	390T	1834R	4
Toy-Gai	Clinical sample	dog	Italy	390T	1834G	1
Koa-Cro	Clinical sample	dog	Italy	390T	1834G	1
Zeo-sci	Clinical sample	dog	Italy	390T	1834G	1
Gia-Spi	Clinical sample	dog	Italy	390T	1834G	1
Grg-Rao	Clinical sample	dog	Italy	390T	1834G	1
Vea-Fri	Clinical sample	dog	Italy	390T	Nd	
Jon-Doe	Clinical sample	dog	Italy	390T	1834G	1
1038U	Clinical sample	human	Italy	390T	1834G	1
1522U	Clinical sample	human	Italy	390T	1834G	1
1536U	Clinical sample	human	Italy	390T	1834G	1

1538U	Clinical sample	human	Italy	390T	1834G	1
1578U	Clinical sample	human	Italy	390G	Nd	
1810U	Clinical sample	human	Italy	390G	Nd	
2618U	Clinical sample	human	Italy	390T	1834G	1
2619U	Clinical sample	human	Italy	390T	1834G	1
1	Clinical sample	dog	Pantelleria (Italy)	390T	1834G	1
4	Clinical sample	dog	Pantelleria (Italy)	390T	1834A	6
5	Clinical sample	dog	Pantelleria (Italy)	390T	1834A	6
6	Clinical sample	dog	Pantelleria (Italy)	390T	1834A	6
9	Clinical sample	dog	Pantelleria (Italy)	390T	1834A	6
10	Clinical sample	dog	Pantelleria (Italy)	390T	1834A	6
12	Clinical sample	dog	Pantelleria (Italy)	390T	1834A	6
13	Clinical sample	dog	Pantelleria (Italy)	390T	Nd	
14	Clinical sample	dog	Pantelleria (Italy)	390T	1834G	1
15	Clinical sample	dog	Pantelleria (Italy)	390T	Nd	
16	Clinical sample	dog	Pantelleria (Italy)	390T	1834A	6
19	Clinical sample	dog	Pantelleria (Italy)	390T	Nd	
20	Clinical sample	dog	Pantelleria (Italy)	390T	Nd	
21	Clinical sample	dog	Pantelleria (Italy)	390T	1834R	4
22	Clinical sample	dog	Pantelleria (Italy)	390T	1834G	1
24	Clinical sample	dog	Pantelleria (Italy)	390T	Nd	
26	Clinical sample	dog	Pantelleria (Italy)	Nd	1834A	
27	Clinical sample	dog	Pantelleria (Italy)	390T	1834A	6
28	Clinical sample	dog	Pantelleria (Italy)	390T	1834A	6

[Table 7] Genotyping results summary of strains and clinical samples/isolates processed by qPCR-ME65 and qPCR-GPI88. Nd: not detected

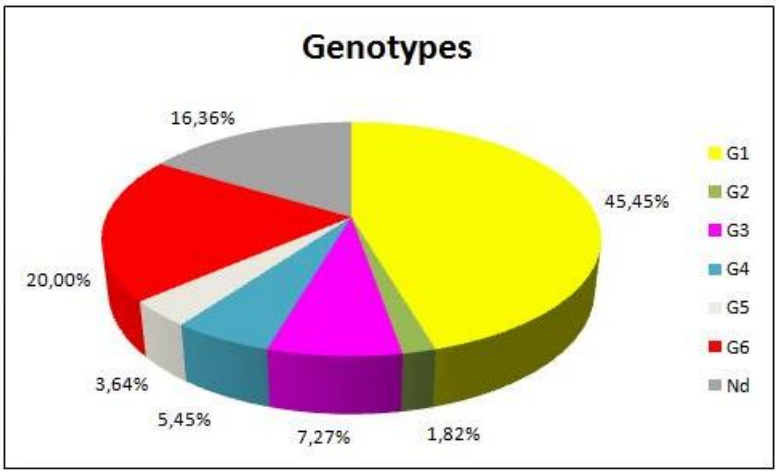

[Figure 9] Genotype distribution in tested samples. Nd: not determined

Genotype 1 resulted the most frequent genotype in human and canine population independently to the geographical region. Interestingly, the genotype 6 (390T/1834A) was found only in Pantelleria island with a prevalence of 68.8% (Figure 10)

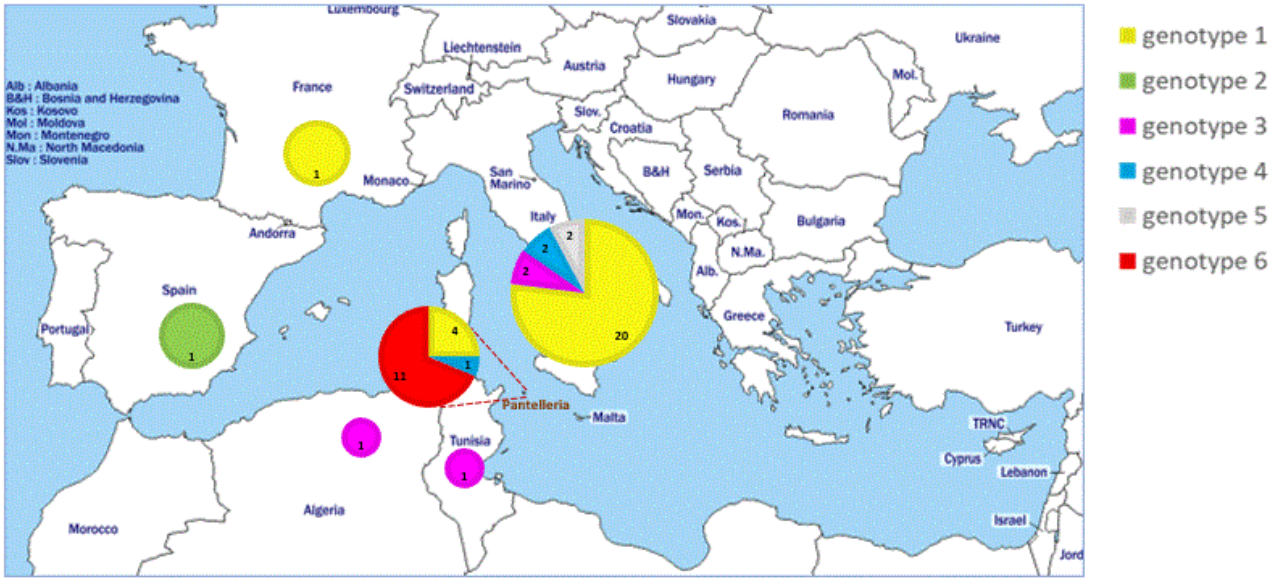

[Figure 10] Geographical distribution of the six genotypes identified

4. Discussion

The taxonomy of the *Leishmania* genus is very complex and has been revised several times during the years according to biochemical and biological characteristics of the parasites (Bates, 2007). In this study, we focused on *L. infantum* species, the main causative agent of CanL and human VL and CL. The *Leishmania* typing at species and strains level is important for epidemiology studies, (Gramiccia et al., 2013), for the identification of new reservoirs and to predict the clinical course of infection, particularly in humans (dermotropic and viscerotropic strains) (Kuhls et al., 2008). The reference technique for *Leishmania* genus typing is the MLEE (World Health Organization 2010), which is based on the electrophoretic mobility of various enzymes obtained from the promastigotes. According to this technique, *Leishmania* species are classified in zymodemes also called MON. In Italy, MON-1 and MON-72 are the most represented *L. infantum* zymodemes in infected dogs, while human infections are caused by a more heterogeneous zymodeme population (Gramiccia et al., 2013), suggesting that the dogs are not the only reservoirs of infection, and pointing out the importance of epidemiological studies. A recent work by Castelli et al. conducted in Sicily (Italy) on *Leishmania* isolates from humans and dogs, revealed that 71 out of 78 samples (91%) were MON-1, which was confirmed as the predominant strain in the Mediterranean area; the remaining 7 samples (9%) were non-MON-1 (Castelli et al., 2020). In particular, the non-MON-1 strains were isolated from humans. In this view, more and more works have investigated the role of other mammalians as *Leishmania* reservoirs. For example, hare (*Lepus granatensis*) (Molina et al., 2012) and rabbit (Garcia 2014) have been indicated as potential sources of *L. infantum*. In Madrid, two cases of infection have been reported in orangutans (*Pongo pygmaeus pygmaeus*) in the Primate Rehabilitation Center (Miró et al., 2017) and in wolves (*Canis lupus*) (Oleaga et al., 2018). Other research groups (Pennisi and Persichetti, 2018) studied feline leishmaniasis (FeL) as an emerging disease in domestic cats of endemic areas (Mediterranean basin, Iran and Brazil), evidencing similarities with CanL. Moreover, recent studies conducted in Central Italy have shown that donkeys can also be affected by leishmaniasis (Nardoni et al., 2019).

As already discussed, the MLEE technique presents some limitations including the need for parasite cultivation. In these years, the use of biomolecular techniques such as MLMT (Gouzelou et al., 2012) and MLST (Mauricio et al., 2006) has increased. In order to identify

polymorphisms useful for *L. infantum* typing in the Mediterranean region, we designed a custom MLST panel and the sequencing of 9 *L. infantum* strains and clinical isolates was performed. Phylogenetic analysis showed that only one sample, Leo-Ani, isolated from a patient with CL in the Marche region, clustered independently from the other *L. infantum* strains/isolates. Based on MLST panel results, an informative polymorphism on GPI genes (1834A/G) has been identified and selected to develop a qPCR-HRM-based assay for clinical samples screening, used in association with an updated genotyping method previously developed and applied by Ceccarelli et al. on ME gene (Ceccarelli et al., 2018). The two PCR assays have been tested on 9 clinical isolates and 38 human and canine clinical samples from central/south Italy and Pantelleria island showing a good sensitivity (97.4% and 78.9% for qPCR-ME65 and qPCR-GPI88 on clinical samples, respectively). Thanks to the pre-amplification step, it was possible to apply this method to clinical samples without parasite isolation. Compared to other biomolecular approaches for *Leishmania* typing, performed on clinical strains and isolates (Mauricio et al., 2006; Zemanová et al., 2007), this represents an important advantage useful for fast screening in epidemiological studies. In our previous work it has been shown that the polymorphism 390T on malic enzyme gene was associated to zymodemes MON-1, 72, 201; here, with the simultaneous use of the two polymorphisms, it was possible to distinguish the strain MHOM/IT/93/ISS822 (MON-201) from MON-1, 72 exploiting the heterozygosity results found in position 1834 (confirmed by sequencing). The presence of heterozygosity was also found in the clinical isolate V2921 (MON-1) and clinical samples Els-Mai, Dae-Dio, and number 21. The heterozygosity has also been described in other cases involving metabolic enzymes of *Leishmania donovani* complex (Zemanová et al., 2007), in association with the geographical origin of the parasite (Gaunt et al., 2003).

Despite the increase in discrimination power compared to our previous publication (Ceccarelli et al., 2018), no genotypic differences were found between the MON-1 and MON-72 (G1) zymodemes. However, this may not represent an issue. In fact, the MON-1, 72 are the most represented zymodemes in dogs, therefore the identification of genotypes different from G1 could be useful to understand the exact role of the dog in the transmission of the pathogen and to identify other reservoirs of infection for humans. The only exception was the reference strain MHOM/TN/80/IPT1, which, despite being a MON-1, presents a genotype G3. This may be due to the geographical origin of this strain (Tunisia) compared to

the European strains/isolates. Excluding Pantelleria island, 77.8% and 80.0% of human and canine clinical samples/isolates resulted G1. Considering the correlation between G1 and MON-1, the results can be considered in agreement with the literature data (MON-1 frequency is attested between 70% and 90%) (Bulle et al., 2002; Kuhls et al., 2008; Castelli et al., 2020). Moreover, the clinical isolates Leo-Ani and Bra-Aii resulted G3 like MHOM/TN/80/IPT1. This seems to confirm the genotypic heterogeneity within the MON-1 zymodeme, as described in other works (Reale et al., 2010). Nevertheless, if Bra-Aii clusters with MHOM/TN/80/IPT1 in the MLST panel, placing in favor of the possibility that it is a MON-1, Leo-Ani clustered independently. Regarding Pantelleria island, only 25.0% of canine clinical isolates/samples resulted G1 while 68.8% is associated with the genotype G6 (390T/1834A), not found in other geographical areas. To confirm this finding on a larger scale, the evaluation of this genotype in a database of Wellcome Sanger Institute containing whole-genome sequence data for over 500 *Leishmania* isolates is planned. Generally, an MLST approach would require about ten target sequences to have an adequate capacity for discrimination. The genotyping method based on HRM-assays proposed in this work, using only two molecular targets, was able to distinguish 6 different genotypes. Among them, the most represented was the G1 which showed a strong correlation (although not univocal) with MON-1, 72 zymodemes group.

5. Conclusion

A total of 9 *L. infantum* isolates/strains have been sequenced by an MLST panel encoding for 14 metabolic enzymes. The analysis of these sequences, together with sequences available in the database, allowed us to identify interesting polymorphisms exploitable to differentiate the most common *L. infantum* zymodemes in the Mediterranean basin. In particular, two HRM-based assays were developed to differentiate the genotype 390T/G and 1834A/G, in ME and GPI genes. The application on 9 clinical isolates and 38 clinical samples allowed us to identify 6 different genotypes. The genotype G1 (390T/1834G), correlated with zymodemes MON-1,72 allowing for the rapid identification of the most common *L. infantum* zymodemes. These assays have been successfully applied to clinical samples, without the need for parasite isolation.

In conclusion, this approach could find application as a fast screening in epidemiological studies for the characterization of *L. infantum* strains, in the identification of new reservoirs of infection, and to investigate the genetic variability of *L. infantum* in border territory in the Mediterranean.

References

Aït-Oudhia, K., Harrat, Z., Benikhlef, R., Dedet, J.P., Pratlong, F., 2011. Canine Leishmania infantum enzymatic polymorphism: A review including 1023 strains of the Mediterranean area, with special reference to Algeria. Acta Trop. https://doi.org/10.1016/j.actatropica.2011.03.001

Bates PA. Transmission of Leishmania metacyclic promastigotes by phlebotomine sand flies. Int J Parasitol. 2007 Aug;37(10):1097-106. doi: 10.1016/j.ijpara.2007.04.003. Epub 2007 Apr 18. PMID: 17517415; PMCID: PMC2675784.

Bulle B, Millon L, Bart JM, Gállego M, Gambarelli F, Portús M, Schnur L, Jaffe CL, Fernandez-Barredo S, Alunda JM, Piarroux R. Practical approach for typing strains of Leishmania infantum by microsatellite analysis. J Clin Microbiol. 2002 Sep;40(9):3391-7. doi: 10.1128/JCM.40.9.3391-3397.2002. PMID: 12202583; PMCID: PMC130734.

Castelli G, Bruno F, Caputo V, Fiorella S, Sammarco I, Lupo T, Migliazzo A, Vitale F, Reale S. Genetic tools discriminate strains of Leishmania infantum isolated from humans and dogs in Sicily, Italy. PLoS Negl Trop Dis. 2020 Jul 24;14(7):e0008465. doi: 10.1371/journal.pntd.0008465. PMID: 32706789; PMCID: PMC7406075.

Ceccarelli M, Galluzzi L, Migliazzo A, Magnani M. Detection and characterization of Leishmania (Leishmania) and Leishmania (Viannia) by SYBR green-based real-time PCR and high resolution melt analysis targeting kinetoplast minicircle DNA. PLoS One. 2014b Feb 13;9(2):e88845. doi: 10.1371/journal.pone.0088845. PMID: 24551178; PMCID: PMC3923818.

Ceccarelli M, Galluzzi L, Sisti D, Bianchi B, Magnani M. Application of qPCR in conjunctival swab samples for the evaluation of canine leishmaniasis in borderline cases or disease relapse and correlation with clinical parameters. Parasit Vectors. 2014a Oct 21;7:460. doi: 10.1186/s13071-014-0460-3. PMID: 25331737; PMCID: PMC4207623.

Ceccarelli, M., Diotallevi, A., Andreoni, F., Vitale, F., Galluzzi, L., Magnani, M., 2018. Exploiting genetic polymorphisms in metabolic enzymes for rapid screening of Leishmania infantum genotypes. Parasit. Vectors. https://doi.org/10.1186/s13071-018-3143-7

Diotallevi, A., Buffi, G., Corbelli, G., Ceccarelli, M., Ortalli, M., Varani, M., Magnani, M., and Galluzzi, L. (2021) In vitro reduced susceptibility to pentavalent antimonials of a *Leishmania infantum* isolate from a human cutaneous leishmaniasis case in central Italy. *Microorganism* 9 (6), 1147. DOI: 10.3390/microorganisms9061147

García N, Moreno I, Alvarez J, de la Cruz ML, Navarro A, Pérez-Sancho M, García-Seco T, Rodríguez-Bertos A, Conty ML, Toraño A, Prieto A, Domínguez L, Domínguez M. Evidence of Leishmania infantum infection in rabbits (Oryctolagus cuniculus) in a natural area in Madrid, Spain. Biomed Res Int. 2014;2014:318254. doi: 10.1155/2014/318254. Epub 2014 Mar 3. PMID: 24724079; PMCID: PMC3958779.

Gaunt MW, Yeo M, Frame IA, Stothard JR, Carrasco HJ, Taylor MC, Mena SS, Veazey P, Miles GA, Acosta N, de Arias AR, Miles MA. Mechanism of genetic exchange in American trypanosomes. Nature. 2003 Feb 27;421(6926):936-9. doi: 10.1038/nature01438. PMID: 12606999.

Gouzelou, E., Haralambous, C., Amro, A., Mentis, A., Pratlong, F., Dedet, J.P., Votypka, J., Volf, P., Toz, S.O., Kuhls, K., Schönian, G., Soteriadou, K., 2012. Multilocus microsatellite typing (MLMT) of strains from Turkey and cyprus reveals a novel monophyletic L. donovani Sensu Lato group. PLoS Negl. Trop. Dis. 6. https://doi.org/10.1371/journal.pntd.0001507

Gramiccia, M., 2003. The identification and variability of the parasites causing leishmaniasis in HIV-positive patients in Italy. Ann. Trop. Med. Parasitol. 97, 65–73. https://doi.org/10.1179/000349803225002543

Gramiccia, M., Scalone, A., Di Muccio, T., Orsini, S., Fiorentino, E., Gradoni, L., 2013. The burden of visceral leishmaniasis in Italy from 1982 to 2012: a retrospective analysis of the multi-annual epidemic that occurred from 1989 to 2009. Euro Surveill. Bull. Eur. sur les Mal. Transm. = Eur. Commun. Dis. Bull. 18, 20535. https://doi.org/10.2807/1560-7917.ES2013.18.29.20535

Hall, T.A. 1999. "BioEdit: A User-Friendly Biological Sequence Alignment Editor and Analysis Program for Windows 95/98/NT." *Nucleic Acids Symposium Series* 41: 95–98. https://doi.org/citeulike-article-id:691774.

Kuhls K, Chicharro C, Cañavate C, Cortes S, Campino L, Haralambous C, Soteriadou K, Pratlong F, Dedet JP, Mauricio I, Miles M, Schaar M, Ochsenreither S, Radtke OA, Schönian G. Differentiation and gene flow among European populations of Leishmania infantum MON-1. PLoS Negl Trop Dis. 2008 Jul 9;2(7):e261. doi: 10.1371/journal.pntd.0000261. PMID: 18612461; PMCID: PMC2438616.

Kuhls, K., Alam, M.Z., Cupolillo, E., Ferreira, G.E.M., Mauricio, I.L., Oddone, R., Feliciangeli, M.D., Wirth, T., Miles, M.A., Schönian, G., 2011. Comparative microsatellite typing of new world leishmania infantum reveals low heterogeneity among populations and its recent old world origin. PLoS Negl. Trop. Dis. https://doi.org/10.1371/journal.pntd.0001155

Mauricio, I.L., Yeo, M., Baghaei, M., Doto, D., Pratlong, F., Zemanova, E., Dedet, J.P., Lukes, J., Miles, M.A., 2006. Towards multilocus sequence typing of the Leishmania donovani complex: Resolving genotypes and haplotypes for five polymorphic metabolic enzymes (ASAT, GPI, NH1, NH2, PGD). Int. J. Parasitol. 36, 757–769. https://doi.org/10.1016/j.ijpara.2006.03.006

Millán, J., Ferroglio, E., Solano-Gallego, L., 2014. Role of wildlife in the epidemiology of Leishmania infantum infection in Europe. Parasitol. Res. https://doi.org/10.1007/s00436-014-3929-2

Miró, G., Müller, A., Montoya, A., Checa, R., Marino, V., Marino, E., Fuster, F., Escacena, C., Descalzo, M.A., Gálvez, R., 2017. Epidemiological role of dogs since the human leishmaniosis outbreak in Madrid. Parasit. Vectors 10, 209.

Molina R, Jiménez MI, Cruz I, Iriso A, Martín-Martín I, Sevillano O, Melero S, Bernal J. The hare (Lepus granatensis) as potential sylvatic reservoir of Leishmania infantum in Spain. Vet Parasitol. 2012 Nov 23;190(1-2):268-71. doi: 10.1016/j.vetpar.2012.05.006. Epub 2012 May 23. PMID: 22677135.

Nardoni S, Altomonte I, Salari F, Martini M, Mancianti F. Serological and Molecular Findings of *Leishmania* Infection in Healthy Donkeys (*Equus asinus*) from a Canine Leishmaniosis Endemic Focus in Tuscany, Italy: A Preliminary Report. Pathogens. 2019 Jul 9;8(3):99. doi: 10.3390/pathogens8030099. PMID: 31323973; PMCID: PMC6789632.

Nei M. and Kumar S. (2000). Molecular Evolution and Phylogenetics. Oxford University Press, New York.

Oleaga A, Zanet S, Espí A, Pegoraro de Macedo MR, Gortázar C, Ferroglio E. Leishmania in wolves in northern Spain: A spreading zoonosis evidenced by wildlife sanitary surveillance. Vet Parasitol. 2018 May 15;255:26-31. doi: 10.1016/j.vetpar.2018.03.015. Epub 2018 Mar 19. PMID: 29773132.

Pennisi MG, Persichetti MF. Feline leishmaniosis: Is the cat a small dog? Vet Parasitol. 2018 Feb 15;251:131-137. doi: 10.1016/j.vetpar.2018.01.012. Epub 2018 Feb 2. PMID: 29426470; PMCID: PMC7130840.

PRATLONG, F., LAMI, P., RAVEL, C., BALARD, Y., DEREURE, J., SERRES, G., BAIDOURI, F. EL, DEDET, J.-P., 2013. Geographical distribution and epidemiological features of Old World Leishmania infantum and Leishmania donovani foci, based on the isoenzyme analysis of 2277 strains. Parasitology 140, 423–434. https://doi.org/10.1017/S0031182012001825

Reale S, Lupo T, Migliazzo A, Di Mauro C, Ciprì V, Calderone S, Manna L, Vitale F. Multilocus microsatellite polymorphism analysis to characterize Leishmania infantum strains isolated in Sicily. Transbound Emerg Dis. 2010 Apr;57(1-2):37-41. doi: 10.1111/j.1865-1682.2010.01131.x. PMID: 20537100.

Schönian, G., Nasereddin, A., Dinse, N., Schweynoch, C., Schallig, H. D. F. ., Presber, W., & Jaffe, C. L. (2003). PCR diagnosis and characterization of Leishmania in local and imported clinical samples. *Diagnostic Microbiology and Infectious Disease*, *47*(1), 349–358. https://doi.org/10.1016/S0732-8893(03)00093-2

Vitale F, Bruno F, Migliazzo A, Galante A, Vullo A, Graziano R, D'Avola S, Caputo V, Castelli G. Cross-sectional survey of canine leishmaniasis in Pantelleria island in Sicily. Vet Ital. 2020 Dec 31;56(2):103-107. doi: 10.12834/VetIt.2059.10976.3. Epub 2020 Jul 14. PMID: 32761581.

Wilm, Andreas and Aw, Pauline Poh Kim and Bertrand, Denis and Yeo, Grace Hui Ting and Ong, Swee Hoe and Wong, Chang Hua and Khor, Chiea Chuen and Petric, Rosemary and Hibberd, Martin Lloyd and Nagarajan, Niranjan (2012). LoFreq: a sequence-quality aware, ultra-sensitive variant caller for uncovering cell-population heterogeneity from high-throughput sequencing datasets. In Nucleic Acids Research, 40 (22), pp. 11189-11201. [doi:10.1093/nar/gks918]

World Health Organization, 2010. Control of the leishmaniases., World Health Organization technical report series.

Ye J, Coulouris G, Zaretskaya I, Cutcutache I, Rozen S, Madden TL. PrimerBLAST: a tool to design target-specific primers for polymerase chain reaction. BMC Bioinformatics. 2012;13:134.

Zemanová E, Jirků M, Mauricio IL, Horák A, Miles MA, Lukes J. The Leishmania donovani complex: genotypes of five metabolic enzymes (ICD, ME, MPI, G6PDH, and FH), new targets for multilocus sequence typing. Int J Parasitol. 2007 Feb;37(2):149-60. doi: 10.1016/j.ijpara.2006.08.008. Epub 2006 Sep 18. PMID: 17027989.

CHAPTER 6

This chapter consists of a report regarding an autochthonous case of CL in a patient living in central Italy with an unsatisfactory response to treatment with intralesional Meglumine Antimoniate (the isolated parasites were reported in the previous chapter with the sample ID Leo-Ani). After the molecular characterization, we demonstrated the reduced susceptibility to SbIII through *in vitro* assay, helping the medical team in choosing a different therapeutic approach.

Case report published in Microorganism

DOI: 10.3390/microorganisms9061147 Volume 9, Issue 6, 2021, 1147

microorganisms

MDPI

Case Report

In Vitro Reduced Susceptibility to Pentavalent Antimonials of a *Leishmania infantum* Isolate from a Human Cutaneous Leishmaniasis Case in Central Italy

Aurora Diotallevi [1,†], Gloria Buffi [1,†], Giovanni Corbelli [2], Marcello Ceccarelli [1], Margherita Ortalli [3], Stefania Varani [3,4], Mauro Magnani [1] and Luca Galluzzi [1,*]

[1] Department of Biomolecular Sciences, University of Urbino "Carlo Bo", 61029 Urbino, Italy; aurora.diotallevi@uniurb.it (A.D.); g.buffi@campus.uniurb.it (G.B.); m.ceccarelli3@campus.uniurb.it (M.C.); mauro.magnani@uniurb.it (M.M.)
[2] Unit of Infectious Diseases, Marche Nord Hospital,61122 Pesaro, Italy; giovanni.corbelli@ospedalimarchenord.it
[3] Unit of Microbiology, IRCCS Polyclinic S.Orsola-Malpighi, 40138 Bologna, Italy; margherita.ortalli@gmail.com (M.O.); stefania.varani@unibo.it (S.V.)
[4] Department of Experimental, Diagnostic and Specialty Medicine, Alma Mater Studiorum University of Bologna, 40126 Bologna, Italy
* Correspondence: luca.galluzzi@uniurb.it
† These authors contributed equally.

Abstract

Cutaneous leishmaniasis (CL) caused by *Leishmania* (*Leishmania*) *infantum* is endemic in the Mediterranean basin. Here we report an autochthonous case of CL in a patient living in central Italy with an unsatisfactory response to treatment with intralesional Meglumine Antimoniate and *in vitro* demonstration of reduced susceptibility to SbIII. Parasitological diagnosis was first achieved by histopathology on tissue biopsy and the patient was treated with a local infiltration of Meglumine Antimoniate. Since the clinical response at 12 weeks from the treatment's onset was deemed unsatisfactory, two further skin biopsies were taken for histopathological examination, DNA extraction and parasite isolation. *L. (L.) infantum* was identified by molecular typing. The low susceptibility to Meglumine Antimoniate was confirmed in vitro: the promastigotes from the patient strain showed significantly lower susceptibility to SbIII (the active trivalent form of antimonial) compared to the reference strain MHOM/TN/80/IPT1. The patient underwent a new treatment course with intravenous liposomal Amphotericin B, reaching complete healing of the lesion. Additional studies are needed to confirm the

epidemiological and clinical relevance of reduced susceptibility to SbIII of human *L.* (*L.*) *infantum* isolate in Italy.

Keywords: *Leishmania infantum*; antimonials; resistance; cutaneous leishmaniasis;

---

1. Introduction

Leishmaniases are parasitic diseases transmitted by sandflies showing heterogeneous clinical manifestation, depending on the *Leishmania* species and host health status. About 20 species of *Leishmania*, mainly belonging to the subgenera *Leishmania* and *Viannia*, can parasitize humans. A comprehensive updated taxonomy of trypanosomatidae, including the genus *Leishmania*, has been recently published [1]. Clinical manifestations range from cutaneous lesions (cutaneous leishmaniasis, CL) to severe systemic multiorgan disease (visceral leishmaniasis, VL). In the Old World (i.e., southern Europe, the Middle East, Asia, and Africa) the etiological agents of CL are *Leishmania* (*Leishmania*) species, such as *L.* (*L.*) *donovani, L.* (*L.*) *infantum, L.* (*L.*) *major, L.* (*L.*) *aethiopica,* and *L.* (*L.*) *tropica* [2]. The lesions generally occur on skin portions easily accessible to sand flies, such as the face or limbs. The CL lesions can manifest as a single nodular or ulcerative lesion at the site of parasite inoculation, called localized cutaneous leishmaniasis (LCL) or as multiple lesions caused by infection propagation, named diffuse cutaneous leishmaniasis (DCL) [3]. In the Mediterranean basin, CL often manifests as a single, painless lesion caused by *L.* (*L.*) *infantum* [4], which represents the etiological agent of CL and VL in humans, as well as canine leishmaniasis (CanL).

In the Old World, intralesional pentavalent antimony compounds (i.e., sodium stibogluconate and Meglumine Antimoniate) are among the first choice for the treatment of uncomplicated CL, while liposomal amphotericin B or other systemic treatments can be used for complicated CL or for immunosuppressed patients [5]. Antimonials are used also in the standard therapy for CanL, either alone, or in combination with allopurinol [6]. Notably, treatment failure due to resistance to antimonials has been described in different studies, mostly in the treatment of *L.* (*L.*) *donovani* VL in the Indian subcontinent [7], and rarely in the Mediterranean region [8],

where treatment efficiency exceeding 95% in HIV-negative individuals has been reported [9].

In recent years, new evidence of CL cases in north-eastern Italy has been documented [10]. However, to the best of our knowledge, human CL cases not responding to antimonials have never been notified in Italy so far. Here, we report an autochthonous CL case due to *L.* (*L.*) *infantum* in central Italy, with unsatisfactory response to treatment with intralesional pentavalent antimony compounds.

2. Description of the Case

A 61-year-old male was referred from the San Salvatore–Muraglia hospital (Pesaro, Italy), in May 2019 as a suspected case of CL, with a skin lesion on the dorsal left forearm with diameter of 5 × 3 cm. The patient reported not having traveled abroad in the previous years. Physical examination did not reveal any clinical sign of pathology, except for the abovementioned lesion. The lesion was biopsied by a dermatologist in aseptic conditions, with histological report of skin characterized by intense chronic limphoplasmocytoid inflammation and presence of histiocytes containing several *Leishmania* amastigotes. The ensuing pathological diagnosis was cutaneous leishmaniasis of the left forearm. Laboratory results showed 5.81 x10^6 erythrocytes, Hb 17.1 g/dl, MCV 88, normal white blood cells, and platelet count and biochemical parameters within normal range. Renal and liver function were also normal, and no autoantibodies were detected. The patient had just been tested for polyglobulia by a hematologist, and he was in clinical follow-up. No evidence of BCR-ABL or Jak2 mutations was reported.

The patient was treated with a local infiltration of Meglumine Antimoniate (Glucantime® vials 1.5 g/5 mL—1 vial every week for a total of 5 weeks) in the skin lesion and along its margins. Twelve weeks after the beginning of therapy the clinical result was not deemed satisfactory by the managing clinicians (Figure 1).

Figure 1. Photograph of the dorsal forearm skin lesion on the patient with cutaneous leishmaniasis, twelve weeks after the beginning of treatment.

After 12 weeks from the beginning of treatment, the patient underwent a second skin biopsy. Maintaining aseptic conditions and after the expression patient's informed consent, two 5 mm diameter biopsies were collected from the nodular lesion. One biopsy was fixed in 4% formalin and sent for microscopic analysis which showed persistence of histiocytes containing *Leishmania* amastigotes. The second biopsy was collected in 5 mL sterile Tobie medium, disrupted by pipetting and divided into two aliquots: one was used for parasite isolation as described previously [11,12] and the other for DNA extraction. The DNA was extracted with the DNeasy Blood & Tissue kit (Qiagen) and amplified by a real-time PCR assay (qPCR-ML) as previously described [13–15]. The qPCR-ML assay gave positive amplification results indicating the presence of *Leishmania* spp DNA in the skin sample. Melting analysis [13] allowed amplicons to be assigned to *Leishmania* (*Leishmania*) subgenus (Figure 2A). The ITS1-PCR RFLP analysis, performed as described by Schönian et al. [16], enabled the identification of *L.* (*L.*) *infantum* species (Figure 2B). The species identification was confirmed by partial sequencing of glucose-6-phosphate isomerase gene and successive alignment against *Leishmania* sequences using the BLASTN algorithm, followed by construction of the phylogenetic tree (Figure 3).

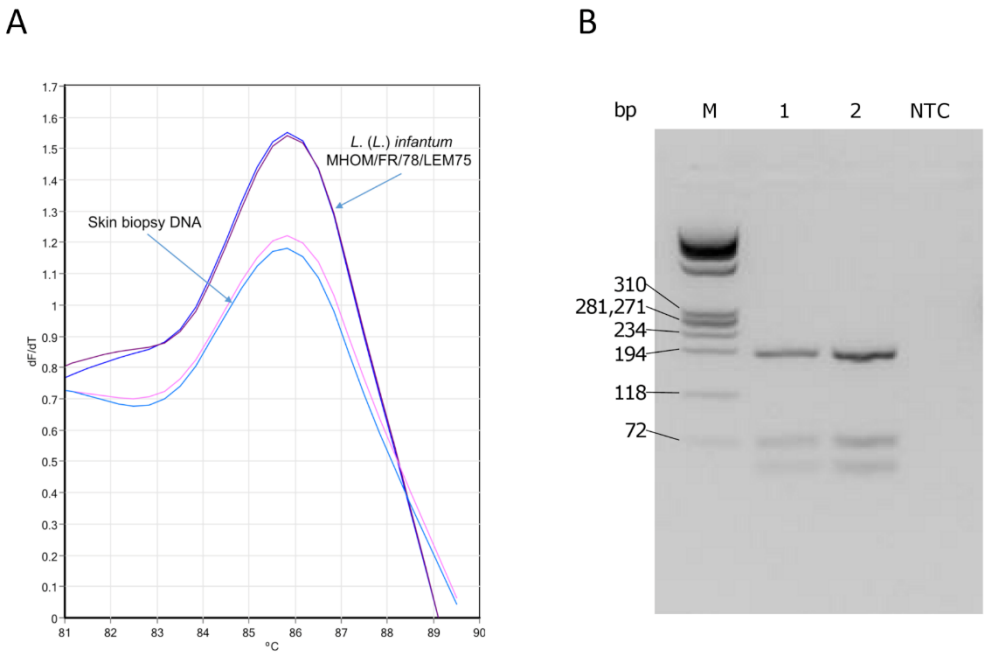

Figure 2. Molecular identification and characterization of the parasite from the skin biopsy. **A)** Melting analysis of qPCR-ML amplicons. A region of kinetoplast DNA (kDNA) was amplified by a qPCR assay using primer pairs MLF/MLR as described previously [13]. Briefly, PCR reactions were carried out in duplicate, in 25 µl volume containing 1 µl template DNA (corresponding to 140 ng DNA) and 24 µl SYBR green PCR master mix (Diatheva srl) with 200 nM of each primer, using a Rotor-Gene 6000 instrument (Corbett life science). The amplification conditions were: 94 °C for 10 min; followed by 45 cycles at 94 °C for 20 s, 60 °C for 20 s, and 72 °C for 20 s. At the end of the run, a melting curve analysis was performed from 82 °C to 90 °C. As positive control, DNA from *L.* (*L.*) *infantum* MHOM/FR/78/LEM75 was used. Melting temperatures of PCR products were overlapping (85.8 °C) indicating that parasites were from *Leishmania* (*Leishmania*) subgenus. **B)** ITS1-PCR RFLP analysis. ITS1 region was amplified by PCR as described previously [16] using primers LITSR 5'-CTGGATCATTTTCCGATG-3' and L5.8 S 5'-TGATACCACTTATCGCACTT-3'. ITS1 PCR products obtained from skin biopsy (1) and *L. (L.) infantum* MHOM/FR/78/LEM75 (2) were digested with 10 U HaeIII enzyme (Thermo Fisher Scientific) at 37 °C for 3 h and visualized on a 3.5% high-resolution MetaPhor (Cambrex) agarose gel stained with GelRed (Biotium). NTC, no template control; M, DNA marker 9.

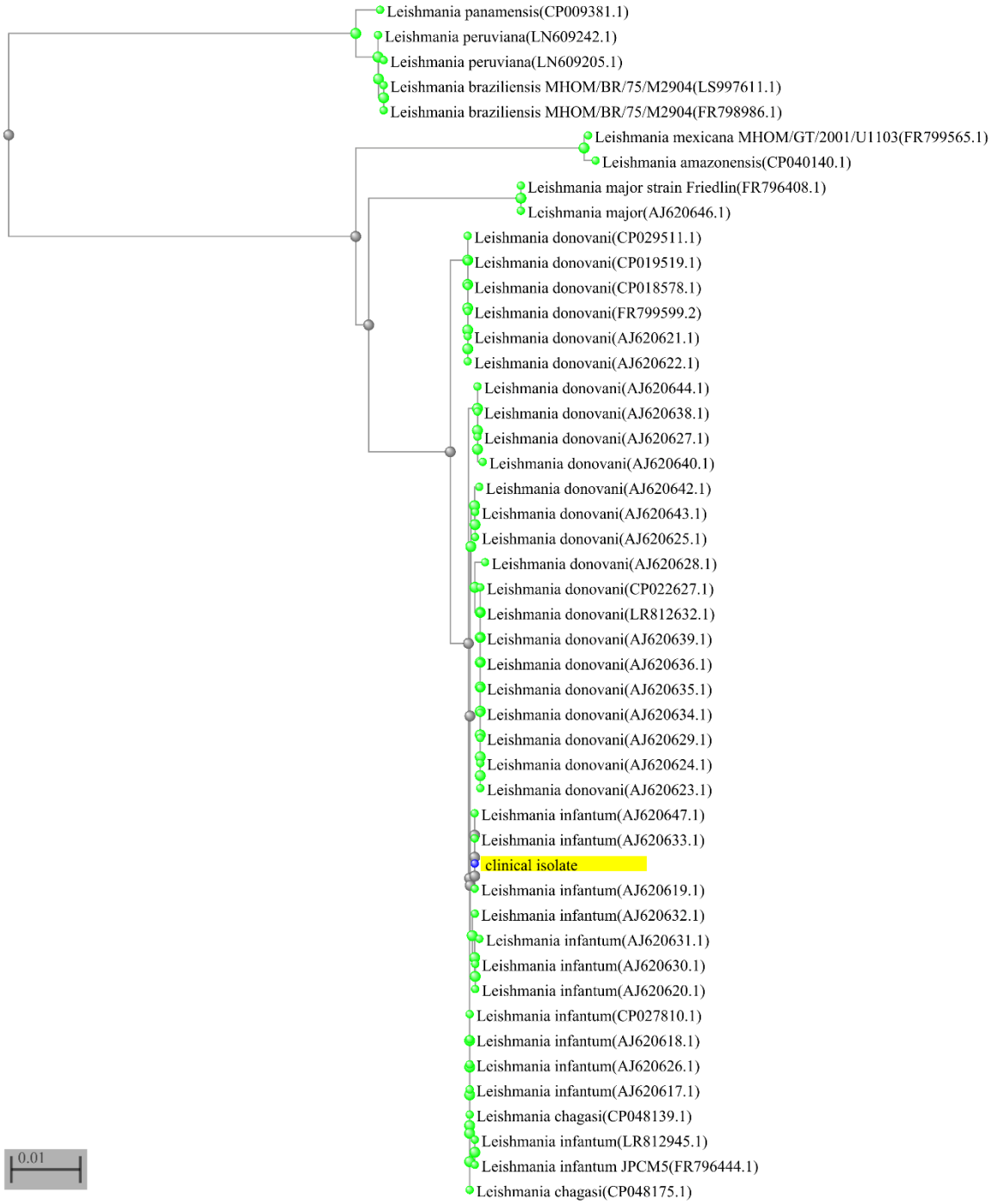

Figure 3. The partial sequence of glucose-6-phosphate isomerase gene (1335 bp) was obtained from isolated parasites in the context of a multilocus sequence typing approach by a customized sequencing panel designed with Ion AmpliSeq™ designer (Thermo-Fisher-Scientific). This panel included 7 primer pairs specific for the glucose-6-phosphate isomerase gene. The library was prepared using Ion AmpliSeq™ library kit plus (Thermo-Fisher-Scientific) following manufacturer's instructions. The library sequencing was performed using the Ion Torrent S5 instrument (Thermo-Fisher-Scientific) and the reads were mapped to *L. infantum* JPCM5 genome (LinJ.12 291520-292854) using Torrent Browser. The consensus sequence was analyzed by BLASTN against *Leishmania* sequences. The results with 100% coverage were selected. A distance tree of pairwise comparisons was visualized by BLAST tree view, using Neighbor Joining algorithm [17]. The sequence of the clinical isolate is highlighted.

Regarding parasite isolation, after 7 days of culture, the liquid phase of Evans' modified Tobie's medium (EMTM) presented numerous motile promastigotes, confirming the presence of viable parasites in the bioptic sample (Figure 4).

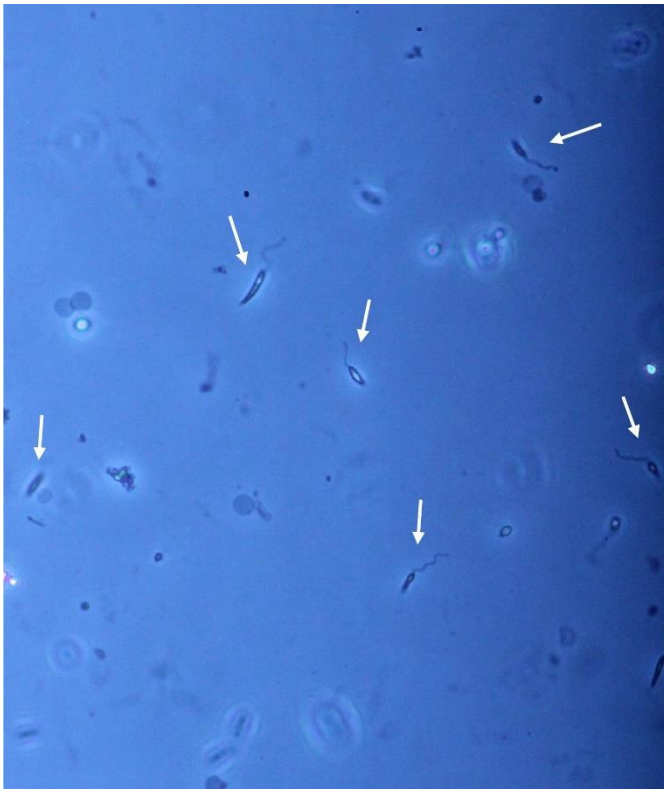

Figure 4. Phase-contrast microscope examination of parasites isolated from the skin biopsy. Individual promastigotes are indicated by arrows (20 X magnification).

Furthermore, the isolate was genotyped by analyzing the nucleotide polymorphism 390 T > G in the malic enzyme gene by High Resolution Melt (HRM) analysis, as described previously [18]. The HRM analysis showed a 390 G genotype (Figure 5), which is not associated with the zymodemes MON-1 (the most common in the Mediterranean basin), MON-72, 201 [18].

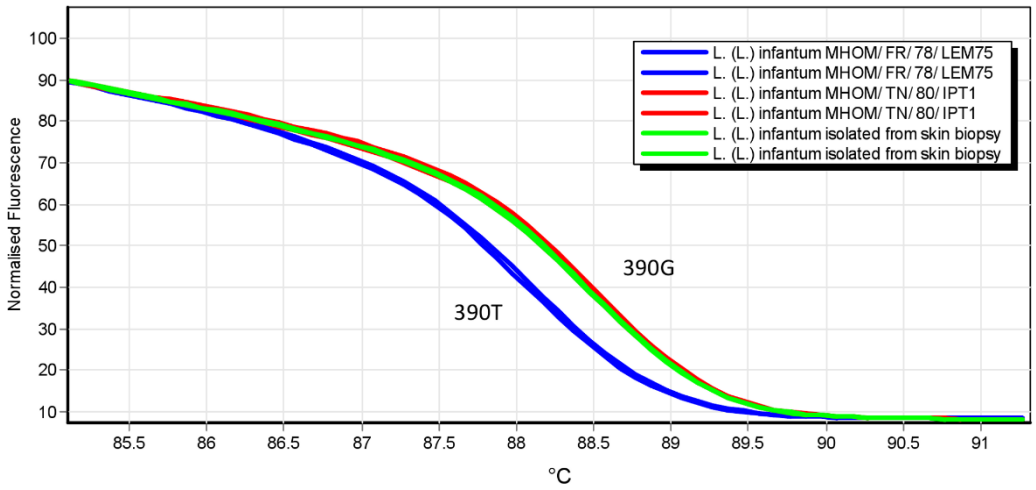

Figure 5. Genotyping of *L. (L.) infantum* clinical isolate through HRM analysis. The malic enzyme gene sequence encompassing the polymorphism 390 T/G was amplified by qPCR-MEint in 25 µl volume containing SYBR green PCR master mix (Diatheva srl) with 200 nM of primers forward (5'-TCAGAACCTTCGCAAGACGA-3') and reverse (5'-CACTTGCCGATGCTGATGC-3'), using a Rotor-Gene 6000 instrument (Corbett life science) [18]. The amplification conditions were: 94 °C for 10 min; followed by 45 cycles at 94 °C for 20 s, 60 °C for 20 s, and 72 °C for 20 s. After amplification, high-resolution melting (HRM) analysis was performed over the range 77–95 °C, rising by 0.1 °C/s and waiting for 2 s at each temperature. Raw HRM curves were normalized by the Rotorgene 6000 v.1.7 software. Controls for genotypes 390 T and 390 G were *L. (L.) infantum* MHOM/FR/78/LEM75 and *L. (L.) infantum* MHOM/TN/80/IPT1, respectively.

To determine whether unresponsiveness to Glucantime® was due to the presence of resistant parasites, the IC_{50} of SbIII (the active trivalent antimonial form) was determined in the promastigotes isolated from the lesion. Briefly, late log/stationary phase promastigotes were resuspended in complete RPMI-PY medium [19] at a density of 2.5 x 10^6 parasites/mL in 96-well plates (100 µL/well). The promastigotes were treated with potassium antimonyl tartrate trihydrate (SbIII) (Sigma-Aldrich) at concentrations of 1, 5, 25, 125, 625 µM for 72 h at 26 °C. The reference strain *L. (L.) infantum* MHOM/TN/80/IPT1 was included as control. Moreover, the promastigotes were also treated with Miltefosine (Sigma–Aldrich). Each condition was repeated sixfold. To evaluate the promastigote viability, the CellTiter 96 H Aqueous Non-Radioactive Cell Proliferation Assay (Promega) was carried out. The parasites derived from the unresponsive patient were significantly less susceptible to SbIII than the reference strain parasites ($p < 0.01$, unpaired t-test with Welch's correction) (Table 1). On the contrary, promastigotes from the clinical isolate appeared more sensitive to Miltefosine compared to the reference strain.

Table 1. In vitro susceptibility tests.

Treatment	*L. (L.) infantum* clinical isolate IC_{50} (µM)	*L. (L.) infantum* MHOM/TN/80/IPT1 IC_{50} (µM)	Unpaired t-test with Welch's correction P-value
Potassium antimonyl tartrate trihydrate (SbIII)	27.06 ± 2.70	13.22 ± 2.11	< 0.01
Miltefosine	1.31 ± 0.14	4.27 ± 0.40	< 0.01

Due to the unsatisfactory clinical response to pentavalent antimony compounds and the in vitro demonstration of low susceptibility to antimonials of the infecting parasitic strain, a new therapy with intravenous liposomal Amphotericin B was administered at the dose of 3 mg/Kg in daily doses for five days, with two further doses at an interval of two weeks. Liposomal Amphotericin B treatment was effective, with healing of the lesion after two months and no major side-effect was reported during the follow-up. The patient did not return with any relapse in the following 6 months.

3. Discussion

A high circulation of *Leishmania* strains causing cutaneous leishmaniasis has been recently observed in northeastern Italy [10]. In the index case, a lack of travel history, the molecular identification of *L. (L.) infantum* and the fact that the patient resided in the Marche region (central Italy) where *L. (L.) infantum* is endemic, strongly suggest an autochthonous origin of the infection.

The diagnosis of CL was initially performed by histology with the detection of leishmanial amastigotes in tissue sections. However, due to treatment unresponsiveness, a second bioptic sample was taken and histological diagnosis was repeated, followed by molecular diagnosis and parasite isolation and characterization.

Treatment failure in leishmaniasis can be caused by drug resistance of the infecting parasite, host factors such as immunity and nutritional status, individual variation in

pharmacokinetics, or other drug-related responses, or whether the parasite resides in tissues accessible to drugs [7]. Antimonials are often the first choice in the treatment of CL and they can be administered intralesionally as well as systemically [20]. In Old World CL, intralesional antimonials have shown >90% cure rates but most of the data are related to *L. (L.) major* infections. [20]. In fact, treatment data are scarce for *L. (L.) infantum* CL lesions [21]. To confirm the first diagnosis and to investigate the lack of response to treatment in the index case, the parasitic strain isolated from the lesion was further characterized with molecular tools and its susceptibility to antimonials was evaluated *in vitro*. Pentavalent antimonials (SbV) such as Meglumine Antimoniate need to be reduced to a trivalent antimonial (SbIII) in order to be active. Since promastigotes cannot reduce SbV to SbIII, the susceptibility test was directly performed with SbIII, the active trivalent antimonial form [22].

The *L*. (*L.*) *infantum* clinical isolate showed significantly lower susceptibility to antimonials than the reference strain (MHOM/TN/80/IPT1), which is itself a VL strain less susceptible to antimonials with respect to CL causing species [23]. At the same time, the clinical isolate exhibited a higher sensitivity to Miltefosine when compared to the reference strain.

Treatment of CanL with Glucantime® is a common practice in many Mediterranean countries, where repeated treatments of dogs have been shown to produce a reservoir of *L*. (*L.*) *infantum* parasites with a decreased sensitivity to antimonials [24,25]. Nevertheless, the clinical isolate of our index case was genotyped as a strain not related to zymodemes MON-1, 72, 201 (polymorphism 390 G in malic enzyme), which include the most common zymodeme circulating in dogs in the Mediterranean basin (MON-1). Therefore, it is unlikely that the strain has canine origin. Since the lower susceptibility to SbIII could not be explained with canine origin of the strain, further investigation on genes involved in inducing antimony-resistant parasites (e.g., AQP1, MRPA, γ-GCS, TR, TDR1) will be needed.

According to the European guidelines [5], CL lesions > 4 cm should be treated with systemic therapy. However, Since the patient presented a single lesion that was slightly above this index, local therapy with Glucantime® was attempted to avoid the toxic effects of the systemic therapy. Nonetheless, after the intralesional therapy, according

to the clinician's judgment, a satisfactory clinical response was not achieved. Subsequent investigations revealed low susceptibility to SbIII. Therefore, the incomplete response to treatment could be due to both an insufficient therapeutic dose and the low susceptibility of the parasite.

In the Old World, Glucantime® failure due to parasite resistance has been reported mostly in *L.* (*L.*) *donovani* strains circulating in the Indian subcontinent. The *L.* (*L.*) *infantum* CL case described here showed decreased susceptibility to Meglumine Antimoniate. Due to the scarcity of data regarding treatment of *L. (L.) infantum* CL lesions, it is possible that some similar cases may not have been reported. Additional studies are needed to confirm the epidemiological and clinical relevance of these findings.

Author Contributions: Conceptualization, L.G., M.C., and G.C.; methodology, A.D., G.B., M.O., S.V., G.C., L.G., and M.C.; investigation, A.D., G.B., M.O., S.V., G.C.; resources, M.M.; writing—original draft preparation, A.D., L.G.; writing—review and editing, S.V., M.O., G.B., M.C., G.C., M.M. All authors have read and agreed to the published version of the manuscript."

Funding: This research was partially funded by the Department of Biomolecular Sciences of the University of Urbino and by FanoAteneo.

Institutional Review Board Statement: Ethical review and approval were waived for this study, since bioptic samples were taken during the normal diagnostic process. However, informed consent was obtained as stated below.

Data Availability Statement: Data sharing not applicable. All presented data are included in the manuscript.

Informed Consent Statement: Informed consent was obtained from all subjects involved in the study.

Conflicts of Interest: The authors declare no conflict of interest.

References

1. Kostygov, A.Y.; Karnkowska, A.; Votýpka, J.; Tashyreva, D.; Maciszewski, K.; Yurchenko, V.; Lukeš, J. Euglenozoa: Taxonomy, diversity and ecology, symbioses and viruses. *Open Biol.* **2021**, *11*, 200407, doi:10.1098/rsob.200407.
2. Reithinger, R.; Dujardin, J.-C.; Louzir, H.; Pirmez, C.; Alexander, B.; Brooker, S. Cutaneous leishmaniasis. *Lancet Infect. Dis.* **2007**, *7*, 581–596, doi:10.1016/S1473-3099(07)70209-8.
3. Van der Auwera, G.; Dujardin, J.-C. Species Typing in Dermal Leishmaniasis. *Clin. Microbiol. Rev.* **2015**, *28*, 265–294, doi:10.1128/CMR.00104-14.
4. Heras-Mosteiro, J.; Monge-Maillo, B.; Pinart, M.; Lopez Pereira, P.; Reveiz, L.; Garcia-Carrasco, E.; Campuzano Cuadrado, P.; Royuela, A.; Mendez Roman, I.; López-Vélez, R. Interventions for Old World cutaneous leishmaniasis. *Cochrane Database Syst. Rev.* **2017**, *2017*, doi:10.1002/14651858.cd005067.pub5.
5. Maroli, M.; Feliciangeli, M.D.; Bichaud, L.; Charrel, R.N.; Gradoni, L. Phlebotomine sandflies and the spreading of leishmaniases and other diseases of public health concern. *Med. Vet. Entomol.* **2013**, *27*, 123–147, doi:10.1111/j.1365-2915.2012.01034.x.
6. Baneth, G.; Shaw, S.E. Chemotherapy of canine leishmaniosis. *Vet. Parasitol.* **2002**, *106*, 315–324, doi:10.1016/S0304-4017(02)00115-2.

7. Ponte-Sucre, A.; Gamarro, F.; Dujardin, J.-C.C.; Barrett, M.P.; López-Vélez, R.; García-Hernández, R.; Pountain, A.W.; Mwenechanya, R.; Papadopoulou, B. Drug resistance and treatment failure in leishmaniasis: A 21st century challenge. *PLoS Negl. Trop. Dis.* **2017**, *11*, e0006052, doi:10.1371/journal.pntd.0006052.
8. Jeddi, F.; Mary, C.; Aoun, K.; Harrat, Z.; Bouratbine, A.; Faraut, F.; Benikhlef, R.; Pomares, C.; Pratlong, F.; Marty, P.; et al. Heterogeneity of molecular resistance patterns in antimony-resistant field isolates of Leishmania species from the western mediterranean area. *Antimicrob. Agents Chemother.* **2014**, *58*, 4866–4874, doi:10.1128/AAC.02521-13.
9. Gradoni, L.; Soteriadou, K.; Louzir, H.; Dakkak, A.; Toz, S.O.; Jaffe, C.; Dedet, J.-P.; Campino, L.; Cañavate, C.; Dujardin, J.-C. Drug regimens for visceral leishmaniasis in Mediterranean countries. *Trop. Med. Int. Heal.* **2008**, *13*, 1272–1276, doi:10.1111/j.1365-3156.2008.02144.x.
10. Gaspari, V.; Ortalli, M.; Foschini, M.P.; Baldovini, C.; Lanzoni, A.; Cagarelli, R.; Gaibani, P.; Rossini, G.; Vocale, C.; Tigani, R.; et al. New evidence of cutaneous leishmaniasis in north-eastern Italy. *J. Eur. Acad. Dermatol. Venereol.* **2017**, *31*, 1534–1540, doi:10.1111/jdv.14309.
11. Galluzzi, L.; Diotallevi, A.; De Santi, M.; Ceccarelli, M.; Vitale, F.; Brandi, G.; Magnani, M. Leishmania infantum Induces Mild Unfolded Protein Response in Infected Macrophages. *PLoS ONE* **2016**, *11*, e0168339, doi:10.1371/journal.pone.0168339.
12. Diotallevi, A.; De Santi, M.; Buffi, G.; Ceccarelli, M.; Vitale, F.; Galluzzi, L.; Magnani, M. Leishmania Infection Induces MicroRNA hsa-miR-346 in Human Cell Line-Derived Macrophages. *Front. Microbiol.* **2018**, *9*, 1019, doi:10.3389/fmicb.2018.01019.
13. Ceccarelli, M.; Galluzzi, L.; Migliazzo, A.; Magnani, M. Detection and Characterization of Leishmania (Leishmania) and Leishmania (Viannia) by SYBR Green-Based Real-Time PCR and High Resolution Melt Analysis Targeting Kinetoplast Minicircle DNA. *PLoS ONE* **2014**, *9*, e88845, doi:10.1371/journal.pone.0088845.
14. Ceccarelli, M.; Galluzzi, L.; Sisti, D.; Bianchi, B.; Magnani, M. Application of qPCR in conjunctival swab samples for the evaluation of canine leishmaniasis in borderline cases or disease relapse and correlation with clinical parameters. *Parasit. Vectors* **2014**, *7*, 460, doi:10.1186/s13071-014-0460-3.
15. Ceccarelli, M.; Buffi, G.; Diotallevi, A.; Andreoni, F.; Bencardino, D.; Vitale, F.; Castelli, G.; Bruno, F.; Magnani, M.; Galluzzi, L. Evaluation of a kDNA-Based qPCR Assay for the Detection and Quantification of Old World Leishmania Species. *Microorganisms* **2020**, *8*, 2006, doi:10.3390/microorganisms8122006.
16. Schönian, G.; Nasereddin, A.; Dinse, N.; Schweynoch, C.; Schallig, H.D.F.; Presber, W.; Jaffe, C.L. PCR diagnosis and characterization of Leishmania in local and imported clinical samples. *Diagn. Microbiol. Infect. Dis.* **2003**, *47*, 349–358, doi:10.1016/S0732-8893(03)00093-2.
17. Saitou, N.; Nei, M. The neighbor-joining method: A new method for reconstructing phylogenetic trees. *Mol. Biol. Evol.* **1987**, *4*, 406–425, doi:10.1093/oxfordjournals.molbev.a040454.
18. Ceccarelli, M.; Diotallevi, A.; Andreoni, F.; Vitale, F.; Galluzzi, L.; Magnani, M. Exploiting genetic polymorphisms in metabolic enzymes for rapid screening of Leishmania infantum genotypes. *Parasit. Vectors* **2018**, *11*, 572, doi:10.1186/s13071-018-3143-7.
19. Castelli, G.; Galante, A.; Verde, V.L.; Migliazzo, A.; Reale, S.; Lupo, T.; Piazza, M.; Vitale, F.; Bruno, F. Evaluation of Two Modified Culture Media for Leishmania infantum Cultivation Versus Different Culture Media. *J. Parasitol.* **2014**, *100*, 228–230, doi:10.1645/13-253.1.
20. Sundar, S.; Chakravarty, J. An update on pharmacotherapy for leishmaniasis. *Expert Opin. Pharmacother.* **2015**, *16*, 237–252.
21. Blum, J.; Buffet, P.; Visser, L.; Harms, G.; Bailey, M.S.; Caumes, E.; Clerinx, J.; Van Thiel, P.P.A.M.; Morizot, G.; Hatz, C.; et al. LeishMan recommendations for treatment of cutaneous and mucosal leishmaniasis in travelers, 2014. *J. Travel Med.* **2014**, *21*, 116–129.
22. Aït-Oudhia, K.; Gazanion, E.; Vergnes, B.; Oury, B.; Sereno, D. Leishmania antimony resistance: What we know what we can learn from the field. *Parasitol. Res.* **2011**, *109*, 1225–1232, doi:10.1007/s00436-011-2555-5.
23. Sarkar, A.; Ghosh, S.; Pakrashi, S.; Roy, D.; Sen, S.; Chatterjee, M. Leishmania strains causing self-healing cutaneous leishmaniasis have greater susceptibility towards oxidative stress. *Free Radic. Res.* **2012**, *46*, 665–673, doi:10.3109/10715762.2012.668186.
24. Gramiccia, M.; Gradoni, L.; Orsini, S. Decreased sensitivity to meglumine antimoniate (Glucantime) of Leishmania infantum isolated from dogs after several courses of drug treatment. *Ann. Trop. Med. Parasitol.* **1992**, *86*, 613–620, doi:10.1080/00034983.1992.11812717.

25. Maia, C.; Nunes, M.; Marques, M.; Henriques, S.; Rolão, N.; Campino, L. In vitro drug susceptibility of Leishmania infantum isolated from humans and dogs. Exp. Parasitol. 2013, 135, 36–41, doi:10.1016/j.exppara.2013.05.015.

Citation: Diotallevi, A.; Buffi, G.; Corbelli, G.; Ceccarelli, M.; Ortalli, M.; Varani, S.; Magnani, M.; Galluzzi, L. *In Vitro* Reduced Susceptibility to Pentavalent Antimonials of a *Leishmania infantum* Isolate from a Human Cutaneous Leishmaniasis Case in Central Italy. *Microorganisms* **2021**, *9*, x. https://doi.org/10.3390/xxxxx

Academic Editor:
Received: 22 April 2021
Accepted: 25 May 2021
Published: 26 May 2021

CHAPTER 7

In this chapter, it is reported the evaluation of a small library of azole-bisindole compounds for their anti-leishmanial potential, in terms of efficacy on *Leishmania infantum* promastigotes and intracellular amastigotes.

Original article submitted to ACS Omega

Submitted version, October 8th, 2021

Phenotype screening of an azole-bisindole chemical library identify URB1483 as a new antileishmanial agent devoid of toxicity on human cells

Aurora Diotallevi[a], Laura Scalvini[b], Gloria Buffi[a], Yolanda Pérez-Pertejo[c], Mauro De Santi[a], Michele Verboni[a], Gianfranco Favi[a], Mauro Magnani[a], Alessio Lodola[b], Simone Lucarini [a,*] and Luca Galluzzi[a]

[a] Department of Biomolecular Sciences, University of Urbino Carlo Bo, 61029 Urbino (PU), Italy;
[b] Department of Food and Drug, University of Parma, 43124 Parma, Italy;
[c] Department of Biomedical Sciences, University of León, 24071 León, Spain.

*Correspondence: simone.lucarini@uniurb.it; Tel.: +39 0722 303333

Abstract

We report the evaluation of a small library of azole-bisindoles for their anti-leishmanial potential, in terms of efficacy on *Leishmania infantum* promastigotes and intracellular amastigotes. Nine compounds showed good activity on *L. infantum* MHOM/TN/80/IPT1 promastigotes with IC_{50} values ranging from 4 to 10 µM. These active compounds were also tested on human (THP-1, HepG2, HaCaT, and Human Primary Fibroblasts) and canine (DH82) cell lines. **URB1483** was selected as the best compound, with no quantifiable cytotoxicity in mammalian cells, to test the efficacy on intracellular amastigotes. **URB1483** significantly reduced the infection index of both human and canine macrophages with an effect comparable to the clinically used drug pentamidine. **URB1483** emerges as a new anti-infective agent with a remarkable antileishmanial activity and no cytotoxic effects on human and canine cells.

Keywords Phenotype screening, Antileishmanial, *Leishmania infantum*, bisindoles, 3,3'-diindolylmethanes.

1. Introduction

Leishmaniasis is a neglected disease caused by protozoan parasites transmitted by phlebotomine sandflies. More than 20 different *Leishmania* species all over the world cause a variety of clinical conditions broadly grouped in cutaneous (CL), mucosal (ML) and visceral leishmaniasis (VL) [1]. The latter, being fatal if untreated, causes 20,000–40,000 deaths across the globe each year [2-3]. More than a million new cases are reported per year and 350 million people are at risk of contracting the infection [1]. Italy is an endemic country, with an increase in cases in the last two decades due to said disease spreading within traditionally endemic regions and to the appearance of autochthonous cases in previously non-endemic areas such as northern continental Italy [2,4]. The most widespread form of leishmaniasis endemic in southern Europe is zoonotic VL, involving humans and domestic dogs (which may serve as main reservoir), sometimes associated with few cases of CL. Both diseases are caused by *L. infantum* [4].

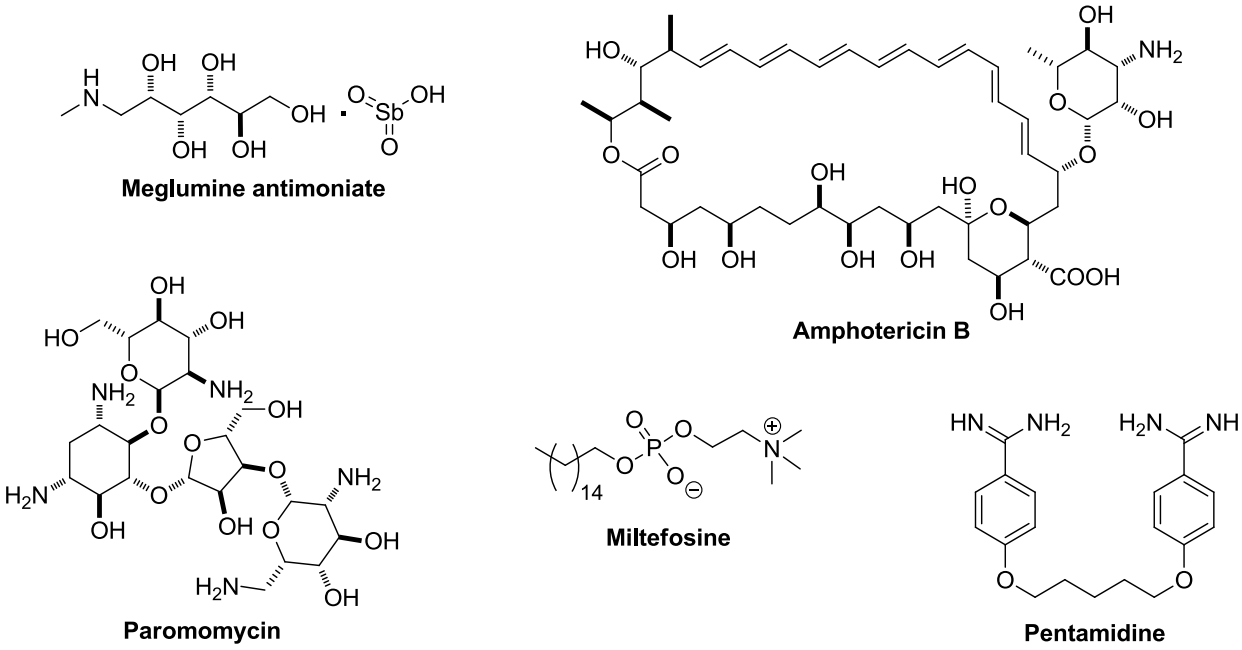

Figure 1. Main commercial drugs against Leishmaniosis.

Although in recent years three vaccine candidates have undergone clinical trials, and half a dozen more are in the pipeline, no efficacious vaccine against leishmaniasis is now available on the market [5]. Moreover, all currently available drugs are inadequate [1] (figure 1). Pentavalent antimonials (one example is meglumine antimoniate, figure 1), the first-line treatment, could not be efficacious due to widespread resistance to the drug. Few VL treatments against leishmaniasis have been introduced during the last decade, each of them having serious limitations. Amphotericin B, one of the most used second-line drug, is effective against antimonial-resistant *Leishmania* strains, but it can induce acute and chronic toxicity. The Amphotericin B liposomal formulation (AmBisome) ameliorates the toxicity

profile; yet its high formulation cost has limited its use [6]. Miltefosine is a highly potent oral drug against VL and CL; however, its use is limited due to high cost, teratogenicity and long treatment. Paromomycin is the cheapest treatment but its use has been associated with severe toxicity. Moreover, this drug requires parenteral administration, needs long treatment and shows region-dependent efficacy. On the other hand, pentamidine is used in combination therapies at low dosages but shows several shortcomings (renal toxicity, myocarditis, diabetes mellitus, hypoglycemia, hypotension and fever) [1].

Due to the serious drawbacks of the available therapeutic options, which are less toxic and more efficacious across all endemic regions, shorter courses and inexpensive drugs are urgently needed. Many research groups around the world have developed several new scaffolds as potential drugs against leishmaniasis [1, 7-10]. Among them, few bis-indoles were reported (figure 2).

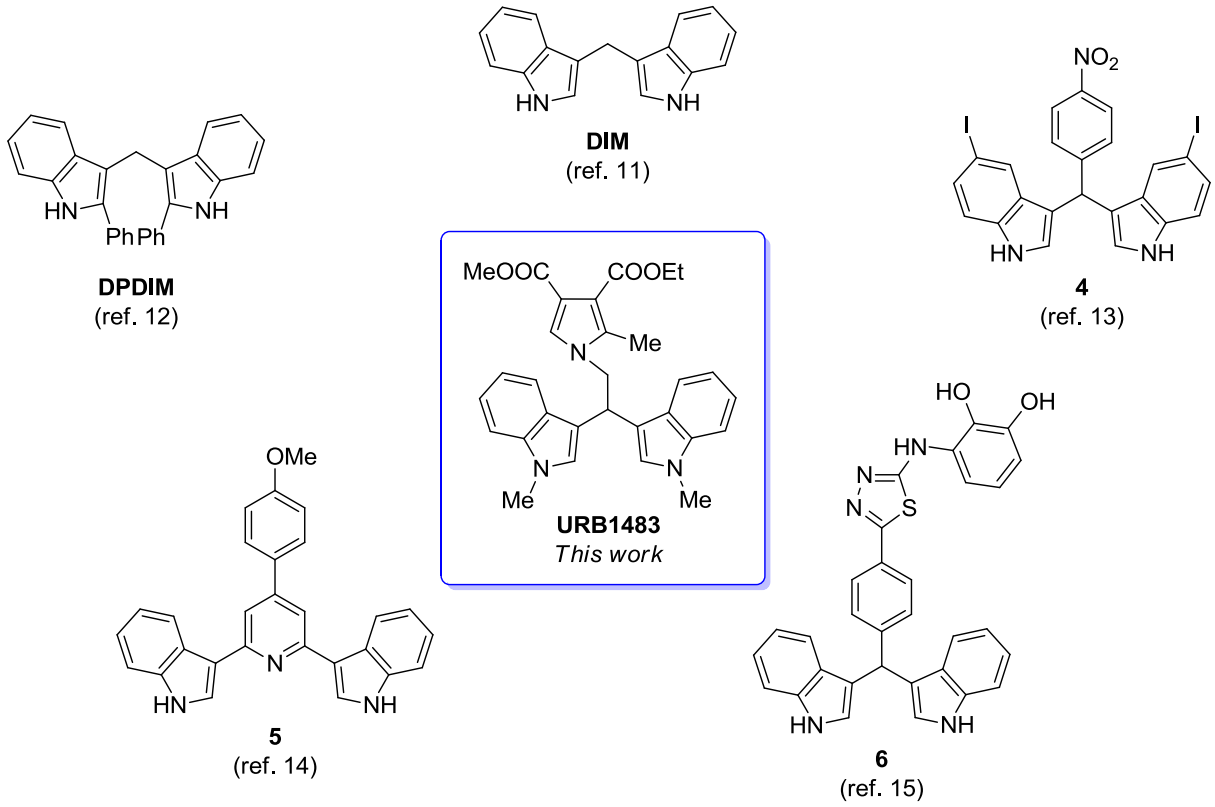

Figure 2. Potential anti-leishmanial agents sharing bis(indolyl) fragment.

The seminal work of Roy and his collaborators reported that 3,3'-diindolylmethane (DIM, figure 2) is an effective inhibitor of *L. donovani* topoisomerase IB [11]. More specifically, the prototypical member of the class, DIM, was reported to act as poison for topoisomerase IB, i.e. similarly to the well-known drug camptothecin (CPT) it stabilizes the topoisomerase–DNA cleavage complex thus blocking the relaxation process [11,12]. In a subsequent work, the same authors reported three new DIM derivatives that were active against a DIM resistant strain of *L. donovani*. In figure 2, 2,2'-

diphenyl-3,3'-diindolylmethane (DPDIM) is shown as the most promising example of the reported DIMs.

In 2013, Bharate and coworkers reported a new aryl-DIM potent class of antileishmanial agents. Among them, compound **4** (figure 2) was the most effective against *L. donovani* promastigotes and amastigotes, showing IC_{50} values lower than 10 μM [13]. However, they did not propose a biological target of the new aryl-DIMs.

The bis(indolyl)-pyridine **5** (figure 2) is the most interesting compound reported by Kalam Khan et al. against *Leishmania* parasites [14] but it is less potent than previously described DIMs and no information about its mechanism of action is available. Very recently, the group of Taha has reported several phenyl-aminothiazole-DIM derivatives as potent antileishmanial agents [15]. In particular, compound **6** (figure 2) has showed outstanding effect on the protozoa with sub-micromolar IC_{50} value. The authors claimed that this new class of compounds may inhibit the pteridine reductase. Yet, no inhibition studies on the isolate enzyme were reported.

As part of our ongoing investigations on the biological activities and applications of bisindole derivatives [16-20] and leishmaniasis [21-24], in the present study, a focused library of selected published azole-bisindole derivatives **1**-**3** (scheme 1 and 2) [20,25] sharing the bis(indolyl) motif with the above mentioned anti-leishmanial agents was screened against several human and canine *L. infantum* promastigote strains. The most active compounds (IC_{50} < 20 μM) were then tested on human and canine macrophages, as well as other human cell lines to check for their potential toxicity. Pyrrole-bisindole **1b**, named **URB1483,** was found to be the most specific compound against parasites and was tested for its efficacy on *L. infantum* infected human and canine macrophage-like cell lines.

2. Results

2.1 Chemistry

The pyrrole-bisindoles **1a-d** and imidazole-bisindoles **2a-f** were synthetized according to previously reported methods [19] starting from the opportune bisindoles **7a-g** and 1,2-diaza-1,3-diene **8a-c** [16,20,25] (scheme 1).

The treatment of bisindole **7** with the opportune propiolate in dichloromethane (DCM) followed by addition of azoalkene **8** in toluene and in the presence of trifluoroacetic acid (TFA) at reflux furnished the corresponding pyrrole-indole **1**. The mechanism of this sequential three-component reaction involves the preliminary formation of enamine intermediate, subsequent Michael addition to azoene system, and final intramolecular heterocyclization with loss of the carbazate residue.

On the other hand, the indole-imidazole scaffold **2** was synthesized by a conjugate addition of bisindole **7** to **8** in acetonitrile (ACN) at room temperature (rt), followed by the condensation with the paraformaldehyde at reflux. For this three-component reaction, a thermal-assisted 1,5-eletrocyclization of azoalkene-derived azavinyl azomethine ylides appears to be operative. [20]

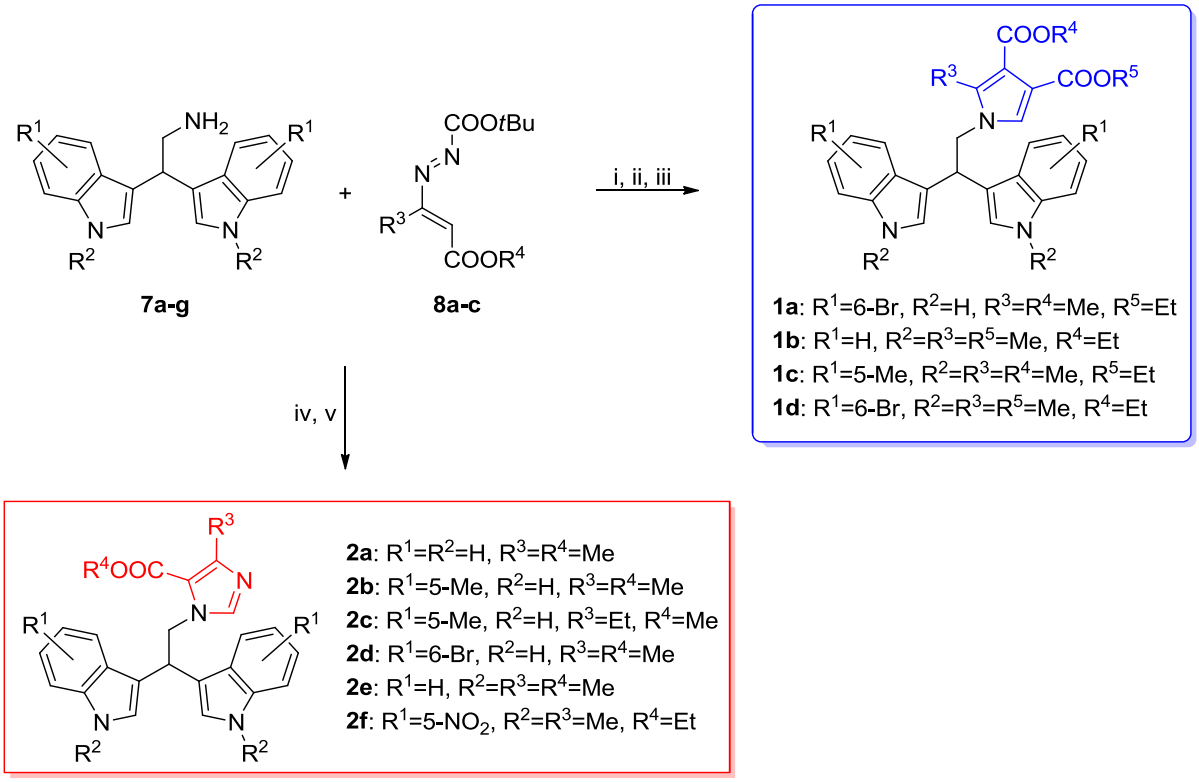

Scheme 1. Reagents and conditions: (i) methyl or ethyl propiolate (R^5), DCM, at room temperature (rt), overnight ; (ii) 1,2-diaza-1,3-diene **8**, toluene, reflux, 2 h; (iii) TFA, reflux, 2-4 h. (iv) 1,2-diaza-1,3-diene **8**, ACN, rt, 1 h; (v) paraformaldehyde, reflux, 4 h.

The triazole-bisindoles **3** were instead synthetized in a single step (Sakai's protocol) from α,α-dichlorotosylhydrazone **9** and bisindole **7** [16,20] respectively in the presence of *N*,*N*-diisopropylethylamine (DIPEA) as a base in ethanol/acetonitrile mixture (Scheme 2). [20]

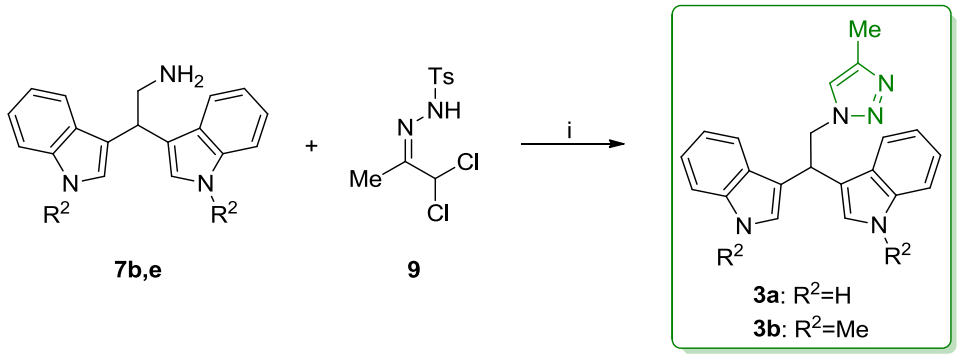

Scheme 2. Reagents and conditions: (i) DIPEA, ethanol, **9** in acetonitrile, 0 °C to rt, 2 h.

2.2 Effect of bisindoles on *L. infantum* promastigote viability

The *in vitro* antileishmanial activity evaluation of bisindole derivatives was carried out by treating *L. infantum* MHOM/TN/80/IPT1 promastigotes for 72h with scalar dilution 1:2 or 2:3 (from 20 to 0.31 µM) of each molecule. As positive controls, *Leishmania* parasites were also treated with pentamidine, non-liposomal amphotericin B and miltefosine. The compounds **1a-b**, **2a-f** and **3b** showed IC_{50} values between 3.66 and 10.09 µM. The compound **1c, 1d**, **3a** and **DIM** showed IC_{50} >20 µM and were not taken into consideration for subsequent experiments (table 1). Next, the activity of bisindoles was evaluated on three *L. infantum* clinical isolates (two canines and one human), confirming the activity of all tested compounds (table 1 and supporting information).

Table 1. Azole-bisindole derivatives potency on *L. infantum* promastigote strains. IC_{50} values for all the strains are reported as mean and 95% confidence interval, from at least three independent experiments. Each experimental condition was conducted at least in duplicate.

Compound	***L. infantum* MHOM/TN/80/IPT1** **IC_{50} (µM) (95% CI)**	***L. infantum* canine clinical isolate 1** **IC_{50} (µM) (95% CI)**	***L. infantum* canine clinical isolate 2** **IC_{50} (µM) (95% CI)**	***L. infantum* human clinical isolate** **IC_{50} (µM) (95% CI)**
1a	6.63 (6.12-7.18)	7.02 (6.53-7.54)	5.72 (5.34-6.13)	6.37 (5.41-7.53)
1b (**URB1483**)	3.66 (3.22 - 4.17)	4.13 (3.84-4.46)	3.66 (3.48-3.85)	7.15 (5.80-8.91)
1c	>20 (42.5%)[a]	n.t.[b]	n.t.[b]	n.t.[b]
1d	>20 (10.6%)[a]	n.t.[b]	n.t.[b]	n.t.[b]
2a	9.98 (9.21- 10.80)	6.81 (6.22-7.46)	4.78 (4.58-4.99)	8.13 (7.21-9.12)
2b	7.69 (7.04-8.37)	6.41 (6.03-6.80)	4.97 (4.68-5.27)	6.08 (5.33-6.95)
2c	10.09 (9.42-10.79)	8.67 (7.86-9.55)	6.53 (6.19-6.90)	8.62 (7.84-9.40)
2d	8.46 (7.77-9.15)	9.66 (9.21-10.12)	7.03 (6.47-7.61)	7.50 (6.78-8.25)
2e	4.90 (4.26-5.64)	4.77 (4.50-5.07)	3.57 (3.32-3.84)	5.49 (5.02-6.01)
2f	4.88 (4.39-5.42)	6.77 (6.18-7.40)	5.63 (5.25-6.03)	5.30 (4.93-5.70)
3a	>20 (21.9%)[a]	n.t.[b]	n.t.[b]	n.t.[b]
3b	8.13 (7.15-9.23)	5.66 (5.25-6.12)	5.27 (5.06-5.48)	7.41 (6.61-8.30)
DIM	>20 (9.9%)[a]	>20 (6.3%)[a]	>20 (11.9%)[a]	>20 (22.3%)[a]

Pent	2.56 (2.11-3.22)	1.72 (1.64-1.86)	1.41 (1.34-1.48)	1.49 (1.37-1.62)
Amph B	0.06 (0.05-0.08)	0.12 (0.12-0.13)	0.11 (0.11-0.12)	0.08 (0.07-0.09)
Milt	2.85 (2.47-3.30)	6.57 (6.02-7.18)	6.07 (5.63-6.53)	1.21 (0.98-1.46)

[a] percentage of inhibition at 20 µM; [b] not tested; **Pent**: Pentamidine; **Amph B** : non-liposomal amphotericin B; **Milt**: miltefosine.

2.3 Cytotoxic effect of bisindoles in human and canine cell lines

The cytotoxicity of the most active compounds **1a**, **1b** (**URB1483**), **2a-f** and **3b** was evaluated in THP-1, DH82, HEPG2, HaCaT and human primary fibroblasts (HPF) cells, in term of concentrations of drug required to reduce cell viability by 50% (CC_{50}). At first, to test the viability of THP-1 and DH82 cells following bisindoles treatment, cells were treated for 72h with each compound at five different concentrations (2, 10, 20, 80, 200 µM). Notably, **URB1483** did not show quantifiable toxicity in both cell lines. The other compounds showed a cytotoxicity >20 µM in both cell lines, with the exception of compound **2d** (15.44 and 18.92 µM in THP-1 and DH82 cells, respectively) and **1a** (11.09 µM in DH82 cells) (table 2 and supporting information).

Table 2. Azole-bisindole derivatives CC_{50} values on THP-1 and DH82 cells

Compund	**THP-1**		**DH82**	
	CC_{50} (µM) (95% CI)	**Selectivity index (CC_{50}/IC_{50}[a])**	**CC_{50} (µM) (95% CI)**	**Selectivity index (CC_{50}/IC_{50}[a])**
1a	124.40 (90.87-193.40)	18.76	11.09 (8.14-13.96)	1.67
1b (**URB1483**)	> 200 (2.1%)[b]	> 55	> 200 (15.4%)[b]	> 55
2a	37.89 (25.21-58.56)	3.79	35.31 (29.31-42.15)	3.54
2b	26.87 (16.70-36.92)	3.49	24.82 (20.98-29.01)	3.22
2c	38.63 (26.41-59.05)	3.83	23.52 (19.96-28.85)	2.33
2d	15.44	1.83	18.92	2.24

	(12.82-18.95)		(15.40-24.01)	
2e	55.44 (24.60-79.61)	11.31	24.30 (20.72-29.27)	4.96
2f	35.11 (21.54-49.87)	7.19	> 200 (42.9%)[b]	> 41
3b	> 200 (33%)[b]	> 25	31.86 (22.61-45.54)	3.92
Pent	103.1 (72.64-179.2)	40.27	10.59 (7.88-12.85)	4.14
Amph B	2.75 (1.50-3.76)	45.83	>200 (41.5%)[b]	> 3333
Milt	27.78 (22.54-35.51)	9.75	95.88 (86.21-108.90)	33.64

[a] selectivity index calculated considering IC_{50} on *L. infantum* MHOM/TN/80/IPT1; [b] percentage of inhibition at 200 µM; **Pent**: Pentamidine; **Amph B**: non-liposomal amphotericin B. **Milt**: miltefosine.

Next, the CC_{50} was evaluated in DH82, HepG2, HaCaT cell lines and HPF cells after 24 h treatment with serially diluted bis-indole compounds (2, 10, 20 µM). In this case, incubations were carried out for 24 hours to evaluate the cytotoxicity in actively dividing cells. In these experiments, the CC_{50} values were >20, indicating low cytotoxicity of the bisindole derivatives also in these cell lines. Interestingly, the CC_{50}/24h values of the reference compound non-liposomal amphotericin B were between 4.6 and 17.26 µM (Table S1, supporting information).

2.4 Efficacy of compound URB1483 on *L. infantum* intracellular amastigotes

Based on the analysis of the IC_{50} and CC_{50} obtained on *L. infantum* promastigotes and THP-1 or DH82 cells, respectively, **URB1483** was found to be the most effective and yet selective compound against the parasites and, therefore, it was selected for further experiments.

The infection of human monocytic THP-1 cell line was conducted with *L. infantum* MHOM/TN/80/IPT1 as described in methods. Infected macrophages were treated with compound **URB1483** or pentamidine (used as positive control) for 72h. The infection index was significantly reduced following the treatment with **URB1483**, in a dose-dependent manner (one-way ANOVA $p< 0.001$) (figure 3A), evocative of specific mechanism of action.

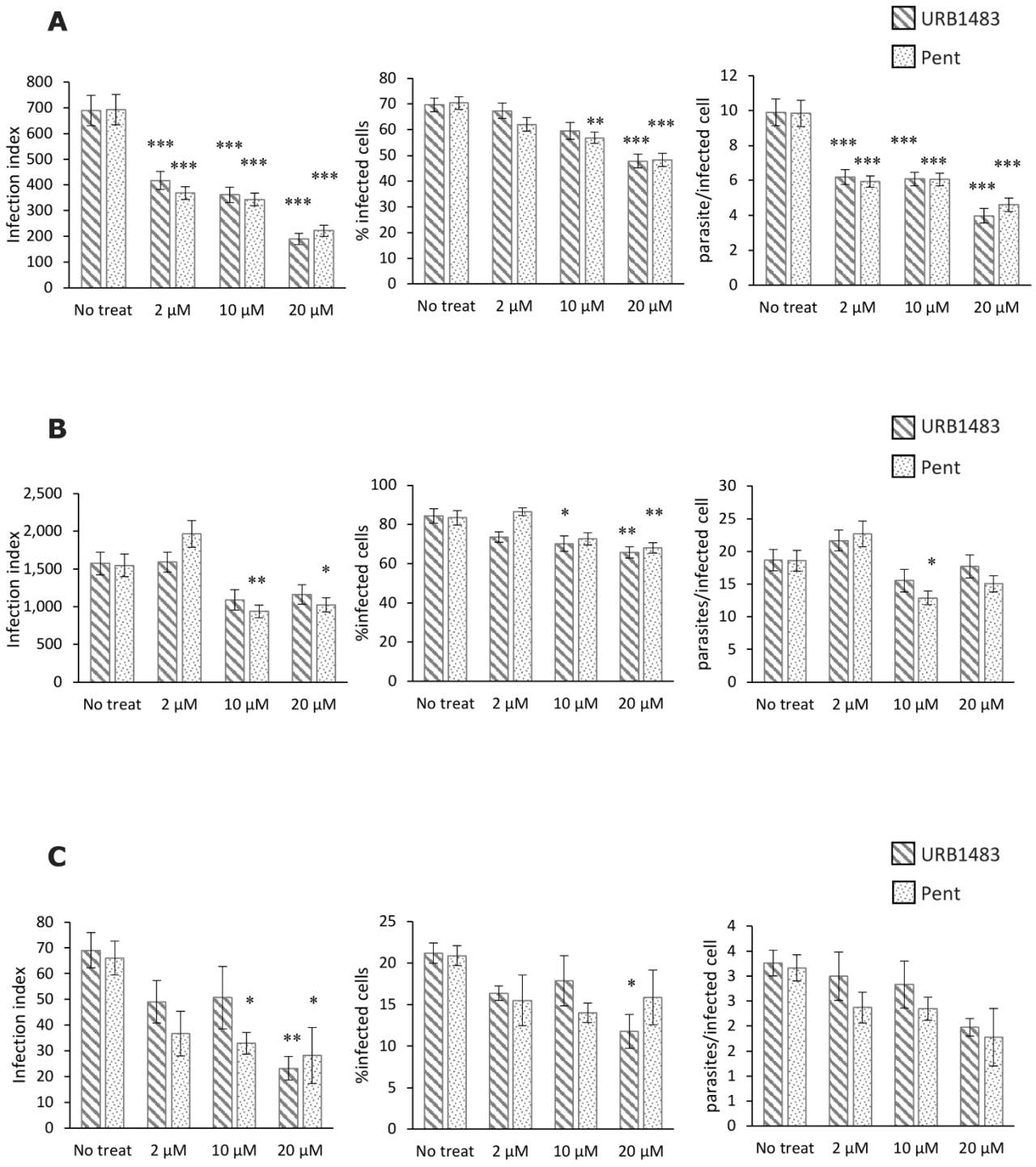

Figure 3. Effect of **URB1483** and **Pent** on intracellular *L. infantum* amastigotes. **A**) THP-1 cells infected with *L. infantum* MHOM/TN/80/IPT1; **B**) THP-1 cells infected with *L. infantum* human clinical isolate; **C**) DH82 cells infected with *L. infantum* MHOM/TN/80/IPT1. In all cases cells were infected for 24 h at 37°C; the drugs were added, and infection index was calculated after 72 h of treatment. Data are expressed as mean ± SEM of three independent experiments. Each experimental condition was conducted at least in duplicate. * $p < 0.05$, ** $p < 0.01$, ***$p < 0.001$.

Interestingly, the percentage of infected cells and the average number of amastigotes per infected cell decrease in a dose-dependent manner, in both **URB1483** and pentamidine treatments. The THP-1 cells were also infected with the *L. infantum* human clinical isolate. In this case, the parasite resulted to be less susceptible to both **URB1483** and **Pent**, compared to the reference strain MHOM/TN/80/IPT1 (figure 3B).

The same infection and treatment protocols were also performed with the DH82 cell line. In DH82 cells infected with MHOM/TN/80/IPT1 strain, the infection index decreased significantly at the higher dose (20 µM) in both **URB1483** ($p < 0.01$) and pentamidine ($p < 0.05$) treated cells (figure 3C). It is noteworthy that **Pent** had a cytotoxic effect on DH82 cells after 72 h treatment (table 2) (not observed after 24h treatment), in contrast to **URB1483**, which did not significantly affect the cells viability (figure 4).

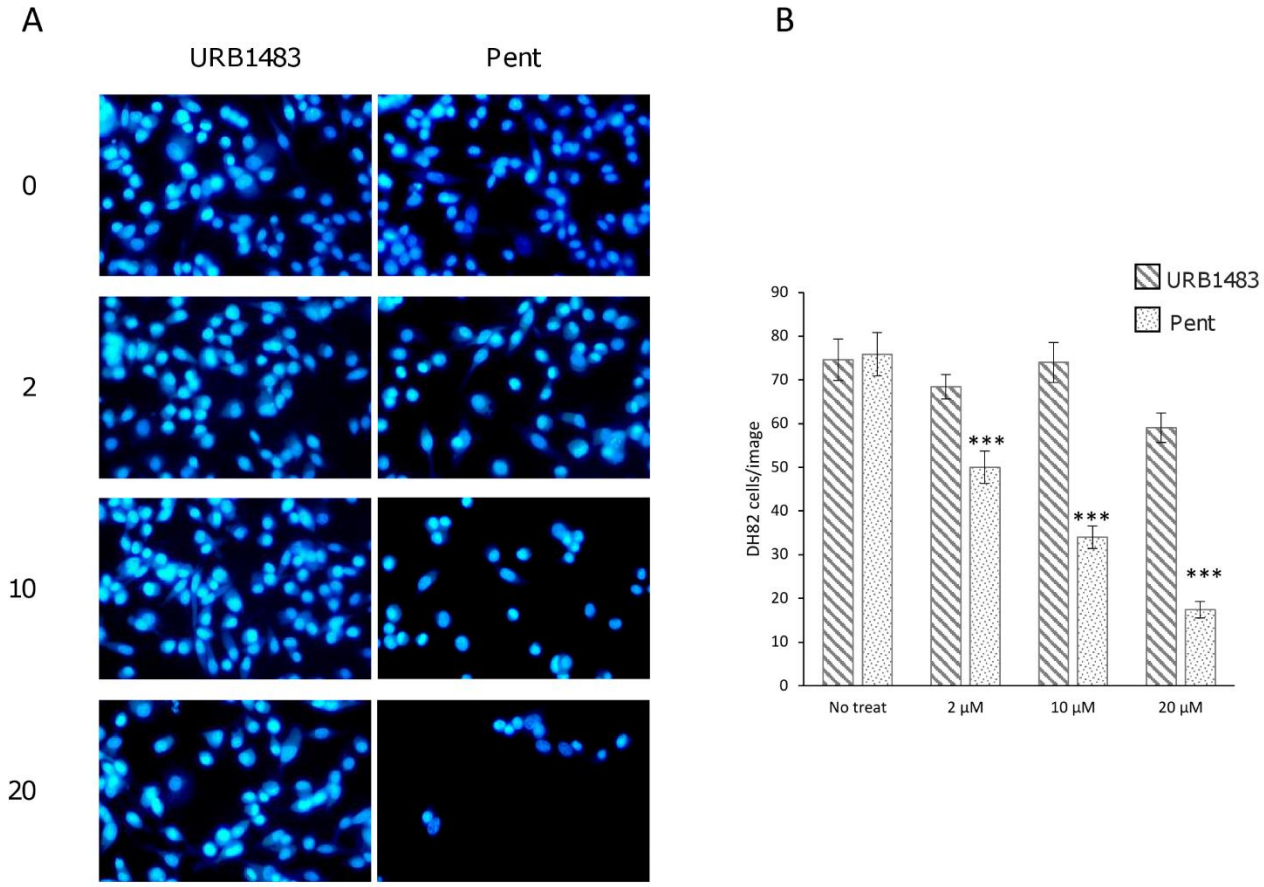

Figure 4. Cytotoxic effect of treatment with pentamidine (**Pent)**, in contrast to **URB1483**, on DH82 cells after 72 h treatment. **A**) Uninfected DH82 cells were treated with **URB1483** or **Pent** for 72h at the concentration of 0, 2, 10, 20 µM and stained with Hoechst dye for fluorescence microscope observation. **B**) The effect of treatment was monitored by calculating the number of cells, considering at least five images per treatment condition. Data are means ± SEM; ***$p < 0.001$.

The two-way ANOVA followed by Bonferroni post hoc test did not show significant differences in infection indexes between treatments with compound **URB1483** and pentamidine in all experiments (see supporting information, Table S2), accounting for similar effects of the two molecules.

2.5 *L. donovani* topoisomerase IB as potential target

Prompted by the encouraging results obtained on both *L. infantum* promastigote and *L. infantum* intracellular amastigotes, we searched for molecular target responsible for the antileishmanial activity displayed by compound **URB1483**. Literature data point to topoisomerase IB as the most likely target for bis-indole compounds [11,12]. The antileishmanial activity displayed by the bis-indolyl derivative **DIM** has been linked to the ability of this compound to block DNA relaxation with a mechanism similar to that of topotecan [26], i.e., stabilizing the formation of a ternary complex composed by the inhibitor itself, the leishmanial enzyme topoisomerase IB and double strand DNA. We thus performed molecular modelling investigations assuming that URB1483 could interact with the topoisomerase IB-DNA complex by targeting the same binding site recognized by topotecan. At first, a three-dimensional model of *L. donovani* topoisomerase I bound to DNA-topotecan complex was built using available structural information in the PDB, i. e., the human form of topoisomerase I bound to DNA and topotecan (PDB ID 1K4T), and the *L. donovani* form of topoisomerase I bound to nicked DNA (PDB ID 2BS9), by following the computational protocol reported by Roy et al. (see method section for details) [12]. This strategy appeared reasonable as the comparison between these two topoisomerase structures reveals that, despite a diverse architecture (monomeric the human, dimeric the *L. donovani* isoform), all of the amino acid residues that line the topotecan-binding pocket are entirely conserved between the two species [27].

The resulting model of *L. donovani* topoisomerase IB bound to topotecan was employed to identify binding mode for **URB1483** that could account for its specific mechanism of action. Docking simulations point to a pose for **URB1483** to some extent resembling the one experimentally observed for topotecan (figure 5), with one indolyl fragment well superposed on the A-ring of topotecan and one terminal carboxylic acid ethyl ester installed on the pyrrole nucleus occupying nearly the same space of the lactone E-ring of topotecan. The second indolyl fragment of **URB1483** protruded in a broad cavity of topoisomerase IB, normally occupied by solvent bulk. This additional cavity is targeted by other classes of topoisomerase poisons such as indolocarbazole and indenoisoquinoline derivatives [28], which place a bulky group in this region (figure S6, supporting information).

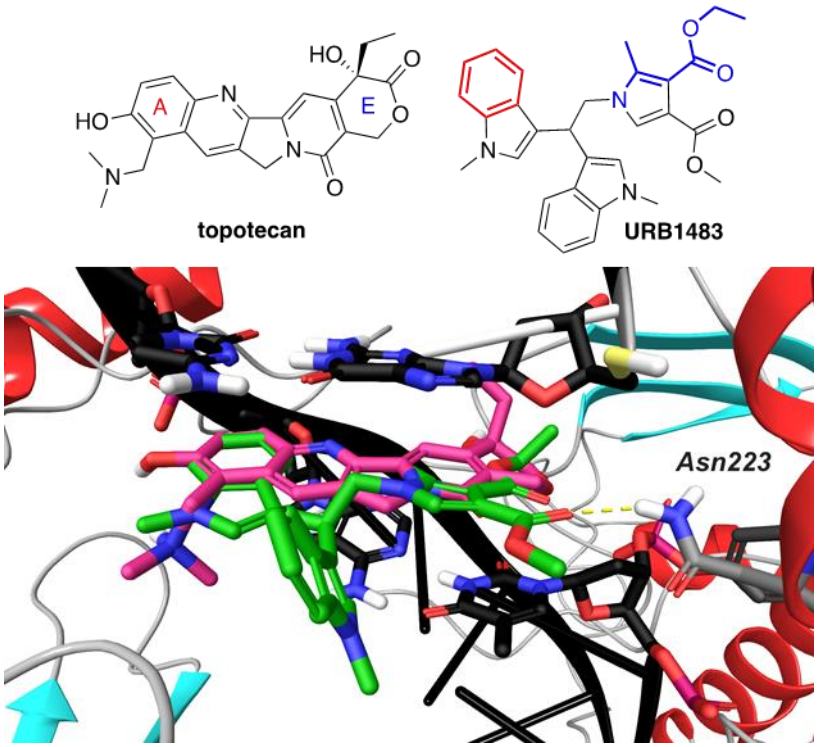

Figure 5. Molecular model of **URB1483** (green carbons) docked in the CPT binding site present in the topoisomerase IB - DNA complex (dark grey carbon atoms). The structure of topotecan (pink carbon atoms) is also displayed for comparison. The secondary structure of topoisomerase IB is represented by red (α-helices) or cyan (β-strands) cartoons, while the secondary structure of the DNA (namely, 22-base pair duplex oligonucleotide) is represented by black cartoons.

Prompted by these computational results, the inhibitory activity of **URB1483** was assessed on *L. donovani* topoisomerase IB by means of a plasmid relaxation assay (figure S7, supporting information). This assay detects the different electrophoretic mobility of the DNA supercoiled plasmid converted, by the enzyme, to its relaxed forms, in the presence of increasing concentrations of the compound. Gathered data indicate that **URB1483** does not inhibit DNA relaxation at all the tested concentrations (up to 50 μM).

Therefore, further investigations, not necessarily based on the structural similarity between **DIM** and **URB1483**, to identify a molecular target accounting for the anti-leishmania activity of pyrrole-bisindole derivatives will be needed.

2.6 Stability studies of URB1483

Chemical stability data were measured by LC/MS approaches for **URB1483** to preliminary assess its *in vitro* PK profile. Gratifyingly our analyses revealed that **URB1483** exhibited a favorable chemical

stability both in physiological solution and in cellular medium. In both conditions, the chemical stability was almost quantitative with more than the 90% of **URB1483** remaining unaltered after 72 h.

3. Discussion

Leishmaniasis is one of the most dangerous neglected tropical diseases, second only to malaria in parasitic causes of death [5]. Caused by global warming, the endemic regions of leishmaniasis are continuously spreading to non-tropical areas, including Europe. So far, no vaccine against leishmaniasis is on the market. Approved drugs in second- and third-line treatments are currently limited and/or exorbitantly priced (i.e. amphothericin B; paromomycin; miltefosine; pentamidine) with few of them being effective on antimonial-resistant *Leishmania* strains. Moreover, the use of these agents on infected patients is seriously hampered by the insurgence of acute and/or chronic toxicity. Therefore, there is an urgent need for developing safe, effective, and affordable drugs for the treatment of leishmaniasis. To fill this therapeutic gap, several research groups introduced new classes of active compounds against leishmaniasis, including bisindole derivatives.

In this context, a phenotypic screening of our small library of previously reported azole-bisindoles **1-3** (scheme 1-2) [20,25] against four human and canine *L. infantum* strains was performed. With few exceptions, all bisindoles, belonging to three different classes (pyrroles **1**, imidazoles **2** and triazoles **3**), showed good activity against the analyzed *L. infantum* promastigotes with IC_{50} values lower than 10 μM (table 1).

Conversely, pyrrole-bisindole **1c** is less active than the other compounds, **1d** and triazole-bisindole **3a** are nearly inactive. At this stage, it seems that an additional nitrogen containing aryl substituent could increase the potency of the simple bisindole scaffold (**DIM** was almost inactive at 20 μM). In the pyrrole class **1**, a double substitution of the indole rings is detrimental for their activity (compounds **1c** and **1d** showed low activity). All the imidazole derivatives **2** are active in all four *L. infantum* promastigote strains, and in particular **2e** and **2f**, having *N*-methylated indoles, are very potent. The methylation of the indole rings seems to play an important role also in the triazole-bisindole derivatives **3** (**3a** is inactive and **3b** showed $IC_{50} < 8$ μM).

The most active azole-bisindoles **1a**, **URB1483**, **2a-f** and **3b** were then tested on human and canine macrophage-like cell lines, as well as other human cell lines to check for their potential toxicity. In general, the imidazole-bisindole derivatives **2** are more toxic than pyrroles **1** and triazole **3b** in all the tested cell lines. Pyrrole-bisindole **URB1483** showed good activity against parasites and the best selectivity index (SI) on both human (THP-1) and canine (DH82) cells (SI > 55, table 2). Moreover, **URB1483** did not show any appreciable toxicity against human hepatocytes, keratinocytes and primary fibroblasts (table S1, supporting information).

Therefore, **URB1483** was tested, in comparison with pentamidine, for its efficacy on *L. infantum* infected human and canine macrophage-like cell lines. The efficacy of compound **URB1483** and pentamidine was not significantly different in human and canine *in vitro* infection models, despite the fact that pentamidine showed lower IC_{50} when compared to **URB1483** in promastigotes (table 1). This may account for a better bioavailability of **URB1483** inside the infected cells. Concerning the human infection model (THP1 cells), the human clinical isolate appeared less susceptible to both drug treatments compared to the reference strain MHOM/TN/80/IPT1. This probably reflects its higher virulence (infection index was twice) and/or its lower susceptibility to treatment with compound **URB1483** (IC_{50} value was about two times higher in the human clinical isolate compared to other strains) (table 1). As regards the canine infection model, it is noteworthy that pentamidine showed high toxicity in DH82 cells at 72 h (table 2 and figure 4), while compound **URB1483** did not show any appreciable toxicity, underlying its potential use also in veterinary applications.

According to literature, topoisomerase IB was identified as a likely biological target for this class of bisindoles, [11,12]. Furthermore, molecular modelling investigations on topoisomerase IB point to a likely binding mode for **URB1483** similar to the one experimentally observed for topotecan. Therefore, **URB1483** was evaluated for its ability to inhibit on topoisomerase IB from *L. donovani*, which shared 98% sequence identity with *L. infantum* isoform. Unexpectedly, **URB1483** failed to inhibit *L. donovani* topoisomerase IB activity, indicating that other targets are likely engaged by this pyrrole-bisindole. Efforts will be taken to discover the target of **URB1483** in our ongoing research on antileishmanial agents.

4. Conclusions

A phenotypic screening of a small library of azole-bisindoles against several human and canine *L. infantum* strains was performed. Most of the tested compounds showed good activity against the promastigotes (IC_{50} values < 10 μM). **URB1483**, a pyrrole-bisindole derivative, showed good activity against parasites and it did not affect viability of canine and human cell lines, with a selectivity index > 55. Moreover, the efficacy of **URB1483** on human and canine *in vitro* infection models was comparable to that of the commercial drug pentamidine. Previous works on the bisindole prototype DIM demonstrated that its antileishmanial activity is due to its ability to block the DNA relaxation activity of *Leishmania* topoisomerase IB. This evidence along with computational studies support the hypothesis that **URB1483** should have worked as topoisomerase IB inhibitor. Biochemical studies on the isolated enzyme ruled out inhibition of topoisomerase IB as mechanism of action for **URB1483**. Even if the search for the biological target is still ongoing, **URB1483** may undoubtedly represent a promising lead compound for the generation of new anti-*Leishmania* agents with low toxicity on host cells.

Experimental Section

5. Materials and Methods

5.1 Chemistry

All organic solvents used in this study were purchased from Sigma–Aldrich (St. Louis, MO, USA), Alfa Aesar (Haverhill, MA, USA), or TCI (Tokyo, Japan). In particular, the antileishmanial drugs pentamidine isethionate salt, non-liposomal amphotericin B and miltefosine, used as positive controls, were purchased from Sigma–Aldrich. Prior to use, acetonitrile, dichloromethane and toluene were dried with molecular sieves with an effective pore diameter of 4 Å. Column chromatography purifications were performed under ‘‘flash” conditions using Merck (Darmstadt, Germany) 230–400 mesh silica gel. Analytical thin-layer chromatography (TLC) was carried out on Merck silica gel plates (silica gel 60 F254), which were visualized by exposure to ultraviolet light and an aqueous solution of cerium ammonium molybdate (CAM). Melting points were determined by Buchi (Gallen, Switzerland) B-540. ^{1}H NMR and ^{13}C NMR spectra were recorded on a Bruker (Billerica, MA, USA) AC 400 or 100, respectively, spectrometer and analyzed using the TopSpin 1.3 (2013) software package. Chemical shifts were measured by using the central peak of the solvent. EI-MS and ESI-MS spectra were recorded with a Shimadzu (Kyoto, Japan) QP-5000 mass spectrometer and with a Waters (Milford, MA, USA) Micromass ZQ spectrometer respectively. The final compounds were analyzed on a ThermoQuest (Italia) FlashEA 1112 elemental analyzer for C, H, and N. The percentages found were within ±0.5% of the theoretical values. All the tested compounds were >95% pure as determined by elemental analysis.

*General procedure for the synthesis of pyrrole-bisindole derivatives **1***

A mixture of the appropriate bisindole **7** [16] (0.4 mmol) and methyl or ethyl propiolate (0.44 mmol) was stirred in DCM (1 mL) overnight at room temperature. A solution of the opportune azoalkene **8** (0.6 mmol) in toluene (4 mL) was added and the reaction was refluxed for 2 h. Catalytic amount of TFA (two drops) was added and the reaction was refluxed for additional 2-4 h (TLC check). After removal of the solvent, the crude mixture was purified by column chromatography on silica gel to afford the corresponding pyrrole-bisindole **1**.

The physicochemical data of compounds **1a-d**, including the purity >95% (determined by elemental analysis), are reported in the supporting information and they are in agreement with those reported in literature [20].

*General procedure for the synthesis of imidazole-bisindole derivatives **2***

To a stirred solution of the appropriate bisindole **7** [16] (0.4 mmol) in ACN (2 mL), the opportune azoalkene **8** (0.4 mmol) was added at room temperature. After the disappearance of the reagents, checked by TLC analysis, (usually 1 h), paraformaldehyde (0.8 mmol) was added, and then the resulting mixture was refluxed for 4 h (TLC check). The solvent was evaporated under reduced pressure and the crude residue was purified by column chromatography to give the corresponding imidazole-bisindole derivatives **2**.

The physicochemical data of compounds **2a-d** [20] and **2e-f** [25], including the purity >95% (determined by elemental analysis), are reported in the supporting information and they are in agreement with those reported in literature.

*General procedure for the synthesis of triazole-bisindole derivatives **3***

To a cooled solution (0 °C) of the appropriate bisindole **7** [16] (0.4 mmol) in ethanol (5 mL) was added DIPEA (2.4 mmol, 6 eq). The solution was stirred for 10 min. after which hydrazine **9** (0.52 mmol, 1.3 eq.) dissolved in acetonitrile (4 mL) was added dropwise to the cooled solution and stirring was continued at room temperature for 2 h (TLC check). After completion of the reaction, all volatiles were removed under reduced pressure and the residue was purified by column chromatography to give the corresponding triazole-bisindole **3**.

The physicochemical data of compounds **3a-b**, including the purity >95% (determined by elemental analysis), are reported in the supporting information and they are in agreement with those reported in literature [20].

5.2 Parasite cultures

The reference strain *L.infantum* MHOM/TN/80/IPT1 (WHO international reference strain) was purchased from ATCC (ATCC® 50134™). Two *L. infantum* strains were isolated from lymph node aspirates of two infected symptomatic dogs, obtained from the veterinary clinic Santa Teresa (Fano, Italy), as previously described [21]. Moreover, one *L. infantum* strain was isolated from a skin biopsy taken during a routine diagnostic process from a patient with CL and previously treated with intralesional injections of glucantime [29]. All *L. infantum* promastigotes were cultured in Evans' Modified Tobie's Medium (EMTM) at 26–28°C. To test bis-indole compounds, the parasites were cultivated in RPMI-PY medium as described previously [30].

5.3 Cell cultures

The human monocytic cell line THP-1 (ECACC 88081201) was cultured in RPMI-1640 medium. The canine macrophage-like cell line DH82 (ATCC® CRL-10389™) and the human hepatocellular carcinoma cell line HepG2 [HEPG2] (ATCC® HB-8065™) were cultured in Eagle's Minimum Essential Medium (EMEM). Human keratinocyte cell line HaCaT (CLS 300493) and Human Primary Fibroblasts (HPF) from healthy subject obtained from upper arm skin biopsies, kindly provided by Dr. Giosuè Annibalini (University of Urbino Carlo Bo), were grown in Dulbecco′s Modified Eagle′s Medium (DMEM). All media were supplemented with 10% (15% for DH82 cells) heat-inactivated Fetal Bovine Serum (FBS), 2 mM L-glutamine, 10 g/l Non-Essential Amino Acid, 1 mM sodium pyruvate, 100 µg/ml streptomycin, 100 U/l penicillin. All cell lines were maintained in a humidified incubator at 37°C and 5% CO_2. All cell culture reagents were purchased from Sigma-Aldrich (St. Louis, MO).

5.4 *L. infantum* promastigotes viability assay

To investigate the bis-indole activity on *L. infantum* strains, the late log/stationary phase promastigotes were resuspended in complete RPMI-PY medium at a density of 2.5 x 10^6 parasites/ml in 96-well plates (100 µl/well). The promastigotes were treated with scalar dilutions 1:2 or 2:3 of the 12 bis-indole compounds (from 20 to 0.31 µM), for 72h at 26 °C. As positive controls, the antileishmanial drugs pentamidine (Sigma–Aldrich) (from 10 to 0.16 µM), non-liposomal amphotericin B (Sigma–Aldrich) (from 1 to 0.0078 µM), and miltefosine (Sigma–Aldrich) (from 20 to 0.31 µM), were included. As negative control, parasites were treated with the vehicle (DMSO). Each condition was carried out in duplicate. To evaluate the promastigotes viability, the CellTiter 96H Aqueous Non-Radioactive Cell Proliferation Assay (Promega), based on the ability of viable cells to convert a soluble tetrazolium salt [3-(4.5-dimethylthiazol-2-yl)-5-(3-carboxymethoxy-phenyl)-2-(4-sulfophenyl)-2H-tetrazolium. MTS] to a formazan product, was conducted. Briefly, 20 µl of MTS/PMS (phenazine methosulfate, Sigma-Aldrich) was added to 100 µl of culture medium and incubated at 26 °C until formazan production. Absorbance was recorded on a Microplate Reader (Benchmark. Bio-Rad) at 492 nm. Results were shown as % of promastigotes growth inhibition compared to control (DMSO). The IC_{50} values was calculated using nonlinear regression curves in GraphPad Prism 8.0 (GraphPad Software, Inc., San Diego, CA). The equation used for data fitting was Y=100/(1+10^((LogIC_{50}-X)*HillSlope)) (hillslope not constrained), where X= log of concentration and Y= Normalized response.

5.5 Cytotoxicity Assay

The cytotoxicity of bis-indole compounds was evaluated in THP-1, DH82, HEPG2, HaCaT and HPF cells. THP-1 cells were resuspended at a density of 5 x 10^6 cells/ml, 100 µl/well were seeded in a 96-well plate and treated with 20 ng/ml phorbol myristic acid (PMA) to induce differentiation into macrophages-like cells for 48h. DH82 cells were seeded in a 96- well plate with a density of 2 x 10^5 cells/well and wait to attach overnight. After cell adhesion to the plate, selected bis-indole compounds were used at concentrations of 2, 10, 20, 80, 200 µM, for 72h at 37°C. Moreover, to test cytotoxicity in actively proliferating cells, DH82, HEPG2, HaCaT, HPF cells were seeded in a 96- well plate with a density of 2 x 10^5 cells/well and wait to attach overnight; afterward, cells were treated with selected bis-indole compounds at concentration of 2, 10, 20 µM, for 24h at 37°C. The negative control, (DMSO), and the antileishmanial drugs pentamidine non-liposomal amphotericin B, and miltefosine, were included in each experiment. Each condition was carried out in duplicate. To evaluate the compound cytotoxicity, the CellTiter 96H Aqueous Non-Radioactive Cell Proliferation Assay (Promega), was conducted as described above. For each compound, the Selectivity Index (SI) was calculated as the ratio between cytotoxicity in THP-1 and DH82 cells (CC_{50}, 72 h) and activity against *L. infantum* promastigotes (IC_{50}, 72 h).

5.6 Anti-amastigote assay on infected cells

The activity of **URB1483** against intracellular amastigotes was evaluated in THP-1- and DH82-infected cells. Briefly, THP-1 cells were seeded in 35 mm dishes with a density of 6 x 10^5 cells/dish and treated with 20 ng/ml phorbol myristic acid (PMA) for 48 h to induce differentiation into macrophage-like cells. After differentiation, cells were infected for 24h with *L. infantum* MHOM/TN/80/IPT1 (or human clinical isolate) promastigotes with a parasite-to-cell ratio of 10:1. Non-internalized promastigotes were then removed and cells were treated with **URB1483** or with the positive control pentamidine at concentrations of 2, 10, and 20 µM, for 72 h. DH82 cells were seeded at a density of 2.5 x 10^5 cells/dish in 35 mm dishes for 24 h. The infection and treatment were performed as described above. Since the vehicle DMSO did not show any toxicity on *L. infantum* promastigotes or on mammalian cells, it was not included in the experiments of infection.

To monitor the infection, cells were washed, formaldehyde/methanol fixed, stained with Hoechst dye and observed with a fluorescence microscope. The infection index (percentage of infected macrophages x the average number of parasites per macrophage) was obtained by counting at least 300 cells for each condition.

5.7 Statistical analysis

The evaluation of IC_{50} in promastigotes and CC_{50} in mammalian cells following bis-indole treatment was performed by non-linear regression analysis and expressed as means and 95% confidence interval. Statistical analyses of infection indexes were performed using one-way ANOVA followed by Tukey's multiple-comparison post hoc test and two-way ANOVA followed by Bonferroni correction for multiple comparisons. All tests were performed using GraphPad Prism version 8 (GraphPad Software, Inc., La Jolla, CA, USA). A p value ≤ 0.05 was considered significant.

5.8 Molecular modelling

Model Building

Differently from human topoisomerase I (hTopo I) which is produced as a monomeric enzyme composed of a single 765 residue polypeptide chain, *L. donovani* topoisomerase I is a heterodimeric protein composed by a large subunit (LdTOP1L) of 635 residues and a small subunit (LdTOP1S) of 262 residues. Despite this different organization, superposition of LdTOP1LS heterodimer (PDB ID 2B9S) [27] bound to DNA on the structure of hTopo I bound to DNA complexed with topotecan (PDB ID 1K4T) [26] reveals that the amino acids shaping the drug-binding cavity are conserved between the two species. Moreover, both human and *L. donovani* forms undertook similar interactions with the 22-bp DNA duplex oligonucleotide present in both the X-ray structures. The key difference between the two PDB complexes resides on the size of the major groove of the DNA double strand, which is slightly larger in human form, where the topotecan is accommodated. Using available structural information here summarized, a 3D model of *L. donovani* topoisomerase I bound to DNA-topotecan complex was built using Maestro 11.6 [31] within the Schrodinger 2018-2 software, following the computational protocol reported by Roy et al. [12]. In brief, after superposing the backbone atoms of the LdTOP1LS heterodimer on the backbone atoms hTopo I protein**,** the DNA double strand of *Leishmania donovani* isoform was replaced with the DNA double strand present in the hTopo I-DNA-topotecan complex. The resulting LdTOP1LS-DNA-topotecan ternary complex was submitted to a protocol of geometry optimization based on energy minimization using OPLS3e force field [32]. After deletion of topotecan from the binding site, the resulting structure was employed to perform docking simulation with Glide 7.9 software [33].

5.9 Ligand docking

Docking studies were performed with Glide included in the *Schrodinger software package* [34] starting from LdTOP1LS-DNA-topotecan ternary model described above. The docking grid was

centered on the position of topotecan ligand. Dimensions of enclosing and bounding boxes were set to 20 and 10 Å on each side, respectively, and van der Waals radii of protein atoms were not scaled during grid generation. The structure of **URB1483** was built in Maestro and then energy-minimized in implicit solvent (water) with OPLS3e force field to an energy gradient of 0.01 kcal/(mol Å). The minimized ligands were docked within the topotecan binding site (see above) using Glide software in Standard Precision mode with default settings. Poses were ranked according to the Gscore value.

5.10 Stability studies of URB1483

An opportune aliquot of a stock solution of **URB1483** in DMSO (10 mM) were added to physiological solution or EMEM or EMTM (**URB1483** concentration = 50 μM) and maintained at 37 °C. At regular time points, aliquots of the described solutions were sampled, two volumes of MeCN were added, and samples were centrifuged (8000 giri/min, 10 min) and analyzed by HPLC-ESI-MS for percentage of remaining compound over incubation time.

Associated Content

Supporting Information

Supplementary materials include: **i**) Physicochemical data of azole-bisindoles **1**-**3**. **ii**) graphical representations of MTS assays with various concentrations of azole-bisindoles and three commercial drugs used as positive controls on four *L. infantum* promastigote strains (IC_{50} reported in table 1, main text). **iii**) Graphical representations of MTS assays with various concentrations of selected azole-bisindoles and three commercial drugs on human (THP-1) and canine (DH82) macrophages for 72 h treatments (CC_{50} reported in table 2, main text). **iv**) Table S1. Cytotoxicity of selected azole-bisindoles after 24 h treatment in canine DH82 macrophages and three different human cell lines (HEPG2, HaCaT and HPF). **v**) Table S2. Two way Anova results of treatment with compound URB1483 and pentamidine in three different infection models **vi**) Figure S6. Superposition of the docking pose of **URB1483** within the *L. donovani* topoisomerase IB on the indolocarbazole inhibitor **SA315F** reported in the ternary adduct involving DNA and human topoisomerase IB. vii) Inhibition studies of the *L donovani* and Human topoisomerase IB activities by **URB1483**. **viii**) References

Author Information

Corresponding Author

Simone Lucarini - *Department of Biomolecular Sciences, University of Urbino Carlo Bo, 61029 Urbino (PU), Italy;* orcid.org/0000-0002-3667-1207; phone: +390722303333; email: simone.lucarini@uniurb.it

Authors

Aurora Diotallevi - *Department of Biomolecular Sciences, University of Urbino Carlo Bo, Urbino (PU), Italy;* orcid.org/0000-0001-5456-1821

Laura Scalvini - *Department of Food and Drug, University of Parma, Parma, Italy;* orcid.org/0000-0003-3610-527X

Gloria Buffi - *Department of Biomolecular Sciences, University of Urbino Carlo Bo, Urbino (PU), Italy;* orcid.org/0000-0001-6288-8787

Yolanda Pérez-Pertejo - *Department of Biomedical Sciences, University of León, León, Spain;* orcid.org/0000-0003-2361-3785

Mauro De Santi - *Department of Biomolecular Sciences, University of Urbino Carlo Bo, Urbino (PU), Italy;* orcid.org/0000-0003-2983-8344

Michele Verboni - *Department of Biomolecular Sciences, University of Urbino Carlo Bo, Urbino (PU), Italy;* orcid.org/0000-0001-5648-521X

Gianfranco Favi - *Department of Biomolecular Sciences, University of Urbino Carlo Bo, Urbino (PU), Italy;* orcid.org/0000-0003-3112-819X

Mauro Magnani - *Department of Biomolecular Sciences, University of Urbino Carlo Bo, Urbino (PU), Italy;* orcid.org/0000-0001-6456-6626

Alessio Lodola - *Department of Food and Drug, University of Parma, Parma, Italy;* orcid.org/0000-0002-8675-1002

Luca Galluzzi - *Department of Biomolecular Sciences, University of Urbino Carlo Bo, Urbino (PU), Italy;* orcid.org/0000-0002-1747-526X

Author Contributions

M.V., G.F. and S.L. synthesized the azole-bisindole derivatives and studied the stability properties of URB1483. A.D., G.B., M.D.S and L.G. designed and performed biological assays on *L. infantum* protozoa, canine and human cell lines. L.S. and A.L. designed and performed docking studies. Y.P.-P. designed and performed DNA relaxation and agarose cleaving assays on human and *L. donovani* topoisomerase IB. M.M. and S.L. funding acquisition, A.L., S.L., and L.G. analyzed data and wrote the original manuscript. All the authors reviewed and edited the manuscript and they have given approval to the final version.

Notes

The authors declare no competing financial interest.

Acknowledgments

We would like to thank Prof. Alessandro Desideri, Dr. Silvia Castelli (University of Rome "Tor Vergata) and Prof. Rafael Balaña-Fouce (University of Leon, Spain) for the inhibition studies on Human and Leishmania Topoisomerase IB and fruitful discussions. We are also grateful to Dr. Giosuè Annibalini (University of Urbino Carlo Bo) for providing HPF cells and Dr. Lucia Vedovi (University of Urbino Carlo Bo) for the extensive editing of English language and style of the manuscript.

This work was partially supported by University of Urbino Carlo Bo, FANOATENEO and FFABR (fund for basic research activities) from MIUR (Italian Ministry of Education, University and Research).

Abbreviations Used

CL, Cutaneous Leishmaniasis; ML Mucosal Leishmaniasis; VL, visceral leishmaniasis; *L.*, Leishmania; DIM, 3,3'-diindolylmethane; DIMs, 3,3'-diindolylmethane derivatives, CPT, camptothecin; DPDIM, 2,2'-diphenyl-3,3'-diindolylmethane; ACN, acetonitrile; DIPEA, *N*,*N*-diisopropylethylamine; Pent, pentamidine; Amph B, non-liposomal amphotericin B; Milt, miltefosine; HPF, Human Primary Fibroblasts; hTopo I, human topoisomerase IB, LdTOP1L, *L. donovani* topoisomerase IB large subunit; LdTOP1S, *L. donovani* topoisomerase IB small subunit; EMEM, eagle's minimum essential medium; DMEM, Dulbecco′s modified eagle′s medium; FBS, Fetal Bovine Serum; RMSD, root mean square deviation.

References

[1] Nagle, A. S., Khare, S., Kumar, A. B., Buchynskyy, F. S. A., Mathison, C. J. N., Chennamaneni, N. K., Pendem, N., Buckner, F. S., Gelb, M. H., and Molteni, V. (2014) Recent developments in drug discovery for leishmaniasis and human african trypanosomiasis. *Chem. Rev.* 114, 11305–11347. DOI: 10.1021/cr500365f.

[2] Ortalli, M., Mistral De Pascali, A., Longo, S., Pascarelli, N., Porcellini, A., Ruggeri, D., Randi, V., Procopio, A., Re, M. C., and Varani, S. (2020) Asymptomatic *Leishmania infantum* infection in blood donors living in an endemic area, northeastern Italy. *Journal of Infection* 80, 116–120. DOI: 10.1016/j.jinf.2019.09.019.

[3] Catta-Preta, C. M. C., and Mottram, J. C. (2018) Drug candidate and target for leishmaniasis. *Nature* 560, 171–172. DOI: 10.1038/d41586-018-05765-y.

[4] Di Muccio, T., Scalone, A., Bruno, A., Marangi, M., Grande, R., Armignacco, O., Gradoni, L., and Gramiccia, M. (2015) Epidemiology of imported leishmaniasis in Italy: implications for a European endemic country. *PLoS ONE*. 10 (6), e0129418. DOI: 10.1371/journal.pone.0129418.

[5] Srivastava, S., Shankar, P., Mishra, J., and Singh, S. (2016) Possibilities and challenges for developing a successful vaccine for leishmaniasis. *Parasites & Vectors* 9, 277. DOI:10.1186/s13071-016-1553-y.

[6] Ponte-Sucre, A., Gamarro, F., Dujardin, J.-C., Barrett, M. P., López-Vélez, R., García-Hernández, R., Pountain, A. W., Mwenechanya, R., and Papadopoulou, B. (2017) Drug resistance and treatment failure in leishmaniasis: A 21st century challenge. *PLoS Negl. Trop. Dis.* 11, e0006052. DOI:10.1371/journal.pntd.0006052.

[7] Bekhit, A. A., El-Agroudy, E., Helmy, A., Ibrahim, T. M., Shavandi, A., and Bekhit, A. E.-D. A. (2018) *Leishmania* treatment and prevention: natural and synthesized drugs. *Eur. J. Med. Chem.* 160, 229–244. DOI: 10.1016/j.ejmech.2018.10.022.

[8] Sangshetti, J. N., Kalam Khan, F. A., Kulkarni, A. A., Aroteb, R., and Patilc, R. H. (2015) Antileishmanial drug discovery: comprehensive review of the last 10 years. *RSC Advances* 5, 32376–32415. DOI: 10.1039/c5ra02669e.

[9] Razzaghi-Asl, N., Sepehri, S., Ebadi, A., Karami, P., Nejatkhah, N., and Johari-Ahar, M. (2019) Insights into the current status of privileged *N*-heterocycles as antileishmanial agents. *Molecular Diversity* 24, 525–569. DOI: 10.1007/s11030-019-09953-4.

[10] Cavalli, A., and Bolognesi, M. L. (2009) Neglected tropical diseases: multi-target-directed ligands in the search for novel lead candidates against *Trypanosoma* and *Leishmania*. *J. Med. Chem.* 52 (23), 7339-7359. DOI: 10.1021/jm9004835.

[11] Roy, A., Das, B. B., Ganguly, A., Dasgupt, S. B., Khalkho, N. V. M., Pal, C., Dey, S., Giri, V. S., Jaisankar, P., Dey, S., Majumder, H. K. (2008) An insight into the mechanism of inhibition of unusual bi-subunit topoisomerase I from *Leishmania donovani* by 3,3'-di-indolylmethane, a novel DNA topoisomerase I poison with a strong binding affinity to the enzyme. *Biochem. J*. 409**,** 611–622. DOI: 10.1042/BJ20071286.

[12] Roy, A., Chowdhury, S., Sengupta, S., Mandal, M., Jaisankar, P., D'Annessa, I., Desideri, A., and Majumder, H. K. (2011) Development of derivatives of 3,3'-diindolylmethane as potent *Leishmania donovani* bi-subunit Topoisomerase IB poisons. *PLoS ONE*. 6 (12), e28493. DOI: 10.1371/journal.pone.0028493.

[13] Bharate, S. B., Bharate, J. B., Khan, S. I., Tekwani, B. L., Jacob, M. R., Mudududdla, R., Yadav, R. R., Singh, B., Sharma, P. R., Maity, S., Singh, B., Khan, I. A., and Vishwakarma, R. A. (2013) Discovery of 3,3'-diindolylmethanes as potent antileishmanial agents. *Eur. J. Med. Chem.* 63, 435-443. DOI: 10.1016/j.ejmech.2013.02.024.

[14] Kalam Khan, F. A., Zaheer, Z., Sangshetti, J. N., Patil, R. H., and Farooqui, M. (2017) Antileishmanial evaluation of clubbed bis(indolyl)-pyridine derivatives: one-pot synthesis, *in vitro* biological evaluations and *in silico* ADME prediction. *Bioorg. & Med. Chem. Let.* 27, 567–573. DOI: 10.1016/j.bmcl.2016.12.018.

[15] Taha, M., Uddin, I., Gollapalli, M., Almandil, N. B., Rahim, F., Farooq, R. K., Nawaz, M., Ibrahim, M., Alqahtani, M. A., Bamarouf, Y. A., and Selvaraj, M. (2019) Synthesis, anti‐leishmanial and molecular docking study of bis‐indole derivatives. *BMC Chemistry* 13, 102. DOI: 10.1186/s13065-019-0617-4.

[16] Mari, M., Tassoni, A., Lucarini, S., Fanelli, M., Piersanti, G., and Spadoni, G. (2014) Brønsted acid catalyzed bisindolization of α-amido acetals: synthesis and anticancer activity of bis(indolyl)ethanamino derivatives. *Eur. J. Org. Chem.* 18, 3822–3830. DOI: 10.1002/ejoc.201402055.

[17] Salucci, S., Burattini, S., Buontempo, F., Orsini, E., Furiassi, L., Mari, M., Lucarini, S., Martelli, A. M., and Falcieri, E. (2018) Marine bisindole alkaloid: a potential apoptotic inducer in human cancer cells. *Eur. J. Histochem.* 62 (2), 2881. DOI: 10.4081/ejh.2018.2881.

[18] Campana, R., Favi, G., Baffone, W., and Lucarini, S. (2019) Marine alkaloid 2, 2-bis(6-bromo-3-indolyl) ethylamine and its synthetic derivatives inhibit microbial biofilms formation and disaggregate developed biofilms. *Microorganisms* 7 (2), 28. DOI: 10.3390/microorganisms7020028.

[19] Campana, R., Sisti, M., Sabatini, L., and Lucarini, S. (2019) Marine bisindole alkaloid 2,2-bis(6-bromo-3-indolyl) ethylamine to control and prevent fungal growth on building material: a potential antifungal agent. *Applied Microbiology and Biotechnology* 103, 5607–5616. DOI: 10.1007/s00253-019-09895-9.

[20] Mantenuto, S., Lucarini, S., De Santi, M., Piersanti, G., Brandi, G., and Favi, G. (2016) One-pot synthesis of biheterocycles based on indole and azole scaffolds using tryptamines and 1,2-diaza-1,3-dienes as building blocks. *Eur. J. Org. Chem.* 19, 3193–3199. DOI: 10.1002/ejoc.201600210.

[21] Galluzzi, L., Diotallevi, A., De Santi, M., Ceccarelli, M., Vitale, F., Brandi, G., and Magnani, M. (2016) *Leishmania infantum* induces mild unfolded protein response in infected macrophages. *PLoS One*. 11 (12), e0168339. DOI: 10.1371/journal.pone.0168339.

[22] Diotallevi, A., De Santi, M., Buffi, G., Ceccarelli, M., Vitale, F., Galluzzi, L., and Magnani, M. (2018) *Leishmania* infection induces MicroRNA hsa-mir-346 in human cell line-derived macrophages. *Front. Microbiol.* 9, 1019. DOI: 10.3389/fmicb.2018.01019.

[23] Diotallevi, A., Buffi, G., Ceccarelli, M., Neitzke-Abreu, H. C., Gnutzmann, L. V., da Costa Lima, M. S., Di Domenico, A., De Santi, M., Magnani, M., and Galluzzi, L. (2020) Real-time PCR to differentiate among *Leishmania* (*Viannia*) subgenus, *Leishmania* (*Leishmania*) *infantum* and *Leishmania* (*Leishmania*) *amazonensis*: application on Brazilian clinical samples. *Acta Tropica* 201, 105178. DOI: 10.1016/j.actatropica.2019.105178.

[24] Ceccarelli, M., Diotallevi, A., Andreoni, F., Vitale, F., Galluzzi, L., and Magnani, M. (2018**)** Exploiting genetic polymorphisms in metabolic enzymes for rapid screening of *Leishmania infantum* genotypes. *Parasites & Vectors* 11, 572. DOI: 10.1186/s13071-018-3143-7.

[25] Mantenuto, S., Ciccolini, C., Lucarini, S., Piersanti, G., Favi, G., and Mantellini F. (2016) Palladium(II)-catalyzed intramolecular oxidative C–H/C–H cross-coupling reaction of C3,N-linked biheterocycles: rapid access to polycyclic nitrogen heterocycles, *Org. Lett.* 19 (3), 608-611. DOI: 10.1021/acs.orglett.6b03775.

[26] Staker, B. L., Hjerrild, K., Feese, M. D., Behnke, C. A., Burgin, A. B., and Stewart, L. (2002) The mechanism of topoisomerase I poisoning by a camptothecin analog. *Proc. Natl. Acad. Sci. USA* 99 (24), 15387–15392. DOI: 10.1073/pnas.242259599.

[27] Davies, D. R., Mushtaq, A., Interthal, H., Champoux, J. J., and Hol, W. G. (2006) The structure of the transition state of the heterodimeric topoisomerase I of *Leishmania donovani* as a vanadate complex with nicked DNA. *J. Mol. Biol*. 357, 1202-1210. DOI: 10.1016/j.jmb.2006.01.022.

[28] Staker, B. L., Feese, M. D., Cushman, M., Pommier, Y., Zembower, D., Stewart, L., and Burgin, A. B. (2005) Structures of three classes of anticancer agents bound to the human topoisomerase I-DNA covalent complex. *J. Med. Chem.* 48, 2336-2345. DOI: 10.1021/jm049146p.

[29] Diotallevi, A., Buffi, G., Corbelli, G., Ceccarelli, M., Ortalli, M., Varani, M., Magnani, M., and Galluzzi, L. (2021) In vitro reduced susceptibility to pentavalent antimonials of a *Leishmania infantum* isolate from a human cutaneous leishmaniasis case in central Italy. *Microorganism* 9 (6), 1147. DOI: 10.3390/microorganisms9061147.

[30] Castelli, G., Galante, A., Lo Verde, V., Migliazzo, A., Reale, S., Lupo, T., Piazza, M., Vitale, F., and Bruno, F. (2014) Evaluation of two modified culture media for *Leishmania infantum* cultivation versus different culture media. *J. Parasitol.* 100, 228–230. DOI: 10.1645/13-253.1.

[31] Schrödinger Release 2018-2: Maestro, Schrödinger, LLC, New York, NY, 2018.

[32] Roos, K., Wu, C., Damm, W., Reboul, M., Stevenson, J. M., Lu, C., Dahlgren, M. K., Mondal, S., Chen, W., Wang, L., Abel, R., Friesner, R. A., and Harder, E. D. (2019) OPLS3e: Extending Force Field Coverage for Drug-Like Small Molecules. *J. Chem. Theory Comput.* 15, 1863-1874. DOI: 10.1021/acs.jctc.8b01026.

[33] Friesner, R. A., Banks, J. L., Murphy, R. B., Halgren, T. A., Klicic, J. J., Mainz, D. T., Repasky, M. P., Knoll, E. H., Shelley, M., Perry, J. K., Shaw, D. E., Francis, P., and Shenkin, P. S. (2004) Glide: a new approach for rapid, accurate docking and scoring. 1. Method and assessment of docking accuracy. *J Med Chem.* 47, 1739-1749. DOI: 10.1021/jm0306430

[34] Schrodinger, LLC, 2019. New York, NY.

Supporting Information

Phenotype screening of an azole-bisindole chemical library identify URB1483 as a new antileishmanial agent devoid of toxicity on human cells

Aurora Diotallevi[a], Laura Scalvini[b], Gloria Buffi[a], Yolanda Pérez-Pertejo[c], Mauro De Santi[a], Michele Verboni[a], Gianfranco Favi[a], Mauro Magnani[a], Alessio Lodola[b], Simone Lucarini [a,*] and Luca Galluzzi[a]

[a] Department of Biomolecular Sciences, University of Urbino Carlo Bo, 61029 Urbino (PU), Italy;

[b] Department of Food and Drug, University of Parma, 43124 Parma, Italy;

[c] Department of Biomedical Sciences, University of León, 24071 León, Spain.

*Correspondence: simone.lucarini@uniurb.it; Tel.: +39 0722 303333

Table of Contents

Physicochemical data of pyrrole-bisindoles 1

4-Ethyl 3-methyl 1-(2,2-bis(6-bromo-1H-indol-3-yl)ethyl)-2-methyl-1H-pyrrole-3,4-dicarboxylate (**1a**)

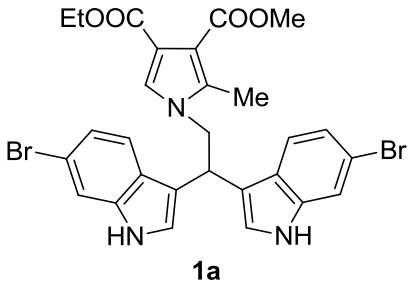

1a

Pyrrole-bisindole **1a** was isolated by column chromatography (ethyl acetate/cyclohexane 25:75) in 70% yield; Yellow solid; mp: 126-128 ° C;

^{1}H NMR (400 MHz, DMSO-d6, 25 ° C): δ = 1.17 (t, *J* = 7.2 Hz, 3 H, OCH_2CH_3), 2.11 (s, 3 H, CH_3), 3.64 (s, 3 H, OCH_3), 4.06 (q, *J* = 7.2 Hz, 2 H, OCH_2CH_3), 4.63 (d, *J* = 8.0 Hz, 2 H, $CHCH_2N$), 4.87 (t, *J* = 8.0 Hz, 1 H, $CHCH_2N$), 6.99 (dd, J_1 = 8.8 Hz, J_2 = 1.6 Hz, 2 H, Ar-H), 7.16 (s, 1 H, Ar-H), 7.37-7.42 (m, 4 H, Ar-H), 7.49 (d, *J* = 1.6 Hz, 2 H, Ar-H), 11.06 (s, 2 H, NH);

^{13}C NMR (100 MHz, DMSO-d6, 25 ° C): δ = 10.7, 14.6, 35.2, 50.9, 51.4, 59.7, 100.0, 114.0, 114.2, 114.4, 115.4, 121.0, 121.6, 124.4, 125.8, 127.5, 135.3, 137.6, 163.7, 165.6;

MS (EI) *m/z* (%) = 627 (M+) (3), 405 (31), 403 (100), 401 (38);

Anal. calcd. for $C_{28}H_{25}Br_2N_3O_4$ (627.32): C 53.61, H 4.02, N 6.70; found: C 53.77, H 3.95, N 6.82.

3-Ethyl 4-methyl 1-(2,2-bis(1-methyl-1H-indol-3-yl)ethyl)-2-methyl-1H-pyrrole-3,4-dicarboxylate (**1b, URB1483**)

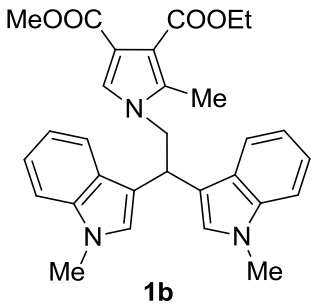

1b

Pyrrole-bisindole **1b** was isolated by column chromatography (ethyl acetate/cyclohexane 35:65) in 37% yield;

pale yellow solid; mp: 121-123 ° C;

^{1}H NMR (400 MHz, DMSO-d6, 25 ° C): δ = 1.19 (t, *J* = 7.2 Hz, 3 H, OCH_2CH_3), 2.19 (s, 3 H, CH_3), 3.60 (s, 3 H, OCH_3), 3.72 (s, 6 H, NCH_3), 4.10 (q, *J* = 7.2 Hz, 2 H, OCH_2CH_3), 4.61 (d, *J* = 7.6 Hz, 2 H, $CHCH_2N$), 4.91 (t, *J* = 7.6 Hz, 1 H, $CHCH_2N$), 6.94 (t, *J* = 7.6 Hz, 2 H, Ar-H), 7.09 (t, *J* = 7.6 Hz, 2 H, Ar-H), 7.22 (s, 1 H, Ar-H), 7.33 (s, 2 H, Ar-H), 7.35 (d, *J* = 8.0 Hz, 2 H, Ar-H), 7.55 (d, *J* = 8.0 Hz, 2 H, Ar-H);

^{13}C NMR (100 MHz, DMSO-d6, 25 ° C): δ = 10.8, 14.5, 32.8, 35.1, 51.3, 59.9, 110.1, 112.5, 113.8, 114.7, 118.9, 119.4, 121.6, 127.2, 127.3, 127.6, 135.3, 137.2, 164.2, 165.0;

MS (EI) *m/z* (%) = 497 (M+) (2), 366 (11), 273 (100);

Anal. calcd. for $C_{30}H_{31}N_3O_4$ (497.58): C 72.41, H 6.28, N 8.44; found: C 72.57, H 6.35, N 8.56.

4-Ethyl 3-methyl 1-(2,2-bis(1,5-dimethyl-1H-indol-3-yl)ethyl)-2-methyl-1H-pyrrole-3,4-dicarboxylate (**1c**)

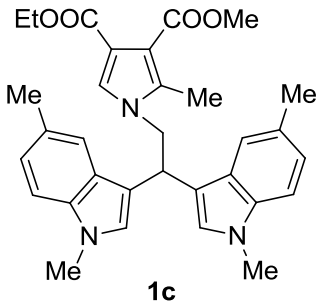

1c

Pyrrole-bisindole **1c** was isolated by column chromatography (ethyl acetate/cyclohexane 30:70) in 40% yield; White solid; mp: 138-140 ° C;

^{1}H NMR (400 MHz, DMSO-d6, 25 ° C): δ = 1.17 (t, *J* = 7.2 Hz, 3 H, OCH_2CH_3), 2.14 (s, 3 H, CH_3), 2.32 (s, 6 H, CH_3), 3.63 (s, 3 H, OCH_3), 3.69 (s, 6 H, NCH_3), 4.07 (q, *J* = 7.2 Hz, 2 H, OCH_2CH_3), 4.52 (d, *J* = 7.6 Hz, 2 H, $CHCH_2N$), 4.82 (t, *J* = 7.6 Hz, 1 H, $CHCH_2N$), 6.92 (dd, J_1 = 8.4 Hz, J_2 = 1.2 Hz, 2 H, Ar-H), 7.17−7.26 (m, 7 H, Ar-H);

^{13}C NMR (100 MHz, DMSO-d6, 25 ° C): δ = 10.8, 14.6, 21.6, 35.0, 32.8, 51.3, 51.8, 59.6, 109.7,

112.3, 114.1, 114.3, 118.9, 123.2, 127.3, 127.4, 127.5, 127.7, 135.4, 135.7, 163.8, 165.6;

MS (EI) *m/z* (%) = 525 (M+) (20), 380 (79), 301 (100);

Anal. calcd. for $C_{32}H_{35}N_3O_4$ (525.64): C 73.12, H 6.71, N 7.99; found: C 72.89, H 6.59, N 8.07.

3-ethyl 4-methyl 1-(2,2-bis(6-bromo-1-methyl-1H-indol-3-yl)ethyl)-2-methyl-1H-pyrrole-3,4-dicarboxylate (**1d**)

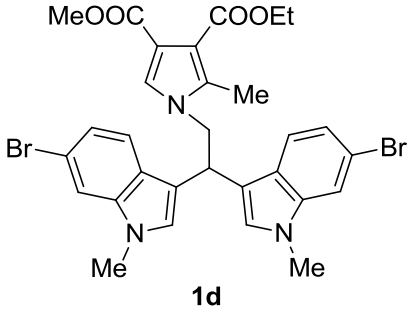

1d

Pyrrole-bisindole **1d** was isolated by column chromatography (ethyl acetate/cyclohexane 40:60) in 31% yield; Pale yellow solid; mp: 93-95 ° C;

^{1}H NMR (400 MHz, DMSO-d6, 25 ° C): δ = 1.19 (t, *J* = 7.2 Hz, 3 H, OCH_2CH_3), 2.13 (s, 3 H, CH_3), 3.62 (s, 3 H, OCH_3), 3.72 (s, 6 H, NCH_3), 4.10 (q, *J* = 7.2 Hz, 2 H, OCH_2CH_3), 4.56 (d, *J* = 8.0 Hz, 2 H, $CHCH_2N$), 4.89 (t, *J* = 8.0 Hz, 1 H, $CHCH_2N$), 7.04 (dd, J_1 = 8.8 Hz, J_2 = 1.6 Hz, 2 H, Ar-H), 7.24 (s, 1 H, Ar-H), 7.35 (s, 2 H, Ar-H), 7.43 (d, *J* = 8.8 Hz, 2 H, Ar-H), 7.63 (d, *J* = 1.6 Hz, 2 H, Ar-H);

^{13}C NMR (100 MHz, DMSO-d6, 25 ° C): δ = 10.8, 14.5, 33.0, 34.7, 51.1, 51.3, 59.9, 112.5, 113.0,
113.8, 114.6, 114.9, 121.1, 121.7, 126.1, 127.3, 128.6, 135.3, 138.0, 164.2, 165.0;
MS (EI) *m/z* (%) = 655 (M+) (3), 433 (31), 431 (100), 429 (38);
Anal. calcd. for $C_{30}H_{29}Br_2N_3O_4$ (655.38): C 54.98, H 4.46, N 6.41; found: C 55.12, H 4.41, N 6.32.

Physicochemical data of imidazole-bisindoles 2

Methyl 1-(2,2-di(1H-indol-3-yl)ethyl)-4-methyl-1H-imidazole-5-carboxylate (**2a**)

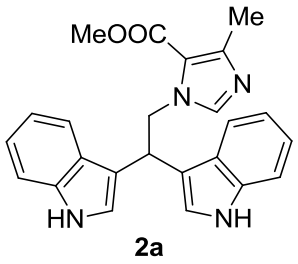

2a

Imidazole-bisindole **2a** was isolated by column chromatography (ethyl acetate/cyclohexane 70:30) in 75% yield;

Pale yellow solid; mp: 224-226 ° C;

^{1}H NMR (400 MHz, DMSO-d6, 25 ° C): δ = 2.22 (s, 3 H, CH_3), 3.80 (s, 3 H, OCH_3), 4.82-4.97 (m, 3 H, $CHCH_2N$), 6.87 (t, *J* = 7.6 Hz, 2 H, Ar-H), 6.99 (t, *J* = 7.6 Hz, 2 H, Ar-H), 7.20 (s, 1 H, Ar-H), 7.24 (s, 2 H, Ar-H), 7.28 (d, *J* = 8.0 Hz, 2 H, Ar-H), 7.53 (d, *J* = 8.0 Hz, 2 H, Ar-H), 10.83 (s, 2 H, NH);

^{13}C NMR (100 MHz, DMSO-d6, 25 ° C): δ = 15.6, 35.1, 50.6, 51.2, 111.3, 114.8, 117.4, 118.1, 118.7, 120.8, 122.7, 126.4, 136.3, 141.7, 146.8, 161.0;

MS (EI) *m/z* (%) = 398 (M+) (100);

Anal. calcd. for $C_{24}H_{22}N_4O_2$ (398.46): C 72.34, H 5.57, N 14.06; found: C 72.45, H 5.62, N 13.93.

Methyl 1-(2,2-bis(5-methyl-1H-indol-3-yl)ethyl)-4-methyl-1Himidazole-5-carboxylate (**2b**)

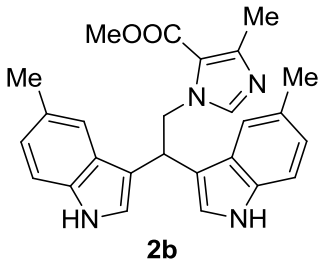

2b

Imidazole-bisindole **2b** was isolated by column chromatography (ethyl acetate/cyclohexane 70:30) in 69% yield;

Pale yellow solid; mp: 207-209 ° C;

^{1}H NMR (400 MHz, DMSO-d6, 25 ° C): δ = 2.27 (s, 3 H, CH_3), 2.32 (s, 6 H, CH_3), 3.84 (s, 3 H, OCH_3), 4.75-4.97 (m, 3 H, $CHCH_2N$), 6.85 (d, *J* = 8.0 Hz, 2 H, Ar-H), 7.17-7.23 (m, 5 H, Ar-H), 7.31 (s, 2 H, Ar-H), 10.70 (s, 2 H, NH);

^{13}C NMR (100 MHz, DMSO-d6, 25 ° C): δ = 16.1, 21.8, 35.6, 51.2, 51.7, 111.6, 114.8, 118.0, 118.8, 122.9, 123.3, 127.0, 127.2, 135.2, 142.2, 147.4, 161.5;

MS (EI) *m/z* (%) = 426 (M+) (100);

Anal. calcd. for $C_{26}H_{26}N_4O_2$ (426.51): C 73.22, H 6.14, N 13.14; found: C 73.08, H 6.08, N 13.26.

Methyl 1-(2,2-bis(5-methyl-1H-indol-3-yl)ethyl)-4-ethyl-1Himidazole-5-carboxylate (**2c**)

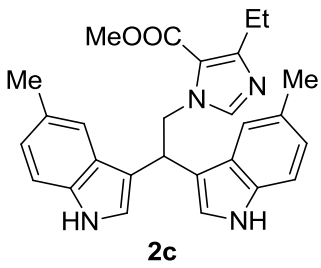

2c

Imidazole-bisindole **2c** was isolated by column chromatography (ethyl acetate/cyclohexane 70:30) in 85% yield;

Pale Yellow solid; mp: 161-163 ° C;

^{1}H NMR (400 MHz, DMSO-d6, 25 ° C): δ = 1.05 (t, *J* = 7.6 Hz, 3 H, CH_2CH_3), 2.31 (s, 6 H, CH_3), 2.68 (q, *J* = 7.6 Hz, 2 H, CH_2CH_3), 3.82 (s, 3 H, OCH_3), 4.77-4.94 (m, 3 H, $CHCH_2N$), 6.85 (d, *J* = 8.4 Hz, 2 H, Ar-H), 7.15-7.24 (m, 5 H, Ar-H), 7.27 (s, 2 H, Ar-H), 10.70 (s, 2 H, NH);

^{13}C NMR (100 MHz, DMSO-d6, 25 ° C): δ = 14.0, 21.8, 22.6, 35.5, 51.4, 51.7, 111.5, 114.9, 117.2, 118.7, 122.9, 123.3, 126.9, 127.2, 135.1, 142.3, 152.9, 161.5;

MS (EI) *m/z* (%) = 440 (M+) (8), 273 (100);

Anal. calcd. for $C_{27}H_{28}N_4O_2$ (440.54): C 73.61, H 6.41, N 12.72; found: C 73.76, H 6.49, N 12.60.

Methyl 1-(2,2-bis(6-bromo-1H-indol-3-yl)ethyl)-4-methyl-1Himidazole-5-carboxylate (**2d**)

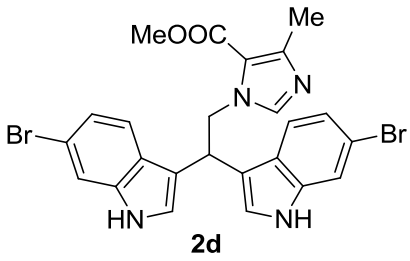

2d

Imidazole-bisindole **2d** was isolated by column chromatography (ethyl acetate/cyclohexane 80:20) in 72% yield; Brown solid; mp: 197-199 ° C;

^{1}H NMR (400 MHz, DMSO-d6, 25 ° C): δ = 2.26 (s, 3 H, CH_3), 3.80 (s, 3 H, OCH_3), 4.91-4.96 (m, 3 H, $CHCH_2N$), 7.01 (dd, J_1 = 8.4 Hz, J_2 = 1.6 Hz, 2 H, Ar-H), 7.22 (s, 1 H, Ar-H), 7.30 (d, *J* = 2.0 Hz, 2 H, Ar-H), 7.40 (d, *J* = 8.4 Hz, 2 H, Ar-H), 7.50 (d, *J* = 1.6 Hz, 2 H, Ar-H), 11.04 (s, 2 H, NH);

^{13}C NMR (100 MHz, DMSO-d6, 25 ° C): δ = 16.1, 35.4, 51.0, 51.8, 114.2, 114.5, 115.4, 117.9, 120.8, 121.6, 124.4, 125.9, 137.6, 142.2, 147.4, 161.5;

MS (EI) *m/z* (%) = 556 (M+) (100), 401 (32), 403 (100), 405 (39);

Anal. calcd. for $C_{24}H_{20}Br_2N_4O_2$ (556.25): C 51.82, H 3.62, N 10.07; found: C 51.95, H 3.66, N 9.94.

Methyl 1-[2,2-bis(1-methyl-1H-indol-3-yl)ethyl]-4-methyl-1Himidazole-5-carboxylate (**2e**)

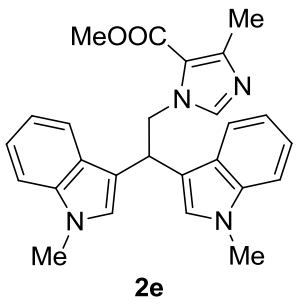

2e

Imidazole-bisindole **2e** was isolated by column chromatography (ethyl acetate/cyclohexane 70:30) in 72% yield; White solid; mp: 168-170 ° C;

^{1}H NMR (400 MHz, DMSO-d6, 25 ° C): δ = 2.25 (s, 3 H), 3.72 (s, 6 H), 3.82 (s, 3 H), 4.92 (m, 3 H), 6.95 (dt, J_1 = 8.0 Hz, J_2 = 0.8 Hz, 2 H), 7.10 (dt, J_1 = 8.0 Hz, J_2 = 0.8 Hz, 2 H), 7.26 (s, 2 H), 7.33 (s, 1 H), 7.35 (d, *J* = 8.0 Hz, 2 H), 7.56 (d, *J* = 8.0 Hz, 2 H);

^{13}C NMR (100 MHz, DMSO-d6, 25 ° C): δ = 16.1, 32.8, 35.2, 51.3, 51.8, 110.1, 114.6, 118.0, 118.9, 119.3, 121.5, 127.3, 127.6, 137.1, 142.3, 147.3, 161.5;

MS (EI) *m/z* (%) = 426 (11) (M+), 273 (100);

Anal. calcd. for $C_{26}H_{26}N_4O_2$ (426.51): C 73.22, H 6.14, N 13.14; found: C 73.36, H 6.06, N 13.25.

Ethyl 1-[2,2-bis(1-methyl-5-nitro-1H-indol-3-yl)ethyl]-4-methyl-1H-imidazole-5-carboxylate (**2f**)

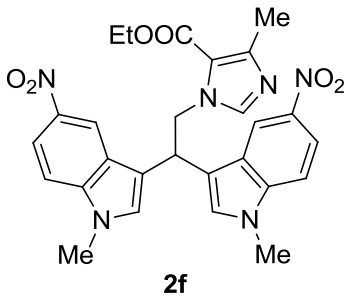

2f

Imidazole-bisindole **2f** was isolated by crystallization (ethyl acetate/cyclohexane) from crude in 54% yield (114.6 mg); Yellow solid; mp: 227-229° C;

^{1}H NMR (400 MHz, DMSO-d6, 25 ° C): δ = 1.27 (t, *J* = 7.2 Hz, 3 H), 2.23 (t, 3 H), 3.85 (s, 6 H), 4.28 (q, *J* = 7.2 Hz, 2 H), 4.89 (d, *J* = 7.6 Hz, 2 H), 5.17 (t, *J* = 7.2 Hz, 1 H), 7.37 (s, 1 H), 7.57-7.62 (m, 4 H), 8.00 (dd, J_1 = 8.8 Hz, J_2 = 2.0 Hz, 2 H), 8.40 (d, *J* = 2.0 Hz, 2 H);

^{13}C NMR (100 MHz, DMSO-d6, 25 ° C): δ = 14.5, 16.0, 33.5, 34.4, 51.9, 60.4, 110.8, 116.3, 117.0, 117.3, 118.3, 126.4, 131.7, 139.9, 140.9, 142.2, 147.6, 161.1;

MS (EI) *m/z* (%) = 530 (100) (M+);

Anal. calcd. for C27H26N6O6 (530.53): C 61.13, H 4.94, N 15.84; found: C 61.01, H 5.02, N 15.73.

Physicochemical data of triazole-bisindoles 3

3,3'-(2-(4-Methyl-1H-1,2,3-triazol-1-yl)ethane-1,1-diyl)bis(1H-indole) (**3a**)

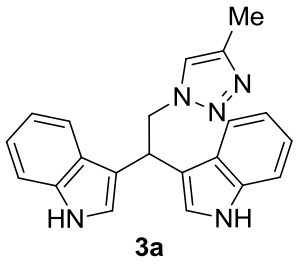

3a

Triazole-bisindole **3a** was isolated by column chromatography (ethyl acetate/cyclohexane 60:40) in 100% yield;

Pale yellow solid; mp: 224-226 ° C;

^{1}H NMR (400 MHz, DMSO-d6, 25 ° C): δ = 2.12 (s, 3 H, CH_3), 5.04-5.16 (m, 3 H, C*H*$_2$C*H*N), 6.91 (t, *J* = 7.6 Hz, 2 H, Ar-H), 7.03 (t, *J* = 7.6 Hz, 2 H, Ar-H), 7.31-7.35 (m, 4 H, Ar-H), 7.54 (d, *J* = 8.0 Hz, 2 H, Ar-H), 7.68 (s, 1 H, Ar-H), 10.86 (s, 2 H, NH);

^{13}C NMR (100 MHz, DMSO-d6, 25 ° C): δ = 10.9, 35.5, 53.9, 111.9, 115.3, 118.7, 119.2, 121.4, 122.8, 123.2, 126.8, 136.8, 141.7;

MS (EI) *m/z* (%) = 341 (M+) (4), 109 (100);

Anal. calcd. for $C_{21}H_{19}N_5$ (341.41): C 73.88, H 5.61, N 20.51; found: C 73.75, H 5.72, N 20.39.

3,3'-(2-(4-Methyl-1H-1,2,3-triazol-1-yl)ethane-1,1-diyl)bis(1-methyl-1Hindole) (**3b**)

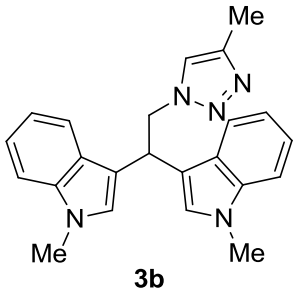

3b

Triazole-bisindole **3b** was isolated by column chromatography (ethyl acetate/cyclohexane 55:45) in 90% yield; White solid; mp: 168-170 ° C;

^{1}H NMR (400 MHz, DMSO-d6, 25 ° C): δ = 2.11 (d, *J* = 0.4 Hz, 3 H, CH_3), 3.71 (s, 6 H, NCH_3), 4.97-5.15 (m, 3 H, C*H*$_2$C*H*N), 6.96 (t, *J* = 7.6 Hz, 2 H, Ar-H), 7.10 (t, *J* = 7.6 Hz, 2 H, Ar-H), 7.30 (s, 2 H, Ar-H), 7.35 (d, *J* = 8.0 Hz, 2 H, Ar-H), 7.55 (d, *J* = 8.0 Hz, 2 H, Ar-H), 7.75 (q, *J* = 0.4 Hz, 1 H, Ar-H);

^{13}C NMR (100 MHz, DMSO-d6, 25 ° C): δ = 10.9, 32.8, 35.0, 54.0, 110.1, 114.6, 118.9, 119.2, 121.6, 122.9, 127.1, 127.4, 137.2, 141.8;

MS (EI) *m/z* (%) = 369 (M+) (7), 273 (72), 109 (100);

Anal. calcd. for C23H23N5 (369.46): C 74.77, H 6.27, N 18.96; found: C 74.91, H 6.19, N 19.08.

Figure S1a. MTS assay of pyrrole-bisindole derivatives **1** on *L. infantum* MHOM/TN/80/IPT1 promastigotes

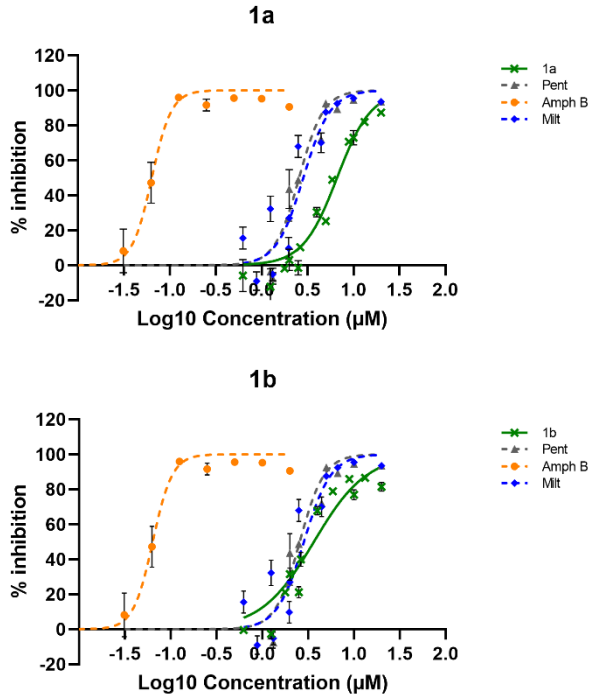

Figure S1b. MTS assay of pyrrole-bisindole derivatives **1** on *L. infantum* canine clinical isolate 1 promastigotes

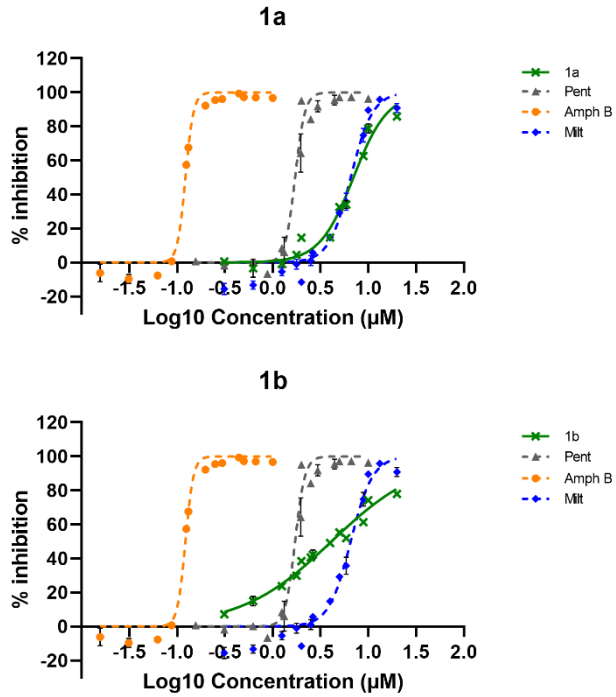

Figure S1c. MTS assay of pyrrole-bisindole derivatives **1** on *L. infantum* canine clinical isolate 2 promastigotes

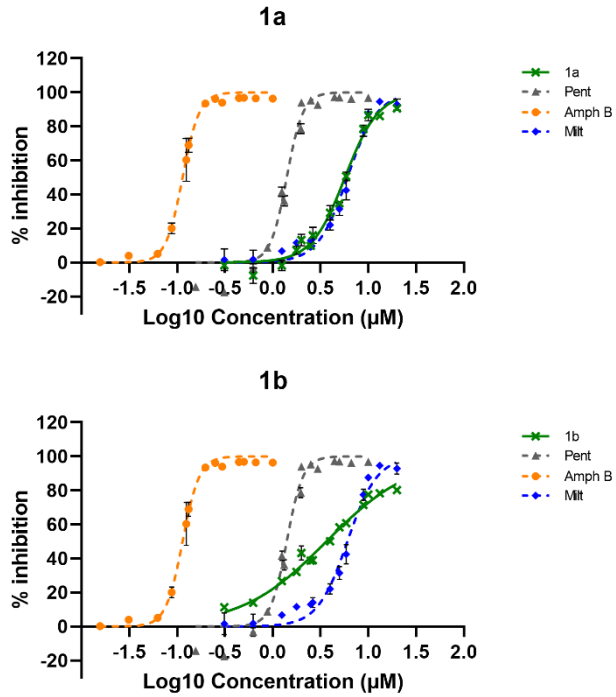

Figure S1d. MTS assay of pyrrole-bisindole derivatives **1** on *L. infantum* human clinical isolate promastigotes

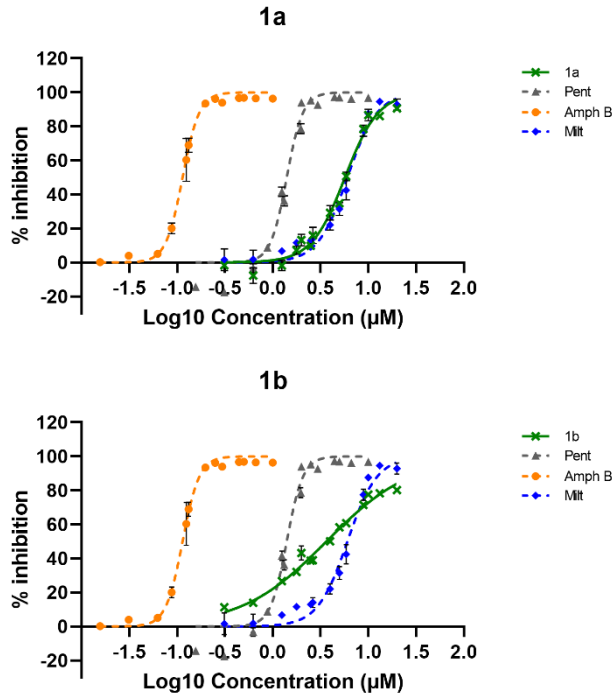

Figure S2a. MTS assay of imidazole-bisindole derivatives **2** on *L. infantum* MHOM/TN/80/IPT1 promastigotes

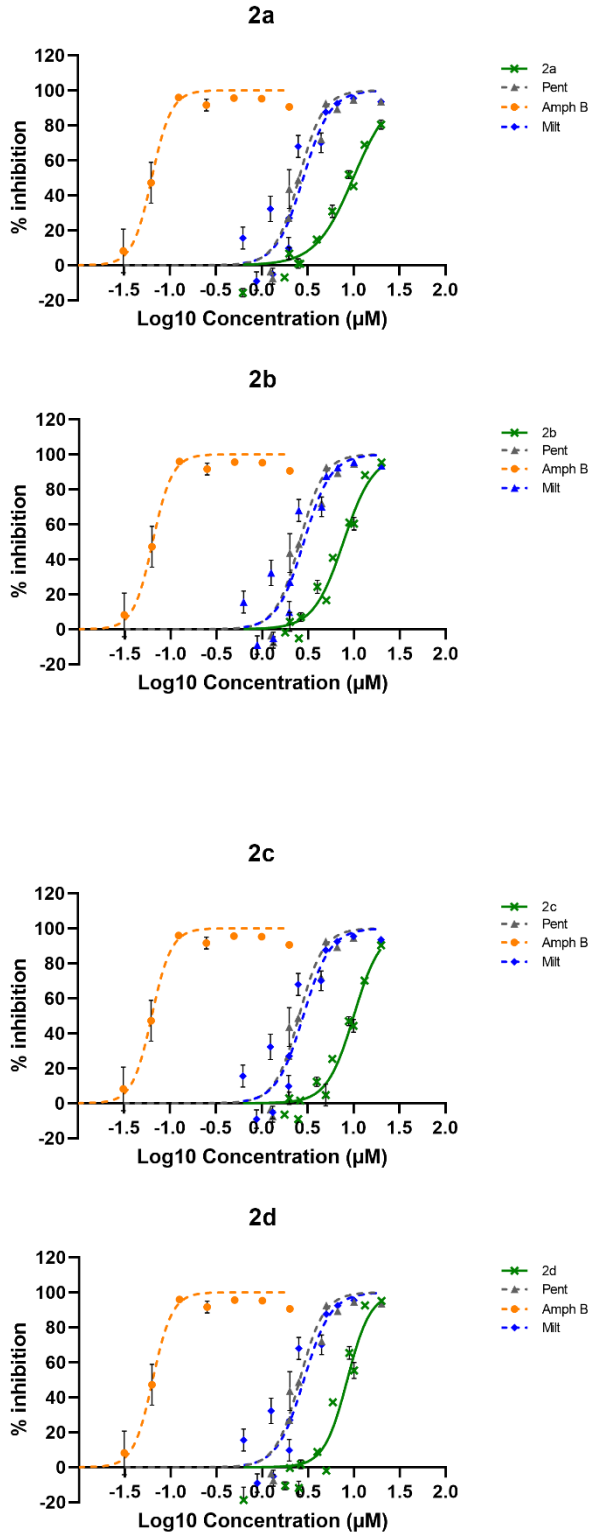

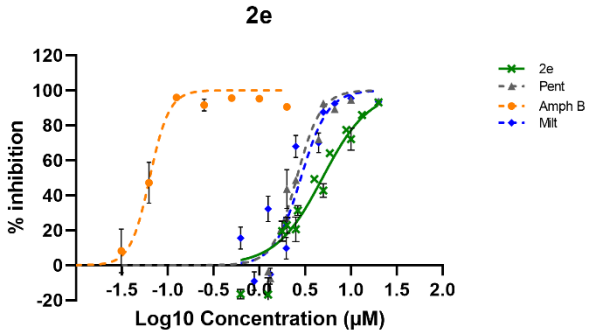
2e
% inhibition
120
100
80
60
40
20
0
-20
-1.5
-1.0
-0.5
0.0
0.5
1.0
1.5
2.0
Log10 Concentration (μM)
2e
Pent
Amph B
Milt

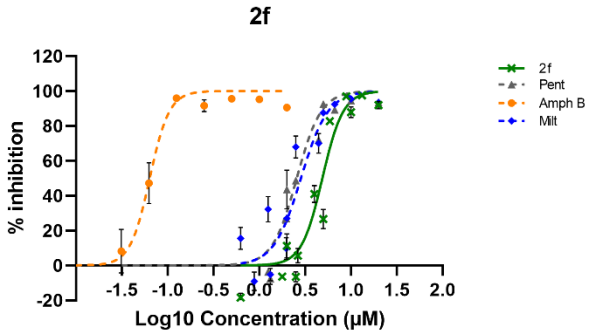
2f
% inhibition
120
100
80
60
40
20
0
-20
-1.5
-1.0
-0.5
0.0
0.5
1.0
1.5
2.0
Log10 Concentration (μM)
2f
Pent
Amph B
Milt

Figure S2b. MTS assay of imidazole-bisindole derivatives **2** on *L. infantum* canine clinical isolate 1 promastigotes

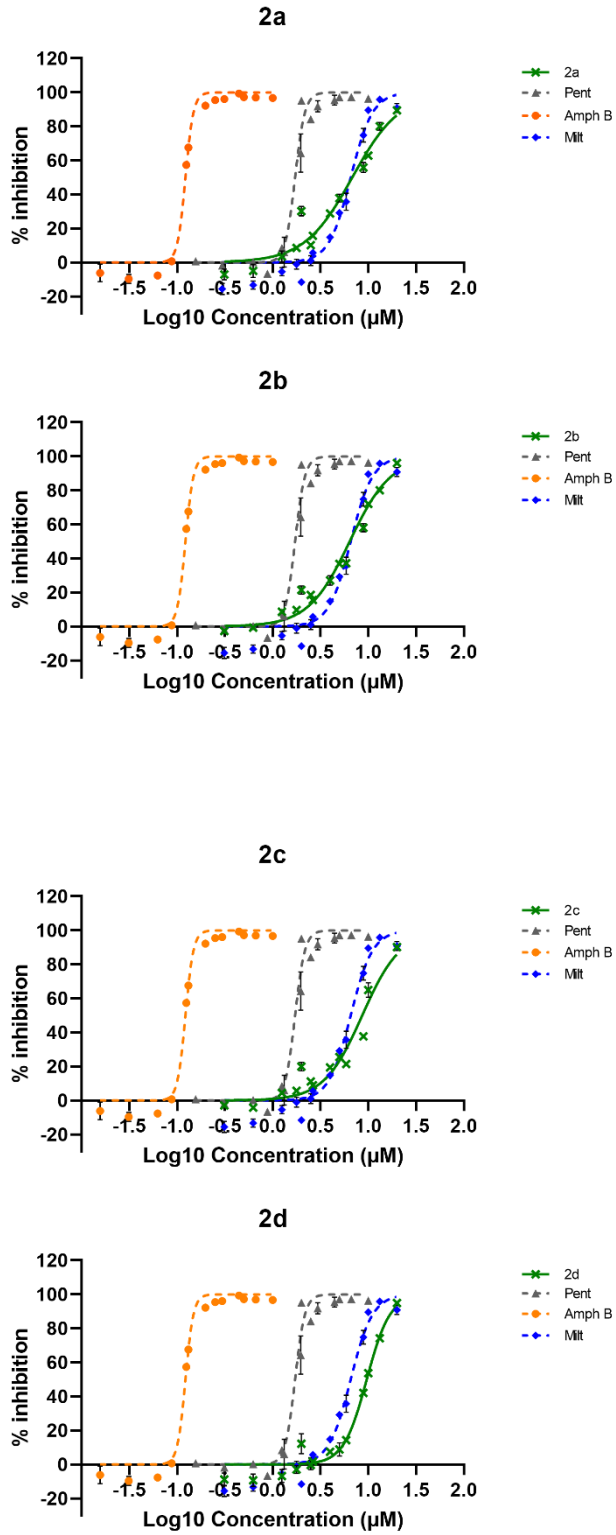

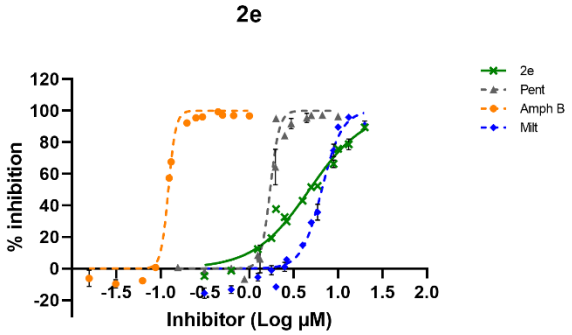
2e
% inhibition
Inhibitor (Log µM)
2e
Pent
Amph B
Milt

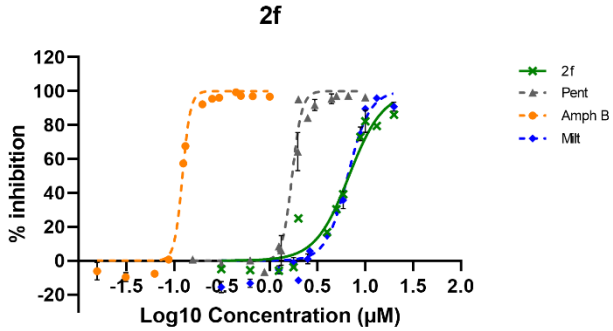
2f
% inhibition
Log10 Concentration (µM)
2f
Pent
Amph B
Milt

Figure S2c. MTS assay of imidazole-bisindole derivatives **2** on *L. infantum* canine clinical isolate 2 promastigotes

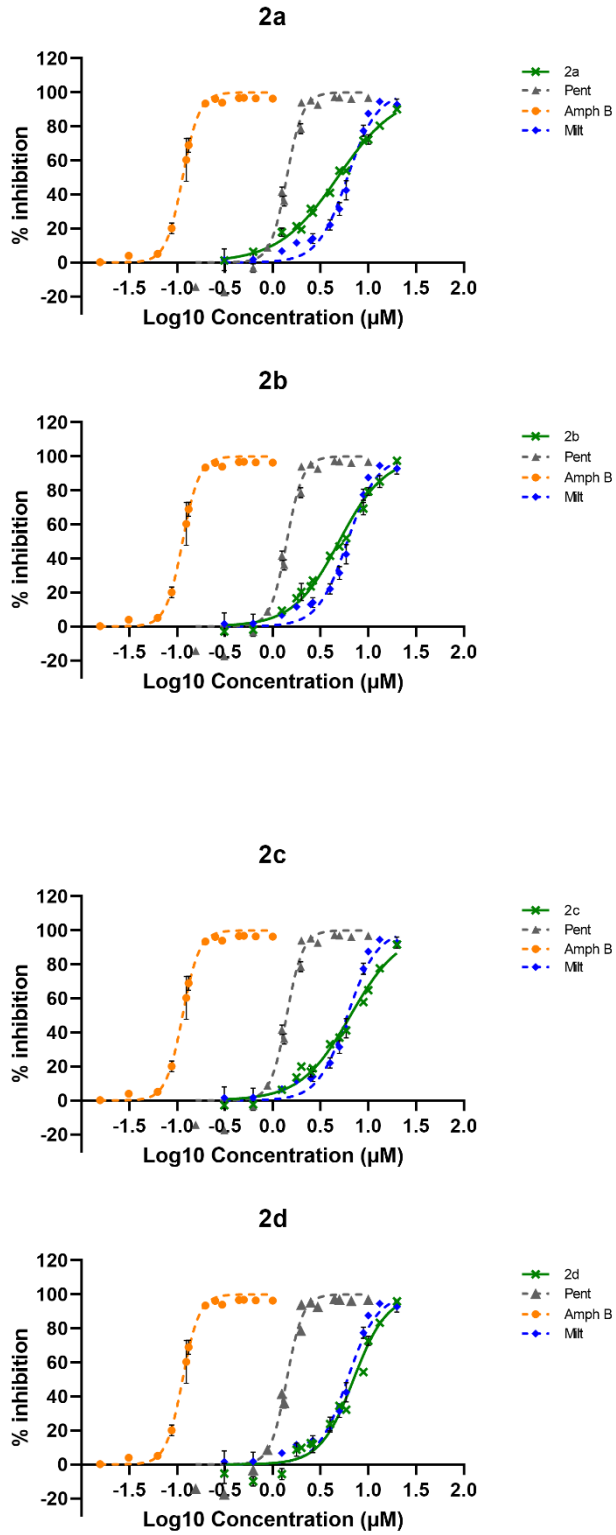

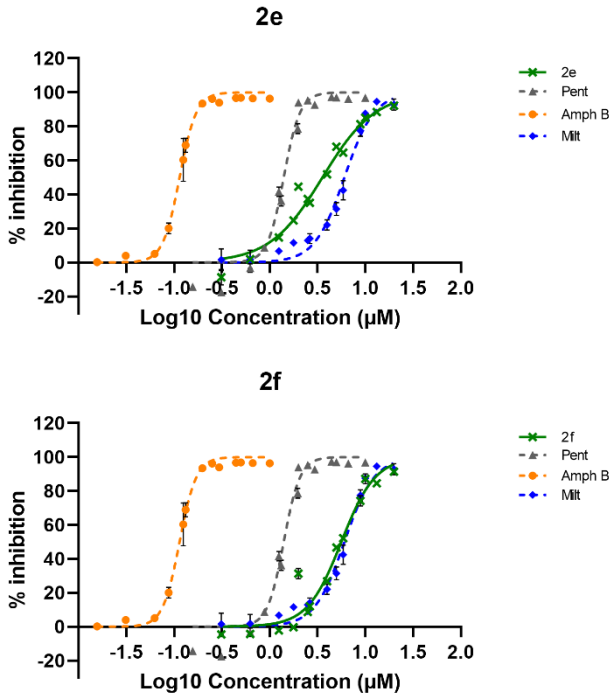
2e
% inhibition
120
100
80
60
40
20
0
-20
-1.5
-1.0
-0.5
0.0
0.5
1.0
1.5
2.0
Log10 Concentration (μM)
2e
Pent
Amph B
Milt

2f
% inhibition
120
100
80
60
40
20
0
-20
-1.5
-1.0
-0.5
0.0
0.5
1.0
1.5
2.0
Log10 Concentration (μM)
2f
Pent
Amph B
Milt

Figure S2d. MTS assay of imidazole-bisindole derivatives **2** on *L. infantum* human clinical isolate promastigotes

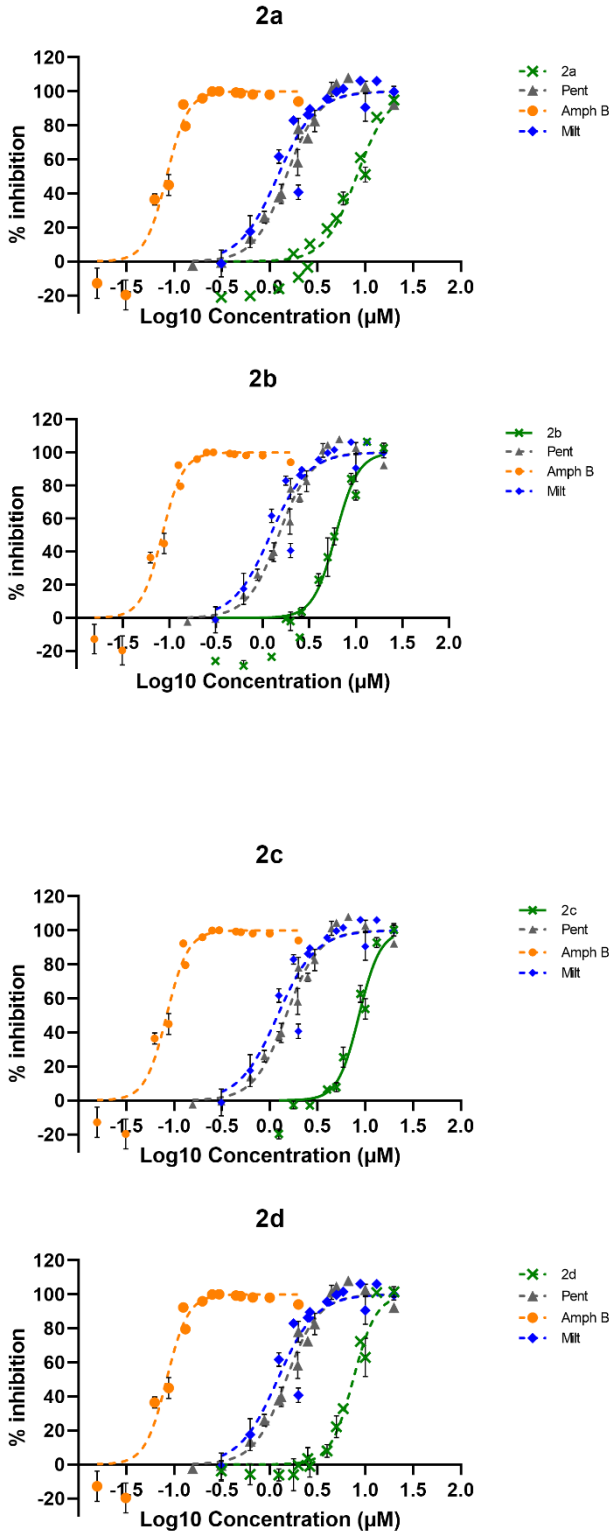

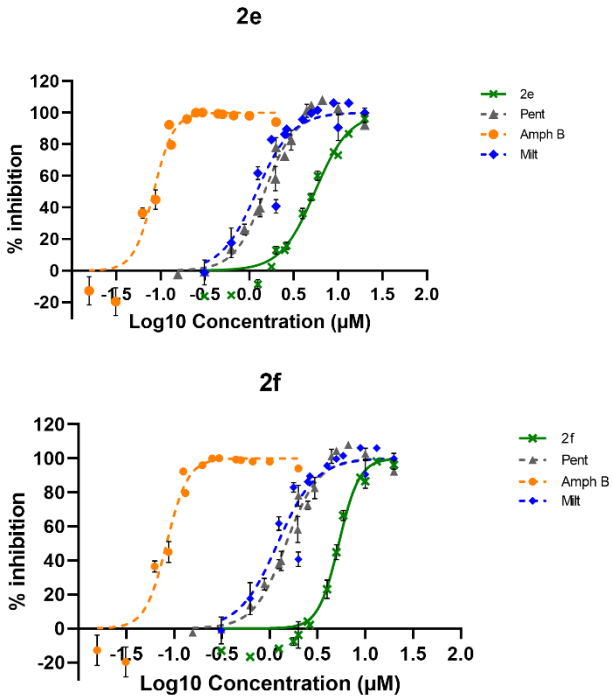
2e
% inhibition
Log10 Concentration (μM)
2e
Pent
Amph B
Milt
2f
% inhibition
Log10 Concentration (μM)
2f
Pent
Amph B
Milt

Figure S3a. MTS assay of triazole-bisindole derivative **3b** on *L. infantum* MHOM/TN/80/IPT1 promastigotes

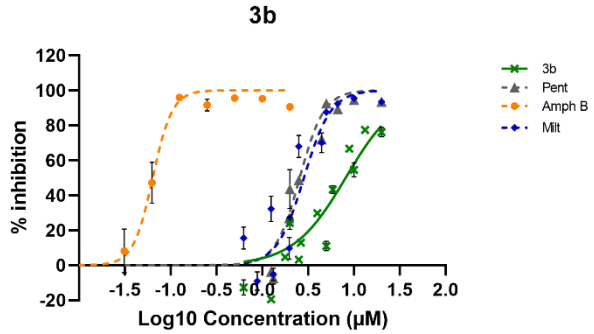

Figure S3b. MTS assay of triazole-bisindole **3b** on *L. infantum* canine clinical isolate 1 promastigotes

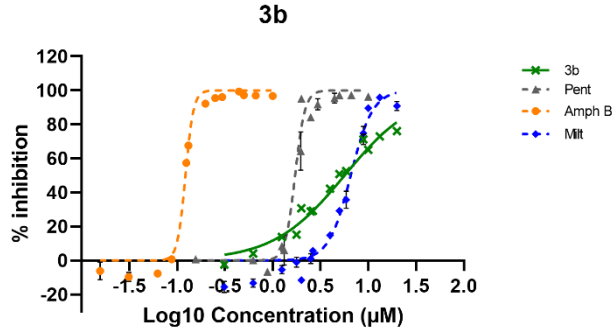

Figure S3c. MTS assay of triazole-bisindole **3b** on *L. infantum* canine clinical isolate 2 promastigotes

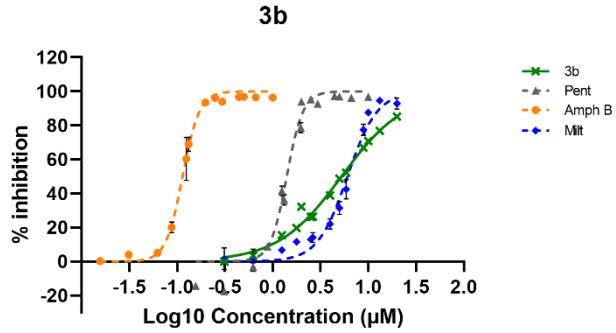

Figure S3d. MTS assay of triazole-bisindole **3b** on *L. infantum* human clinical isolate promastigotes

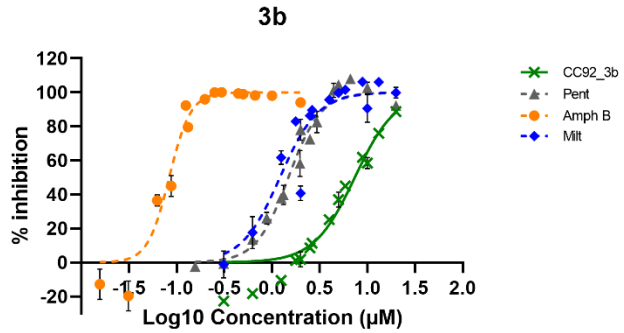

Figure S4a. Toxicity test by MTS assay with selected azole-bisindoles **1** and **3b** on THP-1 cells

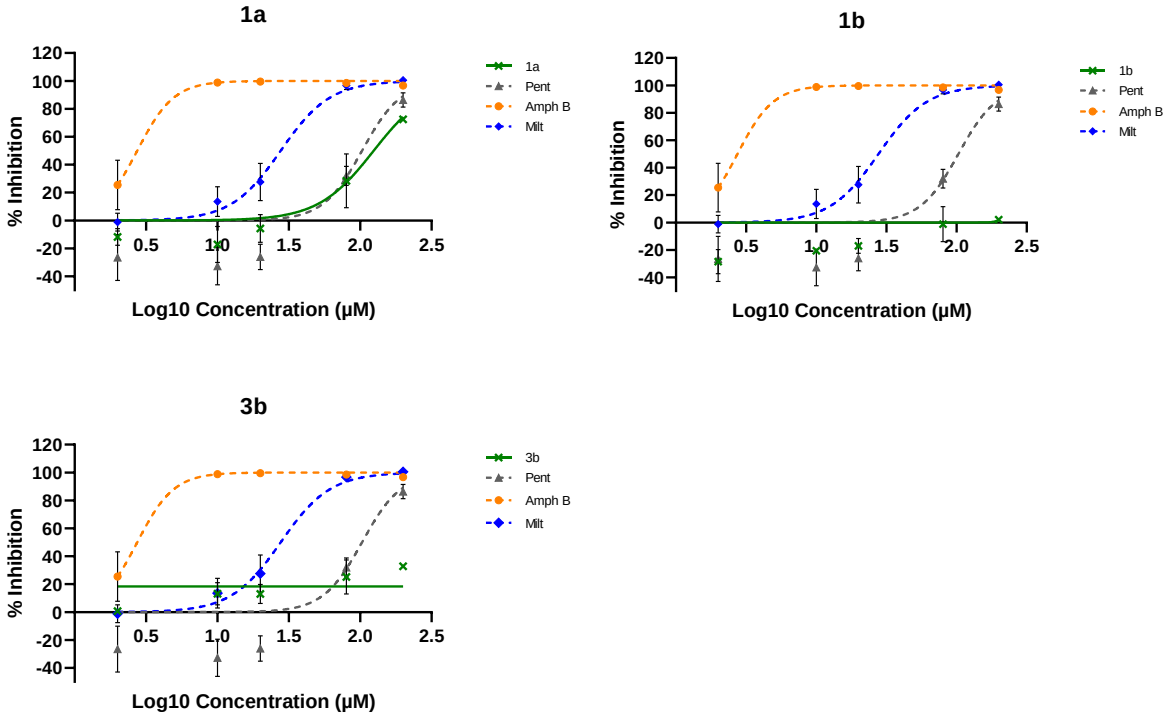

Figure S4b. Toxicity test by MTS assay with imidazole-bisindole derivatives **2** on THP-1 cells

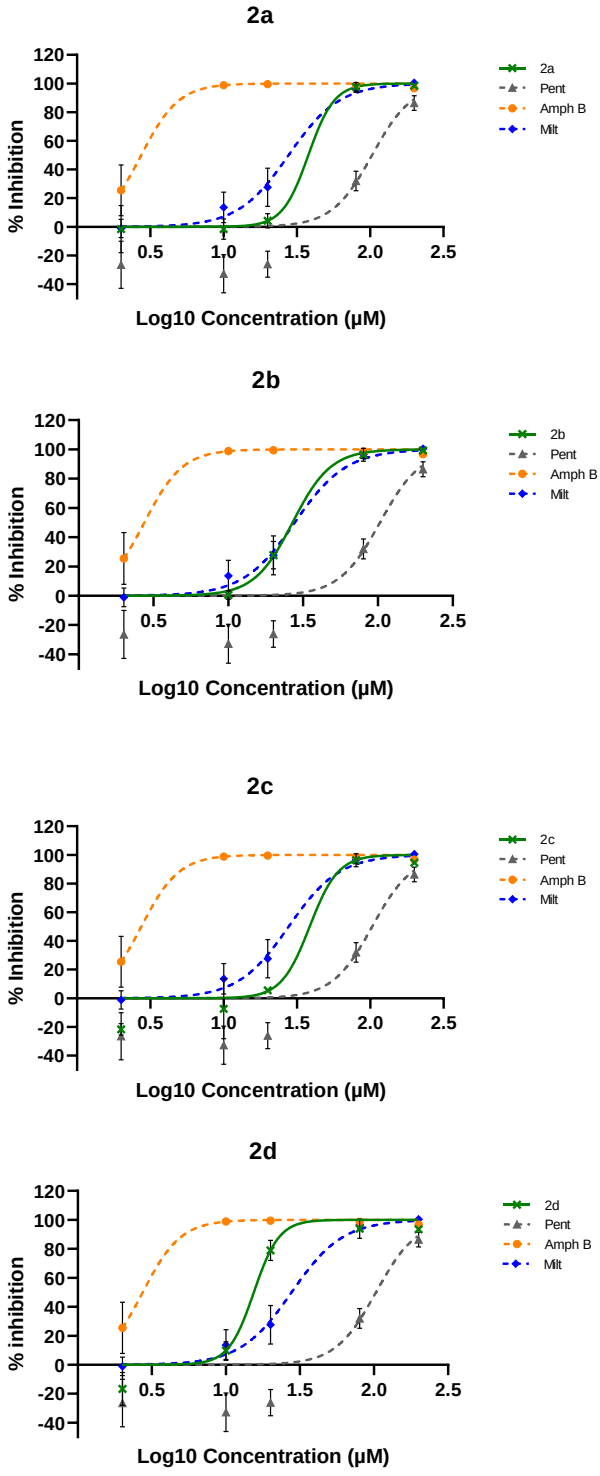

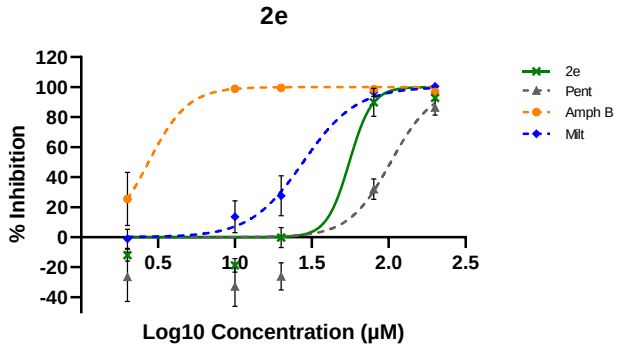
2e
120
100
80
60
40
20
0
-20
-40
% Inhibition
0.5
1.0
1.5
2.0
2.5
Log10 Concentration (µM)
2e
Pent
Amph B
Milt

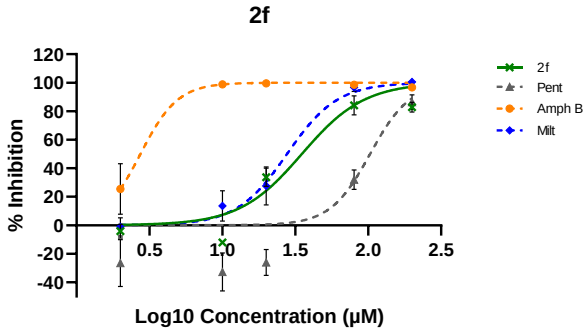
2f
120
100
80
60
40
20
0
-20
-40
% Inhibition
0.5
1.0
1.5
2.0
2.5
Log10 Concentration (µM)
2f
Pent
Amph B
Milt

Figure S5a. Toxicity test by MTS assay with selected azole-bisindoles **1** and **3b** on DH82 cells (72h treatments).

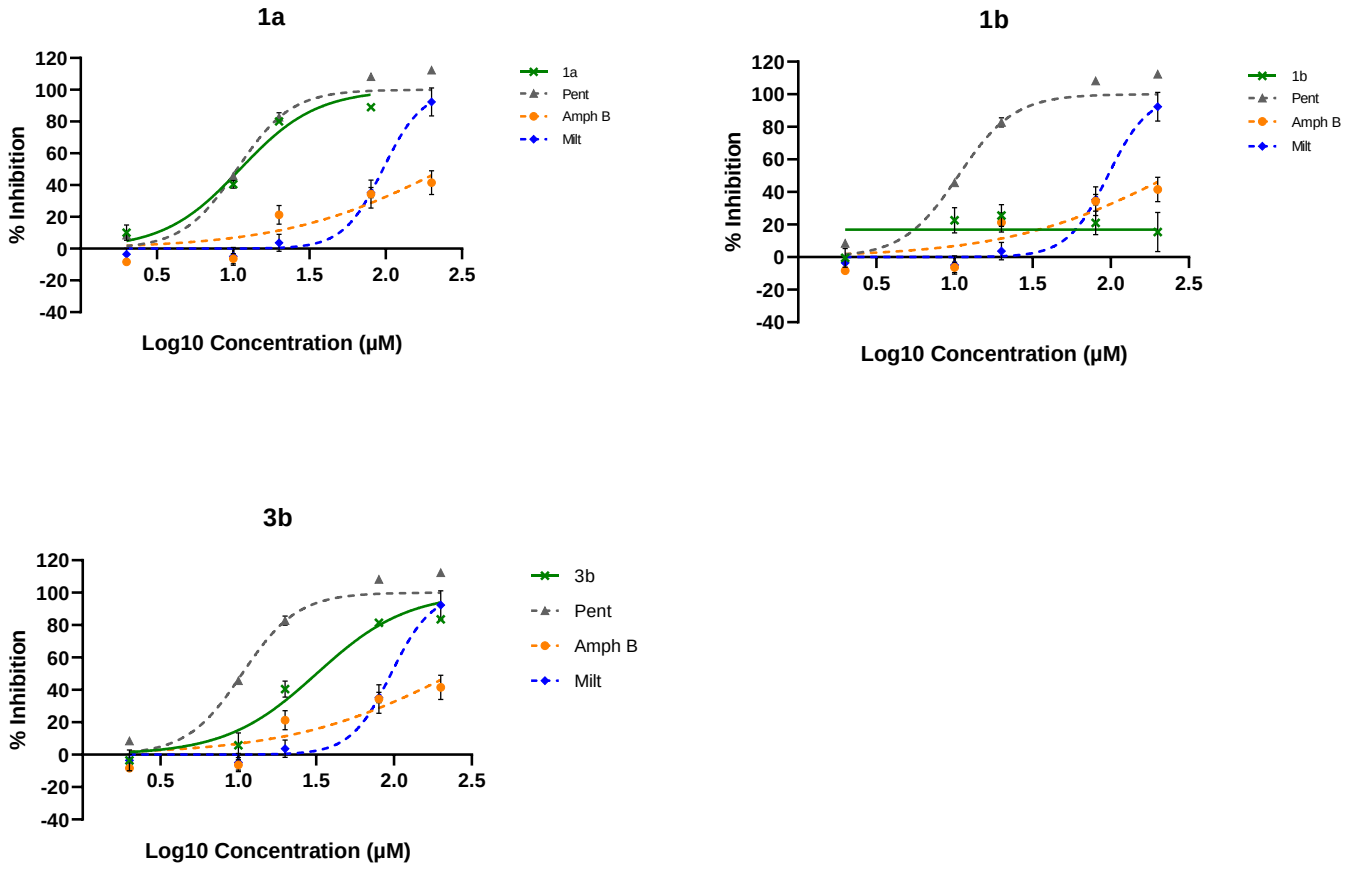

Figure S5b. Toxicity test by MTS assay with imidazole-bisindole derivatives **2** on DH82 cells (72h treatments).

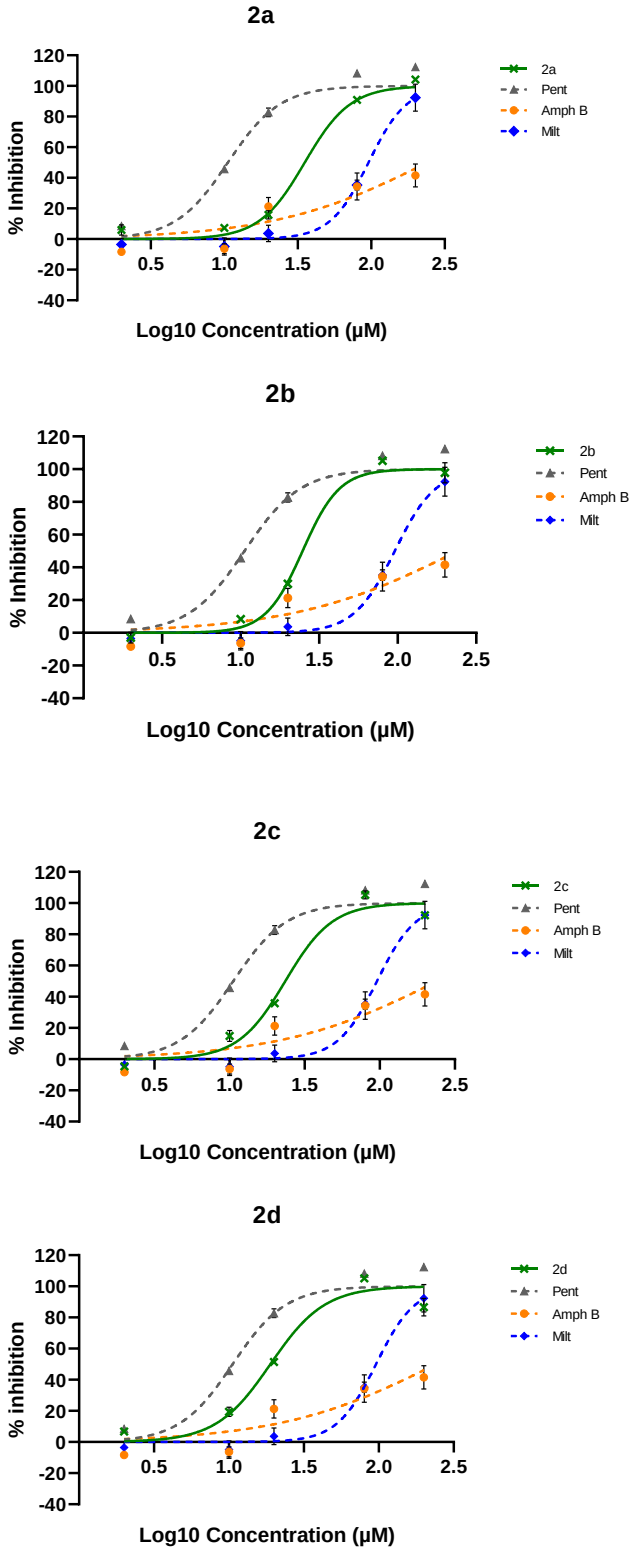

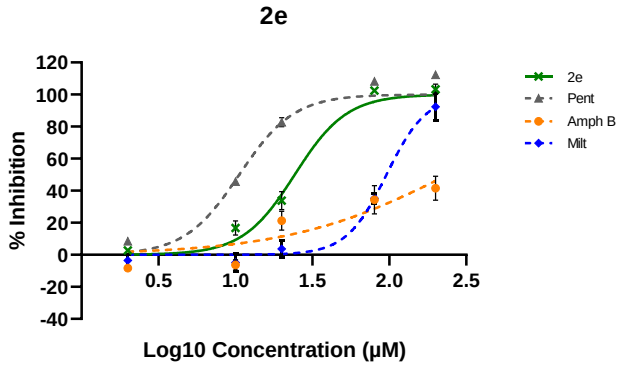
2e
% Inhibition
120
100
80
60
40
20
0
-20
-40
0.5
1.0
1.5
2.0
2.5
Log10 Concentration (µM)
2e
Pent
Amph B
Milt

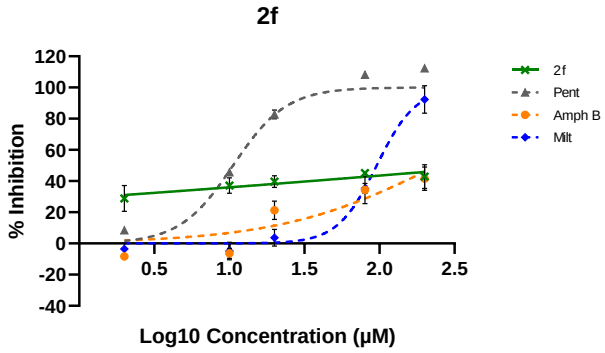
2f
% Inhibition
120
100
80
60
40
20
0
-20
-40
0.5
1.0
1.5
2.0
2.5
Log10 Concentration (µM)
2f
Pent
Amph B
Milt

Table S1. Azole-bisindole derivatives **1-3** toxicity on DH82, HepG2, HaCaT, and HPF cell lines. CC_{50} values for all the strains are reported as mean and 95% confidence interval

	DH82 **CC_{50} (µM)** **(95% CI)**	**HepG2** **CC_{50} (µM)** **(95% CI)**	**HaCaT** **CC_{50} (µM)** **(95% CI)**	**HPF** **CC_{50} (µM)** **(95% CI)**
1a	> 20 (12.1%)*	> 20 (n.e.)*.	> 20 (11.8%)*	> 20 (6.5%)*
URB1483 (**1b**)	> 20 (n.e.)*.	> 20 (n.e.)*.	> 20 (17.8%)*	> 20 (8.2%)*
1c	> 20 (n.e.)*.	> 20 (n.e.)*.	> 20 (9.5%)*	> 20 (n.e.)*.
2a	> 20 (n.e.)*.	> 20 (n.e.)*.	> 20 (9.7%)*	> 20 (12.0%)*
2b	> 20 (11.3%)*	> 20 (n.e.)*.	> 20 (12.2%)*	> 20 (13.8%)*
2c	> 20 (6.1%)*	> 20 (n.e.)*.	> 20 (23.0%)*	> 20 (6.7%)*
2d	> 20 (n.e.)*.	> 20 (n.e.)*.	> 20 (28.8%)*	> 20 (n.e.)*.
2e	> 20 (n.e.)*.	> 20 (n.e.)*.	> 20 (12.6%)*	> 20 (5.1%)*
2f	> 20 (20.5%)*	> 20 (10.2%)*	> 20 (3.7%)*	> 20 (21.1%)*
3b	> 20 (17.9%)*	> 20 (n.e.)*.	> 20 (9.6%)*	> 20 (17.1%)*
Pent	> 20 (n.e.)*.	> 20 (n.e.)*.	> 20 (11.2%)*	> 20 (n.e.)*.
Amph B	17.26 (13.72-23.95)	4.60 (3.65-5.80)	7.95 (6.44-9.66)	5.03 (3.50-6.89)
Milt	> 20 (43.9%)*	> 20 (37.9%)*	> 20 (45.5%)*	> 20 (46.2%)*

HPF: Human Primary Fibroblasts. **Amph B**: non-liposomal amphotericin B. **Milt**: miltefosine.

Pent: Pentamidine.

n.e. no effects were observed following these treatments

*in parenthesis the percentage of inhibition at 20 µM was reported

Table S2. Two way Anova results of treatment with compound **URB1483** and pentamidine (**Pent**) in three different infection models

Infection model	**Source of Variation**	**% of total variation**	**P value**
THP1 cells infected with *L. infantum* MHOM/TN/80/IPT1	Interaction	0.32	0.7149
	URB1483 or **Pent**	0.03	0.7353
	Treatment	44.46	<0.0001
THP1 cells infected with *L. infantum* human clinical isolate	Interaction	2.54	0.1668
	URB1483 or **Pent**	0.02	0.8341
	Treatment	23.41	<0.0001
DH82 cells infected with *L. infantum* MHOM/TN/80/IPT1	Interaction	3.01	0.5513
	URB1483 or **Pent**	1.44	0.3185
	Treatment	33.28	0.0003

Figure S6. Superposition of the docking pose of **URB1483** (**1b**, green carbon atoms) within the *L. donovani* topoisomerase IB (black carbon atoms) on the indolocarbazole inhibitor **SA315F** (orange carbon atoms) reported in the ternary adduct involving DNA and human topoisomerase IB (1SEU.pdb, see ref. 28 main text), after structural alignment of the C-alpha atoms of the enzymes.

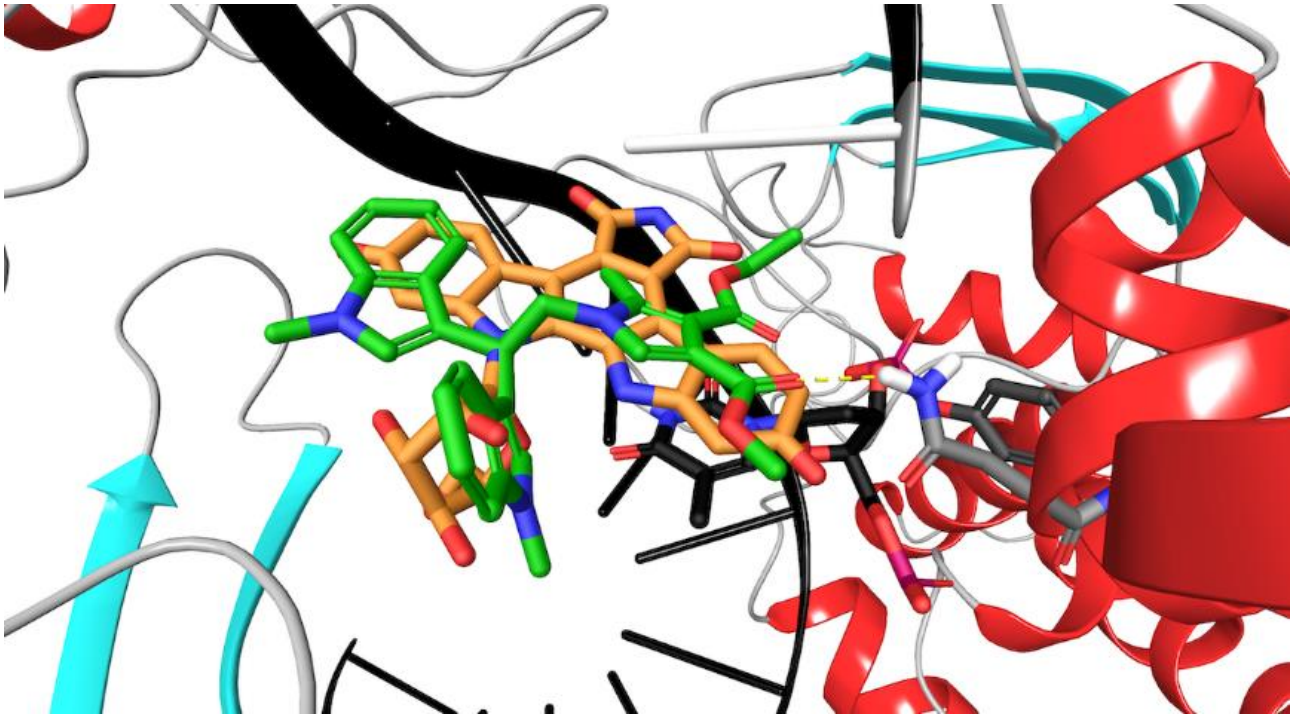

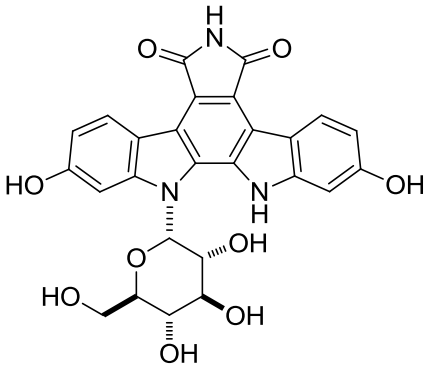

SA315F

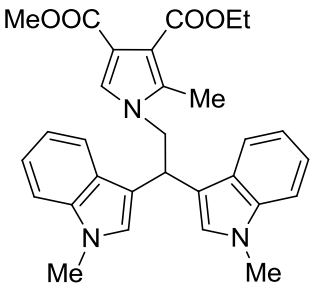

URB1483

Inhibition studies of the *L donovani* and Human topoisomerase IB activities

Results

Relaxation assay and agarose cleavage assay showed that **URB1483** does not inhibit both Leishmania and human TopIB at any tested concentration.

URB1483 was not active at any concentration used at short time (figure S7, panel A) and at longer time (figure S7, panel B). (**DAT**), a relaxation inhibitor of the *Leismania* enzyme (positive control), inhibits both the leishmanial and human enzymes. Camptothecin (**Cpt**) was effective as human enzyme inhibitor and less effective with the Leishmania version.

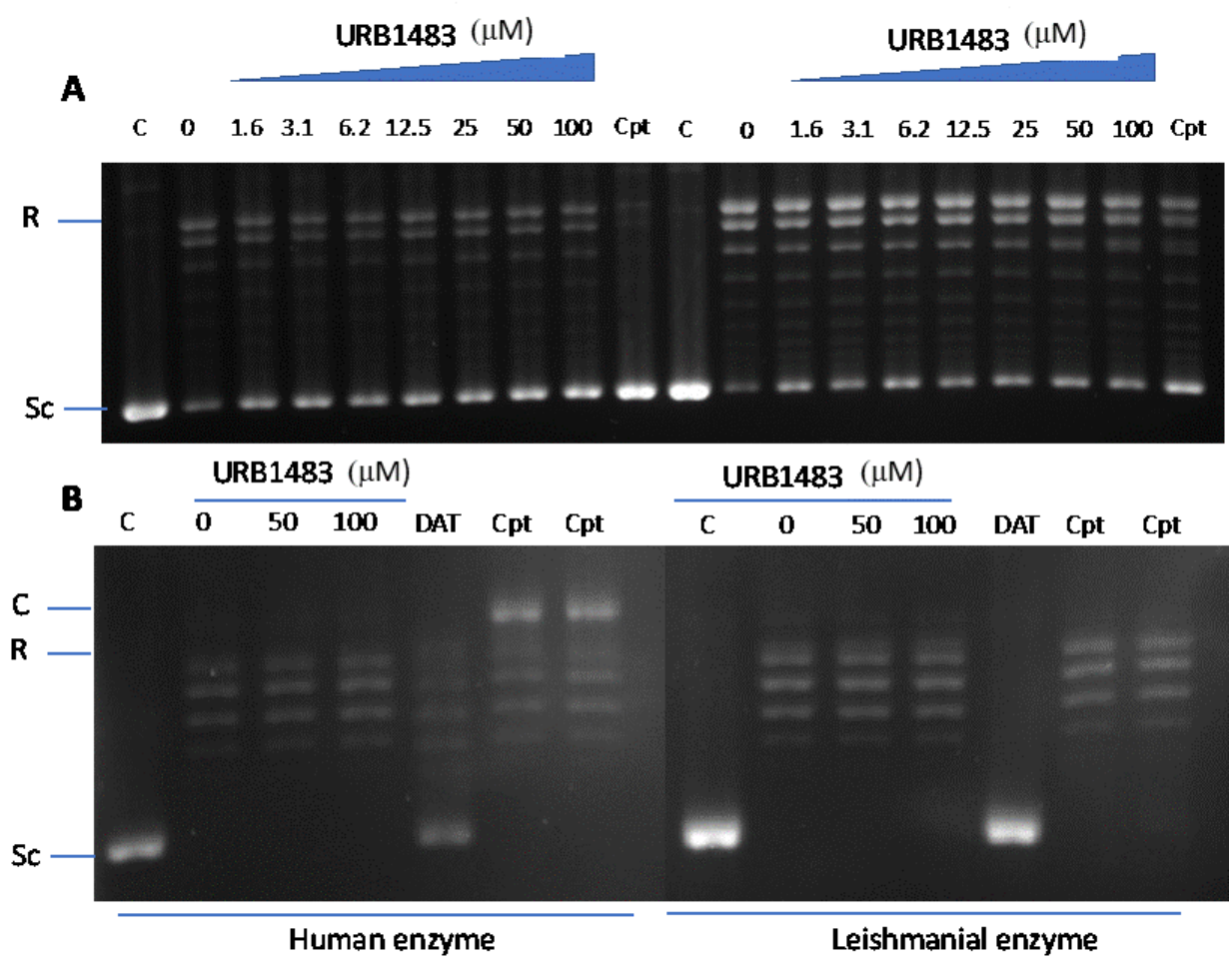

Figure S7: Relaxation of negative supercoiled plasmid DNA by Human and *L. donovani* topoisomerase IB in the presence of increasing concentrations of the **URB1483**. **A**) 2 min preincubation; **B**) 30 min incubation. The reaction products were separated in 1% agarose gel and visualized with ethidium bromide. In lane 1 only the supercoiled DNA substrate is

present. S.C. and R. represent the supercoiled substrate and the relaxed DNA plasmid respectively.

Figure S8 shows agarose cleavage assay with **URB1483**, cpt (top panel) and DAT, bottom panel, (see differences in the position of supercoiled (Sc), relaxed (R) and cleavage (C) bands). CPT produces clear C band in human (not in leishmania) and DAT inhibit the relaxation of DNA (it does induce formation of ternary cleavage complexes).

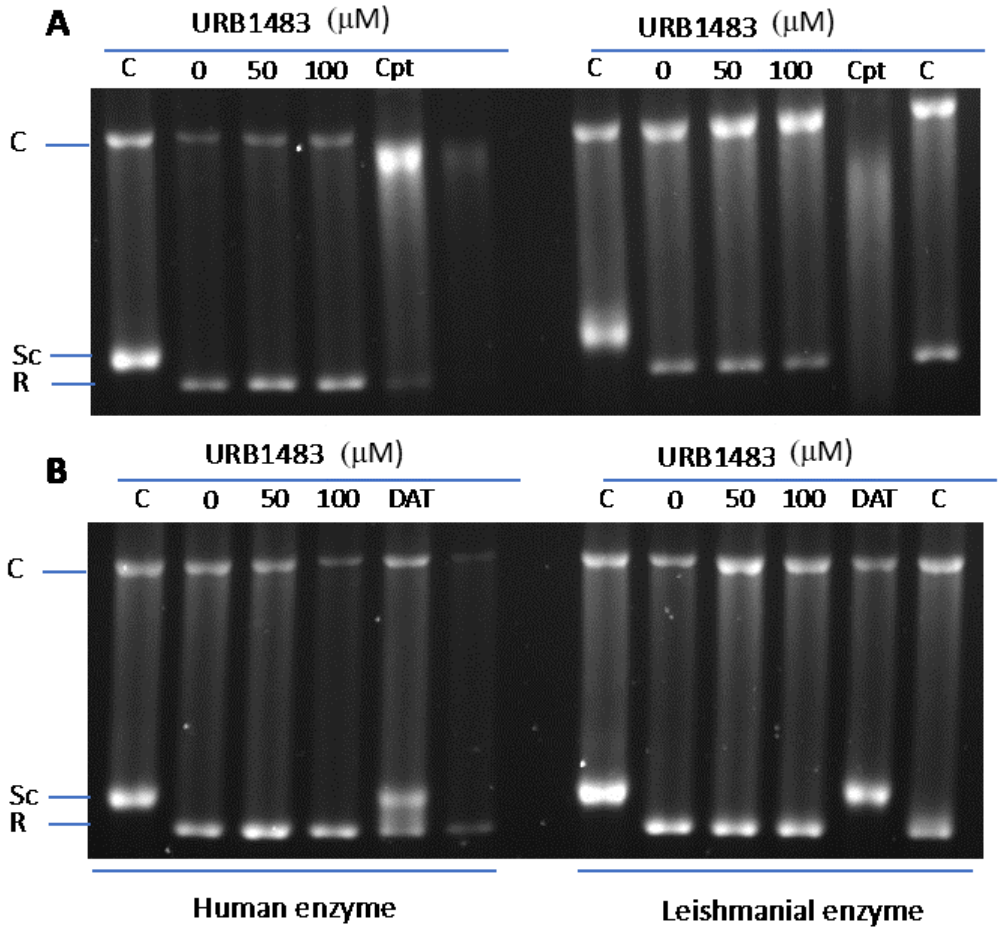

Figure S8: Agarose cleaving assay by Human and *L. donovani* topoisomerase IB in the presence of increasing concentrations of **URB1483** and **A**) with Cpt or **B**) DAT. The reaction products were separated in 1% agarose gel and visualized with ethidium bromide. In lane 1

only the supercoiled DNA substrate is present. S.C. and R. represent the supercoiled substrate and the relaxed DNA plasmid respectively.

Material and Methods

Both recombinant human (hTopIB) and leishmanial (LTopIB) were synthesized and purified from a *Saccharomyces cerevisiae* platform according to Tejería et al [1].

The compound was tested using two different assays. The standard relaxation assays and the agarose cleaving assay.

In the first case (relaxation assay) one unit of purified LTopIB or hTopIB was incubated for 30 min at 37 ºC in the presence of 0.5 μg of supercoiled pSK DNA, 10 mM Tris-HCl buffer pH 7.5, 5 mM $MgCl_2$, 0.1 mM EDTA, 15 μg/mL bovine serum albumin, 150 mM KCl along with different concentrations of the compound, in a final volume of 20 μL. The reaction was stopped by the addition of 4 μL loading buffer (5% sarkosyl, 0.12% bromophenol blue, 25% glycerol). The topoisomers were resolved in 1% agarose gels by electrophoresis in 0.1 M Tris borate EDTA buffer (pH 8.0) at 2 V/cm for 16 h and visualized with UV illumination after ethidium bromide (0.5 μg/mL) staining.

In the agarose cleaving assay 20 μL of reaction mixture (containing one unit of purified LTopIB or hTopIB, 0.5 μg supercoiled pSK; 10 mM Tris-HCl pH 7.5; 5 mM MgCl2; 0.1 mM EDTA; 150 mM KCl; 15 μg/mL bovine serum albumin) along with the different compounds were incubated at 37 °C during 4 min. Reactions were stopped by adding 1% SDS (final concentration), digested with 1 mg/mL proteinase K at 37 °C during 2 h and extracted with phenol/chloroform. DNA was separated by gel electrophoresis in 1% agarose containing 0.1 μg/mL ethidium bromide in 0.1 M Tris borate EDTA buffer (pH 8.0) at 4 V/cm for 16 h. Gels were visualized with UV illumination. Fifty micromolar CPT or DAT [2] were used as positive controls.

References

[1] Tejería, A., Pérez-Pertejo, Y., Reguera, R.M., Rubiales, G., Palacios, F. Antileishmanial effect of new indeno-1,5-naphthyridines, selective inhibitors of Leishmania infantum type IB DNA topoisomerase. *European Journal of Medicinal Chemistry*, **2016**, *124*, 740-749.

[2] Carballeira NM, Morales-Guzman C, Alvarez-Benedicto E, Torres-Martinez Z, Delgado Y, Griebenow KH, Tinoco AD, Reguera RM, Perez-Pertejo Y, Carbajo-Andres R, Balana-Fouce R. First Total Synthesis of ω-Phenyl Δ6 Fatty Acids and their Leishmanicidal and Anticancer Properties. *Curr Top Med Chem.* **2018**, *18* (5), 418-427.

CHAPTER 8

In this chapter, we report the screening of a library of indole-derivative compounds for their potential anti-parasitic effect, in terms of efficacy on *L. infantum* promastigotes and amastigotes, and on *T. brucei* bloodstream trypomastigotes. Moreover, the efficacy of two compounds, including the compound URB1483, identified in the previous study (chapter 7) was tested in an in-vivo *Leishmania* infection model.

This work was performed at the Institute of Research and Innovation in Health (i3s) - University of Porto (Portugal) under the supervision of Professor Anabela Cordeiro-da-Silva and Dr. Nuno Santarem.

All the data were obtained by the author of this thesis during the work period at the University of Porto.

(Unpublished data)

Research for new scaffolds against *trypanosomatidae*: indole-derivatives compounds against *Leishmania infantum* and *Trypanosoma brucei* parasites

Abstract

The protozoa *Leishmania* and *Trypanosoma brucei* are the etiological agents of leishmaniases and Human African Trypanosomiasis (HAT), which belong to Neglected Tropical Diseases (NTDs). Because of their worldwide distribution, they represent a concern for global health. The treatments available are poor and present several limitations such as high costs, toxicity, and the appearance of resistant strains. In this view, the discovery of new potential drug candidates remains a challenge. In this work we report the screening of a library of indole-derivative compounds for their potential anti-parasitic effect, in terms of efficacy on *Leishmania infantum* promastigotes and *Trypanosoma* bloodstream trypomastigotes. Four and ten compounds showed good activity on *Leishmania* and *Trypanosoma*, respectively, showing an IC_{50} < 5 μM. In particular, three of them were active at a concentration < 1 μM. The compounds were also tested on human THP-1-derived macrophages to evaluate the cytotoxicity. Finally, two compounds have been tested in an *in-vivo Leishmania* infection model. The infected BALB/c mice have been treated with 5mg/Kg of drug for ten days. The formulation resulted well tolerated by the animals but, unfortunately, at this dosage, the treatments did not revert the infection and did not significantly reduce the parasite burden in the mice's organs. In conclusion, the good results obtained in *in-vitro* assays suggest indole-derivative compounds as promising antiparasitic agents and represent the bases for further optimization and formulation studies.

1. Introduction

Neglected Tropical Diseases (NTDs) are a group of several conditions mainly prevalent in tropical areas, where they mostly affect impoverished communities affecting health, social and economic conditions of over one billion people (WHO). They include parasitic infections caused by trypanosomatids, such as Human African Trypanosomiasis (HAT, also known as African sleeping sickness) and leishmaniasis caused by *Trypanosoma brucei* and different species of *Leishmania,* respectively. These parasites belong to

Kinetoplastea class, are flagellated and are characterized by a particular life cycle that involves a vector stage and a mammalian host. Two different species are responsible for HAT: *T. brucei gambiense* causes chronic African trypanosomiasis and it is endemic in the west and central Africa. *T. brucei rhodesiense*, is related with acute African trypanosomiasis spread in eastern and southern Africa. Parasites are transmitted by the bite of infected tsetse fly belonging to *Glossina* spp. During the blood meal, the insect injects metacyclic trypomastigotes into skin tissue. The parasites enter the lymphatic system and pass into the bloodstream muting into bloodstream trypomastigotes. From the bite site, they reach other body fluids such as lymph and spinal fluid and continue to replicate. Unlike *Leishmania*, the entire life cycle of African trypanosomes is represented by extracellular stages (Figure 1).

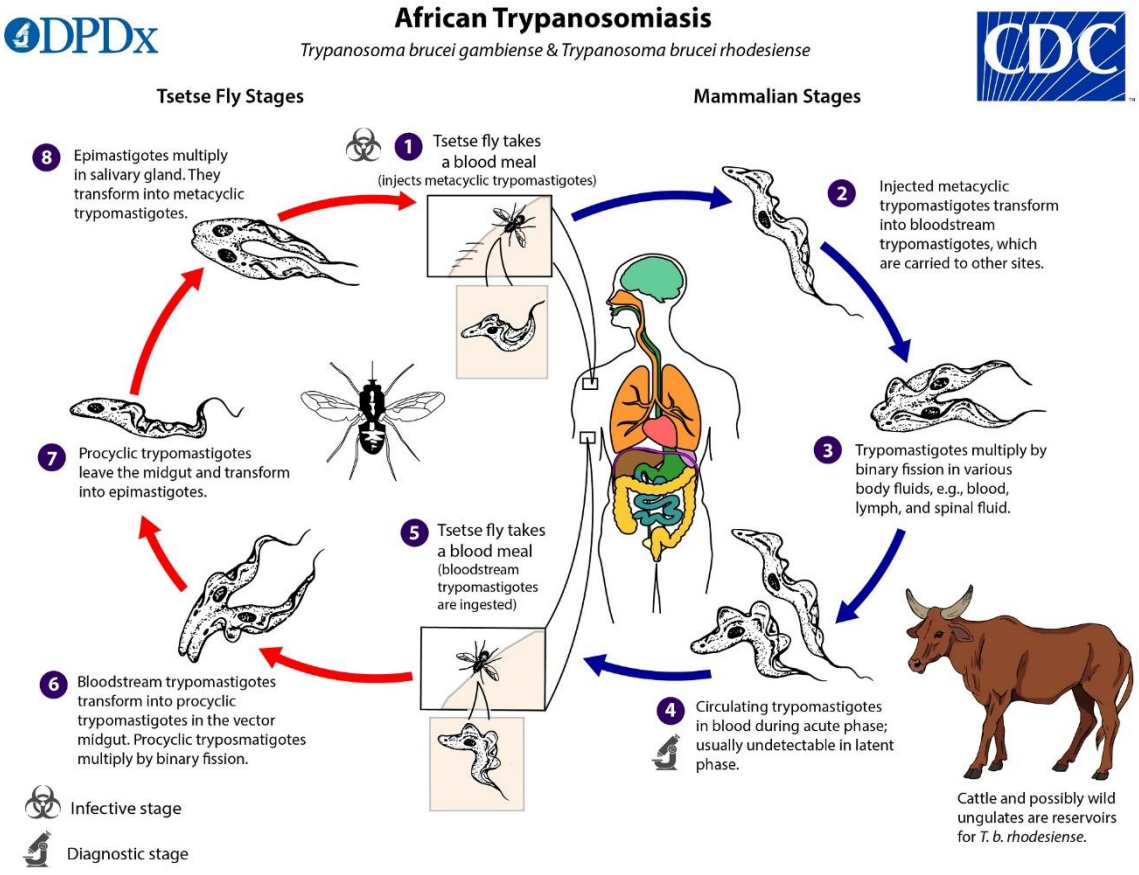

[Figure 1] African trypanosomiasis life cycle
(https://www.cdc.gov/dpdx/trypanosomiasisafrican/index.html)

The disease occurs in two stages. In the first stage (haemolymphatic) the trypanosomes multiply in subcutaneous tissues, blood and lymph and nonspecific signs and symptoms such as fever, headache, itching and lymphadenopathy occur. In the second stage (meningoencephalitic) the parasites cross the blood-brain barrier to infect the central nervous system causing a variety of neuropsychiatric manifestations including sleep disorders (hence the name of the disease), changes of behavior, confusion, sensory disturbances, and poor coordination. Severe cardiac involvement with perimyocarditis is also observed. Without treatment, sleeping sickness is considered fatal although cases of healthy carriers have been reported (WHO). The treatment choice depends on disease stage and species involved. At the moment there are five drugs available (Table 1): pentamidine, suramin, melarsoprol, eflornithine (administrated as monotherapies), and nifurtimox–eflornithine combination therapy (NECT) (Avery et al., 2013). Pentamidine and suramin are used for early-stage HAT caused by *T. b. gambiense* and *T. b. rhodiense*, respectively.

Drug	Structure	Comments	Efficacy
Suramin	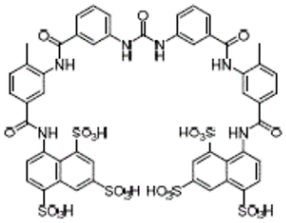	• i.v. • Toxicity.	• Effective against hemolymphatic stage of Rhodesian trypanosomiasis.
Pentamidine	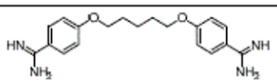	• i.m. • Toxicity.	• Effective against hemolymphatic stage of Gambian trypanosomiasis only.
Melasoprol	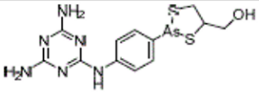	• i.v. • Suitable for second-stage disease. • High toxicity. • High levels of treatment failure in some regions.	• Effective against meningoencephalic stage of both forms of the disease. It is used only for Rhodesian trypanosomiasis.
Eflornithine	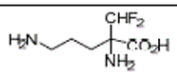	• i.v. • Suitable for second-stage disease. • High cost. • Not efficacious against *T.b. rhodesiense.*	• Most effective against meningoencephalic stage of Gambian trypanosomiasis. Effective in monotherapy or in combination with nifurtimox.
NECT	Eflornithine-Nifurtimox combination	• Suitable for second-stage disease. • Reduced cost and duration compared to monotherapy.	

[Table 1] Current treatment available for HAT (i.v. intravenous; i.m. intramuscular)
(Adapted from Kourbeli et al., 2021)

Pentamidine is an aromatic diamine and acts by preventing the synthesis of trypanosomal proteins, nucleic acids, phospholipids, and folate. Its mechanism of action includes the inhibition of the enzymes participating in the polyamine synthesis and the RNA polymerase activity (Simarro et al., 2012). It is relatively toxic, and patients need to be monitored during therapy (Kourbeli et al., 2021). **Suramin** seems to act by inhibiting glycerophosphate oxidase, serine oligopeptidase, and the RNA-editing ligase of the trypanosome's kinetoplast (Wiedemar et al., 2020). It is administrated for five weekly intravenous injections at a concentration of 20 mg/kg. For the second-stage treatment, eflornithine, either in monotherapy or in combination with nifurtimox, and melarsoprol are approved. **Melarsoprol** is the combination of melarsen oxide (a trivalent organic arsenical) with dimercaprol. This drug is associated with many adverse drug reactions, but the most severe is the encephalopathic syndrome (ES) that can be fatal (Seixas et al., 2020). Melarsoprol could be replaced by the much safer **eflornithine**. Nevertheless, eflornithine requires huge doses of administrations (56 infusions during 14 days in 14 liters of sterile saline) which represents an important limitation in rural areas with poor accessibility to hospital and medical care. Moreover, it presents high risk of resistance. In 2009, the nifurtimox-eflornithine combination therapy (**NECT**) was added to the WHO essential drug list, replacing the more toxic drug, melarsoprol. However, NECT is not effective for the treatment of late-stage T. b. *rhodesiense* HAT, and in this condition, melarsoprol remains the first choice (WHO). More recently, the orally available drug **fexinidazole** has been approved to treat both stages of *T. brucei gambiense* HAT and has been added to the WHO treatment guidelines; and **acoziborole**, formerly known as SCYX-7158, has been advanced to Phase II/III clinical trials for HAT (Klug et al., 2021). Since the treatments available have problems related to poor efficacy, difficulties in administration, side effects and resistance, the need to discover new affordable drugs remains pivotal. Several groups around the world are working on the development of new scaffolds with potential anti-*trypanosomatidae* effects. As already reported in Chapter 7, some works mentioned bis-indoles as anti-leishmanial compounds. Briefly, a work showed that 3,3'-diindolylmethane (DIM) is active on *L. donovani* inhibiting the enzyme topoisomerase IB of *Leishmania* (Roy et al., 2008) while a new aryl-DIM class has been reported as antileishmanial agents (Bharate et al., 2013). Moreover,

bis(indolyl)-pyridine and phenyl-aminothiazole-DIM derivatives showed good IC_{50} value (Kalam Kan et al., 2017; Taha et al., 2019). On the other hand, little is reported in the literature on the efficacy of indole derivatives on *T. brucei.* Recently Klug et al. (2021) identified a series of 3,5-disubstituted-7-azaindoles as growth inhibitors of *T. brucei.* In this study, we report the screening of a library of indole-derivative compounds previously synthesized (Mantenuto et al., 2016-2017; Ciccolini et al., 2018) at the Department of Biomolecular Science (University of Urbino) for their potential anti-parasitic effect, in terms of efficacy on *Leishmania infantum* promastigotes and *Trypanosoma* bloodstream trypomastigotes. A single experiment was performed also in-vivo on BALB/c mice infected by *L. infantum* axenic amastigotes.

2. Material and methods

2.1- Compounds

The 35 DIM-derivatives compounds tested in this work have been provided by Prof. Simone Lucarini (Department of Biomolecular Science, University of Urbino) and have been previously synthesized (Mantenuto et al., 2016-2017; Ciccolini et al., 2018). Compounds belong to eight different classes (Table 2). All the compounds were soluble in dimethyl sulfoxide (DMSO) and have been resuspended at a final concentration of 10 mM and stored at -20°C in the dark. To perform the efficacy and toxicity tests they were thawed and diluted in the specific medium to the required concentration without exceeding 1% of DMSO.

Name	Structure	Reference
Bisindole-pyrrole		
GB01	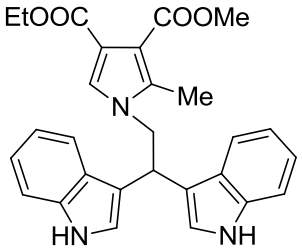	[3]
GB02 (1a)	[Confidential]	[1]
GB03 (1c)	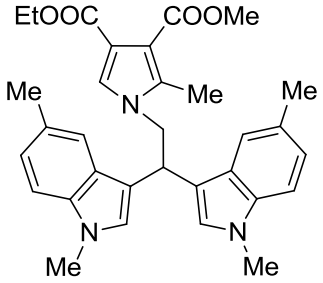	[1]
GB04 (1d)	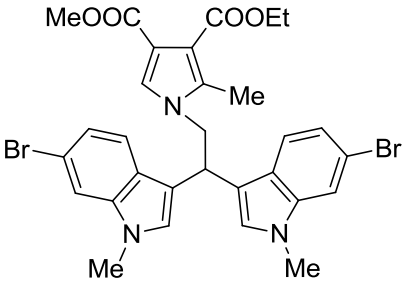	[1]
GB36 (1b-URB1483)	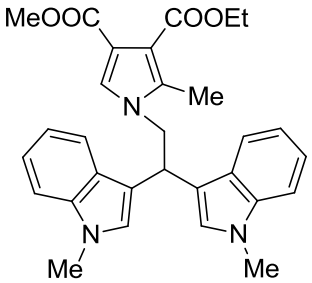	[1]

Bisindole-imidazole		
GB05	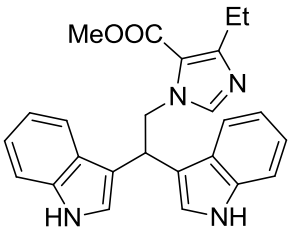	Unpublished
GB06 (2b)	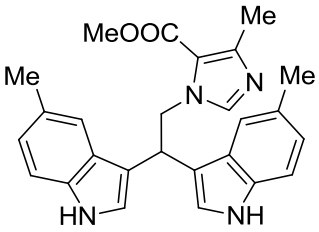	[1]
GB07 (2c)	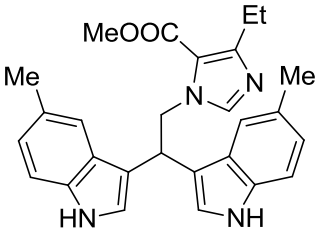	[1]
GB08 (2d)	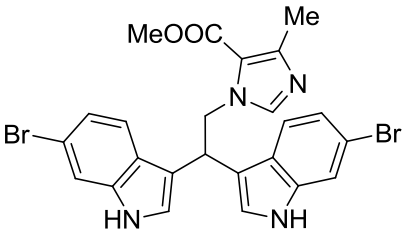	[1]
GB09	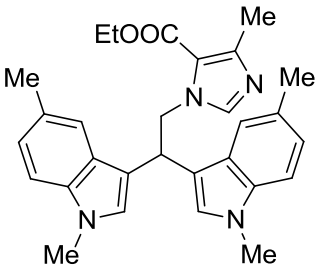	[1]
GB10	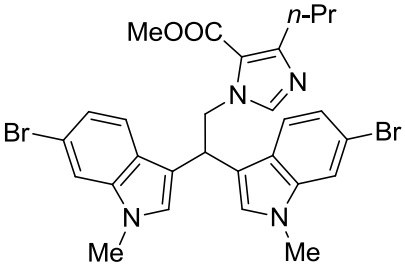	[1]
Bisindole-triazoles		

GB11 (3a)	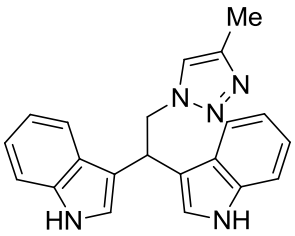	[1]
GB12 (3b)	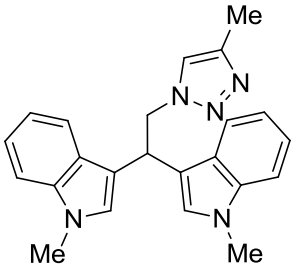	[1]
GB13	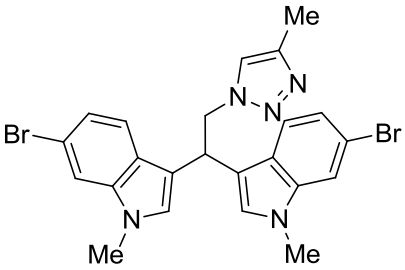	[1]
Planar Rigid Bisindole-Imidazoles		
GB14	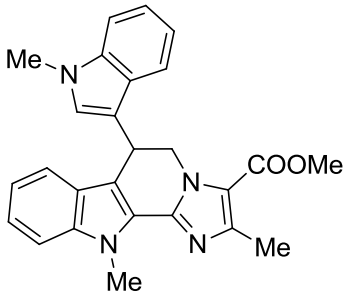	[2]
GB15	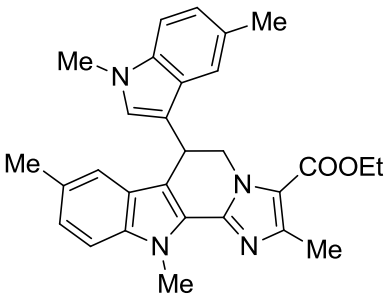	[2]

GB16	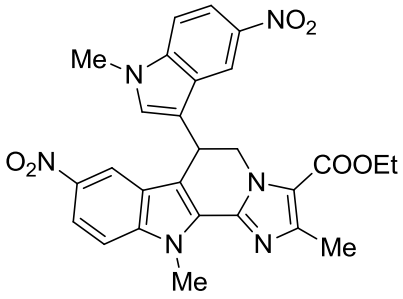	[2]
Planar semi-rigid Indoline-Indole-Pyrrole		
GB17	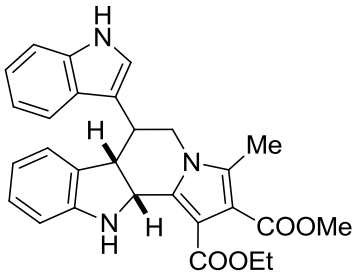	[3]
Rigid indole-Pyrroles		
GB18	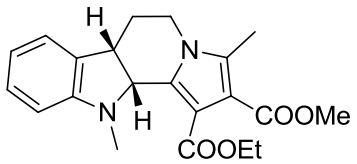	[3]
GB19	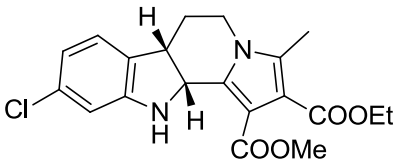	[3]
GB20	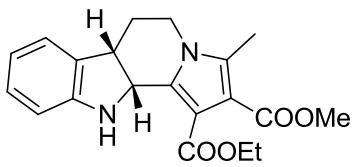	[3]
GB21	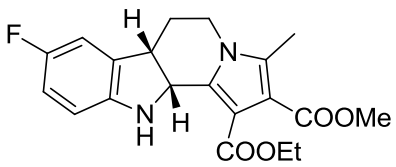	[3]

GB22	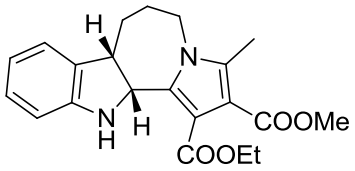	[3]
GB23	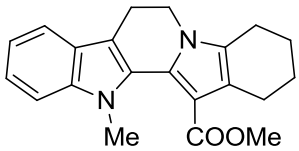	[2]
GB24	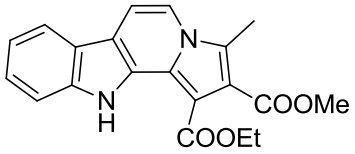	[3]
Rigid Indole-Imidazoles		
GB25	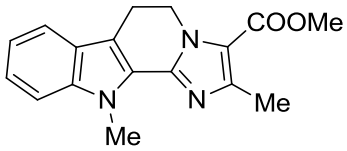	[2]
GB26	[Confidential]	[2]
GB27	[Confidential]	Unpublished
GB28	[Confidential]	[2]
GB29	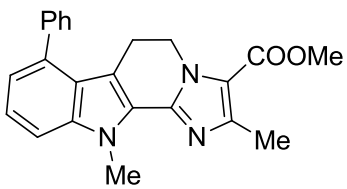	[2]

GB30	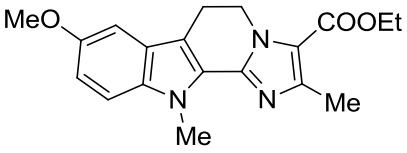	[2]
GB31	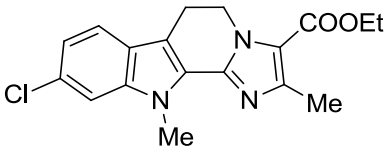	[2]
GB32	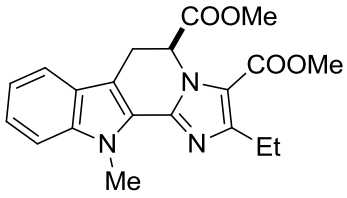	[2]
Rigid Indole-Triazoles		
GB33	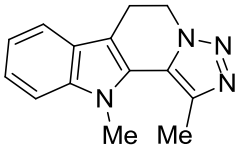	[2]
GB34	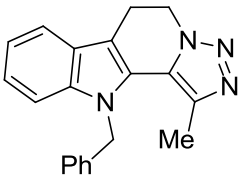	[2]
3,3'-diindolylmethane (DIM)		
GB35	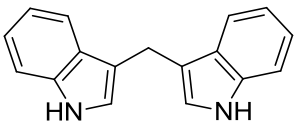	

[Table 2] Compounds tested in this study. The compounds with second name in the brackets have been already tested on *L. infantum* with comparable results (paper submitted see chapter 7).
[1] Mantenuto et al., 2016 [2] Mantenuto et al., 2017 [3] Ciccolini et al., 2018.

2.2- Parasite cultures

Promastigotes from the *L. infantum* strain (MHOM/MA/67/ITMAP-263) were grown in 5 ml on a T25 flasks in Schneider's insect medium supplemented with 10% heat-inactivated Fetal Bovine Serum (FBS), 200U/ml penicillin/streptomycin, 6 µg/ml Phenol

Red and 5 mM HEPES. The cultures were maintained in an incubator at 27° and diluted to $2x10^5$/ml every 5 days. For the assays the parasites used were equivalent to late/log with two or three days of culture.

T. b. brucei Lister 427 strain bloodstream forms were grown in a humidified incubator at 37 °C, 5% CO_2 in complete HMI-9 medium (Hirumi and Hirumi, 1989) supplemented with 10% heat-inactivated Fetal Bovine Serum (FBS) and 100 UI/mL penicillin/streptomycin. Parasites maintenance was done in T25 ventilated flasks by subpassage at a concentration of 1x10^^{4}/ml every 2 days.

Luciferase-expressing *L. infantum* (MHOM/MA/67/ITMAP-263) axenic amastigotes (Sereno et al., 2001) were maintained in MAA/20 (axenic amastigote medium) (Sereno et al., 1998) at 37 °C, 5% CO_2 environment with subculture every 7 days at $1x10^6$/ml in 5 ml on T25 ventilated flasks.

All cell culture reagents were purchased from Lonza-Bioscience (Morrisville, NC).

2.3- Cell cultures

Human leukemia cell line, THP-1 (ATCC® TIB-202™) were cultured in RPMI-1640 medium supplemented with 10% heat-inactivated Fetal Bovine Serum (FBS), 2 mM L-glutamine, 100 UI/mL penicillin/streptomycin, 20 mM HEPES. Cell line was maintained in a humidified incubator at 37°C and 5% CO_2 by subculture every three days in 20 ml of media at a concentration of $2x10^5$/ml in a T75 flask. All cell culture reagents were purchased from Lonza-Bioscience (Morrisville, NC).

2.4- In-vitro evaluation of compounds activity against *T. brucei* and *L. infantum*

The compounds efficacy against *T. brucei* bloodstream forms and *L. infantum* promastigotes was evaluated using a resazurin-based assay (Borsari et al., 2016). The anti-parasitic activity was first investigated at single dose at 20 µM and then, the compounds associated with activity >50% at 20 µM were further evaluated in a dose-response curve. Parasites were added to 100 µl of serial dilutions of compounds in supplemented complete medium at a final cell density of $1x10^4$/ml and $1x10^6$/ml for *Trypanosome* and *Leishmania*, respectively, in a final volume of 200 µl. As positive controls, the antitrypanosomal pentamidine and the antileishmanial miltefosine drugs, were included. Each condition was carried out in duplicate. Following 72h incubation at

the specific conditions for each parasite, 20 µl of a 0.5 mM resazurin solution was added and plates were incubated for a further 4 h under the same conditions. The assay is based on the ability of viable cells to reduce resazurin (7-Hydroxy-3H-phenoxazin-3-one 10-oxide), a dye with a blue to purple color and weak fluorescence, to the pink-colored and highly fluorescent resorufin (7-Hydroxy-3H-phenoxazin-3-one). Fluorescence was measured at 544 nm and 590 nm excitation and emission wavelength, respectively, using a Synergy 2 Multi-Mode Reader (Biotek, Winooski, VT, USA). Results were shown as % of parasite growth inhibition compared to control (untreated parasites) and represent the average of at least three independent experiments. The effect was evaluated by the determination of the IC50 value (concentration required to inhibit growth in 50%) and calculated by non-linear regression curves using GraphPad Prism version 8.0.2 for Windows (GraphPad Software, San Diego CA, USA).

2.5- Cytotoxicity Assay

The cytotoxicity effect of compounds on THP-1-derived macrophages was assessed by the colorimetric MTT assay (3-(4,5-dimethylthiazol-2-yl)-2,5-diphenyl tetrazolium bromide) as previously described (Magoulas et al., 2021), with some modifications. Briefly, THP-1 cells were resuspended in RPMI complete medium at a density of 5 x 10^5 cells/ml and 100 µl/well were seeded in a 96-well plate and were differentiated into macrophages by addition of 40 ng/mL of phorbol-myristate 13-acetate (PMA, Sigma, Saint Louis, MI, USA) for 24 h followed by replacement with fresh medium and cultivated for additional 24 h. Subsequently, cells were incubated with 100 µl of compounds ranging from 100 to 12.5 µM after dilution in the RPMI complete medium containing a maximum amount of 1% DMSO. For interesting compounds, the dose-response curve was performed to calculate the exact $CC_{50.}$ Each condition was carried out in duplicate or triplicate. After 72 h of incubation at 37°C 5% CO_2, the medium was removed and 200 µl of 0.5 mg/mL MTT solution diluted in RPMI was added. Plates were incubated for an additional 4 h to allow viable cells to convert MTT into a purple formazan product. Solubilization of formazan crystals was achieved by the addition of 2-propanol and absorbance was read at 570 nm using a Synergy 2 Multi-Mode Reader (Biotek, Winooski, VT, USA). Cytotoxicity was evaluated by the determination of the CC_{50}

value (drug concentration that reduced the percentage of viable cells in 50**%**) and calculated by non-linear regression analysis using GraphPad Prism version 8.0.2 for Windows (GraphPad Software, San Diego, CA, USA). The results represent the average of at least three independent experiments. For each compound, the Selectivity Index (SI) was calculated as the ratio between cytotoxicity in THP-1 (CC_{50}, 72 h) and activity against parasites (IC_{50}, 72 h).

2.6- In-vitro evaluation of anti-amastigotes activity on infected cells

The best ten efficient and not-toxic compounds against *Leishmania* promastigotes have been tested on *L. infantum* intracellular amastigotes according to the literature (Sereno et al., 1998) with some modifications. Briefly, THP-1 cells were resuspended in RPMI complete medium at a density of 5 x 10^5 cells/ml and 100 µl/well were seeded in a 96-well plate and were differentiated into macrophages by addition of 40 ng/mL of phorbol-myristate 13-acetate (PMA, Sigma, Saint Louis, MI, USA) for 24h followed by replacement with fresh medium for more 24 h. After that, cells were infected for 4 h with *L. infantum* axenic amastigotes expressing luciferase in a macrophage:amastigotes ratio of 1:20 at 37 °C, 5% CO_2. Non-internalized parasites were washed, and compounds were added at different concentrations in a final volume of 100 µL. The anti-parasitic activity was first investigated at single dose at 10 µM and then, the compounds associated with activity >50% at 10 µM were further evaluated in a dose-response curve. As positive controls miltefosine was included. Each condition was carried out in quadruplicate. After 72 h of incubation, the media was substituted by 100 µL of PBS and 25 µL of Glo-lysis buffer from the Steady-Glo Luciferase Assay System (Promega, Madison, WI, USA) was added. The plates have been placed in an agitator at 100 rpm for 10 minutes at room temperature. Finally, 30 µL of the Steady-Glo reagent (Promega, Madison, WI, USA) was added to the plate and was incubated for 15 min in the dark at the same conditions. 100 µL of solution was transferred to white-bottom 96-well plates. The luminescence intensity was read using a Synergy 2 Multi-Mode Reader (Biotek, Winooski, VT, USA). The antileishmanial effect was evaluated by the determination of the IC_{50} value and calculated by the non-linear regression analysis using GraphPad Prism

version 8.0.2 for Windows (GraphPad Software, San Diego CA, USA). The results represent the average of at least three independent experiments.

2.7- Ethical statement

The I3S Animal Ethics Committees approved all the experiments carried out on mice and the project was licenced by the Portuguese National Authority for Animal Health, in accordance with the statements on the directive 2010/63/EU of the European Parliament and Council.

2.8- In-vivo evaluation of anti-amastigotes activity on BALB/c mice infected with *L. infantum* axenic amastigotes

Among the compounds tested against *Leishmania*, the two showing better activity and low cytotoxicity (i.e. GB26, GB36-URB1483 of the previous chapter), have been selected for the *in-vivo* evaluation on a BALB/c mice infection model. Six-to seven-week-old BALB/c mice were purchased from Charles River or the i3S animal facility. *L. infantum* axenic amastigotes expressing episomal luciferase were cultured in complete cell-free medium MAA/20 at 37°C with 5% CO_2. Amastigotes recovered from five-day old cultures were washed twice with PBS and resuspended at a concentration of $1x10^9$ parasites/ml (Mendes Costa et al., 2019). A total of 21 mice have been infected with 100 µL of parasite suspension containing $1x10^8$ parasites. The injection was performed intra-venous (IV) in the mice's tail. Treatments started 21 days post-infection for 10 consecutive days. After solubility and stability studies, compounds have been resuspended in 5% DMSO, 60% of 100% PEG 400 (Molecular Dimensions), 35% distillated H_2O in a final volume of 800 µL. The injection solution has been prepared fresh every day to avoid compound precipitation. As negative and positive controls, 4 mice have been treated with PEG 400 solution without compounds and 4 with miltefosine (stock solution 20mg/ml in distillated water). The administration took place intraperitoneally (IP) with 100 µL/mouse at a concentration of 5mg/kg. The treatment and control groups were as follows:

- 5 uninfected mice (healthy)
- 5 infected and untreated mice

- 4 mice infected and treated with 20mg/kg/day miltefosine oral administration (OP) (positive control)
- 4 mice infected and treated with 5mg/kg/day SM414 (GB26) IP
- 4 mice infected and treated with 5mg/kg/day SM318 (GB36) IP
- 4 mice infected and treated with 3g/kg/day of the vehicle (PEG 400) IP (negative control)

Mice weight has been checked every 2 days. After 10 days of treatment, mice have been anesthetized with 2.5% isofurane and euthanized with cervical dislocation. After that, spleen, liver, and femur bone marrow have been removed for parasite load calculation. Spleen and liver have been weighted and bone marrow cells have been counted with automatic cell counter EVE^{TM} (NanoEnTek). Organ homogenates (1 mg of spleen and 10 mg of liver) and 10^5 bone marrow cells were subjected to serial dilutions in triplicate in Schneider's Insect medium in 96-well microtitration plates. The plates were incubated at 27 °C for 15 days and then each well was inspected for the presence or absence of promastigotes and checked to find the final dilution for which the well contained at least one parasite (Tavares et al., 2019). The number of parasites per gram of organ (parasite burden) is calculated as follows: [(geometric mean of reciprocal titer from each triplicate / mass of homogenized organ) × reciprocal fraction of the homogenized organ inoculated into the first well]. For bone marrow the number of parasites is calculated per 10^5 cells using the formula: [(geometric mean of reciprocal titer from each triplicate / number of cells) × reciprocal fraction of the cells inoculated into the first well]. For graphical representation log transformation is applied to the parasite load to reduce right skewness.

2.9- Statistical analysis

The evaluation of IC_{50} in parasites and CC_{50} in THP1 cells was calculated by the non-linear regression analysis using GraphPad Prism version 8.0.2 for Windows (GraphPad Software, San Diego CA, USA) and expressed as means and 95% confidence interval. The statistical analysis for the *in-vivo* experiments was performed by Ordinary one-way ANOVA with Dunnett's multiple comparisons test (single pooled variance). A p value ≤ 0.05 was considered significant.

3. Results

3.1- Effect of compounds on parasites viability

The anti-parasitic activity on *L. infantum* and *T. brucei* was first evaluated at single dose at 20 µM for 72h. The compounds that showed activity > 50% at 20 µM were further evaluated in a dose-response curve starting from 20 µM. Regarding *L. infantum,* 21 compounds showed an IC_{50} > 20 µM (Table 3), 9 compounds had a value between 6.00 and 11.98 µM, while the compounds GB01, GB12, GB26, GB27, GB28, GB36 showed an IC_{50} ≤ 5.82 µM. Notably, GB26 and GB28 had a value of 0.39 µM and 0.43 µM, respectively, sensibly lower compared with the reference drug miltefosine (IC_{50} = 13.88 µM). The dose-response curves of these compounds are shown in Figure 2 panel A compared with miltefosine. The curve represents the % of growth parasites inhibition at increasing compound concentrations.

Compound	**THP1** **CC_{50} (µM) (95% CI)**	***L. infantum* promastigotes** **IC_{50} (µM) (95% CI)**	**Selectivity index (CC_{50}/IC_{50}) on *L. infantum* promastigotes**
GB01	75.85 (67.15 - 87.82)	5.09 (4.61- 5.59)	14.90
GB02-1a	28.24 (26.58 - 30.01)	6.00 (5.66 - 6.38)	4.71
GB03-1c	>100	>20.00	-
GB04-1d	>100	>20.00	-
GB05	>100	>20.00	-
GB06-2b	25< CC_{50}<50	8.96 (8.55 - 9.36)	2.79<SI<5.58
GB07-2c	25< CC_{50}<50	8.81 (8.29 - 9.33)	2.84<SI<5.68
GB08-2d	12.5< CC_{50}<25	8.02 (7.53 - 8.53)	1.56<SI<3.11
GB09	25< CC_{50}<50	11.98 (11.23 - 12.82)	2.09<SI<4.17
GB10	77.73 (67.82 - 91.37)	>20.00	-
GB11-3a	>100	>20.00	-
GB12-3b	101.1 (76.02 - 152.4)	4.58 (4.13 - 5.07)	22.07

GB13	>100	11.96 (11.22 - 12.79)	>8.36
GB14	50< CC_{50}<100	>20.00	-
GB15	>100	>20.00	-
GB16	>100	>20.00	-
GB17	>100	9.24 (8.63 - 9.91)	>10.82
GB18	>100	>20.00	-
GB19	50< CC_{50}<100	>20.00	-
GB20	>100	>20.00	-
GB21	>100	>20.00	-
GB22	>100	>20.00	-
GB23	>100	9.19 (8.26 - 10.30)	>10.88
GB24	>100	>20.00	-
GB25	50< CC_{50}<100	>20.00	-
GB26	**>100**	**0.39 (0.34 - 0.45)**	**>256.41**
GB27	>100	5.82 (4.81 - 7.05)	>17.18
GB28	**113.4 (95.64 - 141.6)**	**0.43 (0.40 - 0.47)**	**263.72**
GB29	50< CC_{50}<100	>20.00	-
GB30	50< CC_{50}<100	>20.00	-
GB31	25< CC_{50}<50	>20.00	-
GB32	>100	10.22 (9.43 - 11.13)	>9.78
GB33	25< CC_{50}<50	>20.00	-
GB34	25< CC_{50}<50	>20.00	-
GB36-1b (URB1483)	**>100**	**4.05 (3.50 - 4.67)**	**>24.69**
GB35-3-3' DIM	50< CC_{50}<100	>20.00	-
Miltefosine	28.70 (26.53 - 31.04)	13.88 (12.66 - 15.19)	2.07

[Table 3] Indole derivatives potency on *L. infantum* promastigotes and cytotoxicity on THP1 cells. IC_{50} values are reported as mean and 95% confidence interval from at least three independent experiments. In bold, the three best compounds in terms of SI

Regarding *T. brucei,* 13 compounds showed an IC_{50} > 20 µM (Table 4), 12 compounds between 5.00 and 20.00 µM, while 10 compounds had values ≤ 5.00 µM. GB02 resulted the best compound (IC_{50} = 0.83 µM). The dose-response curves of the two best compounds (GB02-GB11) are shown in Figure 2 panel B.

Compound	**THP1** **CC50 (µM) (95% CI)**	***T. brucei* bloodstream form** **IC50 (µM) (95% CI)**	**Selectivity index (CC50/IC50) on *T. brucei* bloodstream form**
GB01	75.85 (67.15 - 87.82)	3.74 (3.49 - 3.99)	20.28
GB02-1a	**28.24 (26.58 - 30.01)**	**0.83 (0.76 - 0.90)**	**34.02**
GB03-1c	>100	3.92 (3.79 - 4.04)	>25.51
GB04-1d	>100	3.74 (3.52 - 3.97)	>26.74
GB05	>100	14.79 (14.12 - 15.46)	>6.76
GB06-2b	25< CC_{50}<50	4.37 (4.18 - 4.47)	5.72<SI<11.44
GB07-2c	25< CC_{50}<50	4.30 (3.92 – 4.72)	5.81<SI<11.63
GB08-2d	12.5< CC_{50}<25	3.97 (3.60 - 4.19)	3.15<SI<6.30
GB09	25< CC_{50}<50	6.95 (6.30 - 7.45)	3.60<SI<7.19
GB10	77.73 (67.82 - 91.37)	3.60 (3.41 - 3.76)	21.59
GB11-3a	**>100**	**2.58 (2.49 - 2.68)**	**>38.76**
GB12-3b	101.1 (76.02 - 152.4)	20.08 (18.74 - 22.29)	5.03
GB13	>100	5.14 (4.79 - 5.52)	>19.46
GB14	50< CC_{50}<100	11.81 (10.92 - 12.80)	4.23<SI<8.48
GB15	>100	6.51 (5.65 - 7.53)	>15.36
GB16	>100	>20.00	-
GB17	**>100**	**3.23 (2.96 - 3.52)**	**>30.96**
GB18	>100	>20.00	-
GB19	50< CC_{50}<100	7.78 (7.29 - 8.32)	6.43<SI<12.85
GB20	>100	>20.00	-

GB21	>100	>20.00	-
GB22	>100	>20.00	-
GB23	>100	11.62 (10.78 - 12.51)	>8.61
GB24	>100	18.14 (14.82 - 24.33)	>5.51
GB25	50< CC_{50}<100	>20.00	-
GB26	>100	>20.00	-
GB27	>100	>20.00	-
GB28	113.4 (95.64 - 141.6)	>20.00	-
GB29	50< CC_{50}<100	>20.00	-
GB30	50< CC_{50}<100	17.33 (14.45 - 22.11)	2.89<SI<5.77
GB31	25< CC_{50}<50	>20.00	-
GB32	>100	5.04 (4.59 - 5.54)	>19.84
GB33	25< CC_{50}<50	>20.00	-
GB34	25< CC_{50}<50	>20.00	-
GB36-1b (URB1483)	>100	5.71 (5.57 - 5.85)	>17.51
GB35-3-3' DIM	50< CC_{50}<100	11.11 (10.33 - 11.93)	4.50<SI<9.00
Pentamidine	52.30 (46.88 - 58.84)	0.0015 (0.0014 – 0.0016)	34866.67

[Table 4] Indole derivatives potency on *T. brucei* and cytotoxicity on THP1 cells. IC_{50} values are reported as mean and 95% confidence interval from at least three independent experiments. In bold, the three best compounds in terms of SI

Taken all the results together, and considering 10 µM as threshold, 15 compounds were not active (green square), 5 and 9 compounds were specific for *Leishmania* and *Trypanosoma*, respectively (blue and grey squares). Finally, 7 compounds were active on both although with different efficacy (red square) (Figure 3).

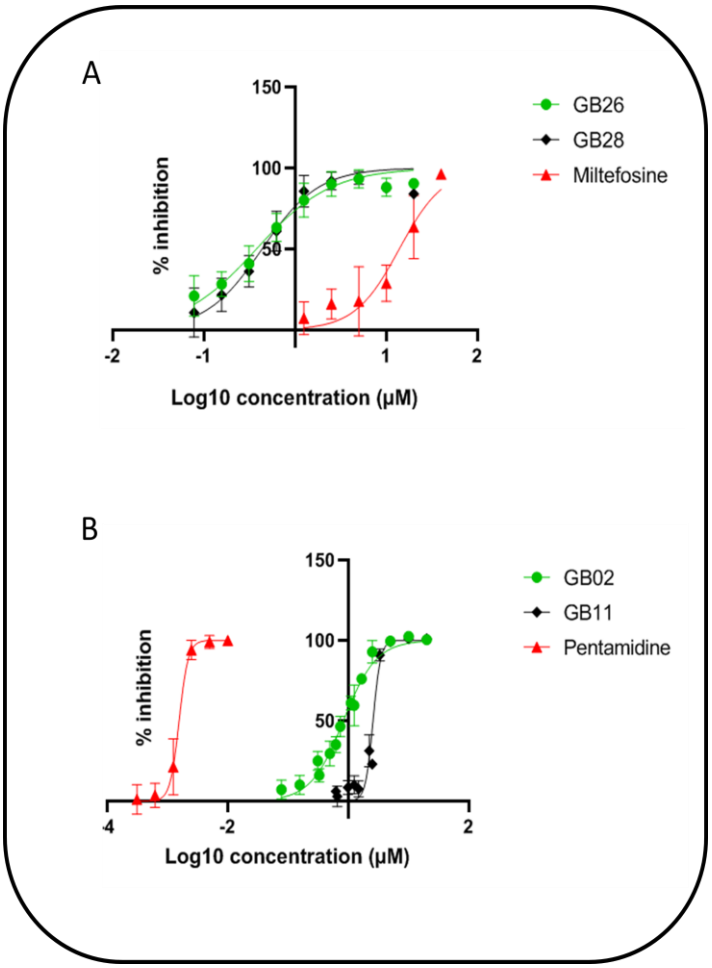

[Figure 2] Dose-response curves. The curve represents the % of growth parasites inhibition at increasing compound concentrations and represent the average of at least three independent experiments. [A*] L. infantum* [B] *T. brucei*. (GraphPad Prism version 8.0.2)

3.2- Cytotoxic effect of bisindole compounds in human THP-1 cell line

The cytotoxicity of the compounds was evaluated on THP-1 to calculate the CC_{50}. First, the viability assay was achieved by incubating cells with different concentrations of each compound (100, 50, 25, 12.5 µM) for 72h to individuate the CC_{50} interval. Subsequently, for interesting compounds, the dose-response curve was performed to calculate the exact CC_{50}. The results are summarized in Table 3 and 4 (second column) and represent the average of at least three independent experiments. The imidazole-bisindole derivatives resulted toxic on cells and were not particularly active on the parasites. Interestingly, the compounds GB26, GB28 and GB36 were not toxic on THP1 resulting in good SI on *Leishmania* parasites, if compared with miltefosine (Table 3, fourth column). In the same way, GB11 and GB17 resulted not toxic and showed good SI on *Trypanosoma* parasites. GB02 had a CC_{50} of 28.24 µM. Nevertheless, because of the low IC50, the SI is comparable with the two other compounds (Table 4, fourth column).

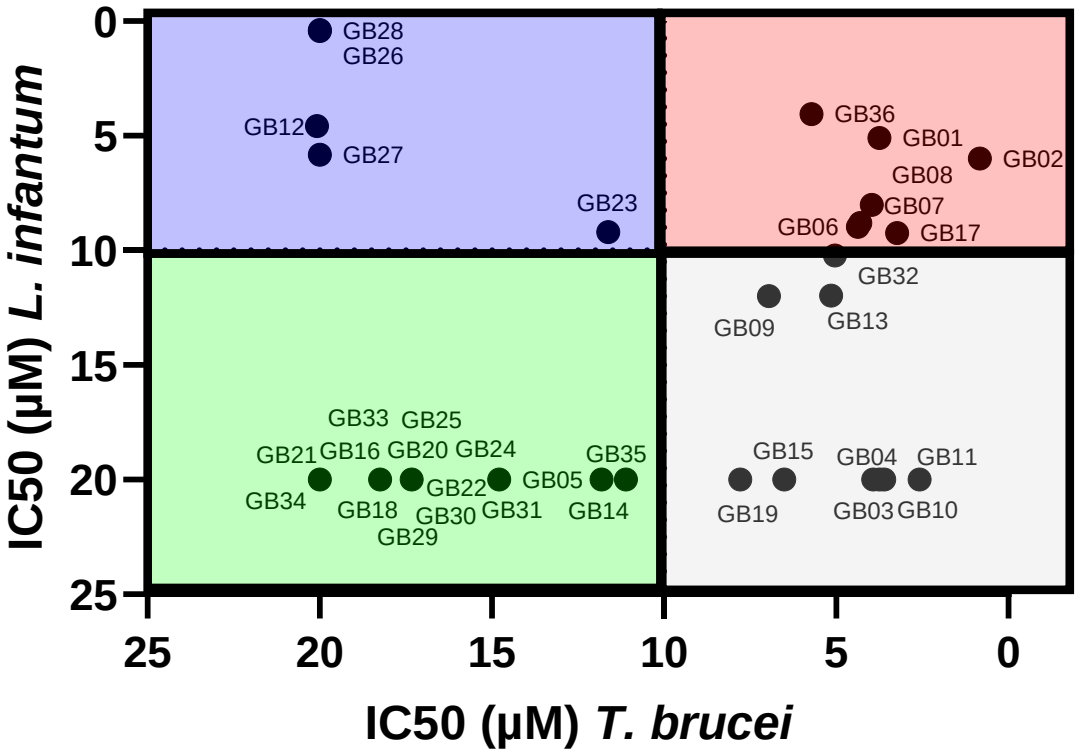

[Figure 3] Correlation graph. The axes represent the values of IC50 and have been set from highest to lowest. Green square: not active compounds; blue square: compounds active on *Leishmania*; grey square: compounds active on *Trypanosoma*; red square: compounds active on both parasites. Some dots overlap. (GraphPad Prism version 8.0.2)

3.3- Efficacy of compounds on *L. infantum* intracellular amastigotes

The ten best compounds in terms of SI on *Leishmania* promastigotes have been selected to be evaluated on *L. infantum* intracellular amastigotes. Human monocytic THP-1 cells were infected with *L. infantum* axenic amastigotes as described in methods. After 4 h, macrophages have been treated with 10 µM of the compound. Miltefosine was used as positive control. Five compounds showed an activity < 50% at 10 µM and were not taken into consideration for subsequent experiments (Table 5). Regarding the other five compounds, a dose-response curve was performed to calculate the exact IC_{50}. Compared with IC_{50} on promastigotes, the values resulted dramatically higher except for GB02 and GB36. On the other hand, miltefosine showed high efficacy to fight cell infection.

Compound	Percentage (% ±SD) of growth parasite inhibition at 10 µM	*L. infantum* intracellular amastigotes IC_{50} (µM) (95% CI)	Selectivity index (CC_{50}/IC_{50}) on *L. infantum* intracellular amastigotes
GB01	49%±7%	11.62 (9.64 - 14.41)	6.53
GB02-1a	79%±6%	5.04 (3.73 - 7.43)	5.60
GB12	39%±13%	>10	-
GB17	48%±7%	>10	-
GB23	36%±8%	>10	-
GB26	**62%±8%**	**6.46 (4.04 - 13.00)**	**>15.48**
GB27	43%±12%	>10	-
GB28	54%±15%	15.98 (10.75 - 32.27)	7.10
GB32	45%±7%	>10	-
GB36-1b (URB1483)	**71%±13%**	**3.59 (2.89 - 4.47)**	**>27.86**
Miltefosine	96%±6%	0.47 (0.44 - 0.50)	61.06

[Table 5] Indole derivatives potency on *L. infantum* amastigotes. IC_{50} values are reported as mean and 95% confidence interval from at least three independent experiments. In bold, the two best compounds in terms of SI

3.4- Efficacy of compounds on BALB/c mice infected with *L. infantum* axenic amastigotes

Considering the results on intracellular amastigotes, compounds GB26 and GB36 have been selected for *in-vivo* experiments. Twenty-one BALB/c mice have been infected with $1x10^8$ *L. infantum* axenic amastigotes intravenous. After 21 days post-infection, mice have been treated for 10 days, as described in methods. Miltefosine and PEG 400 administration were included as positive and negative control, respectively. Every 2 days, mice have been checked to control the weight and the presence of stress signs. The formulation administered in 60% PEG 400 was well tolerated by the mice that did not show any alteration either in physical or behavioral status. The only change was found in mice treated with miltefosine where a weight decrease of 10% occurred from

the second treatment. Nevertheless, a weight loss ≤ 20% is considered physiological (Figure 4).

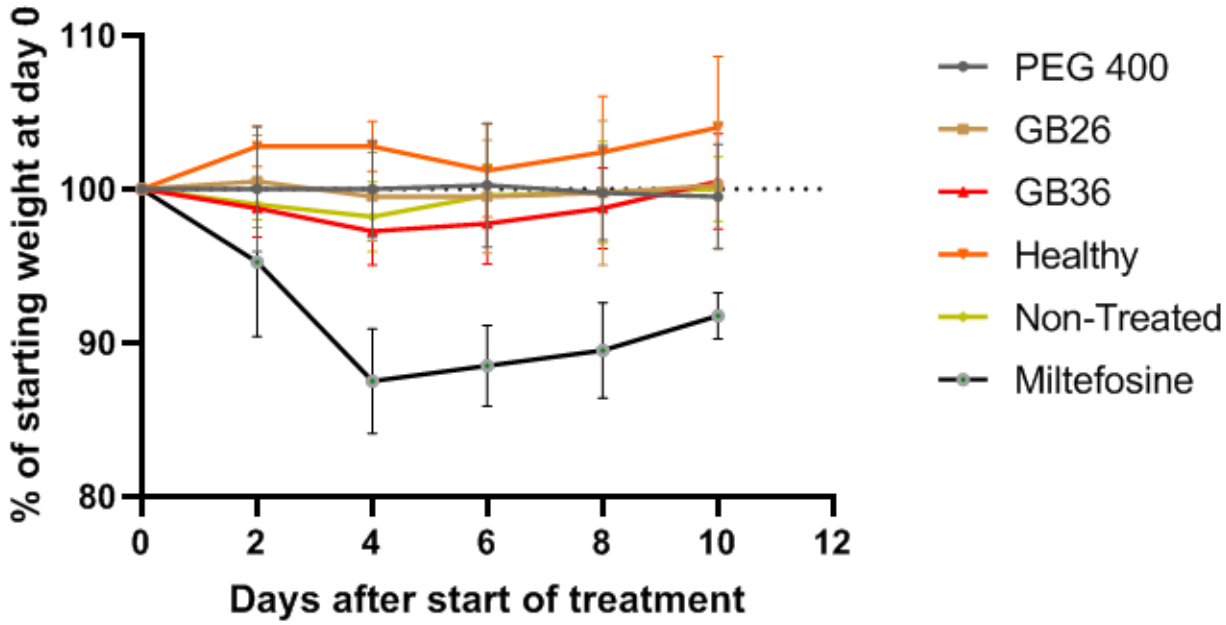

[Figure 4] Mice's weight variation during 10 days of treatment. Each dot represents the average and the SD. (GraphPad Prism version 8.0.2).

After 10 days of treatment, mice have been euthanized and spleen, liver, and femur bone marrow have been removed. Since *Leishmania* infection is associated with splenohepatomegaly, the organs weight has been considered to evaluate the treatment efficacy. The infected animals presented significantly heavier spleens than the non-infected (healthy) animals. The treated animals with effective drugs are expected to have a reversion of this increased spleen weight. This occurred only in miltefosine treated group that presented average spleen weights significantly lower to the non-treated and comparable with healthy group (Ordinary one-way ANOVA with Dunnett's multiple comparisons test. Single pooled variance) (Figure 5 panel A) The data on liver shows no differences among all the groups probably because our infection model did not originate hepatomegaly (Figure 5 panel B)

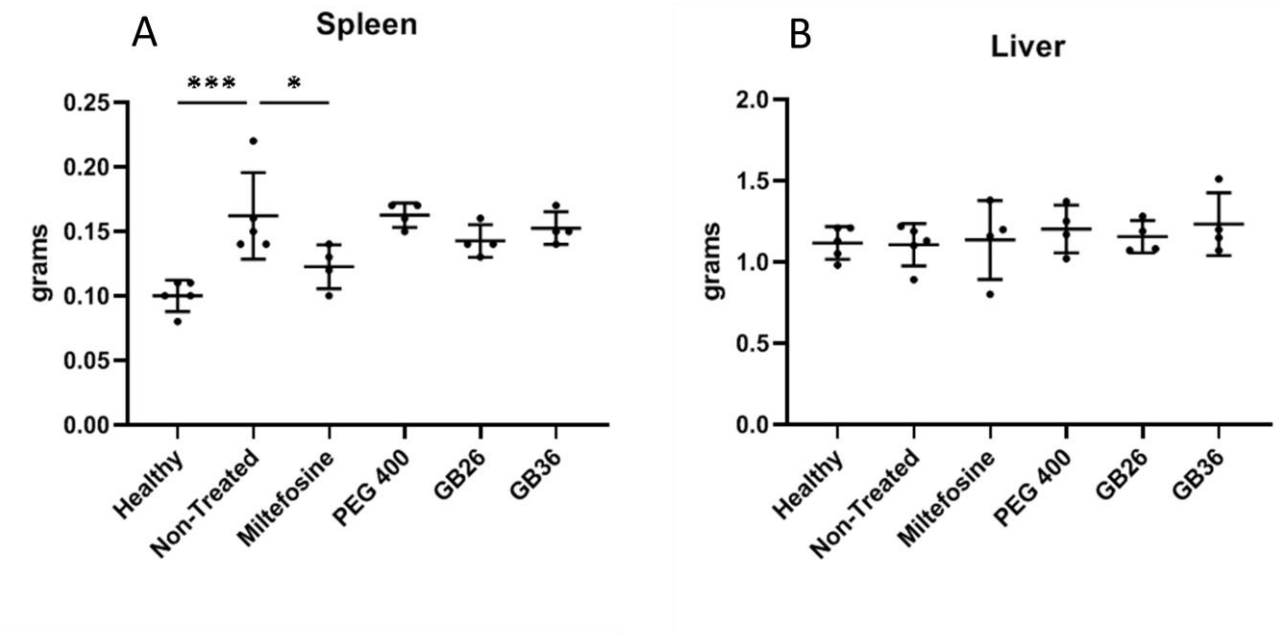

[Figure 5] Organs' weight at the end of 10 days of treatment. The scatter dot plot represents the Mean ± SD. Ordinary one-way ANOVA with Dunnett's multiple comparisons test (single pooled variance). *p ≤ 0.05 *** p ≤ 0.001 (GraphPad Prism version 8.0.2).

Moreover, in order to evaluate the efficacy of the treatment to fight infection, the calculation of the parasite burden was performed using the gold standard limiting dilution assay. Organ homogenates (1 mg of spleen and 10 mg of liver) and $1x10^5$ bone marrow cells were subjected to serial dilutions in 96-well microtitration plates and were incubated at 27 °C for 15 days to find the final dilution for which the well contained at least one parasite. Results showed that miltefosine was able to reduce the parasite burden in all the organs (more than 99,9%) (Figure 6). In particular, no parasites were detected in the liver after the miltefosine treatment (considering the limit of detection of the technique) (Figure 6, panel A). Unfortunately, no other treatment was able to significantly reduce parasite burden in any organ. (Ordinary one-way ANOVA with Dunnett's multiple comparisons test; single pooled variance)

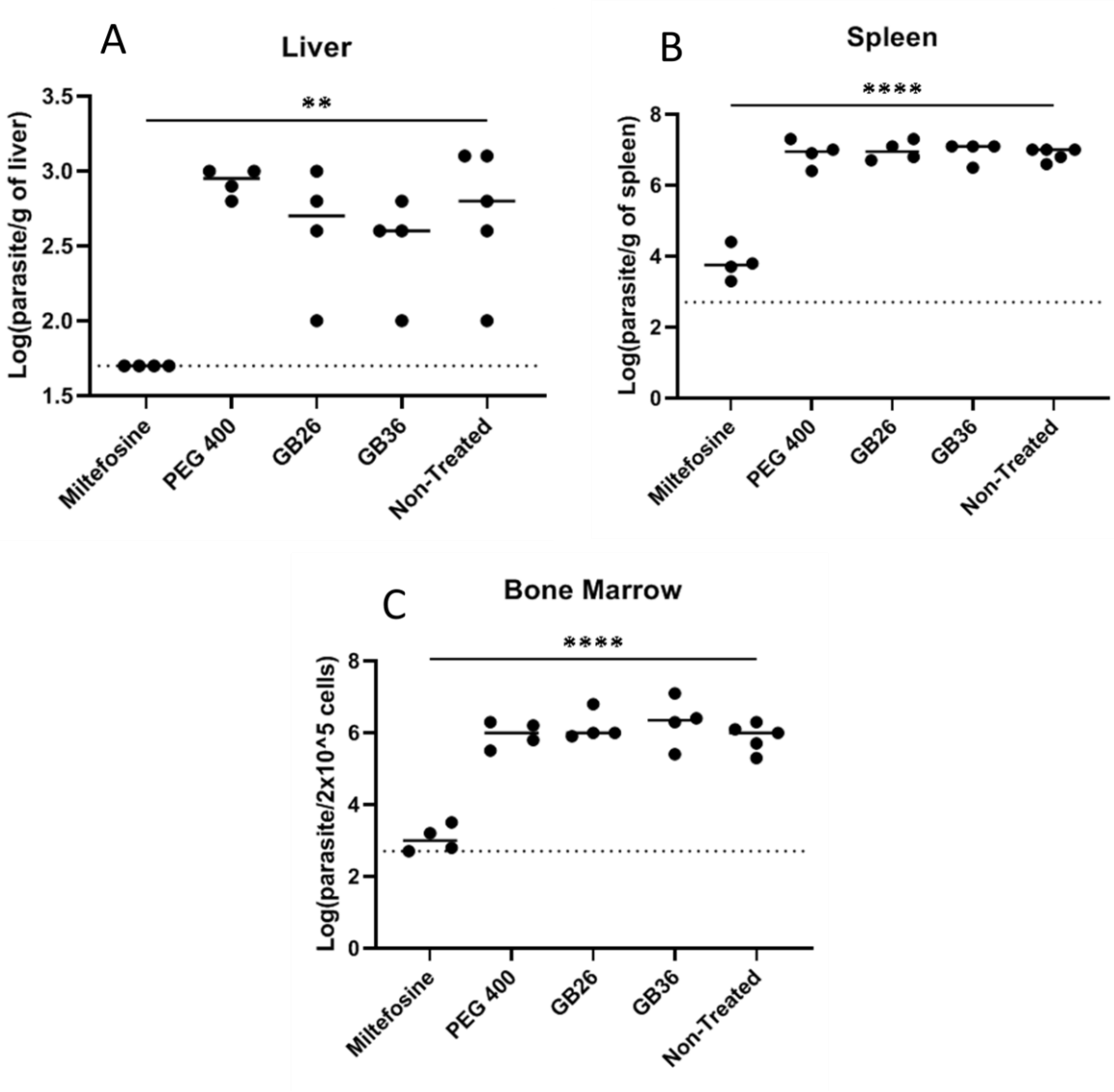

[Figure 6] Parasite burden in liver, spleen and bone marrow. The scatter dot plot represents the Median. Ordinary one-way ANOVA with Dunnett's multiple comparisons test (single pooled variance). **p ≤ 0.01 **** p ≤ 0.0001. The dashed line in the graphs represents the limit of detection of the technique (GraphPad Prism version 8.0.2).

4. Discussion

According to the WHO, neglected tropical diseases affect more than 1 billion people, primarily poor populations living in tropical and subtropical geographical territories. Despite the efforts to improve prevention strategies and surveillance programs, they represent a global health concern. Among them, leishmaniasis and human African trypanosomiasis are two of the most important. In particular, human leishmaniasis is second only to malaria in terms of deaths for parasitic diseases. Moreover, because of

climate changes and migrations, parasites are spreading in non-endemic areas, including non-tropical areas. Up to now, there are no vaccinations available, and the common treatments present limitations related to high costs, difficulties in administration, side effects and toxicity, and, more important, they became less effective due to the emergence of resistant strains. In this context, the development and discovery of safe and effective drugs remain a challenge. Several research groups proposed new classes of compounds with potential anti-parasitic effects, including indole-derivatives. Based on the information present in the literature and on the results previously obtained with the phenotypic screening of a small library of azole-bisindoles (chapter 7, submitted paper), we decided to extend the screening to new compounds and to test them on *L. infantum* and *T. brucei.* The eight classes of indole tested showed different results in terms of efficacy on parasites. In general, the imidazole-bisindole derivatives are more toxic than other classes in THP1 cell line, resulting in lower selectivity indices. GB14 and GB15 (planar Rigid Bisindole-Imidazoles) showed some solubility problems following subsequent thawing, causing problems in the results reproducibility. Concerning *T. brucei,* the most active classes were bisindole-pyrrole, bisindole-triazoles (excepted for GB12), and planar semi-rigid Indoline-Indole-Pyrrole (GB17) with IC_{50} values lower than 10 µM. As already shown on *Leishmania* in the previous work, and also on *T. brucei,* the addition of a nitrogen containing aryl substituent increases the potency compared with the simple bisindole scaffold (DIM showed an IC_{50} > 10 µM). In the pyrrole class, the addition of bromine at the indole rings significantly increases effectiveness. On the other hand, double substitution is detrimental for the activity (compounds GB02 showed high activity than GB04, although with higher cytotoxicity) (Table 4). Compared with pentamidine, the selectivity indexes were not particularly interesting since the reference drug effectiveness lies in the nanomolar range. Nevertheless, due to the toxicity and the use limited to the first phase of the disease, it is not conclusive on clinical applicability. Regarding *Leishmania*, in addition to the pyrrole URB1483 (GB36) identified in the previous work, another class of compounds, rigid Indole-Imidazoles, showed interesting IC_{50} on *in-vitro* promastigotes. In particular, GB26 and GB28, characterized respectively by ethyl and n-propyl substitution on imidazole ring, had IC_{50}

< 1 μM. The potency was clearly higher compared with miltefosine, as well as the SI (Table 3).

Subsequently, the ten best compounds in terms of SI on *Leishmania* promastigotes have been selected to be evaluated on *L. infantum* intracellular amastigotes. In general, compared with IC_{50} on promastigotes, the values resulted dramatically higher probably due to a bioavailability problem of compounds inside the infected cells. On the contrary, miltefosine showed high efficacy to fight cell infection (Table 5). Considering the results on intracellular amastigotes, compounds GB26 and GB36 have been selected for *in-vivo* experiments on infected BALB/c mice. After the solubility evaluation, mice have been treated IP with 5mg/kg of compound resuspended in 60% PEG 400. The formulation resulted well tolerated and no toxicity symptoms occurred. The parasite burden evaluated in spleen, liver and bone marrow showed that only miltefosine was able to heal mice from infection (Figure 6). Unfortunately, the treatment with GB26 and GB36 compounds did not reduce significantly parasite burden in any organ indicating therapeutic failure under these conditions. The good results on *in-vitro* assays suggest indole-derivative compounds as promising antiparasitic agents and represent the bases for further studies in terms of compounds optimization and solubility and bioavailability improvement. In this view, an effective delivery system using nanocarriers such as liposomes or decorated liposomes to improve selective uptake from macrophages could be pivotal for further *in-vivo* studies. Moreover, the molecular target(s) as well as mechanism of action of this class of compounds still need to be investigated.

5. Conclusion

The phenotypic screening of a library of indole-derivative compounds for their potential anti-parasitic effect against *L. infantum* and *T. brucei* was performed. Several classes of compounds showed good activity on in-vitro assay showing an IC_{50} < 5 μM and not relevant cytotoxicity on THP1 cell line. The ten less toxic and more active compounds were selected to test the efficacy on *Leishmania* intracellular amastigotes and two of them have been tested on an *in-vivo* infection model. After 21 days of infection, BALB/c mice have been treated with 5mg/Kg of drug for ten days. The formulation resulted well tolerated by the animals but, unfortunately, at this dosage, the treatments did not be

able to revert the infection and reduce the parasite burden in the mice's organs. Despite the negative results of *in-vivo* experiments, these findings allow us to identify a new promising class of compound against *L. infantum* (rigid Indole-Imidazoles) and a new scaffold active on *T. brucei* representing the bases for further optimization and development studies.

Acknowledgments

I would like to thank the Parasite Disease group of the Institute of Research and Innovation in Health (i3s) - University of Porto (Portugal), in particular the group chief Professor Anabela Cordeiro-da-Silva, my supervisor Dr. Nuno Santarem and my lab mate Dr. Ricardo Monteiro for hospitality and knowledge sharing. Thanks also to Professor Simone Lucarini for providing compounds tested in this work.

References

Avery, V.; Buckner, F.; Baell, J.; Fairlamb, A.; Michels, P.A.; Tarleton, R. Ask the Experts: Drug discovery for the treatment of leishmaniasis, African sleeping sickness and Chagas disease. Future Med. Chem. 2013, 5, 1709–1718

Bharate, S. B., Bharate, J. B., Khan, S. I., Tekwani, B. L., Jacob, M. R., Mudududdla, R., Yadav, R. R., Singh, B., Sharma, P. R., Maity, S., Singh, B., Khan, I. A., and Vishwakarma, R. A. (2013) Discovery of 3,3'-diindolylmethanes as potent antileishmanial agents. *Eur. J. Med. Chem.* 63, 435-443. DOI: 10.1016/j.ejmech.2013.02.024.

Borsari C, Luciani R, Pozzi C, Poehner I, Henrich S, Trande M, Cordeiro-da-Silva A, Santarem N, Baptista C, Tait A, Di Pisa F, Dello Iacono L, Landi G, Gul S, Wolf M, Kuzikov M, Ellinger B, Reinshagen J, Witt G, Gribbon P, Kohler M, Keminer O, Behrens B, Costantino L, Tejera Nevado P, Bifeld E, Eick J, Clos J, Torrado J, Jiménez-Antón MD, Corral MJ, Alunda JM, Pellati F, Wade RC, Ferrari S, Mangani S, Costi MP. Profiling of Flavonol Derivatives for the Development of Antitrypanosomatidic Drugs. J Med Chem. 2016 Aug 25;59(16):7598-616. doi: 10.1021/acs.jmedchem.6b00698. Epub 2016 Aug 5. PMID: 27411733.

Ciccolini C., M Mari M.,, S Lucarini S., Mantellini F., Piersanti G., Favi G. (2018) Polycyclic Indolines by an Acid-Mediated Intramolecular Dearomative Strategy: Reversing Indole Reactivity in the Pictet-Spengler-Type Reaction. Advanced Synthesis & Catalysis 360 (21), 4060-4067 doi.org/10.1002/adsc.201800981

Hirumi H., Hirumi K. Continuous cultivation of *Trypanosoma brucei* blood stream forms in a medium containing a low concentration of serum protein without feeder cell layers. *J. Parasitol.* 1989;75:985–989

Kalam Khan, F. A., Zaheer, Z., Sangshetti, J. N., Patil, R. H., and Farooqui, M. (2017) Antileishmanial evaluation of clubbed bis(indolyl)-pyridine derivatives: one-pot synthesis, *in vitro* biological evaluations and *in silico* ADME prediction. *Bioorg. & Med. Chem. Let.* 27, 567–573. DOI: 10.1016/j.bmcl.2016.12.018.

Klug DM, Mavrogiannaki EM, Forbes KC, Silva L, Diaz-Gonzalez R, Pérez-Moreno G, Ceballos-Pérez G, Garcia-Hernández R, Bosch-Navarrete C, Cordón-Obras C, Gómez-Liñán C, Saura A, Momper JD, Martinez-Martinez MS, Manzano P, Syed A, El-Sakkary N, Caffrey CR, Gamarro F, Ruiz-Perez LM, Gonzalez Pacanowska D, Ferrins L, Navarro M, Pollastri MP. Lead Optimization of 3,5-Disubstituted-7-Azaindoles for the Treatment of Human African Trypanosomiasis. J Med Chem. 2021 Jul 8;64(13):9404-9430. doi: 10.1021/acs.jmedchem.1c00674. Epub 2021 Jun 22. PMID: 34156862; PMCID: PMC8412142.

Kourbeli V, Chontzopoulou E, Moschovou K, Pavlos D, Mavromoustakos T, Papanastasiou IP. An Overview on Target-Based Drug Design against Kinetoplastid Protozoan Infections: Human African Trypanosomiasis, Chagas Disease and Leishmaniases. Molecules. 2021 Jul 30;26(15):4629. doi: 10.3390/molecules26154629. PMID: 34361781; PMCID: PMC8348971.

Magoulas GE, Afroudakis P, Georgikopoulou K, Roussaki M, Borsari C, Fotopoulou T, Santarem N, Barrias E, Tejera Nevado P, Hachenberg J, Bifeld E, Ellinger B, Kuzikov M, Fragiadaki I, Scoulica E, Clos J, Gul S, Costi MP, de Souza W, Prousis KC, Cordeiro da Silva A, Calogeropoulou T. Design, Synthesis and Antiparasitic Evaluation of Click Phospholipids. Molecules. 2021 Jul 10;26(14):4204. doi: 10.3390/molecules26144204. PMID: 34299479; PMCID: PMC8305768.

Mantenuto, S., Ciccolini, C., Lucarini, S., Piersanti, G., Favi, G., and Mantellini F. (2017) Palladium(II)-catalyzed intramolecular oxidative C–H/C–H cross-coupling reaction of C3,N-linked biheterocycles: rapid access to polycyclic nitrogen heterocycles, *Org. Lett.* 19 (3), 608-611. DOI: 10.1021/acs.orglett.6b03775.

Mantenuto, S., Lucarini, S., De Santi, M., Piersanti, G., Brandi, G., and Favi, G. (2016) One-pot synthesis of biheterocycles based on indole and azole scaffolds using tryptamines and 1,2-diaza-1,3-dienes as building blocks. *Eur. J. Org. Chem.* 19, 3193–3199. DOI: 10.1002/ejoc.201600210.

Mendes Costa D, Cecílio P, Santarém N, Cordeiro-da-Silva A, Tavares J. Murine infection with bioluminescent Leishmania infantum axenic amastigotes applied to drug discovery. Sci Rep. 2019 Dec 12;9(1):18989. doi: 10.1038/s41598-019-55474-3. PMID: 31831809; PMCID: PMC6908656.

Roy, A., Das, B. B., Ganguly, A., Dasgupt, S. B., Khalkho, N. V. M., Pal, C., Dey, S., Giri, V. S., Jaisankar, P., Dey, S., Majumder, H. K. (2008) An insight into the mechanism of inhibition of unusual bi-subunit topoisomerase I from *Leishmania donovani* by 3,3'-di-indolylmethane, a novel DNA topoisomerase I poison with a strong binding affinity to the enzyme. *Biochem. J*. 409**,** 611–622. DOI: 10.1042/BJ20071286.

Seixas, J.; Atouguia, J.; Josenando, T.; Vatunga, G.; Bilenge, C.M.M.; Lutumba, P.; Burri, C. Clinical study on the melarsoprol-related encephalopathic syndrome: Risk factors and HLA association. Trop. Med. Infect. Dis. **2020**, 5, 5

Sereno, D.; Cavaleyra, M.; Zemzoumi, K.; Maquaire, S.; Ouaissi, A.; Lemesre, J.L. Axenically grown amastigotes of Leishmania infantum used as an in vitro model to investigate the pentavalent antimony mode of action. Antimicrob. Agents Chemother. **1998**, 42, 3097–3102.

Sereno D, Roy G, Lemesre JL, Papadopoulou B, Ouellette M. DNA transformation of Leishmania infantum axenic amastigotes and their use in drug screening. Antimicrob Agents Chemother. 2001 Apr;45(4):1168-73. doi: 10.1128/AAC.45.4.1168-1173.2001. PMID: 11257031; PMCID: PMC90440.

Simarro, P.P.; Franco, J.; Diarra, A.; Postigo, J.A.R.; Jannin, J. Update on field use of the available drugs for the chemotherapy of human African trypanosomiasis. Parasitology **2012**, 139, 842–846

Taha, M., Uddin, I., Gollapalli, M., Almandil, N. B., Rahim, F., Farooq, R. K., Nawaz, M., Ibrahim, M., Alqahtani, M. A., Bamarouf, Y. A., and Selvaraj, M. (2019) Synthesis, anti‐leishmanial and molecular docking study of bis‐indole derivatives. *BMC Chemistry* 13, 102. DOI: 10.1186/s13065-019-0617-4.

Tavares, J., Santarém, N. & Cordeiro-da-Silva, A. Quantifcation of Leishmania Parasites in Murine Models of Visceral Infection. Methods Mol Biol 1971, 289–301, https://doi.org/10.1007/978-1-4939-9210-2_16 (2019)

WHO. *Control and Surveillance of Human African Trypanosomiasis.* World Health Organization; Geneva, Switzerland: 2013. (Technical Report Series No. 984)

Wiedemar, N.; Hauser, D.A.; Mäser, P. 100 Years of Suramin. Antimicrob. Agents Chemother. **2020**, 64, 1–14

CHAPTER 9

Previously it has been shown that *L. infantum* induces a mild but significant increase in endoplasmic reticulum (ER) stress expression markers to promote parasites' survival in human and murine infected macrophages. Moreover, it was demonstrated that the miRNA hsa-miR-346, induced by the UPR-activated transcription factor sXBP1, was significantly upregulated in human macrophages infected with different *L. infantum* strains. However, no literature exists regarding the ER stress response and miR-346 expression in infected dogs, which represent important reservoirs for *Leishmania* parasite. Therefore, this study aimed to investigate these pathways in the canine monocyte cell line DH82 infected by *Leishmania* spp. and to evaluate the presence of cfa-miR-346 in plasma of healthy and infected dogs.

(Unpublished data)

Cfa-miR-346 is a potential plasma biomarker of canine leishmaniasis

Abstract

Leishmaniases are a group of anthropo-zoonotic parasitic diseases caused by a protozoan of the *Leishmania* genus, affecting both humans and other vertebrates, including dogs. *L. infantum* is responsible for the cutaneous and visceral form of the disease in humans and CanL in dogs. Previously, we have shown that *L. infantum* induces a mild but significant increase in endoplasmic reticulum (ER) stress expression markers to promote parasites' survival in human and murine infected macrophages. Moreover, we demonstrated that the miRNA hsa-miR-346, induced by the UPR-activated transcription factor sXBP1, was significantly upregulated in human macrophages infected with different *L. infantum* strains. However, no literature exists regarding the ER stress response and miR-346 expression in infected dogs, which represent important reservoirs for *Leishmania* parasite. Therefore, this study aimed to investigate these pathways in the canine macrophagic-like cell line DH82 infected by *Leishmania* spp. and to evaluate the presence of cfa-miR-346 in plasma of healthy and infected dogs. The DH82 cells were infected with *L. infantum* and *L. braziliensis* parasites and the expression of cfa-mir-346, as well as several ER stress markers, was evaluated by quantitative PCR (qPCR) at different time points. As ER stress positive control, cells were treated with 2 μg/ml of tunicamycin. Furthermore, the cfa-miR-346 was monitored in plasma collected from healthy dogs (n=11) and dogs naturally infected by *L. infantum* (n=18).

The results in DH82 cells showed that cfa-mir-346 was induced at both 24 h and 48 h post-infection with all *Leishmania* strains but not with tunicamycin, accounting for a mechanism of induction independent from sXBP1, unlike what was previously observed in human cell lines. Moreover, the cfa-miR-346 expression analysis on dog's plasma revealed a significant increase in infected dogs compared to non-infected dogs. Despite the cfa-miR-346 appears to be an infection marker in dogs affected by Leishmaniasis, its role during *Leishmania* infection needs to be further elucidated.

1. Introduction

Leishmaniasis includes a group of anthropo-zoonotic diseases caused by a protozoan belonging to the *Leishmania* genus, which can have different hosts, like humans, dogs, or wild animals (Abbate et al., 2019; Risueño et al., 2018). According to WHO data, leishmaniasis shows a worldwide distribution, involving at least 98 countries, with the highest number of cases in developing countries (Alvar et al., 2012). Italy, in particular the southern regions (including Sicily and Sardinia), is a country highly endemic for leishmaniasis caused by *Leishmania* (*L*.) *infantum*. Nevertheless, cases of canine leishmaniasis (CanL) and human leishmaniasis are largely underestimated due to the lack of notification of new cases, and the difficulty in diagnosing or misdiagnosis (Gaspari et al., 2017). Although a subclinical or self-limiting form was described, CanL represents a very critical problem in veterinary medicine, because the disease can be severe and with fatal exitus (Solano-Gallego et al., 2011). The most frequent signs of CanL are lymphadenopathy, onychogryphosis, cutaneous lesions, weight loss, cachexia, fever and locomotor abnormalities (Baneth et al., 2008).

Leishmania is a dimorphic parasite that develops as promastigotes in the midgut of the sand-fly and as intracellular amastigotes in phagocytic cells, mainly macrophages, of the vertebrate host. *Leishmania* promastigotes enter in the host macrophages, where they survive and replicate within the phagolysosomal environment, subverting the innate immune response and metabolic pathways of the host (Arango Duque & Descoteaux, 2015; Podinovskaia & Descoteaux, 2015).

Among different mechanisms activated by *L. (L.) infantum* to survive and to spread the infection in the host cell, we previously reported the mild induction of the Unfolded Protein Response (UPR) in human monocytic cell lines (U937 and THP-1) and murine primary macrophages (Galluzzi et al., 2016). The mild UPR could represent a common pathogenic mechanism among the different species of *Leishmania* (*Leishmania*), also considering the role of X-box binding protein 1 (XBP1) in the *L. amazonensis* infection highlighted by Dias Teixeira et al. (Dias-Teixeira et al., 2016). The unconventional splicing of XBP1 mRNA, induced by the ER transmembrane protein IRE1, originates a spliced mRNA (sXBP1) encoding an active transcription factor that leads to the expression of chaperones, proinflammatory cytokines (Martinon et al., 2010) and genes involved in the

autophagic response (Margariti et al., 2013). Moreover, Bartoszewski et al., (2011) showed that, during endoplasmic reticulum (ER) stress, sXBP1 induces miR-346 in both human and murine cells. We have previously reported the significant induction of miR-346, in both U937 and THP-1 human cell lines infected with four different strains of *L.* (*L.*) *infantum* and a human clinical isolate of *L*. (*V.*) *braziliensis* (Diotallevi et al., 2018). MicroRNAs have gained more and more relevance in the last years in the context of host-pathogen interaction. In fact, it is known that many intracellular parasites are able to modify the miRNA expression profiles of host cells (Acuña et al., 2020). In particular, in the context of CanL, Bragato et al. reported a differential modulation in the expression of miR-150, miR-451, miR-192, miR-194, and miR-371 in PBMCs of symptomatic dogs naturally infected with *L. infantum*. These miRNAs can target genes involved in the immune response and pathogenesis, such as NF-κB, TNF-α, CD80, and IFN-γ. (Bragato et al., 2018).

In this study we investigated the UPR and the induction of cfa-miR-346 in a canine macrophage-like cell line (DH82) infected with *Leishmania* spp. Furthermore, the presence of cfa-miR-346 in the plasma of non-infected and infected dogs and its potential role as a marker of infection was analyzed.

2. Materials and methods

2.1 *Leishmania* parasites cultivation

Three *L.* (*L.*) *infantum* reference strains (MHOM/TN/80/IPT1, MHOM/FR/78/LEM75 and MHOM/IT/08/31U), and one *L.* (*L.*) *infantum* canine clinical isolate (isolate 42) were provided by the OIE Reference Laboratory National Reference Centre for Leishmaniasis (C.Re.Na.L.) (Palermo, Italy). Moreover, a *L.* (*V.*) *braziliensis* clinical isolate (isolate AN1), identified at the species level by PCR RFLP as described by Schönian et al. (Schönian et al., 2003), was obtained from a pharyngolaryngeal biopsy during routine diagnosis of a human patient with suspect MCL, as previously described (Ceccarelli et al., 2020; Diotallevi et al., 2018). *Leishmania* promastigotes were cultivated at 26-28°C in Evans' Modified Tobie's Medium (EMTM) (Castelli et al., 2014) and stationary promastigotes were transferred to fresh medium (ratio 1:5) every 5-7 days.

2.2 Cell culture and infection

The canine macrophage-like cell line DH82 (ATCC® CRL-10389™) was cultured in an incubator at 37°C and 5% CO_2 in Eagle's Minimum Essential Medium (EMEM) supplemented with 15% heat-inactivated Fetal Bovine Serum (FBS), 2 mM L-glutamine, 10 g/l Non-Essential Amino Acid, 1 mM sodium pyruvate, 100 µg/ml streptomycin, 100 U/l penicillin. For infection experiments, $2.5x10^5$ cells were seeded in 35 mm dishes for 24 hours for cell adhesion. Then, cells were infected with stationary-phase promastigotes of *L.* (*L.*) *infantum* strains/isolate or *L.*(*V.*) *braziliensis* clinical isolate with a parasite-to-cell ratio of 10:1. To exclude the modulation of target genes by the phagocytosis mechanism of macrophages, $2.5x10^6$ promastigotes of *L.* (*L.*) *infantum* MHOM/TN/80/IPT1 and canine clinical isolate 42 were inactivated (heat-killed – HK) at 70°C for 45 minutes and placed into DH82 culture medium. To promote and synchronize cell infection, dishes were centrifuged at 450 x g for 3 minutes at room temperature. After 24h, non-internalized parasites were removed by medium replacement. As ER-stress positive control, cells were treated with 2 µg/ml of tunicamycin for 4 h or with vehicle dimethyl sulfoxide (DMSO) as control. All cell culture reagents were purchased from Sigma-Aldrich (St. Louis, MO). After 6h, 24 h, and 48 h from infection, cells were

directly lysed for gene expression analysis; moreover, one dish for each time point was stained with Hoechst and Acridine Orange dyes and the infection index was calculated by multiplying the percentage of infected macrophages by the average number of parasites per macrophage. At least 300 macrophages were counted for each condition.

2.3 Animals recruitment

To evaluate the presence of cfa-miR-346 in clinical samples, 21 mixed breed dogs from Pantelleria Island (Sicily, Italy), an endemic area for leishmaniasis, were recruited for this study by the C.Re.Na.L. in Palermo (Italy) (Vitale et al., 2020). Additional 8 plasma samples of healthy and infected dogs have been supplied by the veterinary clinic "Santa Teresa" in Fano (Pesaro-Urbino, Italy). All samples were collected for diagnostic purposes during routine examination; oral informed consent was obtained from the owners of dogs. To diagnose CanL, every dog was subjected to physical, clinical, and dermatological evaluation, including the anamnestic history and changes compatible with CanL (e.g., alopecia and desquamation, nodular or ulcerative lesions, exfoliative dermatitis weight loss, lymphadenomegaly). In addition, serological [i.e. IFAT, SNAP test (IDEXX Laboratories, Westbrook, Maine, USA) or Speed Leish K test (BVT Groupe Virbac, La Seyne sur Mer, France] and qPCR-based tests (Vitale et al., 2004) were performed on blood and/or lymph nodal aspirates. In two cases (IDs 42 and 64), *L.* (*L.*) *infantum* amastigotes isolation was obtained as previously described (Castelli et al., 2020). After diagnosis, dogs were divided into two groups: i) non-infected: negative for clinical signs and/or negative IFAT, negative qPCR, negative for SNAP test or for Speed Leish K test; ii) infected: presence of clinical signs, IFAT ≥1:40 and/or positive qPCR, and/or positive SNAP test or Speed Leish K test. Details of samples are summarized in Table 1.

Sample ID	Clinical signs	IFAT	SNAP TEST	qPCR on blood samples	qPCR on Lymph nodal (parasites/ml)	Parasite's isolation	Diagnosis
24	Lymphadenomegaly	Neg	n.a.	Neg	Neg	n.a.	-
29	Neg	Neg	n.a.	Neg	n.a.	n.a.	-
35	Neg	Neg	n.a.	Neg	Neg	n.a.	-
43	Eye signs	Neg	n.a.	Neg	n.a.	n.a.	-
46	Neg	Neg	n.a.	Neg	n.a.	n.a.	-
52	Neg	Neg	n.a.	Neg	n.a.	n.a.	-
54	Neg	Neg	n.a.	Neg	n.a.	n.a.	-
GOA	Neg	Neg	n.a.	n.a.	n.a.	n.a.	-
GON	Neg	Neg	n.a.	n.a.	n.a.	n.a.	-
VIA	Neg	Neg	n.a.	n.a.	n.a.	n.a.	-
ZAR	Neg	Neg	n.a.	n.a.	n.a.	n.a.	-
9	Lymphadenomegaly	1:160	n.a.	Neg	35	n.a.	+
11	Lymphadenomegaly	1:320	n.a.	Neg	n.a.	n.a.	+
23	Skin signs, Lymphadenomegaly	1:320	n.a.	Neg	320	n.a.	+
30	Skin signs, Lymphadenomegaly	1:320	n.a.	Neg	Neg	n.a.	+
31	Skin signs	1:80	n.a.	Neg	30	n.a.	+
32	Neg	1:320	n.a.	Neg	Neg	n.a.	+
40	Skin signs	1:320	n.a.	Neg	45	n.a.	+
42	Neg	1:5120	n.a.	Neg	165000	Pos	+
45	Neg	1:40	n.a.	Neg	165	Bacterial contamination	+
49	Eye signs	1:160	n.a.	Neg	n.a.	n.a.	+
51	Neg	Neg	n.a.	Neg	30	n.a.	+
58	Lymphadenomegaly	1:2560	n.a.	Neg	60	n.a.	+
63	Neg	1:80	n.a.	Neg	225	n.a.	+
64	Skin and eye signs, lymphadenomegaly	1:2560	n.a.	Neg	5700	Pos	+
STA-VOI	Mild periocular dermatisis, anemia, thrombocytopenia	n.a.	Pos	n.a.	n.a.	n.a.	+

MAI-EUI	Alopecia, weight loss, mild onychogryphosis, lymphadenomegal, leucopenia, decline in performance	n.a.	Pos	n.a.	n.a.	n.a.	+
MIA-MAI	Chronic anemia	n.a.	Pos	n.a.	n.a.	n.a.	+
KIO-MEI	Neg	n.a.	Pos	n.a.	n.a.	n.a.	+

[Table 1] Dogs recruited for the study. Pos: positive; neg: negative; n.a.: data not available; +: infected dogs; -: non-infected dogs

2.4 Plasma collection

1 mL of peripheral blood was collected from the jugular vein of each dog and placed into tubes containing ethylene diamine tetraacetic acid (EDTA). Blood was centrifuged at 1500 x g for 15 minutes at 4 °C to separate plasma from the corpuscular part. Plasma collected was further centrifuged at 3000 x g for 15 minutes at 4°C to remove any cellular debris. The supernatant (150 µl) was transferred in a sterile tube and processed as described below.

2.5 RNA isolation and cDNA synthesis

RNA extraction from DH82 infected and non-infected cells was performed with the miRNeasy Mini Kit (Qiagen, Hilden, Germany) after direct lysis with 700 µl of QIAzol Lysis Reagent (Qiagen, Hilden, Germany). RNA extraction from plasma was carried out with Total RNA Purification Kit (Norgen Biotek Corporation, Ontario, Canada) according to the manual instructions specific for plasma. In both cases, extracted RNA was quantified with a NanoVue PlusTM spectrophotometer (GE Healthcare Life Sciences, Piscataway, NJ, United States).

For gene expression analysis in DH82 cells, total RNA (500 ng) was reverse-transcribed using PrimeScriptTM RT Master Mix (Perfect Real Time) (Takara Bio Inc.). For expression analysis of miR-16 and miR-346 in all samples, total RNA (1-5 ng/µl) was reverse-transcribed with the TaqMan™ MicroRNA Reverse Transcription Kit (Applied Biosystems).

2.6 Quantitative Real-Time PCR

The expression of several ER stress markers and GRID1 was evaluated by qPCR as previously described (Galluzzi et al., 2016) with some modifications. Briefly, the qPCR reactions were carried out in duplicate in a final volume of 20 µl using TB Green PreMix ex Taq II Master Mix (Takara Bio Europe, France) and 200 nM primers listed in Table 2. The amplification conditions were: 95 °C for 10 min, 40 cycles at 95 °C for 10 s and 60 °C for 50 s, followed by a melting curve analysis at the end of each run from 65-95 °C, to exclude the presence of non-specific products or primer dimers. As reference gene, GAPDH (glyceraldehydes-3-phosphate dehydrogenase) was selected. To evaluate the expression of cfa-miR-346, the qPCR reactions were performed with a specific Taqman small RNA assay (Applied Biosystems), according to the manufacturer instructions. The amplification protocol was: 95 °C for 10 min, 50 cycles at 95 °C for 15 s and 60 °C for 50 s. The microRNA cfa-miR-16 was used as reference gene (Heishima et al., 2017; Hulanicka et al., 2014). All qPCR reactions were performed in a RotorGene 6000 instrument (Corbett life science, Sydney, Australia). A duplicate non-template control was included for each primer pair reaction as negative control. The relative expression levels were calculated using the $2^{-\Delta\Delta Ct}$ method (Pfaffl, 2001).

Target mRNA	Accession number	Forward primer (5′-3′)	Reverse primer (5′-3′)
Atf3	XM_022420880.1	TTCGCCATCCAGAACAAGCA	GGGCTACCTCAGTTTTCGTG
Atf4	XM_854584.5	TTCTCCAGCGACAAGGCTAA	AAGGCATCCTCCTTTCCGTTG
Chop/ Ddit3	XM_014117187.2	CTGGAAACAAGGAGGAAGAATCA	GGCTCTGGAAGGTGTTCGTG
Gapdh	NM_001003142.2	GTCCCCACCCCCAATGTATC	TCCGATGCCTGCTTCACTAC
Grid1	XM_022417615.1	TACAGCAAGGTGGCGAATCCT	AGGAGCACACAATGAGGGTGA
Hspa5	XM_858292.5	TGGCATAAACCCAGACGAGG	AGGGGACATACATCAAGCAGT
sXbp1	XM_849540.5	CTGAGTCCGCAGCAGGT	TGAACAGAATGCCCAACAGG
uXbp1	XM_849540.5	CCGCAGCACTCAGACTACG	TGAACAGAATGCCCAACAGG

[Table 2] Primers sequence. **Atf3**, Canis lupus familiaris activating transcription factor 3; **Atf4**, Canis lupus familiaris activating transcription factor 4; **Chop**, Canis lupus familiaris DNA damage inducible transcript 3; **Gapdh**, Canis lupus familiaris glyceraldehyde-3-phosphate dehydrogenase; **Grid1**, Canis lupus familiaris glutamate ionotropic receptor delta type subunit 1; **Hspa5**, Canis lupus familiaris heat shock protein family A (Hsp70) member 5; **sXbp1**, Canis lupus familiaris X-box binding protein 1 (spliced); **uXbp1**, Canis lupus familiaris X-box binding protein 1 (unspliced).

2.7 Statistical analysis

Statistical analysis was performed by unpaired t-test or one-way ANOVA with Tukey's multiple-comparison post-test. Values are expressed as mean ± standard deviation (SD). All statistical tests were performed using GraphPad Prism version 5 (GraphPad Software, Inc., La Jolla, CA, USA). A P value ≤ 0.05 was considered statistically significant.

3. Results

3.1 Tunicamycin treatment induces the expression of ER stress markers but not cfa-miR-346 in a canine macrophage-like cell line

Previously it has been shown that *L.* (*L.*) *infantum* could induce a mild but significant increase in ER stress expression markers, including the spliced form of XBP1 (sXBP1), in human and murine infected macrophages (Galluzzi et al., 2016).

To further explore these pathways in a canine cell line, we first determined whether cfa-miR-346 could be induced following ER stress in DH82 cells treated with tunicamycin, an inducer of ER stress through the inhibition of protein N-linked glycosylation. After 4h treatment, the gene expression analysis revealed a significant induction of the ER stress markers (i.e. ATF3, ATF4, CHOP, HSPA5, sXBP1) compared to vehicle DMSO (Unpaired t-test with Welch's correction $p<0.05$) (Fig. 1A). Notably, the unspliced form of XBP1 (uXBP1) resulted downregulated, confirming previous findings in human and murine models. On the contrary, the expression of cfa-miR-346 did not change significantly in response to treatment with Tunicamycin, suggesting a lack of correlation between the upregulation of sXBP1 and the induction of cfa-miR-346 (Fig. 1B).

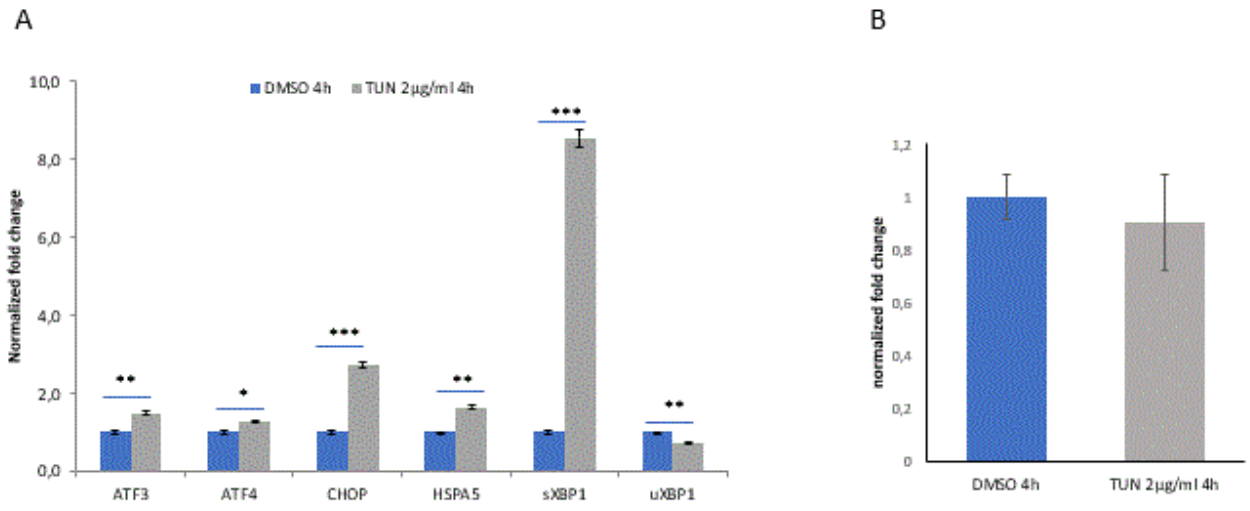

[Figure 1] Tunicamycin treatment induces er stress markers but not mir-346 in DH82 cells. The ER stress expression markers resulted upregulated in DH82 cells treated with tunicamycin 2 µg/ml for 4h (A), while the expression of miR-346 did not change significantly (B). Data are represented as the mean ± SD of technical replicates and are representative of two independent experiments. The graph shows the fold changes in comparison to the control (DMSO). Unpaired t-test *p<0.05 **p<0.01 ***p<0.001

3.2 ER stress response induction by *Leishmania* infection in canine macrophage-like cell line

The ER stress response and induction of cfa-miR-346 were investigated in DH82 cells infected with promastigotes of four *L.* (*L.*) *infantum* strains (i.e. MHOM/TN/80/IPT1, MHOM/FR/78/LEM75, MHOM/IT/08/31U and the canine clinical isolate 42) and a *L.* (*V.*) *braziliensis* human clinical isolate (i.e. AN1) for 24 h and 48 h, as described in methods. The infection indexes are reported in Table 3.

	Infection index 24h	**Infection index 48h**
***L.* (*L.*) *infantum* MHOM/TN/80/IPT1**	143.3 ± 31.1	168.9 ± 58.8
***L.* (*L.*) *infantum* MHOM/FR/78/LEM75**	100.2 ± 22.1	92.7 ± 29.7
***L.* (*L.*) *infantum* MHOM/IT/08/31U**	130.0 ± 10.1	167.8 ± 25.8
***L.* (*L.*) *infantum* canine clinical isolate 42**	189.9 ± 31.9	245.7 ± 50.5
***L.* (*V.*) *braziliensis* human clinical isolate AN1**	185.2 ± 31.2	94.0 ± 26.3

[Table 3] Infection indexes (means ± SD).
Infection index was calculated by multiplying the percentage of infected macrophages by the average number of parasites per macrophage. At least 300 macrophages were counted for each condition.

A significant induction of ER stress expression markers -including sXBP1- was evident after 48h infection with *L. braziliensis*, IPT1 and isolate 42. However, a significant upregulation of cfa-miR-346 was detected at both 24 and 48 hours of infection with all *Leishmania* strains (yellow bar), consolidating the hypothesis that, in the canine cell model, the induction of cfa-miR-346 could not be related to the induction of ER stress expression markers (Fig. 2).

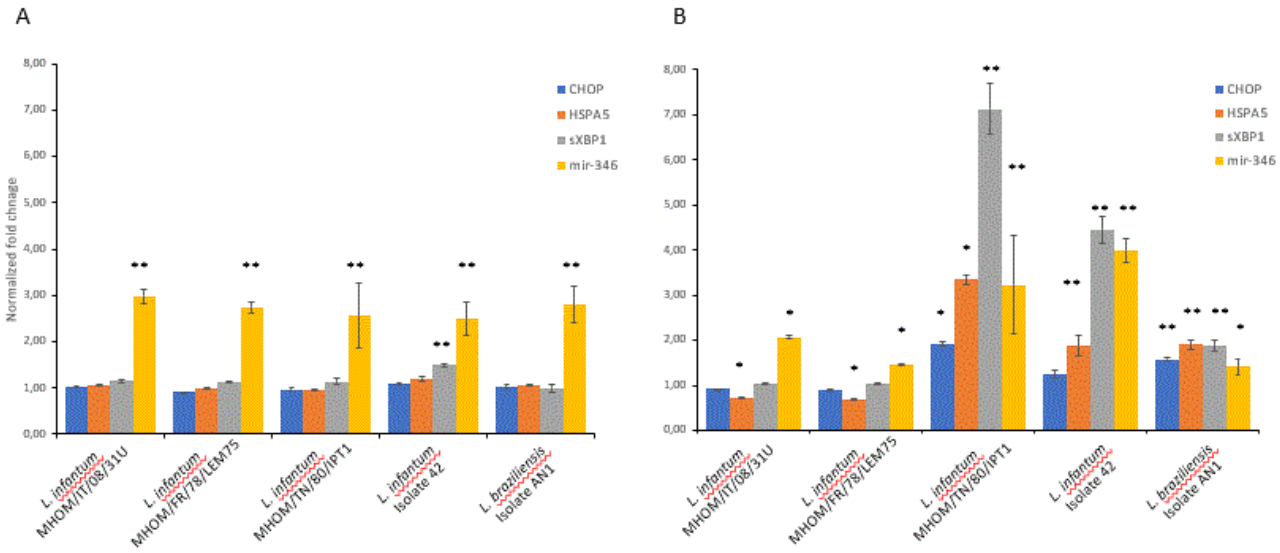

[Figure 2] ER stress markers and mir-346 expression in infected DH82 cells. Gene expression of selected ER stress markers and miR-346 in DH82 cells infected with different *Leishmania* spp. after 24h (A) and 48h (B). Graphs show the fold changes related to the control (non-infected cells). Unpaired t-test with Welch's correction * p <0.05 ** p <0.01

3.3 Cfa-miR-346 induction is related to *Leishmania* spp. active infection and it is independent from GRID1 expression

To deeply analyze the induction of miR-346 following the infection, and therefore to exclude that its regulation was not related to the phagocytosis mechanism of the macrophage, the infection was performed with both live and heat killed (HK) parasites as described in methods.

A significant induction of miR-346 was evident at 6h, 24h, and 48h in cells infected with live parasites. After 6h the induction of mir346 was not significantly different between cells infected with live or HK parasites; however, at 24 and 48 h the mir346 expression in cells treated with HK parasites was significantly lower, dropping close to the values of non-infected controls (Fig. 3). These results further confirm that the induction of miR-346 at 24h and 48h post infection is related to the interaction with the vital pathogen.

As well as hsa-miR-346, Cfa-miR-346, is located in intron 2 of the glutamate ionotropic receptor delta type subunit 1 (GRID1) gene. To investigate if mir-346 upregulation could be due to induction of GRID1, the expression level of GRID1 was evaluated by real-time PCR in infected and non-infected DH82 cells. The real-time PCR assays showed no amplification or amplification with Cq > 33 in some technical replicates, leading to the

conclusion that GRID1 gene was not expressed in either infected or non-infected DH82 cells (data not shown).

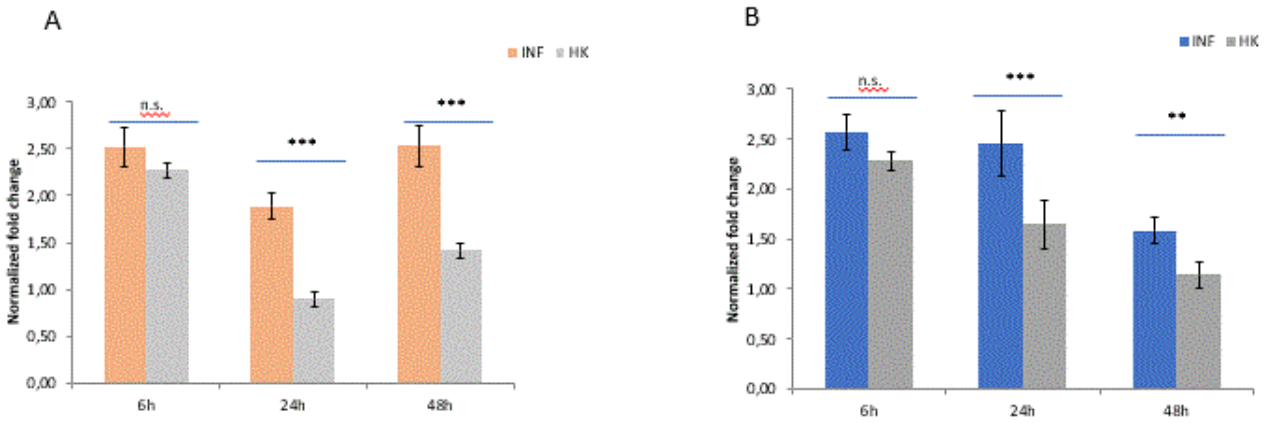

[Figure 3] mir-346 induction is related to active Leishmania infection. miR-346 expression in DH82 cells infected with *L*. (*L*.) *infantum* MHOM/TN/80/IPT1 (A) and canine clinical isolate 42 (B) for 6h, 24h, 48h. Graph shows the fold changes in comparison to non-infected cells (mean ± SD of two independent experiments). One-way ANOVA with Tukey's Multiple Comparison Test. n.s.: not significant, **p<0.01, ***p<0.001

3.4 Cfa-miR-346 expression in plasma of infected dogs

To explore the role of miR-346 in dogs naturally infected with *Leishmania* spp., a study was conducted on 29 mixed breed dogs from Pantelleria island and Marche region (central Italy), both endemic areas for leishmaniasis. The diagnosis of CanL was based on the presence of clinical signs (weight loss, skin and eye signs, lymphadenomegaly) and was confirmed by serological and/or qPCR-based methods, performed on blood and/or lymph node aspirates. In two cases (dog IDs 42 and 64) the isolation of the parasite was also obtained. Following the diagnostics evaluation, the dogs were divided into two groups, infected and non-infected, for *Leishmania* infection. The relative quantity of mir-346 was evaluated in the plasma RNA from all dogs. The results showed that the amount of miR-346 in plasma of dogs naturally infected with *L*. (*L*.) *infantum* is significantly higher compared to non-infected dogs, confirming the previous finding obtained *in vitro* and suggesting the role of miR-346 as a marker of active infection (Fig. 4).

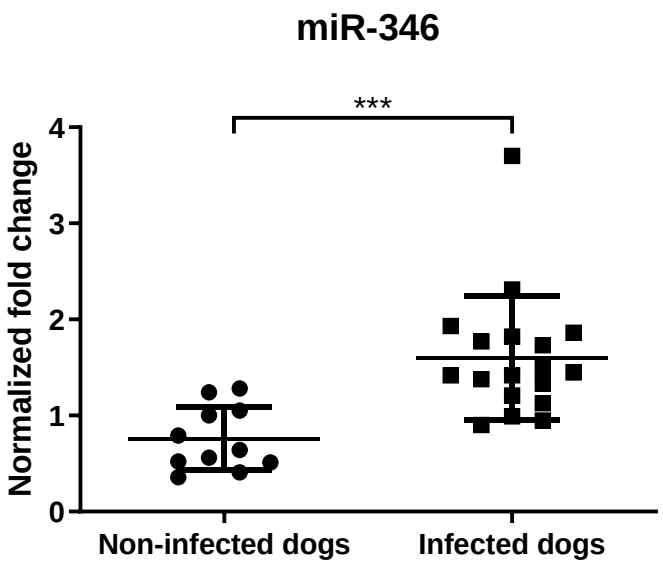

[Figure 4] Relative amount of cfa-miR-346 in plasma of non-infected (n=11) and infected dogs (n=18). The scatter plot graph indicates the mean ± SD. Unpaired t-test ***p<0.001

4. Discussion

Many different mechanisms activated by *Leishmania spp.* to survive within the host cell have been described, e.g. counteracting the antigen presentation and interfering with the macrophage signaling cascade (Podinovskaia & Descoteaux, 2015). Among them, the role of the ER stress and Unfolded Protein Response (UPR), including the activation of IRE1-XBP1 and PERK/eIF2α/ATF4 arms of UPR, have also been investigated (Dias-Teixeira et al., 2016, 2017; Galluzzi et al., 2016). Although dogs are considered of primary importance in the epidemiology of Leishmaniasis, the majority of the current knowledge about *Leishmania*-macrophage interaction comes from cell cultures of murine or human origin. In fact, a limited number of works used the canine monocyte cell line DH82 as cell model to study *Leishmania* infection. The DH82 cells can be considered an M2 subtype macrophage model for leishmaniasis (Nadaes et al., 2020), however, these cells were less permissive to *L. infantum* infection and showed a lower number of amastigotes per macrophages compared to mouse macrophages or human U937 cell line (Maia et al., 2007). This was evident also in the present work, since the infection indexes were rather low compared to human or murine models used in our previous publications (Diotallevi et al., 2018; Galluzzi et al., 2016). This could be explained by the fact that the DH82 canine monocytes were not differentiated by PMA before parasites addition and therefore can multiply during the infection influencing the % of infected macrophages. Moreover, little is known about the surface molecules presented in these cells involved in parasite recognition and uptake. The low infection index could explain the late induction of ER stress markers, which was evident only at 48h post infection, in particular with L. infantum MHOM/TN/80/IPT1 and canine clinical isolate 42. A number of recent studies demonstrated that infections caused by several *Leishmania* species can induce alteration of miRNA profile in human, murine and canine macrophages (Acuña et al., 2020). We have recently investigated mir-346 expression in human U937 and THP-1-derived macrophages infected by *L. infantum* or *L. braziliensis*, finding a significant upregulation of this miRNA during infection (Diotallevi et al., 2018). In this work, we extended these findings to a canine monocyte cell line (DH82) by analyzing the induction of cfa-miR-346 after ER stress induction or *Leishmania* infection. First, we showed that treatment of DH82 cells with tunicamycin significantly induced ER

stress markers (including sXBP1); however, the mir-346 expression did not change, accounting for a sXBP1-independent mechanism of mir-346 induction in this cell line. Nevertheless, the ER stress markers induction with tunicamycin resulted moderate compared to U937, THP1 or murine macrophages (Galluzzi et al., 2016; Diotallevi et al., 2018). In the same way, Nadaes et al., showed general low responsiveness in DH82 stimulated by LPS compared with RAW264.7 cells in terms of reactive oxygen species (ROS) and nitric oxide (NO) production, underling a different activation mechanism in this cell line (Nadaes et al., 2020). On the other hand, the cfa-mir-346 was always significantly upregulated after infection with all *Leishmania* strains and at all times tested, including 24h from infection, when the expression of ER stress markers was still unchanged. Notably, we also showed that induction of mir-346 at early time of infection (6h) can be elicited also by HK parasites; however, cfa-miR-346 upregulation was maintained at later time points (24h and 48h) only in cells infected with viable parasites. Taken together, these data account for a mechanism of cfa-mir-346 induction in canine macrophage-like cells i) depending on active infection and ii) not related to the induction of the ER stress marker sXBP1 (unlike human and mouse cells).

Afterwards, we investigated the presence of cfa-miR-346 in the plasma of dogs naturally infected by *L. infantum* in comparison with plasma obtained from non-infected dogs. Our data showed a significant increase of the cfa-miR-346 expression level in the plasma of infected dogs, suggesting a possible application of the circulating cfa-mir-346 as low-invasive marker of infection. This could help to overcome the limit of PCR-based assays for *Leishmania* detection from whole blood, which presents lower sensitivity compared to bone marrow or lymph node samples (Solano-Gallego et al., 2017), as also demonstrated by qPCR results summarized in Table 1. Interestingly, similar to our findings, Nishimura et al showed that hsa-miR-346 is secreted from macrophages infected by the intracellular pathogen *Mycobacterium avium* complex, which has been demonstrated to elicit ER stress-induced apoptosis in infected macrophages (Go et al., 2019), and proposed that its serum levels could be a potential biomarker of *Mycobacterium avium* complex pulmonary disease activity (Nishimura et al., 2017).

In summary, miR-346 was found to be upregulated in the canine macrophagic-like cell line DH82 infected with four different strains/isolates of *L. (L.) infantum*, as well as

one *L. (V.*) braziliensis isolate, confirming previous findings in human cell lines and pointing to a possible common pathogenic mechanism in human and canine host cells. Moreover, since miR-346 has been shown to be upregulated in the plasma of dogs naturally infected by *L. infantum*, it could be considered a potential biomarker of Leishmaniasis.

Acknowledgments

I would like to thank OIE Reference Laboratory National Reference Centre for Leishmaniasis (C.Re.Na.L.) (Palermo-Italy) and veterinary clinic "Santa Teresa" (Fano-Italy) for providing plasma dog samples.

References

Abbate, J. M., Arfuso, F., Napoli, E., Gaglio, G., Giannetto, S., Latrofa, M. S., Otranto, D., & Brianti, E. (2019). *Leishmania infantum in wild animals in endemic areas of southern Italy*. https://doi.org/10.1016/j.cimid.2019.101374

Acuña, S. M., Floeter-Winter, L. M., & Muxel, S. M. (2020). MicroRNAs: Biological Regulators in Pathogen–Host Interactions. *Cells*, *9*(1), 113. https://doi.org/10.3390/cells9010113

Alvar, J., Vélez, I. D., Bern, C., Herrero, M., & Desjeux, P. (2012). Leishmaniasis Worldwide and Global Estimates of Its Incidence. *PLoS ONE*, *7*(5), 35671. https://doi.org/10.1371/journal.pone.0035671

Arango Duque, G., & Descoteaux, A. (2015). Leishmania survival in the macrophage: where the ends justify the means. *Current Opinion in Microbiology*, *26*, 32–40. https://doi.org/10.1016/j.mib.2015.04.007

Baneth G, Koutinas AF, Solano-Gallego L, Bourdeau P, Ferrer L. Canine leishmaniosis–new concepts and insights on an expanding zoonosis: part one. Trends Parasitol. 2008; 24: 324–330. https://doi.org/ 10.1016/j.pt.2008.04.001 PMID: 18514028

Bartoszewski, R., Brewer, J. W., Rab, A., Crossman, D. K., Bartoszewska, S., Kapoor, N., Fuller, C., Collawn, J. F., & Bebok, Z. (2011). The unfolded protein response (UPR)-activated transcription factor X-box-binding protein 1 (XBP1) induces microRNA-346 expression that targets the human antigen peptide transporter 1 (TAP1) mRNA and governs immune regulatory genes. *The Journal of Biological Chemistry*, *286*(48), 41862–41870. https://doi.org/10.1074/jbc.M111.304956

Bragato JP, Melo LM, Venturin GL, Rebech GT, Garcia LE, Lopes FL, de Lima VMF. Relationship of peripheral blood mononuclear cells miRNA expression and parasitic load in canine visceral leishmaniasis. PLoS One. 2018 Dec 5;13(12):e0206876. doi: 10.1371/journal.pone.0206876. PMID: 30517108; PMCID: PMC6281177.

Castelli, G., Galante, A., Verde, V. Lo, Migliazzo, A., Reale, S., Lupo, T., Piazza, M., Vitale, F., & Bruno, F. (2014). Evaluation of Two Modified Culture Media for Leishmania infantum Cultivation Versus Different Culture Media. *Journal of Parasitology*, *100*(2), 228–230. https://doi.org/10.1645/13-253.1

Castelli G, Bruno F, Caputo V, Fiorella S, Sammarco I, Lupo T, Migliazzo A, Vitale F, Reale S. Genetic tools discriminate strains of Leishmania infantum isolated from humans and dogs in Sicily, Italy. PLoS Negl Trop Dis. 2020 Jul 24;14(7):e0008465. doi: 10.1371/journal.pntd.0008465. PMID: 32706789; PMCID: PMC7406075.

Ceccarelli, M., Buffi, G., Diotallevi, A., Andreoni, F., Bencardino, D., Vitale, F., Castelli, G., Bruno, F., Magnani, M., & Galluzzi, L. (2020). Evaluation of a kDNA-Based qPCR Assay for the Detection and Quantification of Old World Leishmania Species. *Microorganisms*, *8*(12), 2006. https://doi.org/10.3390/microorganisms8122006

Dias-Teixeira, K. L., Calegari-Silva, T. C., dos Santos, G. R. R. M., Dos Santos, J. V., Lima, C., Medina, J. M., Aktas, B. H., & Lopes, U. G. (2016). The integrated endoplasmic reticulum stress response in Leishmania amazonensis macrophage infection: the role of X-box binding protein 1 transcription factor. *FASEB Journal*, *30*(4), 1557–1565. https://doi.org/10.1096/fj.15-281550

Dias-Teixeira, K. L., Calegari-Silva, T. C., Medina, J. M., Vivarini, Á. C., Cavalcanti, Á., Teteo, N., Santana, A. K. M., Real, F., Gomes, C. M., Pereira, R. M. S., Fasel, N., Silva, J. S., Aktas, B. H., & Lopes, U. G. (2017). Emerging Role for the PERK/eIF2α/ATF4 in Human Cutaneous Leishmaniasis. *Scientific Reports*, *7*(1), 17074. https://doi.org/10.1038/s41598-017-17252-x

Diotallevi, A., De Santi, M., Buffi, G., Ceccarelli, M., Vitale, F., Galluzzi, L., & Magnani, M. (2018). Leishmania Infection Induces MicroRNA hsa-miR-346 in Human Cell Line-Derived Macrophages. *Frontiers in Microbiology*, *9*, 1019. https://doi.org/10.3389/fmicb.2018.01019

Galluzzi, L., Diotallevi, A., De Santi, M., Ceccarelli, M., Vitale, F., Brandi, G., & Magnani, M. (2016). Leishmania infantum Induces Mild Unfolded Protein Response in Infected Macrophages. *PLOS ONE*, *11*(12), e0168339. https://doi.org/10.1371/journal.pone.0168339

Gaspari, V., Ortalli, M., Foschini, M. P., Baldovini, C., Lanzoni, A., Cagarelli, R., Gaibani, P., Rossini, G., Vocale, C., Tigani, R., Gentilomi, G. A., Misciali, C., Pesci, S., Patrizi, A., Landini, M. P., & Varani, S. (2017). New evidence of cutaneous leishmaniasis in north-eastern Italy. *Journal of the European Academy of Dermatology and Venereology*, *31*(9), 1534–1540. https://doi.org/10.1111/jdv.14309

Go, D., Lee, J., Choi, J., Cho, S., Kim, S., Son, S., & Song, C. (2019). Reactive oxygen species-mediated endoplasmic reticulum stress response induces apoptosis of Mycobacterium avium -infected macrophages by activating regulated IRE1-dependent decay pathway. *Cellular Microbiology*, *21*(12). https://doi.org/10.1111/cmi.13094

Heishima, K., Ichikawa, Y., Yoshida, K., Iwasaki, R., Sakai, H., Nakagawa, T., Tanaka, Y., Hoshino, Y., Okamura, Y., Murakami, M., Maruo, K., Akao, Y., & Mori, T. (2017). Circulating microRNA-214 and -126 as potential biomarkers for canine neoplastic disease. *Scientific Reports*, *7*(1), 2301. https://doi.org/10.1038/S41598-017-02607-1

Hulanicka, M., Garncarz, M., Parzeniecka-Jaworska, M., & Jank, M. (2014). Plasma miRNAs as potential biomarkers of chronic degenerative valvular disease in Dachshunds. *BMC Veterinary Research*, *10*(1), 205. https://doi.org/10.1186/s12917-014-0205-8

Maia, C., Rolão, N., Nunes, M., Gonçalves, L., & Campino, L. (2007). Infectivity of five different types of macrophages by Leishmania infantum. *Acta Tropica*, *103*(2), 150–155. https://doi.org/10.1016/j.actatropica.2007.06.001

Margariti A, Li H, Chen T, Martin D, Vizcay-Barrena G, Alam S, Karamariti E, Xiao Q, Zampetaki A, Zhang Z, Wang W, Jiang Z, Gao C, Ma B, Chen YG, Cockerill G, Hu Y, Xu Q, Zeng L, 2013. XBP1 mRNA splicing triggers an autophagic response in endothelial cells through BECLIN-1 transcriptional activation. J Biol Chem.; 288(2):859-72. doi: 10.1074/jbc.M112.412783

Martinon F, Chen X, Lee A-H, Glimcher LH, 2010. Toll-like receptor activation of XBP1 regulates innate immune responses in macrophages. Nat Immunol.; 11(5):411-8. doi: 10.1038/ni.1857.

Nadaes, N. R., Silva da Costa, L., Santana, R. C., LaRocque-de-Freitas, I. F., Vivarini, Á. D. C., Soares, D. C., Wardini, A. B., Gazos Lopes, U., Saraiva, E. M., Freire-de-Lima, C. G., Decote-Ricardo, D., & Pinto-da-Silva, L. H. (2020). DH82 Canine and RAW264.7 Murine Macrophage Cell Lines Display Distinct Activation Profiles Upon Interaction With Leishmania infantum and Leishmania amazonensis. *Frontiers in Cellular and Infection Microbiology*, *10*(June). https://doi.org/10.3389/fcimb.2020.00247

Nishimura, T., Tamizu, E., Uno, S., Uwamino, Y., Fujiwara, H., Nishio, K., Nakano, Y., Shiono, H., Namkoong, H., Hoshino, Y., Iwata, S., & Hasegawa, N. (2017). hsa-miR-346 is a potential serum biomarker of Mycobacterium avium complex pulmonary disease activity. *Journal of Infection and Chemotherapy : Official Journal of the Japan Society of Chemotherapy*, *23*(10), 703–708. https://doi.org/10.1016/j.jiac.2017.07.015

Pfaffl, M. W. (2001). A new mathematical model for relative quantification in real-time RT-PCR. *Nucleic Acids Research*, *29*(9), e45. http://www.ncbi.nlm.nih.gov/pubmed/11328886

Podinovskaia, M., & Descoteaux, A. (2015). Leishmania and the macrophage: a multifaceted interaction. *Future Microbiology*, *10*(1), 111–129. https://doi.org/10.2217/fmb.14.103

Risueño, J., Ortuño, M., Pérez-Cutillas, P., Goyena, E., Maia, C., Cortes, S., Campino, L., Bernal, L. J., Muñoz, C., Arcenillas, I., Martínez-Rondán, F. J., Gonzálvez, M., Collantes, F., Ortiz, J., Martínez-Carrasco, C., & Berriatua, E. (2018). Epidemiological and genetic studies suggest a common Leishmania infantum transmission cycle in wildlife, dogs and humans associated to vector abundance in Southeast Spain. *Veterinary Parasitology*, *259*, 61–67. https://doi.org/10.1016/j.vetpar.2018.05.012

Schönian, G., Nasereddin, A., Dinse, N., Schweynoch, C., Schallig, H. D. F. ., Presber, W., & Jaffe, C. L. (2003). PCR diagnosis and characterization of Leishmania in local and imported clinical samples. *Diagnostic Microbiology and Infectious Disease*, *47*(1), 349–358. https://doi.org/10.1016/S0732-8893(03)00093-2

Solano-Gallego, L., Miro, G., Koutinas, A., Cardoso, L., Pennisi, M. G., Ferrer, L., Bourdeau, P., Oliva, G., Baneth, G., & Group, T. L. (2011). LeishVet guidelines for the practical management of canine leishmaniosis. *Parasit.Vectors.*, *4*, 86.

Solano-Gallego, Laia, Cardoso, L., Pennisi, M. G., Petersen, C., Bourdeau, P., Oliva, G., Miró, G., Ferrer, L., & Baneth, G. (2017). Diagnostic Challenges in the Era of Canine Leishmania infantum Vaccines. *Trends in Parasitology*, *33*(9), 706–717. https://doi.org/10.1016/j.pt.2017.06.004

Vitale, F., Reale, S., Vitale, M., Petrotta, E., Torina, A., & Caracappa, S. (2004). TaqMan-based detection of Leishmania infantum DNA using canine samples. *Annals of the New York Academy of Sciences*, *1026*, 139–143. https://doi.org/10.1196/annals.1307.018

Vitale, Fabrizio, Bruno, F., Migliazzo, A., Galante, A., Vullo, A., Graziano, R., Avola, S. D., Caputo, V., & Castelli, G. (2020). *Cross-sectional survey of canine leishmaniasis in Pantelleria island in Sicily*. *February 2017*, 91–95. https://doi.org/10.12834/VetIt.2059.10976.3

FINAL CONCLUSIONS AND FUTURE PERSPECTIVE

Leishmaniases are a group of parasitic diseases caused by protozoa belonging to the *Leishmania* genus. Approximately 20 species are pathogenic to humans and the disease has a worldwide distribution. Italy and the Mediterranean basin are considered endemic areas for canine and human leishmaniasis caused by *L. infantum* species. In some geographical regions, like Latin America, several *Leishmania* species are endemic and simultaneously present. Since various species can cause different forms of the disease, a rapid diagnostic method for species discrimination, particularly in co-existing regions, that does not require parasite isolation, would be needed, not only for epidemiological studies, but also to predict the clinical disease evolution and choose the correct pharmacological therapy. Most of the qPCR assays available are not species-specific and identify only the *Leishmania* genus. We developed a diagnostic approach for *Leishmania* species discrimination based on multiple qPCRs followed by HRM analysis that allowed us to differentiate the subgenera *Leishmania* and *Viannia* and distinguish among *L. infantum*, *L. amazonensis* and *L. mexicana***.** This approach has been implemented with both veterinary and human clinical samples, from Brazil, where *L. infantum*, *L. amazonensis* and *Viannia* subgenus species coexist, and from Mexico, where the main species is *L. mexicana*, which is genetically close to *L. amazonensis*. These studies allowed us to establish a diagnostic algorithm involving 3 different SYBR green-based qPCR assays for the effective discrimination among *Viannia* subgenus, *L*. m*exicana* complex (including *L*. *amazonensis* and *L*. m*exicana* species) and *L*. (*L*.) *infantum*. This approach could be useful in a clinical context in co-endemic regions for different *Leishmania* species to provide a rapid diagnosis and for epidemiological investigations. Furthermore, we showed that our assay designed on kDNA minicircles conserved regions (qPCR-ML) can also amplify the Old World species different from *L. (L.) infantum* [*i.e. L. (L.) donovani*, *L. (L.) major*, *L. (L.) tropica* and *L. (L.) aethiopica*] with good quantification limit; therefore, this assay could be considered as a pan-*Leishmania* assay**.** It is noteworthy that the two closely related species *L. (L.) tropica* and *L. (L.) aethiopica* were distinguished through HRM analysis of qPCR-ML amplicons. However, this could be considered a preliminary result due to the low number of strains analyzed.

Besides the development of tools for *Leishmania* species discrimination, we wanted to find a rapid screening method to explore the genetic variability among the *L. infantum* strains in the Mediterranean region. To this end, a customized sequencing panel targeting 14

housekeeping genes was designed and MLST analysis was performed. The results allowed the selection of two informative polymorphisms on ME and GPI genes (390T/G and 1834A/G, respectively) used to develop two HRM-based assays, which allowed to identify 6 genotypes in *L. infantum* samples collected in the Mediterranean region. This study represents a description of the genetic variability of *L. infantum* through an approach based first on MLST and then on HRM analysis of selected polymorphisms. The HRM assays could be used as fast and cheap tools for epidemiological surveillance of *L. infantum.*

Since *L. (L.) infantum* and *L. (L.) donovani* species are genetically closely related and are part of the same species complex, their molecular differentiation is a challenge. Moreover, they can coexist in the same geographical areas (such as Ethiopia) and cause the same clinical manifestations (VL). Future studies will be aimed to identify genetic polymorphisms that can be exploited to develop molecular assays useful to discriminate between these two species.

Parallel to the identification of a rapid diagnostic method for species discrimination, the mechanisms underlying host-pathogen interaction were investigated. As already known, once that *Leishmania* infection is established, parasites are able to survive and replicate in the host macrophages subverting the host's innate immune response. Among these mechanisms, we previously showed a mild but significant induction of the Unfolded Protein Response (UPR) in human and murine cell lines to promote parasites' survival in the host cells**.** Moreover, we demonstrated that a microRNA, miR-346, related to the UPR-activated transcription factor sXBP1, with a potential role in the immune response modulation, was significantly upregulated in human macrophages infected with different *L. infantum* strains**.** Since dogs represent one of the most important reservoirs of infection for leishmaniasis, in the optic of a "one health" approach, we evaluated, for the first time, the gene expression of some ER stress-related genes and miR-346 by qPCR in a canine macrophage cell line (DH82) infected by either *L.* (*Leishmania)* or *L. (Viannia)* species and we compared the presence of the micro-RNA cfa-miR-346 in plasma of dogs healthy and naturally infected with *L. infantum*. The results in DH82 cells showed that cfa-mir-346 was induced post-infection with all *Leishmania* strain/isolates tested. Moreover, the cfa-miR-346 expression analysis on dogs' plasma revealed a significant upregulation in infected dogs compared to healthy dogs. Despite the role of cfa-miR-346 during *Leishmania* infection needs to be deeply elucidated, these findings seem to identify the miRNA-346 as an infection marker in dogs affected by

leishmaniasis. Over the past decade, it has become clearer how the microRNAs are related to the pathogenesis of leishmaniasis. In this view, in collaboration with IZS Palermo, we are evaluating the miRNome of a human monocytic cell line (U937) differentiated into macrophages infected with *L. infantum* MHOM/IT/08/31U for 24h and 48h, using next-generation sequencing (NGS) approach. Bioinformatics analyses of the data are still ongoing in search of dysregulated metabolic pathways following infection.

Finally, in the last year, we worked on new drug screening and discovery against *trypanosomatidae*. Since the drugs currently available for the treatment of leishmaniasis are expensive, show high toxicity or are subject to drug resistance (as shown in the case report of chapter 6), the rapid identification of drug-resistant strains is important to direct the clinician to more effective treatment; moreover, the progress in the discovery of a safer, affordable, and effective therapeutic alternative is considered peremptory. In this view, we tested a small library of 12 3,3'-diindolylmethane (DIM) derivatives for their anti-leishmanial potential, first in terms of efficacy on *L. infantum* promastigotes and then on intracellular amastigotes. Five compounds showed activity on promastigotes with IC50 values below 10 µM. In particular, the bis-indole compound URB1483 revealed a promising anti-leishmanial activity against both promastigotes and intracellular amastigotes, with low toxicity for the host cells. Starting from these preliminary results, we started a collaboration with the "Institute of Research and Innovation in Health" at the University of Porto. During my activity as visiting research, I tested a library of 35 3,3'-diindolylmethane derivatives, previously synthesized by Prof. Simone Lucarini from the University of Urbino, for their potential antiparasitic effects against *L. infantum* and *Trypanosoma brucei,* the causative agent of African trypanosomiasis. The compounds have been tested in terms of efficacy on the extracellular form, and, after the evaluation of the cytotoxicity on THP1 cells, the molecules have been tested on *L. infantum* intracellular amastigotes. Ten and four compounds resulted active on *T. brucei* and *L. infantum*, respectively, with an IC50 below than 5 µM. These results allowed us to find new promising classes of compounds never tested before. The two best compounds have been selected for the *in vivo* experiments on Balb/C mice infected with *L. infantum* amastigotes. After 3 weeks of infection, the mice have been treated with 5mg/Kg IP of compound for 10 days. Unfortunately, at these conditions, the results did not show differences in terms of molecules efficacy compared with the

untreated mice. Nevertheless, the project is ongoing, and these findings represent the basis for further studies about the pharmacokinetics, pharmacodynamics, solubility test, bioavailability to optimize the new classes of compounds for the development of new therapeutical strategies. In this view, future work will be aimed to develop an effective delivery system using nanocarriers such as liposomes or decorated liposomes to improve selective uptake. Moreover, the molecular target(s) as well as mechanism of action of this class of compounds still needs to be investigated.

In summary, this thesis illustrates our attempt to contribute to the improvement of both diagnostics and therapeutics, in the context of a one health approach, to reduce the burden of this complex and heterogeneous disease.

ACKNOWLEDGMENTS

At the end of this long and exciting travel in the research world, first of all, I would like to express my gratitude to my research group: to my supervisor, Professor Luca Galluzzi, my co-supervisor Dr. Aurora Diotallevi and Dr. Marcello Ceccarelli, thank you for giving me the possibility to start this amazing job, for the support during these years and the knowledge sharing.

I also wish to express my gratitude to Professor Mauro Magnani and to all the people that I had the pleasure to work with at the University of Urbino, in particular to all the colleagues of the Biotechnology section in Fano (PU)

Thanks to all the co-authors for the commitment and work done in the published papers. In particular, Dr. Fabrizio Vitale, Dr. Federica Bruno and Dr. Germano Castelli from the National Reference Center for Leishmaniasis (C.Re.Na.L.) (IZS, Palermo, Sicily).

Thanks to Ph.D. mates, in particular, Dr. Anastasia Ricci, for sharing the beautiful but also difficult moments of this journey.

I also would like to acknowledge the Parasite Disease Group of the “Instituto de Investigação e Inovação em Saúd” (University of Porto – Portugal), in particular, the group chief Professor Anabela Cordeiro-da-Silva and my supervisor Dr. Nuno Santarem for the hospitality and for giving me the possibility to work for eight months in their laboratories.

Last, a special thank you to my parents Gabriele and Laura, my sister Eleonora, my nephews Cecilia and Damiano, my boyfriend Antonio and my friend Sara for always being by my side and supporting me in each moment.

Thank you all.